The Design and Application of Bis-Urea Derived Supramolecular Gelators

FOSTER, JONATHAN,ANDREW

The Design and Application of Bis-Urea Derived Supramolecular Gelators

A thesis submitted for the fulfilment of the requirements for the degree of

Doctor of Philosophy

In the faculty of Science of Durham University

by

Jonathan Andrew Foster

Department of Chemistry

Durham University

South Road

Durham

2012

Abstract The design and application of bis-urea derived supramolecular gelators

A series of amino-acid derived bis-urea gelators were synthesised, some of which show strong gelation in a wide variety of solvents. The gels were probed at the molecular, microscopic and macroscopic levels to gain insights into the gelation behaviour observed. Mixtures of different gelators also result in gels, some of which show different fibre morphologies and X-ray powder patterns to the pure gelators. The series was extended to include fluorescent 1- and 2-pyrenylalanine derived gelators and the fluorescence behaviour of the gels in solution, the gel state, in mixed gels and with the addition of anions was investigated. Tetrabutylammonium-acetate was found to disrupt urea-hydrogen bonding leading to the break-down of the gels, a process which was followed by NMR spectroscopy, rheometry and fluorescence spectroscopy. Two gelators were used to template the formation of porous polymers which SEM and gas adsorption studies show reflect the different fibre morphologies observed in the gels.

The use of supramolecular gels as a medium for controlling the crystallisation of pharmaceutical compounds was developed. Proof of principle for the growth of a wide range of pharmaceutical compounds from a variety of different gels was demonstrated. The supramolecular nature of the gels was exploited by using anions to break down the gels in order to recover the crystals. Comparison of crystals grown from gels with those grown from solution highlighted a number of differences in crystal form, habit and stability. Gelators which mimic the chemical functionality of the drug compound being crystallised were synthesised. A study investigating the crystallisation of 5-methyl-2-[(2-nitrophenyl)amino]-3-thiophenecarbonitrile (ROY) showed some differences in polymorphism when crystallised from a gel designed to mimic ROY compared to generic gels. A placement with the particle science group at GSK explored the potential of supramolecular gels for use in early stage screening of pharmaceutical compounds in an industrial setting.

Acknowledgements

I am very grateful to the EPSRC and GSK for funding my research. To Jonathan Steed for being such an excellent supervisor and for all the opportunities and support he has given me. I would also like to thank Judith Howard and everyone in her group for being so helpful and inclusive. I am grateful to Andrew Craig, Tim Ho and everyone at GSK for giving me such a positive experience of life in industry.

I would like to thank everyone who has helped and collaborated with me during my time at Durham. Marc Piepenbrock and Gareth Lloyd for introducing me to gels and getting me started, Katherina Fucke for keeping me going. Robert Edkins for his help with the fluorescence spectroscopy, David Johnson for helping me with the gas adsorption measurements and Andrew Beeby and Neil Cameron for letting me use their instruments. Steve Cobb, Neil Colgin and Andrew Crawford for synthesising the pyrenylalanine amino acids. Helen Grindley for her help with the SEM. Silvia Imberti at ISIS and Tilo Seydel at the ILL for the opportunity to work with Neutrons. I'd also like to thank the students that I've worked with: Gary Cameron, Miranda Camping, Jenifer Cuestra and Lorenzo Meazza.

This thesis could not have been done without the support of my family who have given me every opportunity and encouragement I could have asked for. In particular I would like to thank my beautiful wife Clare for all her love and support over the past three and a half years, I couldn't have done it without you. This thesis has been an act of worship to an amazing creator God whose universe I have enjoyed learning more about.

Declaration

I declare that all experiments described herein are my own work and were carried out at the Department of Chemistry, University of Durham, under the supervision of Professor Jonathan W. Steed and Professor Judith K. Howard. Several of the gelators used in this thesis were synthesised by other people as acknowledged at the start of the experimental section for each chapter. Details for the synthesis of compounds made by Masters Student Gary Cameron and summer student Jenifer Bernal under my supervision have been included for completeness and to provide a published record. Compounds **20**, **26** and **30** and Figures 24 and 36 in Chapter 2 were previously included in work submitted for my Masters dissertation. The solution phase screen of GSK-D was undertaken by Reshma Chudasama.

Papers

Foster, J.A. & Steed, J.W., Exploiting Cavities in Supramolecular Gels, *Angew. Chem. Int. Ed.*, 2010, **49**, 6718.

Foster, J.A., Piepenbrock, M.-O.M., Lloyd, G.O., Clarke, N., Howard, J.A.K. & Steed, J.W., Anion-switchable supramolecular gels for controlling pharmaceutical crystal growth, *Nat. Chem.*, 2010, **2**, 1037.

Lenthall, J.T., Foster, J.A., Anderson, K.M., Probert, M.R., Howard, J.A.K. & Steed, J.W., Hydrogen bonding interactions with the thiocarbonyl pi-system, *CrystEngComm*, 2011, **13**, 3202.

Piepenbrock, M.-O.M., Clarke, N., Foster, J.A. & Steed, J.W., Anion tuning of chiral bis(urea) low molecular weight gels, *Chem. Commun.*, 2011, **47**, 2095.

Lloyd, G.O., Piepenbrock, M.O.M., Foster, J.A., Clarke, N. & Steed, J.W., Anion tuning of chiral bis(urea) low molecular weight gels, *Soft Matter*, 2012, **8**, 204.

Abbreviations

1D	One Dimensional
2D	Two Dimensional
3D	Three Dimensional
Asp	Aspirin
ACP	Acetaminophen
API	Active Pharmaceutical Ingredient
ATR	Attenuated Total Reflection
Bn	Benzyl
BOC	tert-Butyloxycarbonyl
Bpy	Bipyridine/Bipyridinium
Bu	Butyl
CAF	Caffeine
CBZ	Carbamazepine
Cbz	Carbobenzyloxy
CSD	Cambridge Crystallographic Database
cm	Centimeter
CCD	Charge Coupled Device
$CHCl_3$	Chloroform
conc	Concentration
CGC	Critical Gelation Concentration
CMC	Critical Micelle Concentration
-d	Deuterated
d (NMR)	Doublet
DCM	Dichloromethane
dd (NMR)	Doublet of Doublets
ddd (NMR)	Doublet of Doublet of Doublets
DMF	Dimethylformamide
DMSO	Dimethylsulfoxide
DOSY	Diffusion Ordered Spectroscopy
eq.	Equivalents
ES	Electrospray

Et	Ethyl
EtOAc	Ethylacetate
EtOH	Ethanol
f	Oscillator Strength
FT	Fourier Transform
G′	Storage or elastic shear modulus
G″	Loss or viscous modulus
HOMO	Highest Occupied Molecular Orbital
Hz	Hertz
IBU	Ibuprofen sodium salt
IND	Indomethacin
IR	Infrared
J (NMR)	Coupling Constant
K or Ka	Association Constant
LMW	Low Molecular Weight
LMWG	Low Molecular Weight Gelator
log	Logarithmic
LUMO	Lowest Unoccupied Molecular Orbital
m	Metre
m (NMR)	Multiplet
MALDI	Matrix Assisted Laser Desorption Ionisation
Me	Methyl
MeCN	Acetonitrile
MeOH	Methanol
MS	Mass Spectrometry
NMR	Nuclear Magnetic Resonance
OAc	Acetate
OMe	Methoxide
Pa	Pascal
Ph	Phenyl
PIX	Piroxicam
Pr	Propyl
XRPD	Powder X-Ray Diffracion

q (NMR)	Quintet
ROY	5-Methyl-2-[(2-nitrophenyl)amino]-3-thiophenecarbonitrile
s (NMR)	Singlet
SEM	Scanning Electron Microscopy
SPF	Sparfloxacin
SUL	Sulindac
t (NMR)	Triplet
TBA	Tetrabutylammonium
td(NMR)	Triplet of Doublets
T_{gel}	Solution to gel transition temperature
THE	Theophyline
THF	Tetrahydrofuran
TLC	Thin Layer Chromotography
Tol	Toluene
UV	Ultraviolet
UV-vis	Ultraviolet-visible
vol	Volume
VT	Variable Temperature
w/v	Weight/volume ratio
β	Stepwise Binding Constant
δ	Chemical Shift
λ	Wavelength
ν	Wavenumber
σ	Applied stress

Table of Contents

Chapter 1: Design and application of urea-derived supramolecular gelators

1.1 Introduction

1.1.1 Common Characteristics

Everyday products such as jelly, hair gel, contact lenses and lithium grease are readily identified as gels despite their very different molecular and structural compositions. Gels are materials which have solid-like flow properties despite being predominantly liquid in composition. The gel state arises when solvent is trapped through surface tension by a continuous, sample spanning structure. This structure may be lamellar (e.g. soaps and clays), a covalent polymeric network (e.g. silica gels), a polymeric network formed through physical aggregation (e.g. gelatin) or particulate in nature (e.g. precipitates consisting of highly anisotropic particles).[1]

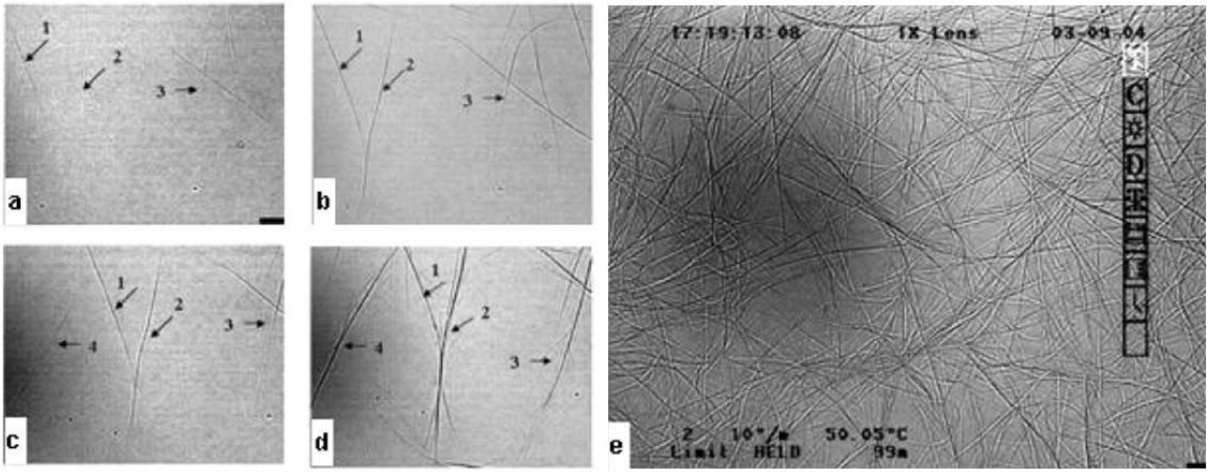

Figure 1 Optical micrographs showing time evolution of a fibrillar gel network upon slow cooling of N-lauroyl-L-glutamic acid di-n-butylamide/propylene glycol: (a) one-dimensional growth of fibres, b) and c) branching of fibres d) aggregation of fibres, e) formation of sample spanning network.[2]

Considerable progress has recently been made in the development and characterisation of supramolecular gels in which the macromolecular networks are assembled through non-covalent interactions. The basic building block of a supramolecular gel is a low molecular weight compound (known as a low molecular weight gelator, LMWG) which typically makes up 1 % of the gel by weight whilst the remaining 99% is solvent. The LMWG undergo an arrested crystallisation stacking together preferentially in one direction to give highly anisotropic structures (Figure 1a). These structures either physically entangle or cross link

through intermolecular interactions to form a sample spanning network which traps large volumes of solvent through surface tension. Because the gel network is held together by supramolecular interactions most LMWGs are thermally reversible and reform upon cooling from a hot solution.

A wide variety of chemical species form supramolecular gels including surfactants,[3] fatty acids,[4] nucleobases,[5] porphyrin derivatives,[6] dendrimers,[7] amino acids,[8] peptides[9] and carbohydrates.[10] These compounds contain a number of motif-forming functional groups which enable the anisotropic aggregation required for gel formation to take place. These include amides, ureas, oxalamides,[11] (-XCONH- hydrogen bonding), carbohydrates (multiple –OH hydrogen bonding), steroids (hydrophobic surfaces), nucleobases (hydrogen bonding and π-π stacking) and long chain alkanes (van der Waals interactions).[12] A variety of host-guest interactions have also been exploited effectively to create supramolecular gels.[13] In addition to a single gelling component, a variety of multi-component gelators have been developed. Such systems may consist of two or more organic components coming together to form a gel,[14-17] incorporation of a metal ion to form a metallo-gel[12, 18, 19] or the inclusion of nano-materials to form composite gels.[20-23]

The nature of the solvent mediates the relative importance of different types of gelator-gelator interactions. In organic solvents aggregation is typically driven by attractive forces between gelator units, such as hydrogen bonding, dipolar interactions, electron transfer and metal-co-ordinated interactions.[24] Such systems are termed organogels.[24] However, such interactions tend to lose their strength in water due to solvation, so it is often less directional hydrophobic effects which dictate hydrogel formation.[25] Stronger attractive components such as salt bridges, metal co-ordination and co-operative hydrogen bonding can also play a role, particularly when shielded from solvent by hydrophobic groups.[26] Some gelators are able to gel both aqueous and organic solvents and such systems are described as amphiphilic gelators.[27]

Although a diverse range of compounds form gels, the delicate balance of interactions required to bring about gel formation means small changes in molecular structure can lead to large differences in gelation behaviour. This may be due to subtle differences in conformation, steric interactions or electronic effects resulting from the different substituents.

Solvent-gelator interactions must also be taken into consideration in terms of the solubility of the gelator, templating effects on the nucleation of different forms and wetting of the gel matrix. These factors make *a priori* predictions about which compounds will form gels and under what conditions difficult and most new classes of gelator are still discovered serendipitously.[28]

One successful attempt to predict the packing of a gel, formed by sonication of melamine and uric acid, was made by Anderson *et al*.[29] They used *ab initio* crystal structure calculation to identify the lowest lattice energy combinations from 250,000 candidate structures, one of which was found to match the X-ray powder pattern of the dried gel. However, these gelators have unusually rigid structures for LMWGs which aided prediction and many gels are not formed under thermodynamic control. Gelators can be polymorphic and in a recent example four different crystal forms were crystallised from gels of the same silver(I) gelator in different solvents.[30] In a number of cases crystallisation of the gelator has been observed to occur over time if the gel is not the thermodynamically stable phase.[17, 31-33]

In comparison to the gelator-gelator interactions, relatively little is known about the role of solvent in gel formation. Smith and co-workers considered the effect of Kamlet-Taft parameters on a series of lysine derived bis-urea gelators with different length alkyl chains.[34] They found that the α parameter (hydrogen bond donor ability) of the solvent was most important in determining whether a gelator network can be established, the β parameter (hydrogen bond acceptor ability) modulates gelator-gelator interactions whilst the π* parameter (polarisability) tunes interactions between gel fibres and solvent molecules. Dissolution studies for a series of pyridine derived compounds showed that room temperature solubility was a poor indicator of gelation ability.[35] However, gelators were found to exhibit higher dissolution enthalpies and entropies than non-gelators consistent with stronger intermolecular interactions and more order in the solid state. Similar findings were observed when the range of gelators was extended to include a series of peptide derived gelators.[36]

1.1.2 Characterising the gel state

The bench-top test to determine whether a compound forms a gel is to invert a vial containing a low concentration of the potential gelator recrystallised from a hot solution; if the mixture doesn't flow then it is considered to have gelled. This is essentially a crude rheometric

measurement and more detailed, quantitative measurements can be made using a rheometer. Gels are viscoelastic materials displaying both solid-like behaviour, characterised by an elastic storage modulus G', and liquid-like viscous behaviour, characterised by the elastic loss modulus G'' (equation 1). Both G' and G'' have units of Pascals. As gels are solid-like in their flow properties, G' is typically an order of magnitude greater than G'' under a weak applied stress (σ). In a gel G' should also be constant over a wide range of frequencies when a low stress is applied.[12, 24, 37, 38]

$$G = G' + iG'' \qquad (1)$$

$$G' = \frac{\sigma_0}{\varepsilon_0}\cos\delta \qquad (2)$$

$$G'' = \frac{\sigma_0}{\varepsilon_0}\sin\delta \qquad (3)$$

At higher stresses the gels shear and begin to flow, a point referred to as the yield stress. This correlates with a drop in G′ below that of G″ indicating liquid like behaviour. This transition can also be observed by monitoring the phase difference (δ) between the applied stress (σ) and resulting strain (ε) which should be close to 0° in the solid-like gels (equations 2 and 3). The magnitude of G' gives an indication about the relative strength of the gel, however small differences in sample preparation and the presence of defects such as air bubbles can lead to significant variation in the values obtained.[24]

The minimum concentration of gelator required to form a gel is termed the critical gelator concentration (CGC) and may be measured by rheometry or more typically the inversion test. The temperature at which the gel-sol transition takes place, known as the T_{gel}, is typically measured using the 'dropping ball' test. A ball bearing is placed on the surface of a gel and the sample gradually heated in a water bath with the point at which the gel can no-longer support the ball bearing defining the T_{gel}. Alternative measurements can be made by rheology, differential scanning calorimetry (DSC) or spectroscopic techniques with the same gel giving disparate readings depending on what level of structural break down is being characterised.[39, 40] The break-down of the gel matrix does not necessarily correlate with dissolution of the gelator and a number of methods have been employed to measure the solubility of the gelator molecules.[34, 35, 41]

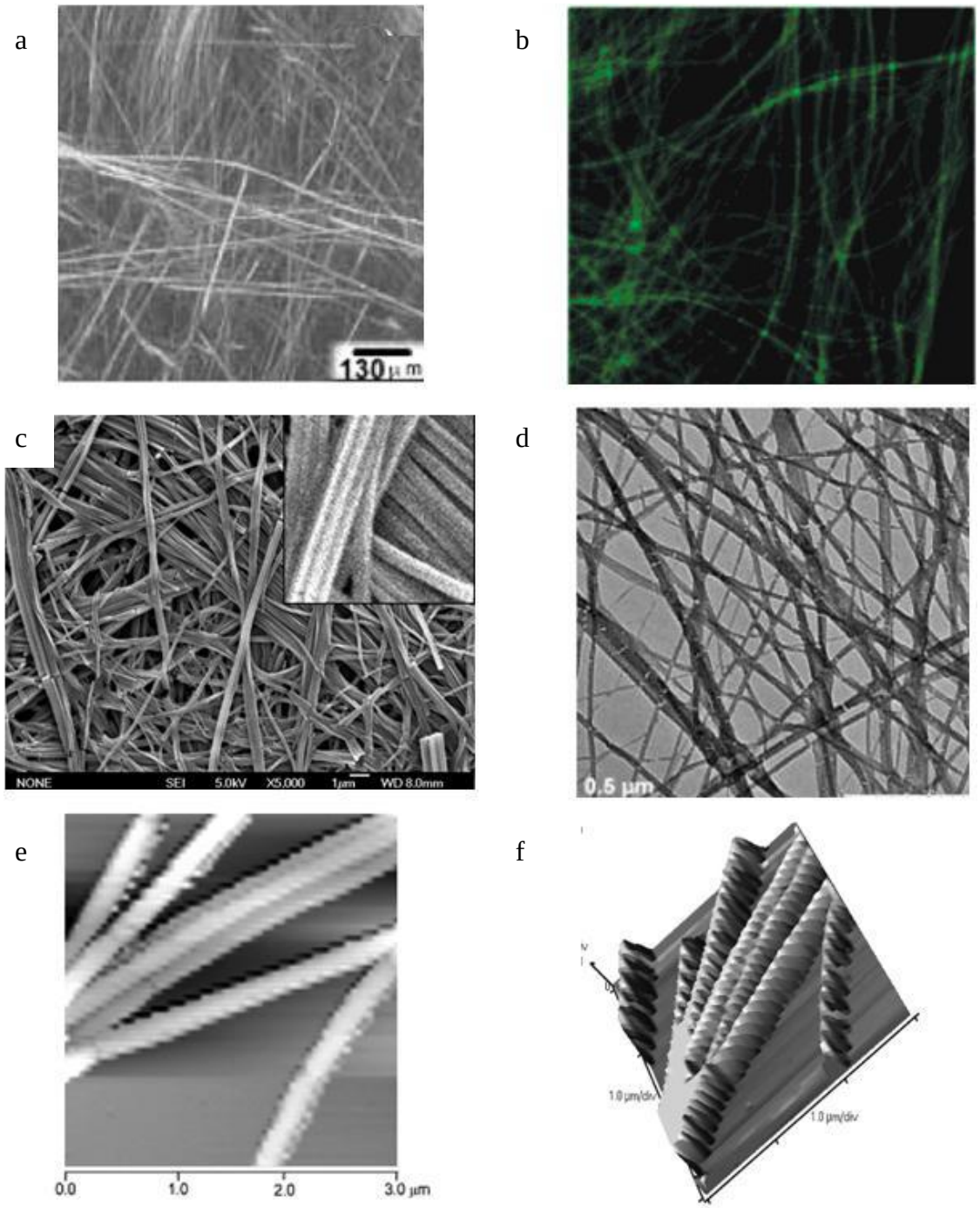

Figure 2 Hydrogel formed by riboflavin and melamine imaged using a) optical microscopy, b) fluorescence microscopy, c) scanning electron microscopy (SEM), d) transmission electron microscopy (TEM), e) atomic force microscopy (AFM) f) 3D reconstruction of e) showing helical fibres.[42]

Optical microscopy provides real time imaging of the gel matrix in its solvated state, allowing dynamic features such the growth of fibres from solution (Figure 1) to be captured.[2] However, it is the wide spread availability of scanning electron microscopy (SEM) in recent years that has allowed detailed images to be built up about the nanoscopic morphology of the

gel matrix and interactions between gel fibres. One limitation of this and related techniques, such as transmission electron microscopy (TEM), is the requirement for high vacuum. Samples are therefore typically viewed as dried xerogels, opening up the possibility of changes in gel structure upon loss of solvent.[36] Cryo-SEM allows for *in situ* de-solvation of the gels minimising the chance of transformations whilst environmental SEM allows imaging of solvated gels, albeit with lower resolution. More detailed imaging techniques such as atomic force microscopy and scanning tunnelling microscopy have also been applied to LMWGs. A good comparison of the different techniques is provided by Saha *et al*. who imaged a hydrogel formed by riboflavin and melamine using a range of techniques as shown in Figure 2.[42]

Single crystal structure determination remains an invaluable tool for understanding how small molecule gelators pack together in the solid state. The relationship between the gel and crystalline state is typically established by comparing X-ray powder diffraction (XRPD) data for the xerogels with calculated patterns derived from crystal structure data, although the possibility of rearrangement upon drying remains.[30, 36] X-ray powder patterns have been run directly on more crystaline gel samples with the broad pattern for the solvent background subtracted to emphasise the gelator peaks.[43] Other diffraction techniques such as small angle X-ray or neutron scattering (SAXS and SANS respectively) provide further information about spacing between gelator molecules.[9, 41] Other techniques such as IR, Raman and NMR spectroscopy have also been used to provide insights into intermolecular interactions.[42, 44]

1.2 Urea derived Gelators

1.2.1 Urea derived gelators

One motif that has proved prolific at bringing about gelation in low molecular weight compounds is the urea moiety. Key to the success of urea derivatives in bringing about gelation is the formation of the α-urea tape motif. Urea groups stack together to form a chain of 6-membered hydrogen bonded rings based on two hydrogen bond donors and one carbonyl acceptor, $C(4)R_2^1(6)$ in graph set nomenclature (Figure 3a).[45] The strength of this interaction between two urea molecules was calculated to be 44.80 kJmol^{-1}.[46] It is these hydrogen bonded chains which typically provide the strong directionality required to form high aspect ratio fibres which (upon physical entanglement) lead to the formation of gels (Figure 3b).

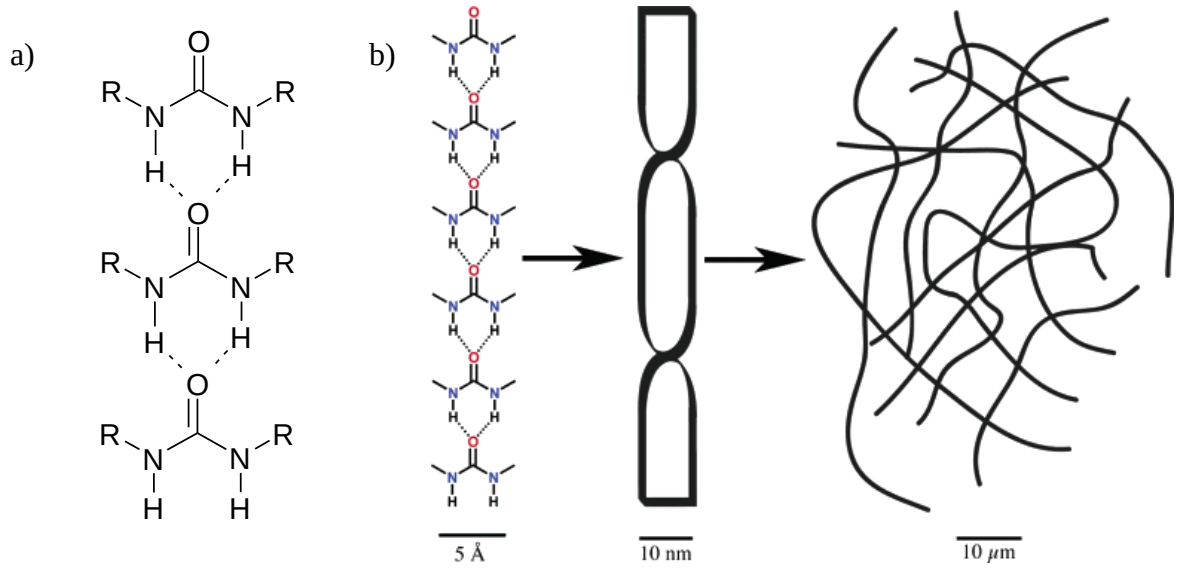

Figure 3 a) Ureas are an example of a functional group which can favourably stack together through hydrogen bonds to give one-dimensional fibrils. b) These fibrils can aggregate to form larger fibres which interweave to create a sample spanning network.[25]

The simplest urea based gelator, and possibly the lowest molecular weight gelator to date, is N,N′-dimethylurea (M_w 88) which forms gels in silicone oil.[46] This compound forms part of a series of related N,N′-dialkylurea gelators with different alkyl chain lengths developed by Weiss and co-workers. The optimum length was found to be the dipropyl derivative with shorter and longer chain lengths requiring higher concentrations of compound to produce a stable gel. Mono-alkylated ureas with primary amido groups are typically more efficiently in hydrogen bonding than secondary amido groups, although the hydrophobic contributions of the alkyl chains are also important.

In a recent paper, Kim *et al*. compared the gelation behaviour of (*R*)- and (*S*)-2-heptylurea with a racemic mixture.[47] The individual enantiomers formed gels in a greater range of solvents at lower concentrations than a racemic mixture or *n*-hexylurea. SEM studies showed 1D structures are formed by the resolved compounds whilst 2D ribbons are formed by the racemic and achiral gelators (Figure 4a and b). The crystal structure obtained for racemic 2-heptylurea (Figure 4c) was found to be in $P2_1/c$, a space group not available to the pure enantiomers potentially explaining the differences in morphology and gelation behaviour observed.

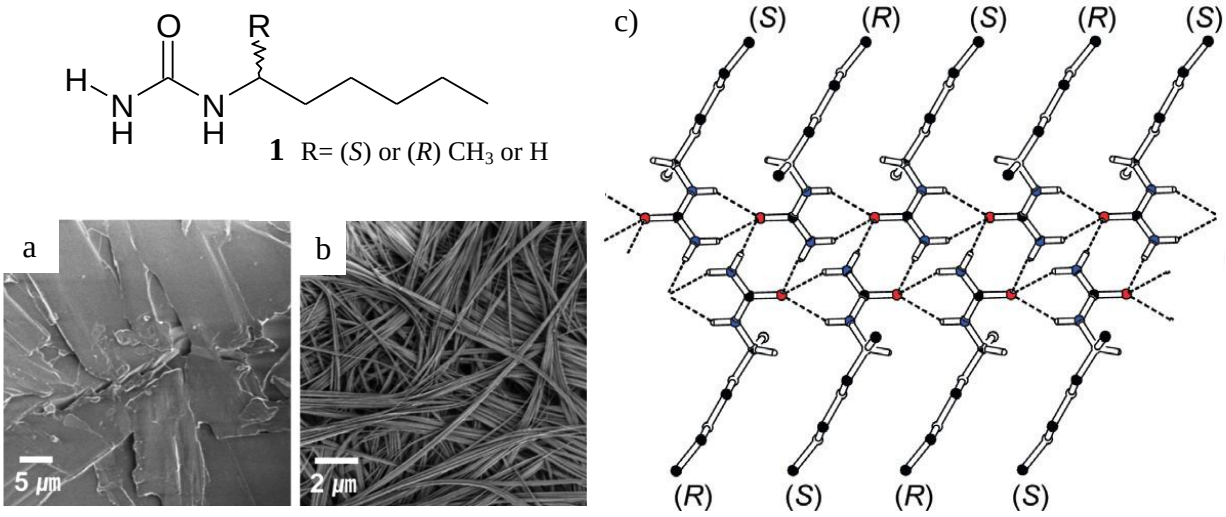

Figure 4 SEM images showing morphologies obtained from 1:1 ethylacetate:hexane for a) rac-2-heptylurea and b) (*s*)-2-helptylurea. c) crystal structure obtained for racemic 2-heptylurea. [47]

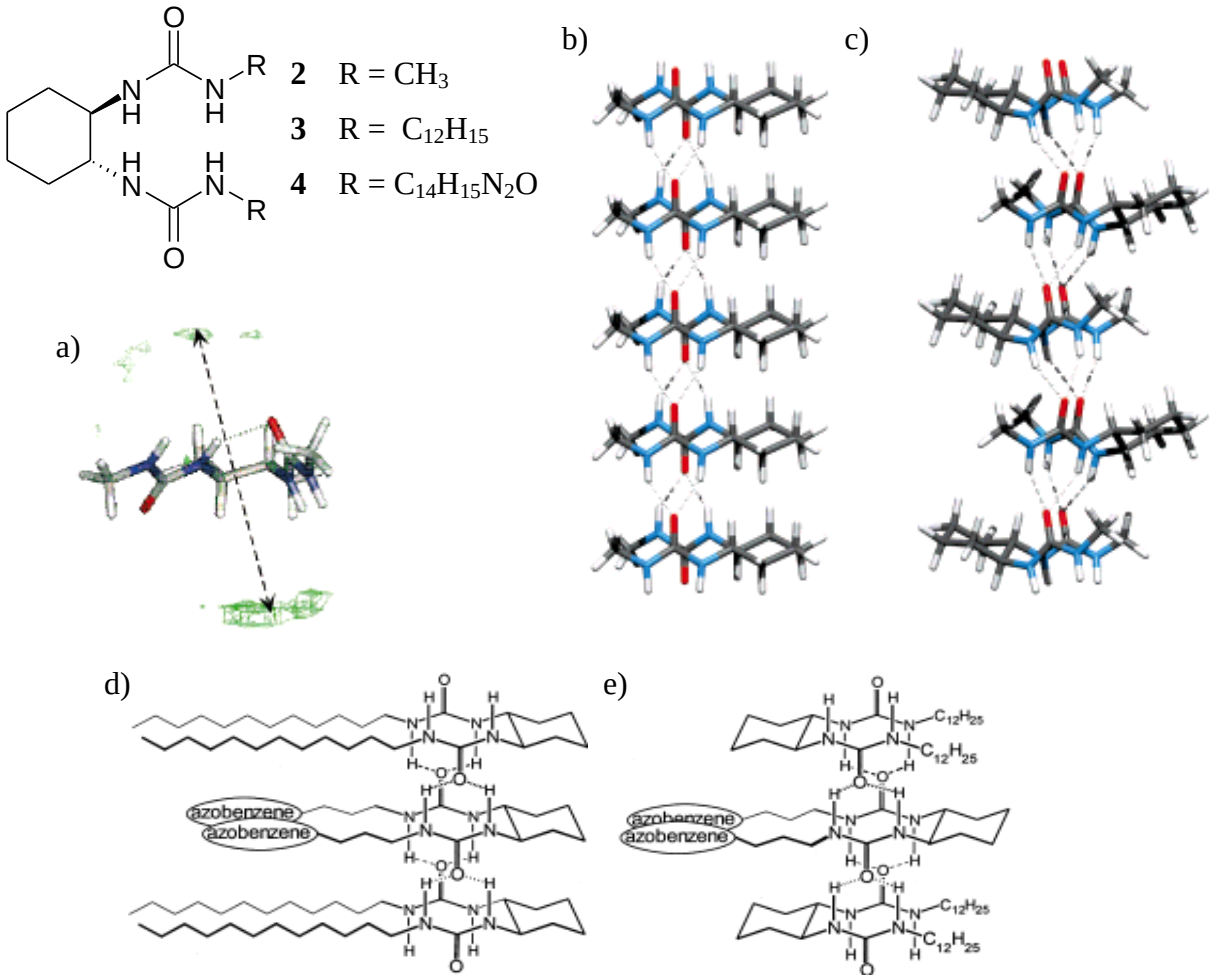

Figure 5 Molecular modelling of compound **2** (R= CH_3) showing a) intramolecular hydrogen bonding in monomer b) anti-parallel and c) parallel hydrogen bonding in stacks.[48] Model for the incorporation of *R,R*-**4** into an aggregate of d) *R,R*-**3** e) *S,S*-**3** showing the distinct environments of the azobenzene groups.

Much of the early work on urea derived gelators was undertaken by Van Esch and co-workers. They developed a series of cyclic bis-ureas including compounds **2**, **3** and **4**. [48-50] Molecular modelling showed compound **2** can potentially adopt either parallel or antiparallel bis-urea chains (Figure 5).[48] On its own an antiparallel arrangement of the monomer is favoured due to an intramolecular hydrogen bond between the urea groups. Parallel and antiparallelstacks are equally favourable and experimental results indicate a number of different phases may be present, potentially within a single gel. A wide range of derivatives based on the same hexane bis-urea structure were synthesised. A study testing the gelation behaviour of derivative **3** in a range of alcohols found that the thermal stability of the gels formed increased with the polarity of the solvent.[49] This is the opposite behaviour to that which is expected if hydrogen-bond formation is the primary driving force for aggregation which indicates that solvophobic interactions from the dodecyl chains is the dominant interaction in the polar solvents tested. 1,2-bis(ureido)cyclohexane derivatives such as compound **3** and the related azobenzene functionalised compound **4** have two stereogenic centres. The *R*,*R*-diasteriomer of compound **4** was found to form a mixed gels with the *R*,*R*- and *S*,*S*-diasteriomers of **3** (Figure 5d and e).[50]

Chiral *S*-phenylethyl end groups were deliberately incorporated into a series of oligomethylene spaced bis-urea gelators developed by Steed and co-workers.[51, 52] For bis-ureas, the two urea tapes may run in the same (parallel) or opposite (antiparallel) direction. In this series, gelation was only observed for even spacer lengths (no. of carbon atoms n = 2-8) where antiparallel bis-urea tapes are formed whilst the parallel urea tapes observed in odd spaced compounds produced only precipitates (Figure 6). The same effect has been observed in a variety of other related systems.[53]

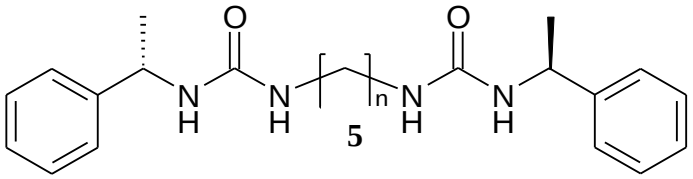

5

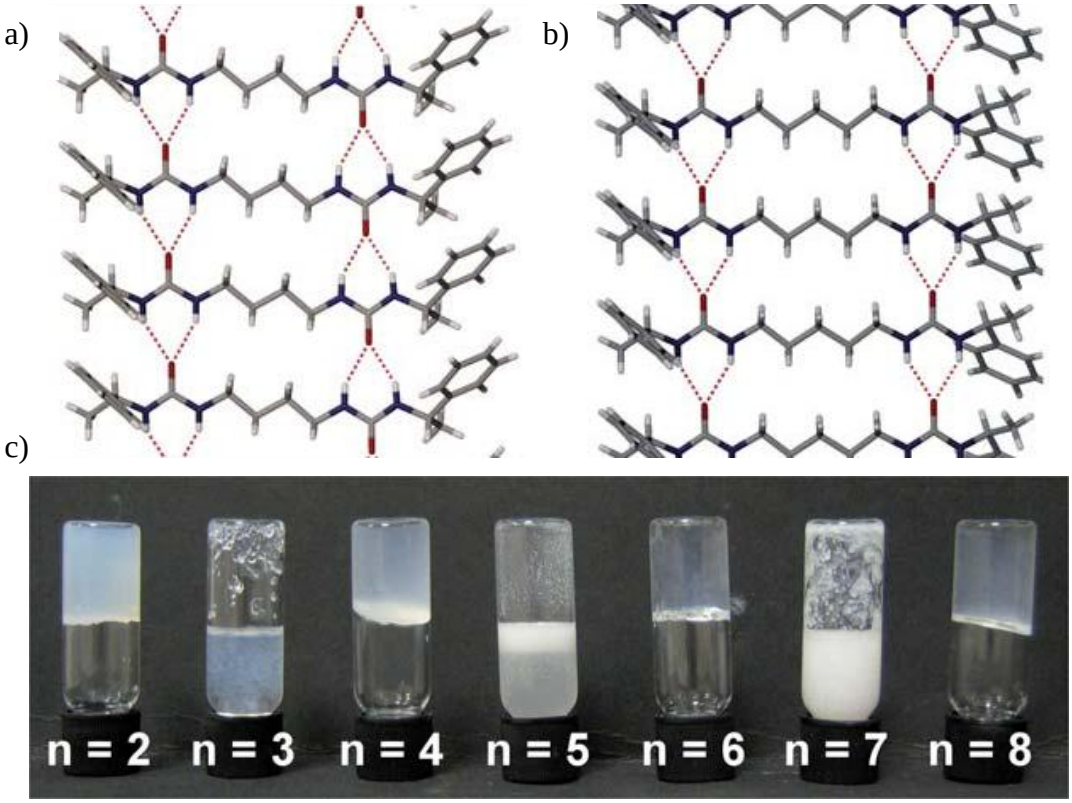

Figure 6 Alternation effect observed in a series of bis-urea gelators **5** (*n*= 2-8) with different lengths of alkane space where *n*= number of alkyl units in spacer (c). Even spacer lengths result in antiparallel bis-urea tapes (a) and give rise to gels whilst odd spacer lengths result in parallel bis-urea tapes (b) and are not associated with gelation.[51]

A number of tripodal ureas have been developed based around a tris(2-aminoethyl)amine core.[54-56] As seen for gelator **6** the urea moiety in one arm undergoes intramolecular hydrogen bonding with the urea in the second arm (Figure 7). The second arm then intermolecularly hydrogen bonds to the third arm of an adjacent molecule and the process is mirrored by the second molecule producing antiparallel urea stacks akin to those seen in bis-urea gelators.[54] Compound **7** is unusual in showing a lamellar, rather than fibrous, morphology (Figure 7c and d). Aggregation into the second dimension is brought about by hydrophobic interactions between the alkyl chains. Aggregation into the third dimension depends upon the solvent from which the gel is crystallised leading to different xerogel morphologies. The wettability of xerogels of **7** was found to depend upon the solvent from which the gel is formed with

contact angles of 80.3° from nBuOH and 146.0° from xylene.[56] A tetra-urea gelator based on a [2.2]paracyclophane-bridged imidazole dimer has also been reported although little structural information is given.[57]

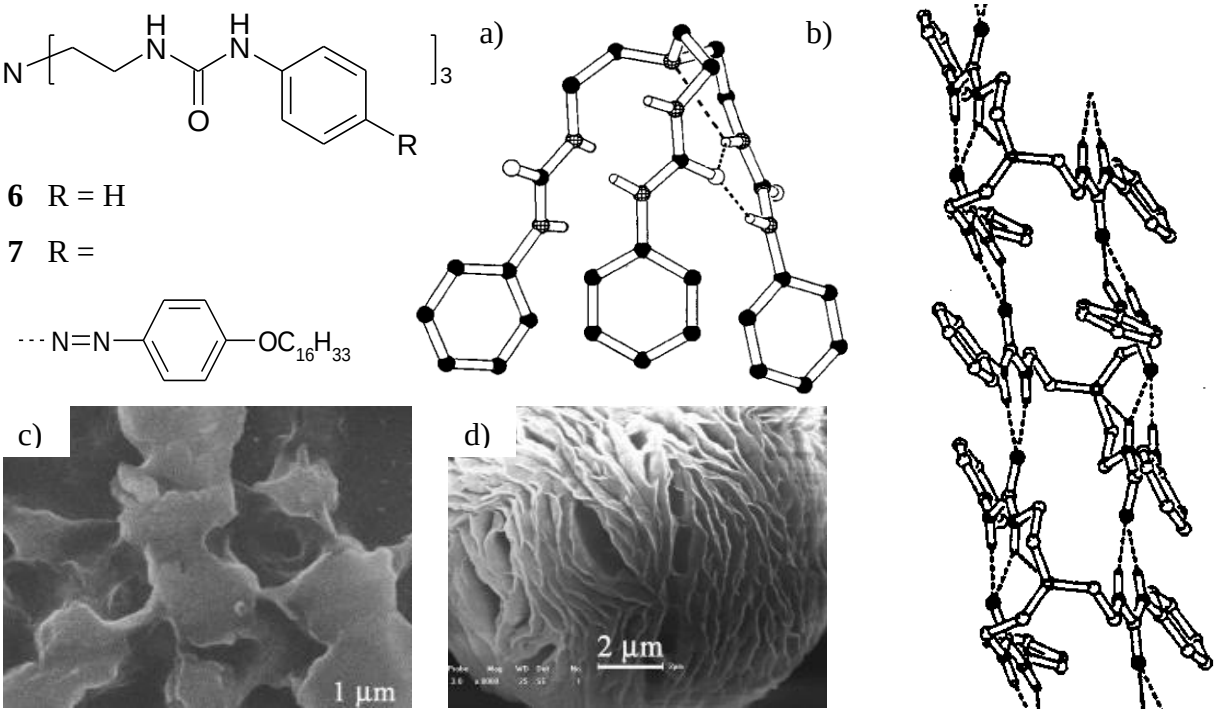

6 R = H

7 R =

Figure 7 X-ray crystallographic structures of **6** showing a) intramolecular hydrogen bonding between urea arms b) formation of antiparallel urea tapes.[54] SEM image of xerogels of **7** showing unusual lamellar structures formed from (c) *n*-BuOH and (d) xylene [56]

The urea carbonyl oxygen atom is not a particularly effective hydrogen bond acceptor and its basicity depends on the electronic and steric properties of the substituents attached to the nitrogen atoms.[38] The presence of electron withdrawing aromatic moieties, such as nitrophenyl groups, results in significant intramolecular CH···O hydrogen bonding making it unavailable for use as a hydrogen bonding acceptor. Interactions with hydrogen bond acceptors present in solvent molecules can result in the formation of inclusion compounds rather than hydrogen bonded polymers (Figure 8a).[58] Recently a series of mono-urea compounds incorporating aromatic rings functionalised with nitro and acid groups have been produced. Many of the gelators, including compounds **8** and **9**, form gels based on a mixture of urea-urea, nitro-urea and carboxylic acid dimerisation and solvent interactions (Figure 8b and c).[59]

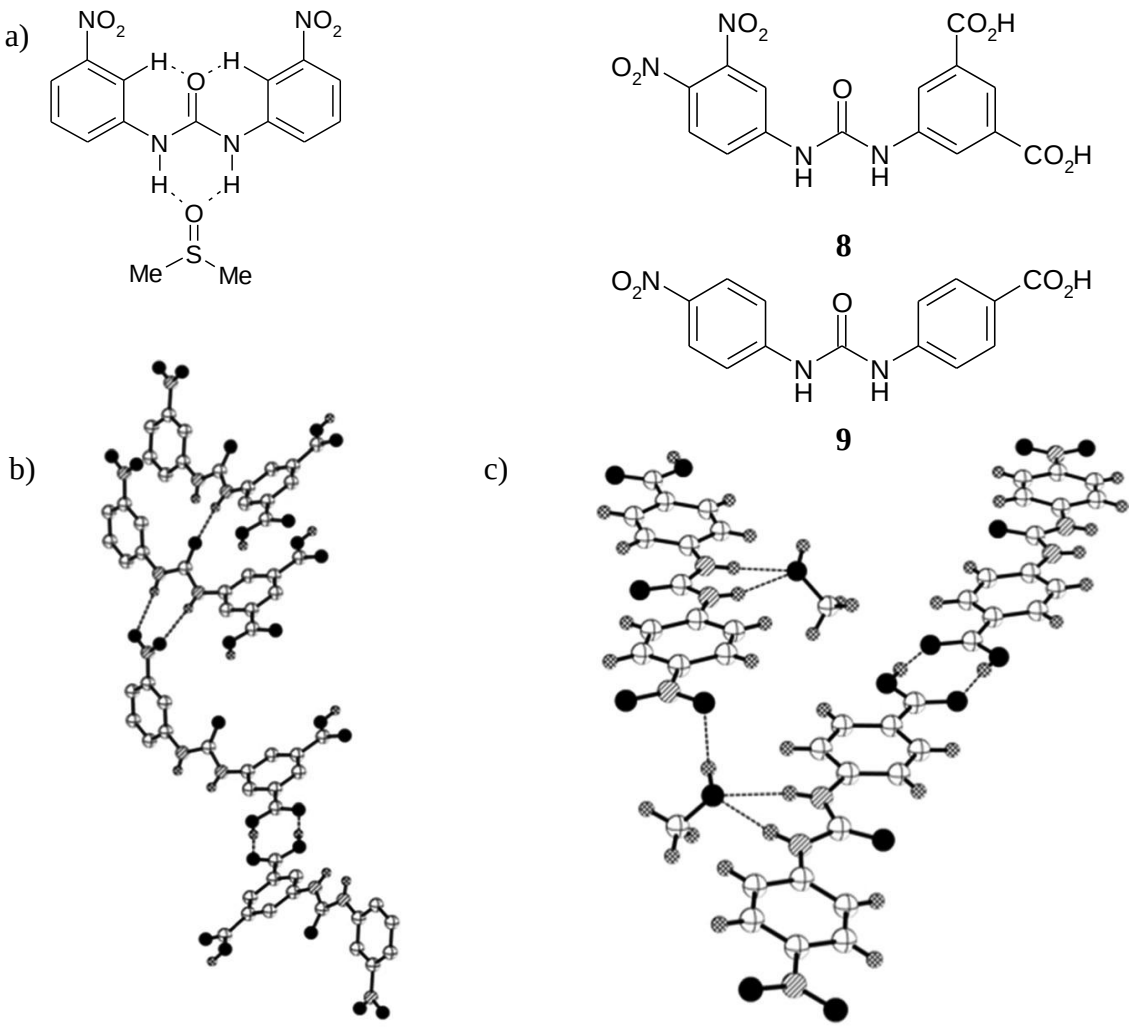

Figure 8 Hydrogen bonding patterns observed in crystal structure including gelators b) **8** and c) **9**.

1.3 Anion tuning of urea derived gelators

Anions have been exploited to disrupt the gelation ability of a variety of bis-urea gelators that form gels based on the α-urea motif.[12, 38, 60-63] Rheological studies undertaken on gels of series **5** show how the addition of increasing equivalents of anion results in a decrease in the elastic storage modulus (*G'*) and yield stress (Figure 9).[51] NMR spectroscopic studies, conducted in acetonitrile above the T_{gel}, showed competing 1:1 binding of the gelator molecules to the anions (K_{11} = 18,000 for **5** *n*= 6 with acetate) versus self association (K_{20} = 6,000 for **5** *n*= 6). Binding was found to be strongest for acetate, followed by chloride then nitrate and was too weak to determine for tetrafluoroborate.

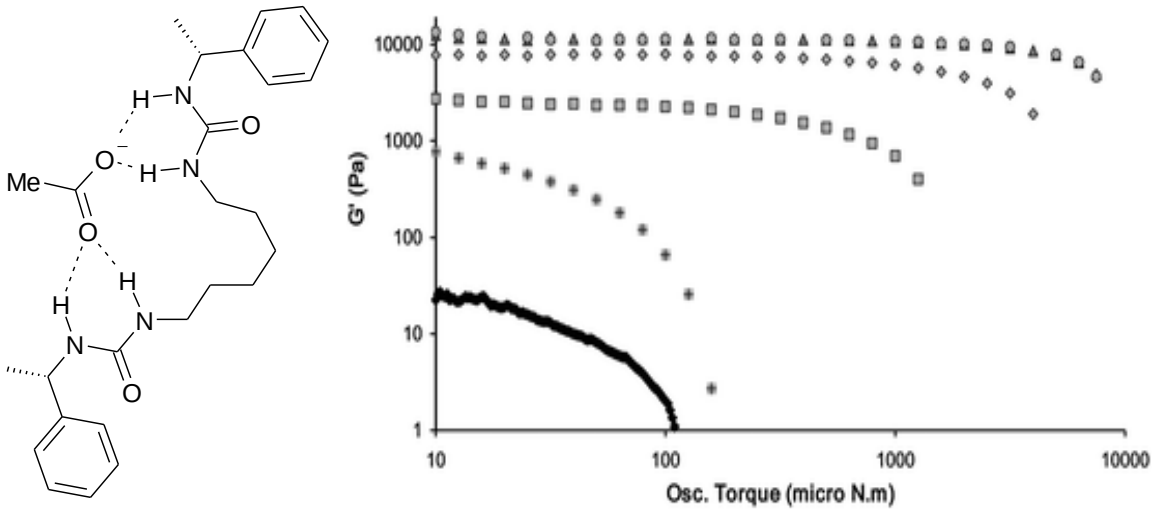

Figure 9 a) Scheme showing binding of **5** *n*= 6 to acetate. b) Graph showing the influence of different anions (0.1 equivalents added as TBA^+ salts) on the storage modulus (*G′*) as a function of oscillatory stress (σ) of the 0.3 % by weight gel of compound **5** *n*= 2 in acetonitrile. The anions added are BF_4^- (△); Br^- (◇); NO_3^- (□); Cl^- (+) and $MeCO_2^-$ (♦) and pure gelator (○).

Insights into this process are gained from tris-urea **10** which forms needle-shaped crystals, rather than gels, in the presence of sodium chloride. The single crystal structure revealed no anion was incorporated into the crystals.[55] The association constant for chloride in DMSO was found to be K_{11} = 1154 and the anion is thought to retard the 1-dimensional growth of gel fibres by reversibly binding to the urea tape. Interestingly the X-ray structure shows **10** forms parallel urea tapes, unlike gelator **6**, and it is thought that the binding of the chloride anions may re-orientate the urea groups. Fluoride ions were found to disrupt the formation of gels of **11**,[64] a process which could be reversed by the addition of trifluoroacetic acid. As well as the disruption of hydrogen bonding, the basicity of fluoride means it may deprotonate the urea group as is observed for a variety of urea derived fluoride sensors.[65, 66]

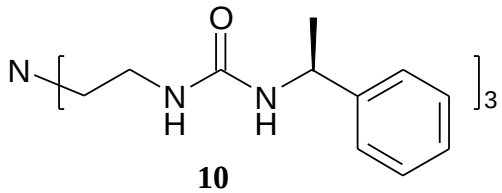

10

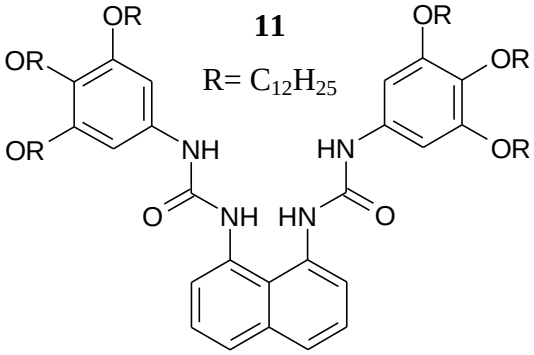

11

R= $C_{12}H_{25}$

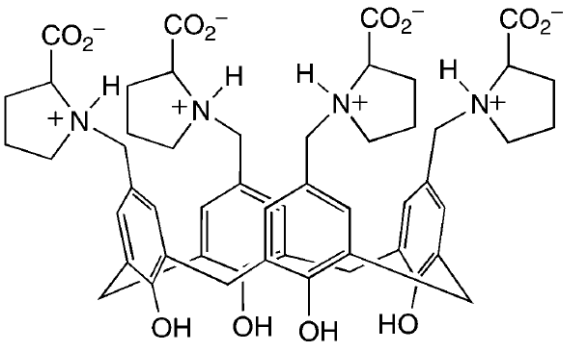

12

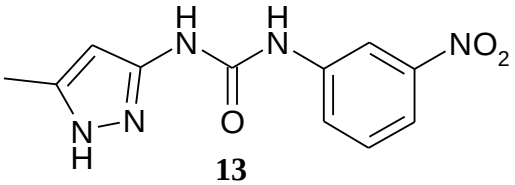

13

The presence of various anions was found to induce gelation in proline functionalised calix[4]arene **12** by Ogden and co-workers.[67] NMR spectroscopy indicated no binding interactions were taking place between the gelator and the anions. The effect of anion was found to correlate well with the Hofmeister series which classifies ions in order of their ability to order water. More hydrated salts (termed kosmotropic) have the effect of strengthening the hydrophobic effect and decreasing the solubility of nonpolar molecules whilst less hydrated salts (termed chaotropic) have the opposite effect. The presence of chaotropic anions, such as nitrate, bromide and chloride induced gel formation whilst **12** remained in solution in the presence of kosmotropic anions such as sulphate.

Pyrazole derived mono-urea based gelator **13** was found to form hydrogels under acidic conditions.[68] The rheology, morphology and structure of the gels formed depends on the identity of the acid used to protonate the gelator. The magnitude of *G′* and yield stress was highest when gels were formed using kosmotropic ions. TEM and SEM imaging revealed chaotropic anions such as BF_4^- and PF_4^- resulted in particulate gels whilst kosmotropic oxyanions such as SO_4^{2-}, HPO_4^{2-}, $EtPO_3^{2-}$ and $MePO_3^{2-}$ produced fibrous morphologies (Figure 9a). Single crystal structural characterisation revealed a number of different highly solvated structures with hydrogen bonding taking place between urea, pyrazole, anion and solvent molecules but no urea tapes (Figure 9c).

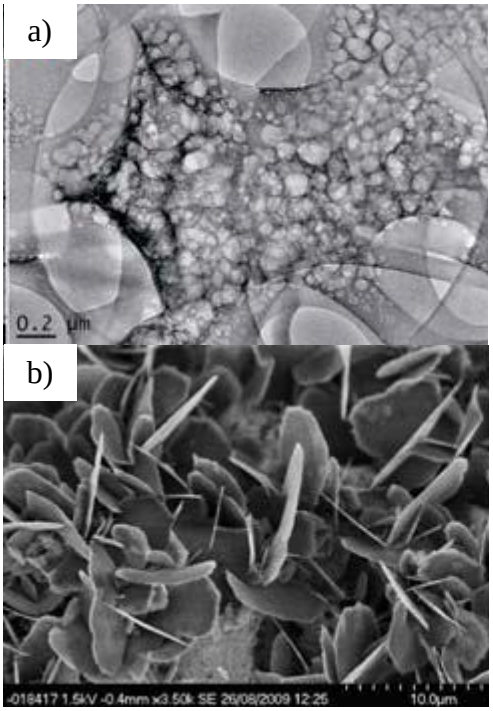

Figure 10 a) TEM image showing of **13** in water acidified with H_2SO_4 b) SEM image showing dried xerogel of **13** acidified with HBF_4 c) molecular structure of BF_4 salt of **13**.

Pyridyl ureas are one class of compound which have been particularly well studied with $NH\cdots N_{pyridyl}$ interactions typically taking place instead of the α-urea motif.[69] These competing motifs were exploited by Steed and co-workers who found that the addition of Ag(I) and Cu(II) salts could be used to dramatically enhance gelation of a number of bis(pyridyl ureas).[18, 19, 70, 71] The metal ions bond preferentially to the pyridyl nitrogen, "turning off" the $NH\cdots N_{pyridyl}$ interactions enabling gel formation through the formation of co-ordination polymers. Mixtures of $CuBr_2$ and **14** in methanol were found not to gel until suddenly shaken at which point a gel rapidly forms. The gel can then be broken down by the addition of TBA-acetate but restored by the addition of further equivalents of copper in the form of $Cu(BF_4)_2$. The mechanism is thought to be linked to the sequestration of the copper(II) ions by the acetate resulting in the formation of a stable complex $[Cu_2(OAc)_4(H_2O)_2]$.[71]

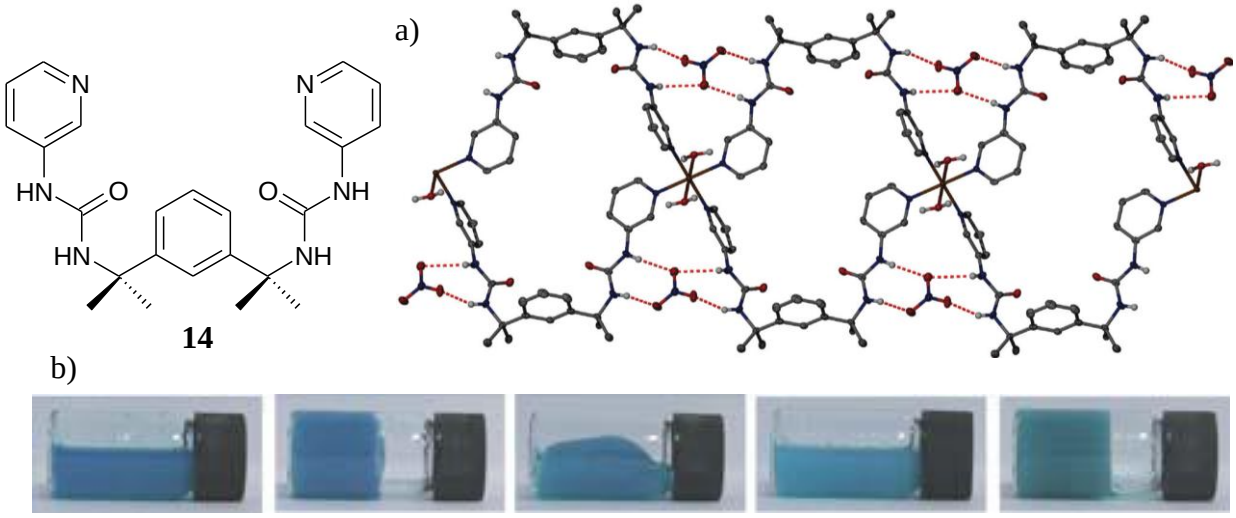

Figure 11 a) Crystal structures obtained for **14** with $Cu(NO_3)_2$ showing metallo polymer $[Cu(\mathbf{14})_2](NO_3)_2.3H_2O.$ 3MeOH of a type potentially responsible for gelation.[19] b) Photo showing mixture of **14** with $CuBr_2$ (0.3 equiv.) in methanol (left to right) before shaking, after shaking, 5 minutes after injection of TBA-acetate, 30 minutes after injection of TBA acetate, and 5 minutes after injection of $Cu(BF_4)_2$ (1 equiv.). [71]

1.4 Applications

Gels have a diverse array of unusual and useful properties which have been exploited in a variety of ways. Until recently, generic polymeric gels have typically been used in bulk applications for use as lubricants and as gelling agents in food and consumer products. However, recent progress in the design and understanding of supramolecular gelators has greatly extended the range of possibilities to include a wide range of high-tech applications.[72, 73]

1.4.1 Responsive materials

Because the network formed by LMWGs is held together by supramolecular interactions, the gel state is inherently reversible and can be turned on and off in response to a variety of stimuli.[74] The majority of LMWGs are thermoreversible, dissolving at high temperatures and re-setting upon cooling, although a more unusual subclass display the opposite behaviour.[75-77] Gels have been designed incorporating functionalities which make them responsive to external stimuli such as pH,[9, 78-80] redox reactions,[81, 82] light[83-85] and ultrasound.[86-88] The presence of specific chemical species such as cations,[12, 19, 71] anions,[60, 78] neutral species[74], or guest molecules[13] can also be used to trigger or disrupt gelation. The transformation of a solution to a gel can lead to an increase in viscosity by a factor of 10^{10} upon gelation.[37] The

ability of gels to elicit such a dramatic change in their properties in response to external stimuli makes them remarkable candidates for use as 'smart' materials.

LMWGs have been used to trap chemical species which are then released in response to a specific chemical stimulus. Incorporating a drug functionality into a gelator which forms a stable gel under physiological conditions but which breaks up in the presence of a particular physiological stimulus (change in pH,[79] salt concentration[89], enzyme[90]) allows for the targeted delivery of a drug to a diseased site. This would reduce the dosage of drug required and so reduce any adverse side effects. The gel matrix can be used to solubilise and transport otherwise hydrophobic drug compounds.[91] A number of pharmaceutically active compounds can be readily modified to form gels with the drug released upon enzyme mediated hydrolysis.[92-94] The opposite approach, whereby a specific enzyme in a bacteria[95] or mammalian cell modifies a soluble small molecule triggering gelation[96] also holds promise as a therapeutic approach.[97]

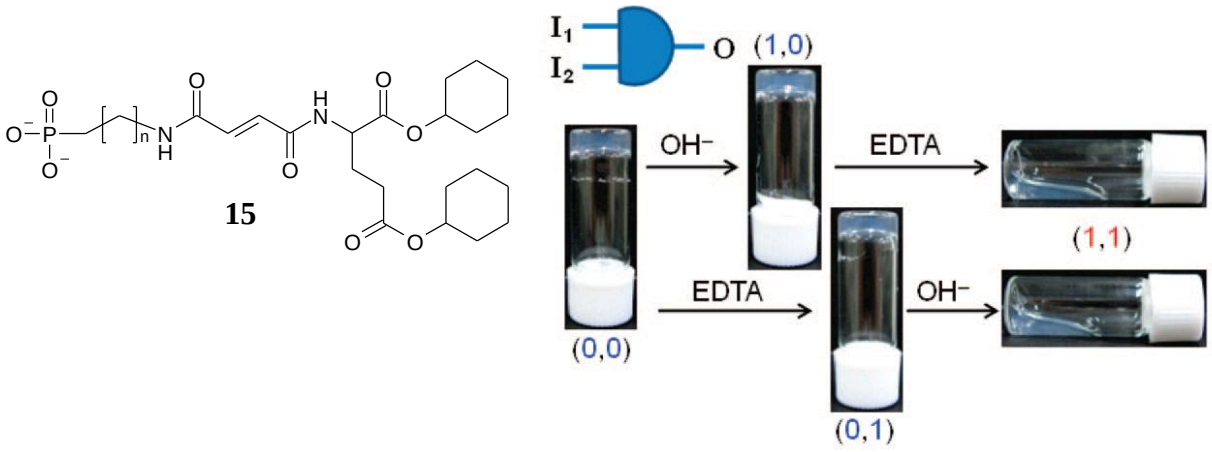

Figure 12 Gels of **15** functioning as an AND gate- with the input of both an increase in pH AND the addition of EDTA (leading to a decrease in calcium ion concentration) in either order required to output dissolution of the gel. [98]

Molecules which respond in different ways to a number of stimuli can act as logic gates. [99] Komatsu *et al.* developed a gelator which is responsive to temperature, pH, calcium ion concentration and irradiation with light; compound **15** in Figure 12. Using different combinations of stimuli they were able to apply AND, OR, NAND and NOR logic operations to control and fine tune the release of substrates from the gel.[98] Photoresponsive hydrogels have also be used as nanolitre reaction vessels with the fusion of gels containing reactants

controlled using light.[100] Rather than undergoing a sol-gel transition, a hydrogel developed by Zhou *et al.* shrank and expanded in response to changes in pH which they showed could be used to control the rate of drug release. [101]

1.4.2 Scaffold material

Hydrogels resemble the extracellular matrix of the body and can provide a scaffold for tissue engineering and matrices for drug delivery.[102] LMWGs offer some advantages in terms of biocompatibility over polymeric systems owing to their supramolecular nature. A number of amphiphilic polypeptide hydrogelators have been used for the *in vitro* culture of liver (progenitor)[103] and collagen producing chondrocytes.[104] Similar gelators have been shown to aid the repair of spinal cord injuries in mice[105] and optical nerve damage in hamsters.[106] The latter gelator was also found to bring about rapid hemostasis in a variety of tissue types, potentially revolutionising the way bleeding is controlled during surgery.[107]

LMWGs can be enhanced with nanoscopic materials in order to take advantage of their unusual properties or to strengthen the gel. Examples include the incorporation of silver nanoparticles,[108] quantum dots,[88] carbon nanotubes (CNTs),[21] buckminsterfullerene (C_{60}),[22] graphene,[20, 109] polymer nanobeads,[110] and up-conversion rare earth nanophosphors (UCNPs)[111] to form composite gels. A particularly impressive example is the mixing of clay nanosheets (CNCs) with a ganadinium functionalised dendrimer which formed self-healing hydrogels capable of forming free standing structures. [23, 112] The hydrogels can be cut and the segments stuck back together to form structures such as the bridge shown in Figure 13.

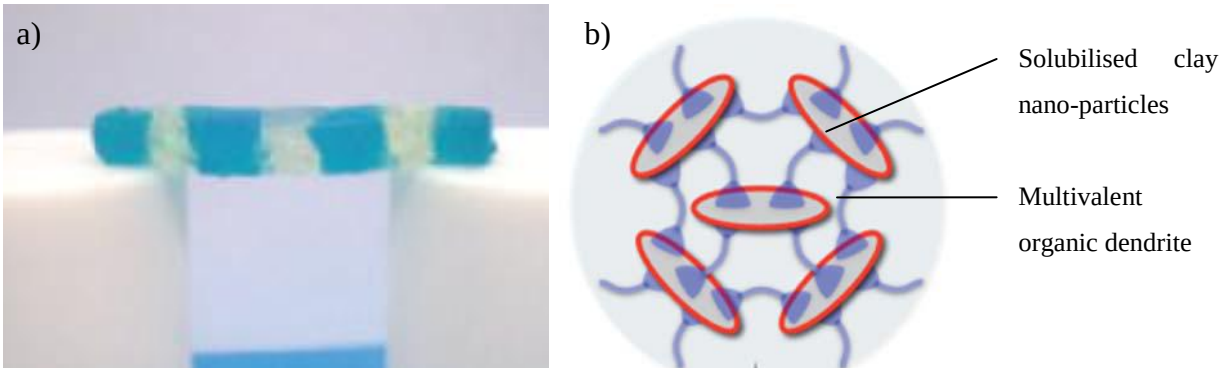

Figure 13 a) A shape-persistant free-standing bridge prepared by fusing together freshly cut blocks of hydrogel (methylene blue was incorporated into alternating blocks). b) Clay nanoparticles solubilised with an anionic surfactant are gelled by a dendritic gelator bearing guanidinium groups.[112]

Polymeric gels are widely used for the separation of compounds owing to their ability to restrict the flow of molecules. The use of LMWGs was used to extend the range of solvents available for electrophoresis to include organic solvents such as acetonitrile.[113] The reversible nature of the gels allows for easy separation of analytes, reactants and products from the matrix and even direct analysis by mass spectrometry. The separation of proteins was achieved using supramolecular gel mimicking the popular SDS-PAGE method.[114] A *n*-hexyl-galactonamide gelator was found to develop a partial charge when a voltage is applied allowing for the separation of neutral compounds by electroosmosis.[115]

Self assembly of a gel scaffold can be used to organise highly conjugated organic molecules for applications such as light harvesting and for use as molecular wires. [116-118] Tetrathiafulvalene (TTF), which is known to conduct in the condensed state, was modified to include an amide hydrogen bonding functionality resulting in the formation of fibrous structures in hexane which gave rise to a gel. A mixed valence state was generated by exposure of the xerogel to iodine vapour producing conductive nanowires.[119] An organic supramolecular light-harvesting antenna was created by encapsulating an energy-accepting molecular wire into an energy donating π-gel scaffold.[6]

1.4.3 Templating

The 'soft' matrix of gels can be 'fixed' in a variety of ways to give permanent, rigid structures. This can be achieved by the positioning of polymerisable functional groups such as on the outside of the gel fibres, such that they can be polymerised to give a permanent covalent structure. [61, 63, 120-123] An alternative approach is to deposit an inorganic material on the inner or outer surface of the gel template to produce an organic-inorganic composite.[124] LMWGs have been used to gel polymer precursors, such as methyl methacrylate, which are then polymerised to give composite materials.[125, 126] These composite materials can have superior physical properties to the pure materials.[127] The supramolecular nature of the gel matrix means it can be removed by washing or chemical treatment of the composite to leave an imprint of the gel structure in the polymer.[128-133]

LMWGs have also been used to template the formation of nanoparticles. Das and co-workers exploited the intrinsic reducing ability of the tryptophan residue for *in situ* synthesis of gold[134] and silver[135] nanoparticles within hydrogels of tryptophan based dipeptide

amphiphiles. Steed found a pyridyl-urea gelator which formed gels in the presence of silver ions, gradually precipitating silver nanoparticles within the gel fibres.[136] The organised structure of supramolecular gels has also been utilised to catalyse a variety of other reactions.[137]

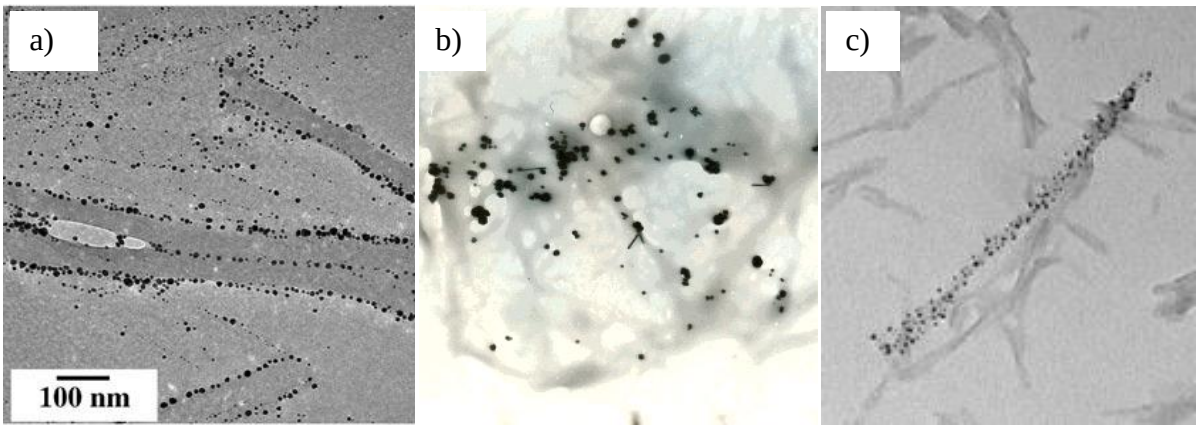

Figure 14 TEM images showing a) gold[138] b) silver[139] and c) silver[140] nanoparticles on gel fibres.

1.5 A medium for crystal growth

1.5.1 Gel Phase Crystal Growth

Crystallisation is enormously important in a variety of natural and commercial processes.[141] Transient fluctuations in a supersaturated solution bring solute molecules together to form molecular clusters or nuclei.[142] A critical nucleus size must be reached before the energy gained from the formation of a crystal lattice is able to offset the increase in surface energy and crystal growth becomes energetically favourable.[143] Nucleation may take place homogeneously between solute molecules in solution or heterogeneously where nucleation is facilitated by small particles or bubbles. Crystallisation proceeds by growth of these critical nuclei until the solution is no longer supersaturated and an equilibrium state is reached. Crystallisation from bulk solution is typically under kinetic control, with metastable polymorphs crystallising first due to a lower energy barrier to nucleation.[144] As the level of supersaturation decreases such crystals become unstable with respect to slower growing but more thermodynamically stable forms which replace them. This process was recognised in 1897 by Ostwald who coined his famous rule of stages.[145]

Polymeric gels have been utilised for over a century for the growth of crystals.[146-150] The gel matrix is often considered to be inert with crystal growth occurring within the macropores between gel fibres. The nature of the gel structure is such that solvent is 'trapped' by gel fibres preventing macroscopic flow of solvent whilst allowing diffusion between pores. This has the effect of suppressing convection currents resulting in continuous, diffusion limited growth of crystal faces. The gel also acts as a soft matrix preventing sedimentation or aggregation of the crystals which can arbitrarily disrupt crystal growth along faces in contact with the vessel walls or other crystals. Heterogeneous nucleation can either be repressed by an inert gel matrix, making homogenous nucleation dominant, or enhanced by an activating gel structure.[150]

A combination of these factors means gels have been utilised for the growth of protein crystals for single crystal structure determination where the size and quality of crystals is particularly important (Figure 15a-b). The lack of sedimentation in gels allows for spatial control of nucleation. This was exploited by Alexander and co-workers who used a laser to induce nucleation in a supersaturated solution of potassium chloride immobilised by an agar gel to spell out the word 'laser' (Figure 15c).[151]

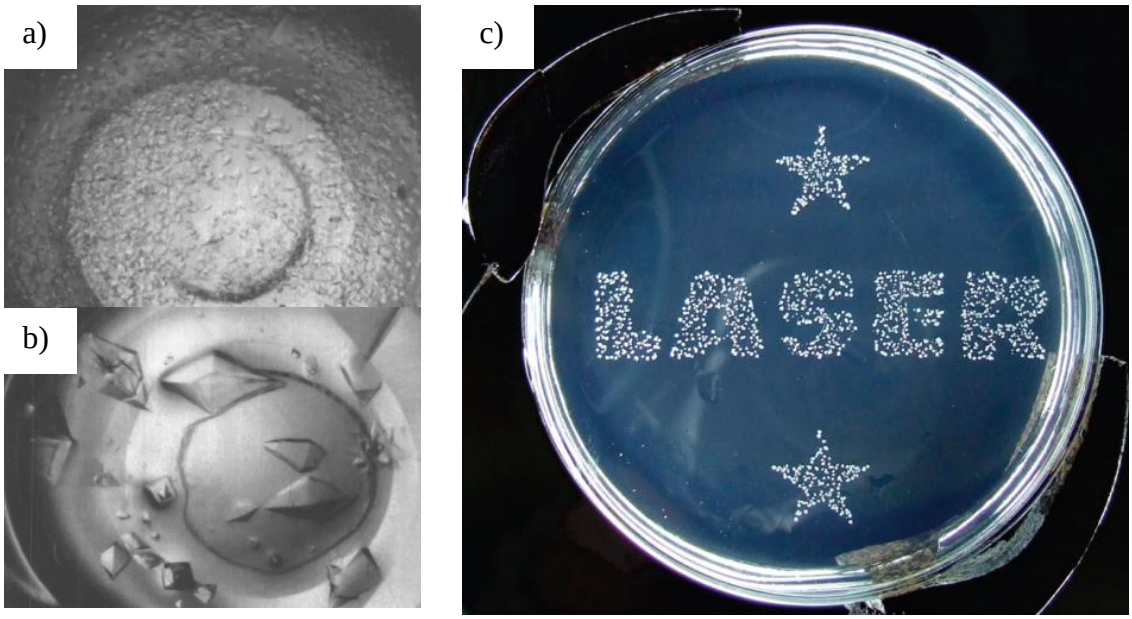

Figure 15 Crystallisation of the protein thaumatin from a) solution and b) silica gel.[152] c) Laser induced nucleation of KCl in agarose gel.

The gel environment has been shown to influence a number of other aspects of crystal growth such as the polymorphism, habit and enantiomorphism of crystals grown from gels. Considerable recent work has been done to try and understand the mechanisms by which gels influence crystallisation in order to gain greater control over the crystallisation process.

1.5.2 Influencing Polymorphism

Figure 16: Growth of modafinil in TMS/methanol/water gels of varying ratios.[153]

A lack of heterogeneous nucleation in gels can lead to higher degrees of supersaturation resulting in conditions far from equilibrium. This potentially allows the formation of single crystals of unstable polymorphs which form outside thermodynamic equilibrium conditions as precipitates using conventional solution based techniques. (±)-2-((diphenylmethyl)sulfinyl)-N-acetamide, marketed as (±)-modafinil, is one such compound. Solution crystallisations close to thermodynamic equilibrium yield stable racemic form I as single crystals whilst metastable racemic form III can only be formed as a powder far from equilibrium (precipitation). Morgan Pauchet *et al.* were able to crystallise form III from a tetramethoxysilane (TMOS) methanol/water gel. By varying the solvent ratio of methanol:water they were able to control the level of supersaturation within the gel (Figure 16). Crystals grown with a 2/7/7 ratio of TMOS/water/methanol were found to give mainly form III alongside some single and twinned crystals of form I. They note that the size and connectivity of the pores, and so the degree of supersaturation, vary within a single gel which may explain the co-existence of different forms. Perhaps of crystallographic interest, the 'stacking fault' which gave rise to the form I twin is repeated periodically to produce form III. The similarity between the structures further explains their concomitant crystallisation.

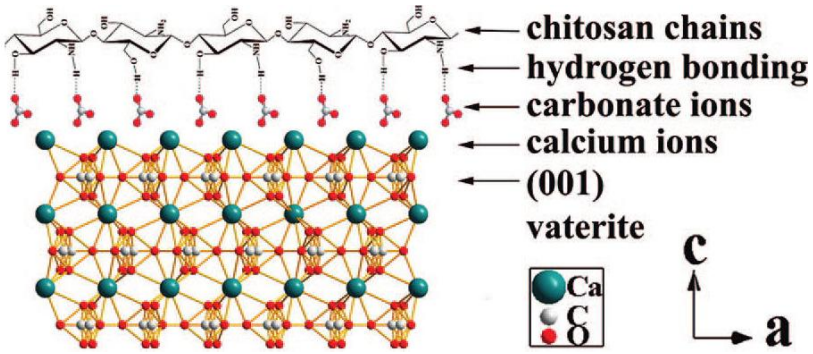

Figure 17: Scheme showing proposed influence of chitosan chains on packing of calcium carbonate ions[154]

Conversely, heterogeneous nucleation may occur on gel fibres with different crystal forms being templated compared to solution. Xiao *et al*.[154] have investigated the effect of chitosan, a linear polysaccharide able to form hydrogels at pH >6, on the crystallisation of calcium carbonate. In the sol, nanoparticles of the thermodynamically favourable calcite form were found with crystal growth thought to be inhibited by surface binding of the polycationic chitosan chains. In the gel phase however, hexagonal plates of the less stable vaterite form were produced. The authors attribute this to heterogeneous nucleation of the $CaCO_3$ on the gel fibres which then stabilise the normally soluble vaterite form. They suggest that the $–NH_2$ and –OH groups on the chitosan chain form strong hydrogen bonds with the carbonate anions which in turn attract calcium cations. This generates a local supersaturated microenvironment at the chitosan gel interface which resembles the alternating layers of ions found in vaterite. This arrangement also stereochemically matches, and so stabilises, the high energy (001) face of vaterite such that it becomes the dominant product.

The crystallisation of model pharmaceutical compounds carbamazepine and ROY were undertaken from cubic polyethylene glycol diacrylate (PEGDA) microgels with different mesh sizes.[155] A number of differences were noted between the polymorphism of the compounds crystallised from solution and microgels with different mesh sizes. The differences are rationalised in Figure 18 which illustrates how at small mesh sizes polymer-solute interactions dominate hindering the solute-solute interactions essential for nucleation. When the mesh size is too large, the nucleation-templating effect of the polymer is less significant. At an intermediate mesh size polymer-aided solute-solute interactions were optimised to bring about nucleation. Optimum mesh sizes were found to enhance selectivity

for the R form of ROY by twenty times and for the nucleation of form II of carbamazepine in the absence of form I as observed in solution.

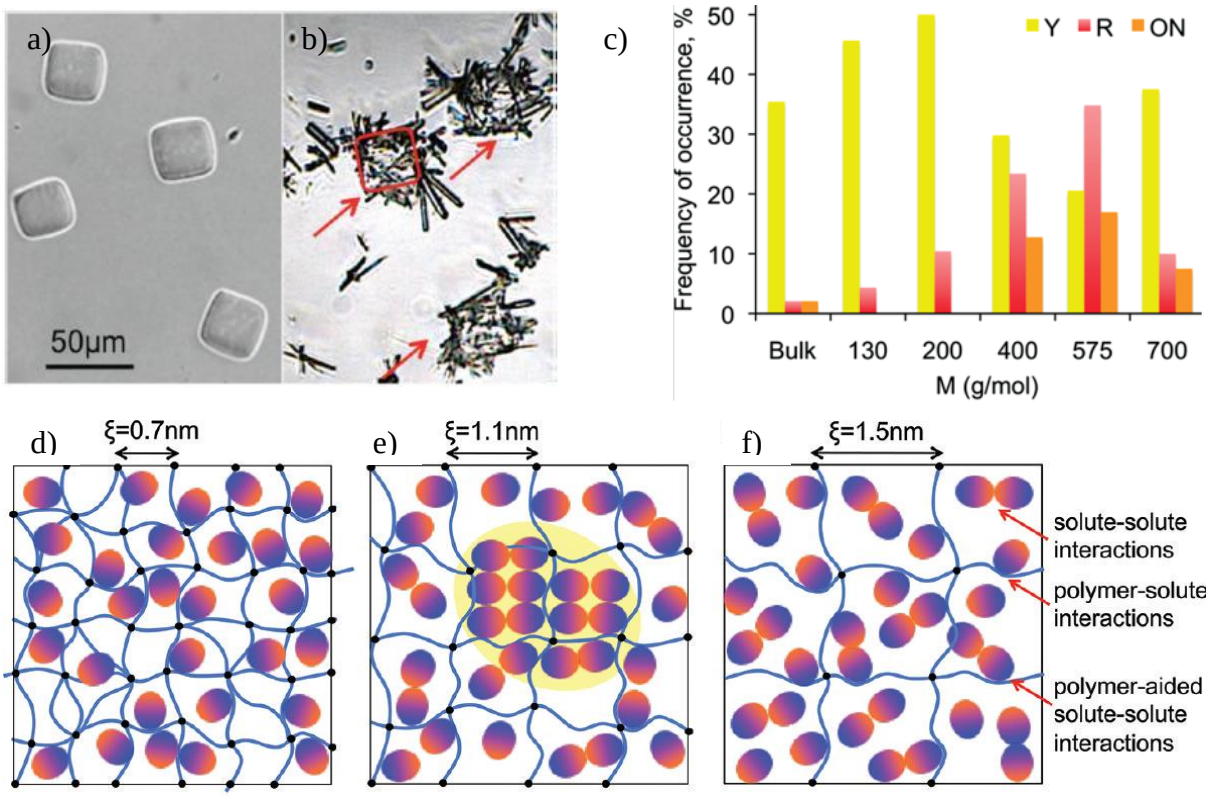

Figure 18 Optical micrographs showing a) cubic PEG microgels b) carbamazepine crystallising in the microgels (shown in red), c) graph showing occurance of different polymorphs of ROY grown from gels with different molecular weights of PEG, (d-f) schematic illustrating the effect of mesh size on nucleation. At small mesh sizes (d) polymer-solute interactions dominate inhibiting solute-solute interactions, at larger mesh sizes (f) solute-solute interactions dominate, at intermediate sizes (e) polymer-solute interactions and spatial confinement jointly facilitate solute-solute interactions creating optimum conditions for nucleation (highlighted by yellow background).

In an interesting adaptation of the gel phase method, Leng *et al.* further slowed down the rate of crystallisation by using alginate, an anionic polysaccharide which forms a metallo-gel in the presence of calcium ions. [156] Diffusion of gaseous carbon dioxide into these gels results in the slow release of calcium ions and crystallisation of calcium carbonate. The mineral is crystallised as micron-sized lens like particles composed of fused nanoparticles of vaterite, stabilised for long periods of time by the alginate.

1.5.3 Influencing Crystal Habit

A comparison of the effect on the habit of asparagine crystals by crystallisation from various polymeric hydrogels was made by Swift and co-workers.[157] Asparagine crystallises from aqueous solutions as a monohydrate with a prismatic morphology determined by up to eighteen different faces. The effects of the different gelators on crystal habit are shown in the table in Figure 19. The dominance of the {012} face in crystals grown from agarose gels was interpreted in terms of hydrogen bonding interactions between the agarose side chains and the crystal surface. The fact that this morphology is dominant for both aqueous and binary water/DMSO mixtures in the presence of agarose, solvent systems that give very different morphologies in solution phase crystallisations, indicates a dominance of gelator effects. Further evidence of the importance of the gel phase was demonstrated by the addition of D-galactose, a monomeric unit of the agarose polymer, which at comparable concentrations showed no modification of the crystal habit. The dominance of {101} faces in crystals from *i*-carrageenan gels was thought to be due to presence of sulphate groups, a hypothesis which appears substantiated by solution growth experiments in the presence of sulphate ions. The complex functionality of gelatin polymers makes such functional group analysis difficult, indeed it was suggested that the size and poor definition of the crystals may be due to the diverse functionalities interacting with different faces.

Media	Morphology	Major face	Minor faces
Aqueous solution		{012}	{101}, {111} {011}, {010}
Agarose (aqueous or binary H_2O / DMSO mixtures)		{012}	{101}
ι-Carrageenan		{101}	{012}
κ-Carrageenan	Ill-defined habits	{012}	?
Gelatin	Dendrites Clusters of tiny crystals	?	?
DMSO/Water		{010}	{101}, {012}
NaCl Na_2SO_4 K_2SO_4		{101} or {001}	{012}, {111}

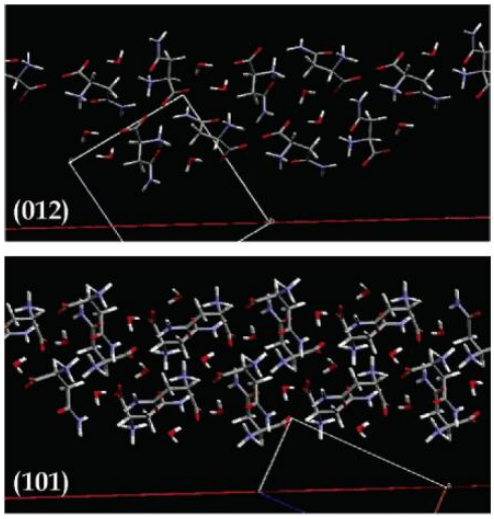

Figure 19: Effect of gel media on crystal morphology and corresponding molecular packing of key faces.[157]

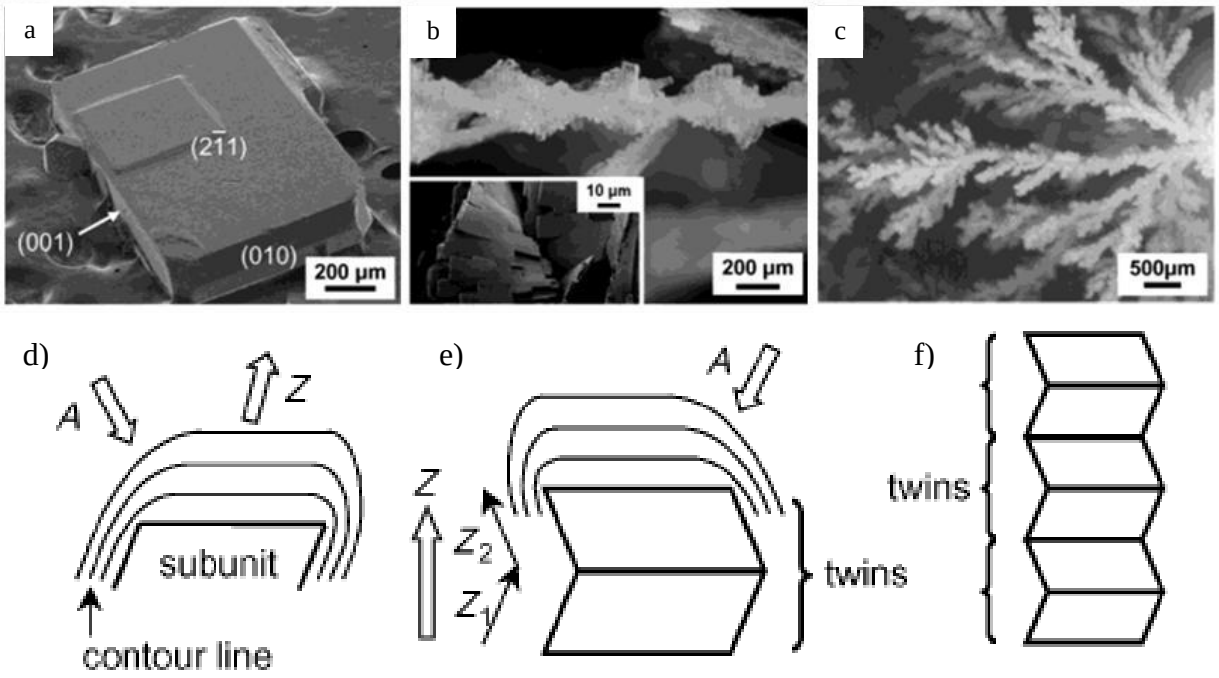

Figure 20 SEM images of $K_2Cr_2O_7$ crystals grown at increasing gel densities a) 5 g/100 ml, b) 25 g/100 ml and c) 35 g/100 ml of gelatin. d) Growth of the crystal occurs fastest asymmetrically along the z direction. However, under the diffusion limited conditions present at high gelator concentration, depletion of material from the surrounding gel means growth of a twin in the direction of the higher concentration gradient, A, becomes favourable. e) Growth therefore occurs along a new direction, Z_2, until the process is reversed leading to the formation of alternating stacks of twinned crystals.

The crystallisation of a range of inorganic salts was undertaken by Oaki and Imai from a range of aqueous gels in order to investigate the effect of gel density on crystal morphology.[158] They observed that as the gel density increased, the morphology of the crystals changed from polyhedral single crystals exhibiting specific habits into dendritic forms consisting of irregularly branched polycrystalline aggregates (Figure 20). This was observed regardless of the type of inorganic compounds or gelling agents. The formation of dendrites was ascribed to instability of the growing surface under the diffusion limited conditions formed in the viscous gel media. It was also speculated that increasing the density of the gel media increases the random noise for crystal growth because the polymer backbone of gel matrixes disturbs the progress of the growing surface. Helical twisting was observed for potassium chromate grown from gelatin (Figure 20b) which was attributed to 'twisted twins'. [159] Figure 20d shows how asymmetric crystal growth occurring along the Z direction depletes the surrounding gel material. Eventually, under the diffusion limited conditions, growth of the twin crystal becomes favourable leading to growth in a second direction Z_2 and

so the formation of twisted stacks of twin crystals. In an extension of this work Oaki and co-workers found that the handedness of the helices, consisting of achiral crystals, could be controlled by the addition of *d*- and *l*- glutamic acids under the diffusion limited conditions of the gel.[160]

In a study by Estroff and co-workers, hydrogels have been coupled with self assembled monolayers to control the crystallisation of calcium carbonate.[161] The ordered surface of the carboxylate terminated self assembled monolayer (SAM) regulates the orientation of the crystals and favours selection of the calcite form. The gel changes the growth kinetics, and thus the morphology of the calcite crystals, resulting in a decrease in the aspect ratio with increasing gel concentration. Etching of gels grown inside the gels indicated incorporation of the gel fibres into the single crystals. The incorporation of gel fibres into crystals has been observed in a number of other systems and can be used to produce composite materials with enhanced physical properties.[127, 162, 163]

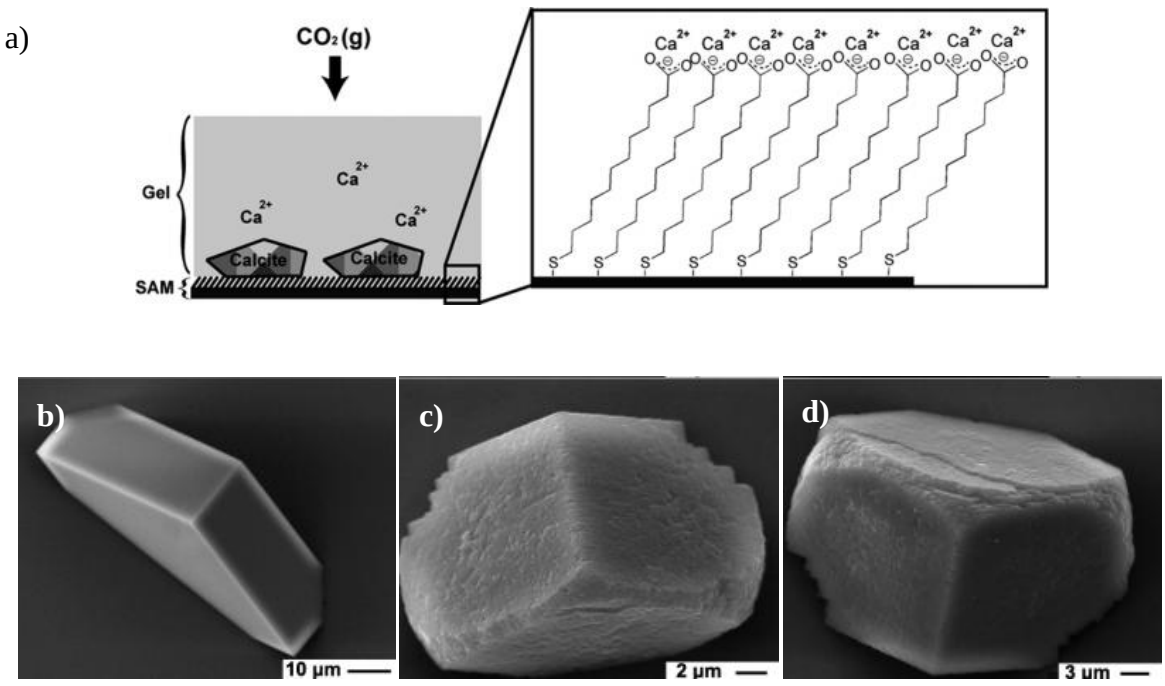

Figure 21 a) Scheme showing crystal growth in gels. SEM images of calcite crystals grown on carboxylateterminated SAMs in (b) solution (c) 1 % w/v agarose gel (d) 2 % w/v agarose gel.

1.5.4 Influencing Enantiomorphism

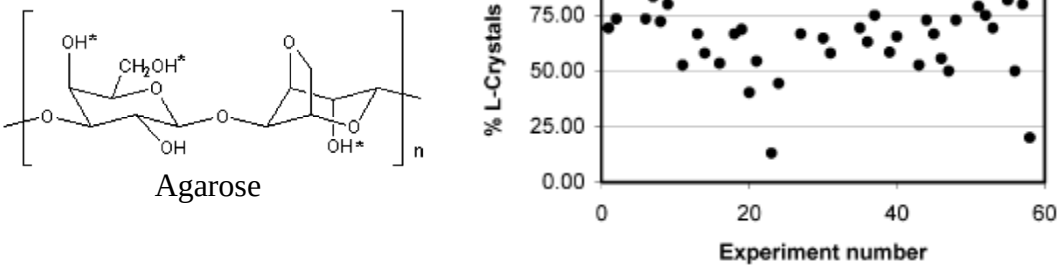

Figure 22: Scattergram showing the percentage *l*-crystals grown by the diffusion of methanol at 24ºC into a gel of 0.75 wt% agarose.[164]

Another interesting feature of crystal morphology over which gels have been shown to exert some influence is the enantiomorph of molecules which crystallise in a chiral space group. $NaClO_3$ is an achiral molecule in solution which crystallises in space group $P2_13$ leading to equienergetic *d*- and *l*- crystal forms. Although individual crystallisations often deviate from the expected ratio, repeated crystallisations under the same conditions tend towards a 50:50 mixture of the two enantiomorphs. Swift and co-workers[164] carried out a large number of crystallisations of $NaClO_3$ from varying concentrations of agarose in water, at different temperatures and with the addition of methanol. They noted that with higher concentrations of gelator the crystals became distorted from their normally cubic morphology and fewer crystals formed. Most interestingly, they found statistically significant enantiomeric excesses (*ee*) of the *d*- or *l*-enantiomorph under different conditions. At low temperatures (6ºC) and high concentrations of agarose (0.75wt%) they found a bias towards *d*-$NaClO_3$ of up to *ee* = 22%. Surprisingly, they found that adding methanol resulted in a bias as high as *ee* = 53% (24ºC, methanol added after 45 days) in favour of *l*-$NaClO_3$. The reasons for these differences are poorly understood but explanations are offered in terms of the structure of agarose which has been shown to adopt a variety of left handed, single and double helices.

1.5.5 Supramolecular gels as a medium for crystal growth

The examples given in sections 1.5.1-1.5.4 refer to crystallisation from polymeric gelators. Despite a number of allusions to the concept,[165-167] the potential of LMWGs as a medium for crystal growth remains largely unexplored with the exception of some elegant work on the use of LMWGs for the growth of calcium carbonate[168] and other inorganic minerals[169] as part

of biomineralisation studies. Related work includes the templation of inorganic-organic hybrid materials and nanoparticles as discussed in section 1.4.3.

The control of crystallisation is commercially important to a wide range of industries including the cosmetic, food and paint sectors. In particular, the control of polymorphism and crystal habit is important in the pharmaceutical industry owing to biological, manufacturing and legal implications. Compared with simple inorganic compounds in which there is little difference between the faces of their crystals, more complex pharmaceutical compounds often crystallise in structures with very different functionalities along different faces. This could potentially allow gels to exert much more profound changes in the habit and packing of growing crystals.

Supramolecular gels offer a number of inherent advantages as a medium for crystallisation over their polymeric counterparts.[170] The reversible nature of the gels allows for easy recovery of crystals from the viscous gel matrix. The addition of a suitable chemical or physical stimulus can be used to break down the gel liberating the crystals to be collected using conventional solution based techniques such as filtration. The diverse array of chemical species which have been found to form gels provides a ready library of gelators which can be matched to the compound being crystallised.[24, 25] In addition to forming hydrogels, a wide variety of LMWGs can form organogels, greatly extending the range of crystallisation conditions than can be generated. This is particularly important for pharmaceutical compounds, many of which are poorly soluble in aqueous solvents. LMWGs are generally readily synthesised and can be inexpensive and biologically compatible making them commercially attractive. The supramolecular nature of the gel fibres may mean that unlike polymeric gels they do not become incorporated into the growing crystals. It is also possible that supramolecular gels will provide a qualitatively different environment for crystal growth which proves to exert novel effects not observed in polymeric systems.

1.6 Conclusion

Low molecular weight gels provide a fascinating example of supramolecular self-assembly and posess a number of unusual properties which present opportunities for use in a variety of high-tech applications. LMWGs are complex, hierarchical materials which require analysis at a range of dimensions using a variety of techniques. Hydrogen bonding interactions between

urea moieties provide the one-dimensional aggregation required to bring about gel formation and a diverse array of urea derived gelators have been developed. Disruption of these hydrogen bonding patterns by the addition of anions provides a mechanism for tuning the gels' rheology. The responsive and reversible nature of supramolecular gels, their unusual combination of liquid and solid-like properties and the ordered gel matrix mean they have found uses in a wide variety of applications. Polymeric gels have been used extensively to influence the morphology and form of crystals, predominantly inorganic compounds crystallised from aqueous media. Supramolecular gels offer a number of potential advantages as a medium for crystal growth, particularly of pharmaceutical compounds.

1.7 Project aims and overview

The aim of this thesis is to create novel urea derived low molecular weight gelators, investigate their structure and properties and develop them for use in a variety of applications, particularly as a medium for crystal growth. In the first three chapters a series of amino acid derived bis-urea compounds are developed. Chapter 2 seeks to establish the relationships between the structure and gelation behaviour of compounds in the series. X-ray crystallography, X-ray powder diffraction, infrared spectroscopy, electron microscopy and rheometry are used to probe different levels of the gel structure. The different gelators are then mixed together in order to further investigate the relationship between the different gelators. The series of gelators is expanded in Chapter 3 to include structurally related pyrenylalanine derivatives with the aim of utilising their fluorescent properties to further investigate gelation behaviour in the series. Anions are introduced in order to disrupt gelation and the process is monitored in solution by NMR spectroscopy and in the gel phase at the macroscopic level by rheology and on a molecular level using fluorescence spectroscopy. In Chapter 4 the different nano-scopic morphologies of gelators in the series are exploited to produce meso-porous polymers with different pore shapes. Electron microscopy and gas adsorption measurements are utilised to characterise and compare the resulting materials.

The second half of the thesis develops the novel application of low molecular weight gelators as a crystallisation medium for pharmaceutical compounds. The basic methodology and proof of principle for the viability of LMWGs as a medium for crystal growth is developed in Chapter 5. The use of anions as a means of recovering crystals grown in low molecular weight gels is also investigated. In Chapter 6 a crystal engineering approach is taken to

designing supramolecular gelators which incorporate functionalities mimicking those of the compound under investigation. The influence of such a ‘designer’ gelator on polymorphism is compared with generic gelators and forms obtained from solution. A collaboration with GlaxoSmithKline sought to apply the use of LMWGs as part of an industrial polymorph screening procedure, the results of which are detailed in Chapter 7. The focus is on developing a generic methodology which can be incorporated into existing screening procedures.

Chapter 2: Gelation-structure relationships in a series of amino acid derived bis-urea gelators

2.1 An arrested crystallisation

The gel state is characterised by solid-like flow properties in a material which is largely liquid in composition. Gel formation can be brought about in a number of distinct ways and four different classes of gel have been distinguished: lamellar structures, disordered covalent polymeric networks, polymeric networks formed through physical aggregation and particulate, disordered structures.[1] Many low molecular weight gelators (LMWGs) fall into this final class of gelators.[19] Gelation in these systems can be thought of as an arrested crystallisation where crystal growth occurs predominantly in one direction resulting in the formation of fibrous aggregates.[24] As with other small molecules they have the potential to pack together in a variety of ways leading to different polymorphs, some of which form gels and others which do not.[17, 30-33]

Bis-ureas are one of a number of well-established motifs which frequently aggregate in the highly anisotropic morphologies necessary for gel formation.[38] However, fibre formation in itself is insufficient to bring about gelation and physical entanglement of fibres must occur to create a three dimensional sample-spanning network capable of trapping solvent through surface tension. Subtle differences in gelator structure, solvent properties and the conditions under which the gel is formed can all play an important role in determining gel formation.

In this chapter we present a systematic study investigating the effects of different substituent groups on the solid state and gel phase behaviour of a series of amino-acid derived bis-urea gelators. Evidence for a variety of different structural motifs is gathered from electron microscopy, crystallographic and solid state analytical data. X-ray single crystal and powder diffraction (XRPD), infrared spectroscopy (IR), differential scanning calorimetry (DSC), scanning electron microscopy (SEM), rheometry and bench top observations are all brought together in order to understand the complex behaviour of this series of gelators and the gels they form.

2.2 Design and Synthesis

Building on previous work within the Steed group[38, 51, 52, 61, 171] and others,[46, 47, 167, 172] a number of design features were deliberately incorporated into the gelators' chemical structure to aid gel formation. Ureas are readily synthesised through the nucleophilic addition of an amine to an isocyanate in good yield. Amino acids are a readily available and cost efficient source of amines which are of particular interest due to their biological importance. The substituent groups (*R*) of the amino acids provide a varied, but well defined, range of functionalities which can be systematically altered in order to study their effect on gel formation.[8, 11, 173] Amino acids also provide a well resolved source of chirality which can frustrate crystallisation by limiting the choice of space groups to Sohnke groups potentially aiding gelation.[8, 47, 51, 174, 175] Methyl ester protected amino acid derivatives were used in order to prevent strong competing hydrogen bonding interactions from the carboxylic acid groups. The length of the oligomethylene spacer (where *n* = number of methylene units) can also be important in bis-urea gelators with compounds possessing an even number of methylene units forming stronger gels due to the anti-parallel arrangement of the bis-urea tapes that they form.[51]

A series of bis-urea compounds were synthesised by the reaction of di-isocyanato alkanes of varying length with two equivalents of the methyl-ester protected *l*-amino-acid to give the corresponding bis-urea, compounds **16**-**31 (**Scheme 1). Full synthetic details are provided in the experimental section. In general, the amino acid methyl ester hydrochloride salt is stirred in chloroform and a slight excess of triethylamine added. The solubility of the mixture depends on the amino acid being used with some compounds dissolving readily at room temperature and others requiring heating, sonication and a greater excess of triethylamine. Small amounts of undissolved material were not found to be problematic and generally dissolved upon the addition of the isocyanate. The isocyanate was dissolved in chloroform and added dropwise to the stirred solution and the mixture was heated under reflux overnight. Individual reactions were never optimised but the initial conditions of heating under reflux for 18 hours proved excessive and shorter reaction times were used for cases where the gelator precipitated from solution upon addition of the isocyanate.

Scheme 1 A series of bis-urea gelators functionalised with different methyl ester protected amino acids and number of methylene units (*n*) in the spacer.

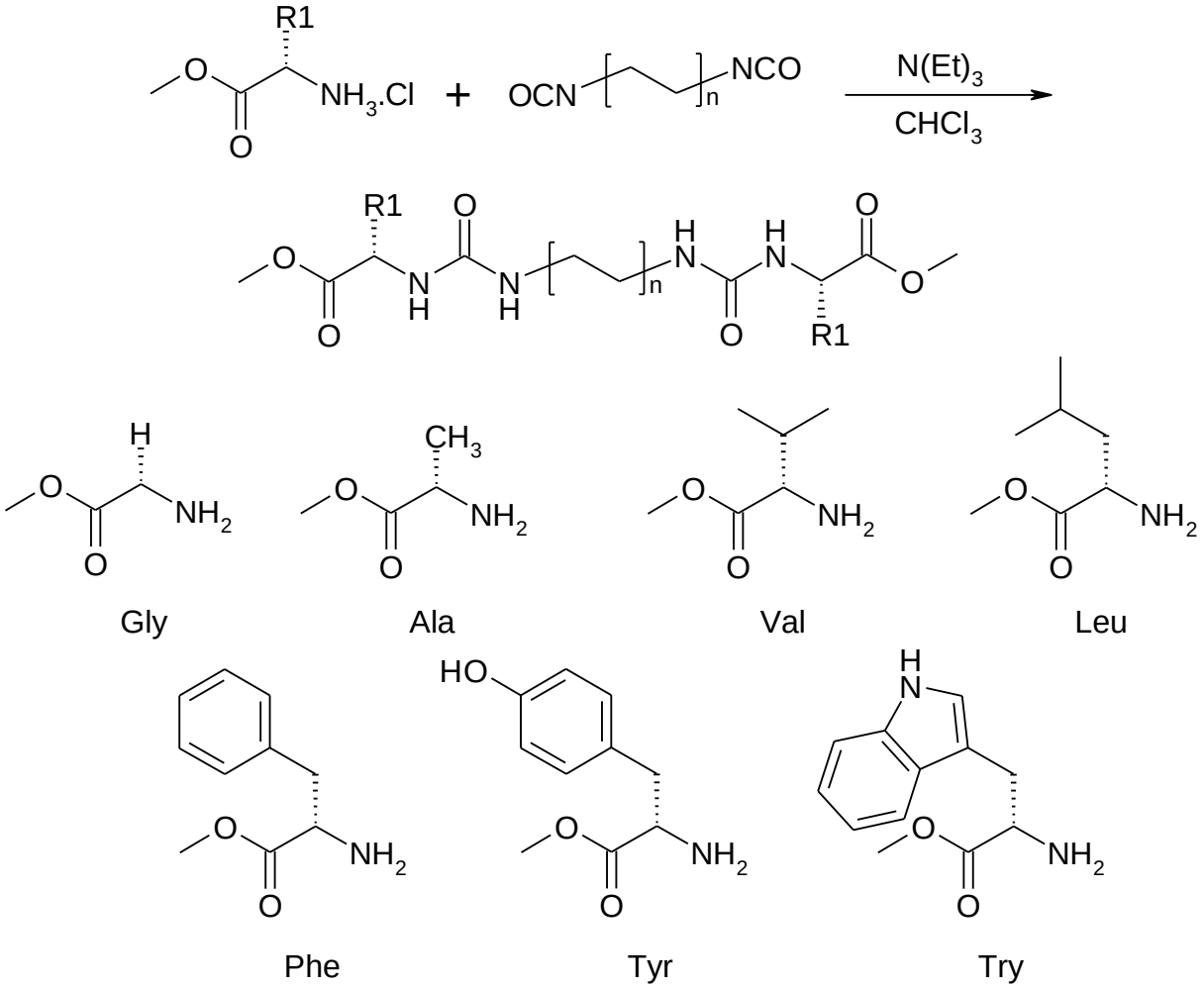

16	*n* = 6	R = H	(Gly)	**24**	*n* = 4	R = Me	(Ala)
17	*n* = 6	R = Me	(Ala)	**25**	*n* = 4	R = iBu	(Leu)
18	*n* = 6	R = iPr	(Val)	**26**	*n* = 4	R = Bn	(Phe)
19	*n* = 6	R = iBu	(Leu)	**27**	*n* = 4	R = $CH_2C_6H_6OH$	(Tyr)
20	*n* = 6	R = Bn	(Phe)	**28**	*n* = 4	R= C_9H_8N	(Try)
21	*n* = 6	R = $CH_2C_6H_6OH$	(Tyr)	**29**	*n* = 2	R = iPr	(Val)
22	*n* = 6	R= C_9H_8N	(Try)	**30**	*n* = 8	R = Bn	(Phe)
23	*n* = 4	R = H	(Gly)	**31**	*n* = 12	R = iBu	(Leu)

Work-up of the reaction largely depends on the solubility of the resulting compound. In cases where the product precipitates from the chloroform it can be isolated by filtration, washed with cold dichloromethane and diethyl ether then dried in a drying pistol. In some cases

additional washing with water was required to fully remove the triethylamine hydrochloride. Where the compound remains dissolved in the reaction mixture, the volume of the chloroform was reduced under vacuum, the impurities extracted with water and the chloroform layer dried and evaporated to give the clean product. In some cases addition of water induced a fine precipitate of the product in the reaction mixture making extraction difficult. In such cases the chloroform was completely removed by evaporation to leave a solid which was ground and washed repeatedly with warm water before filtering and drying. Many of the compounds retained solvent strongly and drying in a heating pistol was required to ensure clean products.

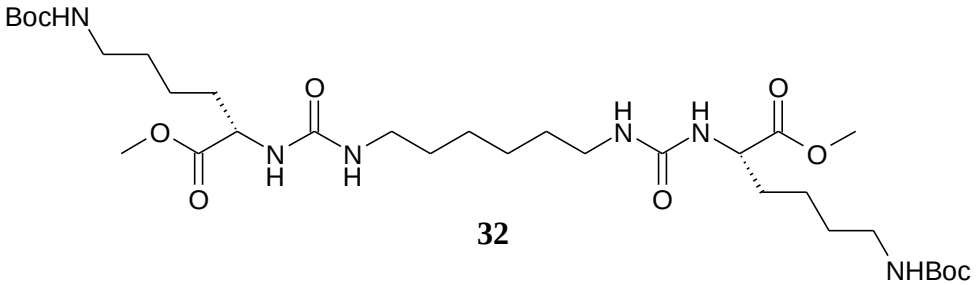

32

l-Lysine methyl ester, with the amine of the R-group Boc protected, was used to successfully synthesise compound **17**. Attempts to remove the Boc protecting group using 1:1 TFA:DCM produced a complex mixture of products. As **17** does not form part of the series of amino acid derived gelators no further work was undertaken on this compound. However, **17** proved to gel a range of solvents without deprotection forming stable gels in toluene and ethyl acetate. Gels initially formed in water but proved unstable with time and quickly broke down. Deprotecting the amine and reacting it with isocyanates or other functional groups to produce extended gelator molecules provides a potentially interesting future line of inquiry, as does its gelation behaviour.[8]

2.3 Characterisation of gelation behaviour

2.3.1 Effect of R-group and solvent on gelation

Hexylene spaced gelators **16**-**22** were screened for gelation behaviour against a range of solvents across the polarity spectrum. An amount corresponding to 1 % weight to volume (% w/v) of the compound relative to the solvent was weighed into a small vial and heated in 1ml of solvent until fully dissolved. The samples were cooled rapidly by placing the vials in a water bath at room temperature and sonicating them briefly when the first signs of precipitation were observed.[176] The results upon cooling to room temperature are recorded in

Table 1. Gel formation was characterised by a simple vial inversion test; if the solvent was fully immobilised it was considered to have gelled. The term partial gel was ascribed to samples where only partial trapping of the solvent occurred. Heating took place in sealed vials using a heat gun and in some cases the dissolution temperature of the compound was above the boiling point of the solvent at atmospheric pressure.

Table 1 Compounds **16-22** screened against a range of solvents for gelation behaviour by heating 1 % w/v of the compound in the corresponding solvent until fully dissolved and recording the results upon cooling

	Compound (*n*=6 and amino acid from which derived)						
	16	**17**	**18**	**19**	**20**	**21**	**22**
Solvent	Gly	Ala	Val	Leu	Phe	Tyr	Try
Water	P	G[a]	I	P	I	P	P
DMSO	S	S	S	S	S	O	S
Acetonitrile	P	G	P	S	G	O	S
Methanol	P	S	S	S	S	O	S
Ethanol	P	G[a]	S	S	S	S	S
Acetone	P	G	P	S	G	O	S
THF	P	G	S	S	S	O	P
DCM	P	PG	S	S	S	O	P
Ethyl acetate	P	G	G	P	G	O	I
Chloroform	P	G	S	S	S	O	S
Diethyl ether	I	I	I	P	I	O	I
Toluene	G	G	P	G	G	O	I
Hexane	I	I	I	I	I	O	I

P = precipitate, S = solution, G = Gel, PG = partial gel, O = oil, I = insoluble with heating, [a] = gel unstable, breaks down over time.

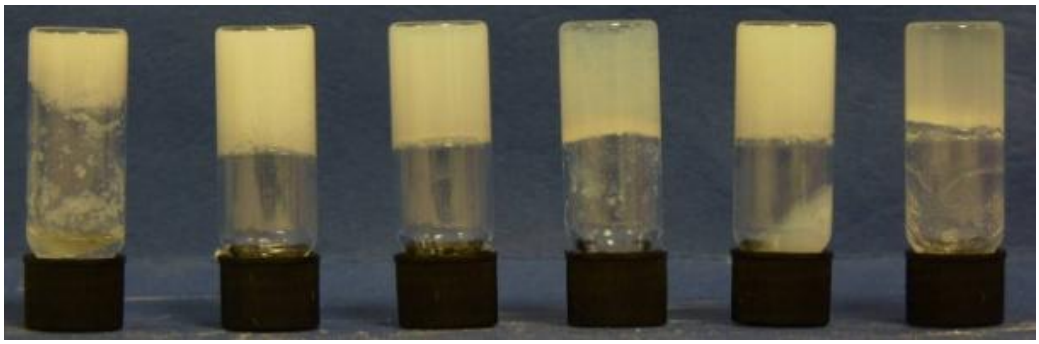

Figure 23 Photograph showing 1 % w/v gels of alanine derived gelator **17** in (left to right) water, acetonitrile, THF, chloroform, ethyl acetate and toluene.

Small changes in R-group across the series result in large changes in the properties of the compounds. Glycine derived gelator **16** rapidly forms strong translucent gels in toluene but precipitates from other solvents. In contrast, alanine derived gelator **17** forms robust gels in

toluene, chloroform, ethyl acetate, THF, acetone and acetonitrile and partial gels in DCM. Gels are also produced in ethanol and water but are unstable, particularly the hydrogels, and rapidly break down to give a precipitate. Moving from a methyl to an isopropyl group, valine derived compound **18** produces only weak gels in ethyl acetate. Leucine derived gelator **19** is markedly more soluble than other compounds remaining in solution in most of the solvents tested. Gels gradually form in toluene over a period of several hours with the viscosity of the solution increasing gradually; a markedly different process to the rapid gelation observed for the other compounds. Phenylalanine derived compound **20** produced robust gels from toluene and ethyl acetate. Weaker, more opaque gels also form in acetone and acetonitrile, however gel formation was poorly reproducible with precipitates or partial gels often obtained using the same procedure. Compound **20** also forms robust gels in a number of aqueous solvent mixtures, namely 1:1 DMSO:water, 3:2 Methanol:water, 1:4 THF:water.

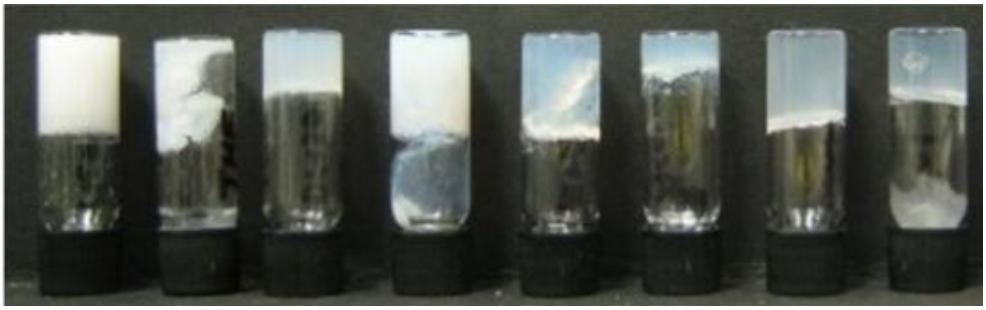

Figure 24 Photograph showing 1 % w/v gels of phenylalanine derived gelator **20** in (left to right) 3:2 MeOH:H_2O, 1:4 THF:H_2O, 1:1 DMSO:H_2O, CH_3CN, Ethyl acetate, Acetone, Benzene, Toluene

Tyrosine derived compound **21** produces immiscible oils in most of the solvents tested. The oil droplets are transparent and stick to the sides of the vial which makes it difficult to ascertain whether they dissolve at high temperatures. Oils form upon the addition of very small amounts of solvent to the dry compound. During the synthesis of **21**, the product is obtained from the chloroform reaction mixture as immiscible oil which NMR spectroscopy indicates contains only small amounts of solvent. A fine white powder could be obtained by drying the oil in a heating pistol or by recrystallization from water. Tryptophan derived compound **22** also showed no evidence of gelation remaining soluble or producing precipitates from all of the solvents tested.

Gelators **16**-**22** are all capable of forming gels, but only do so in certain solvents. Thermally induced gelation requires the compound to be soluble in the solvent at high temperature, but insoluble at low temperature. The gelation behaviour reported in Table 1 refers to mixtures

with 1 % w/v of gelator to aid comparison, however further tests at higher and lower concentrations failed to produce gels in any further solvents. Most of the compounds are poorly soluble in water or apolar solvents such as hexane and diethyl ether. Toluene proved the best solvent for this class of gelator producing the most robust and translucent gels in each series, apart from compound **18** where only ethyl acetate formed gels. In general, gels formed in more polar solvents tended to be more opaque and required sonication and higher concentrations of gelator to ensure complete gelation.

2.3.2 Effect of spacer length on gelation behaviour

Spacer length can play an important role in determining gel formation and an alternation effect is well established for alkylene-spaced compounds,[53, 177] including bis-urea gelators of this type.[51, 52] A number of analogues with different (even) lengths of alkylene spacers (*n*) were investigated.

Table 2 Compounds **23-28** screened against a range of solvents for gelation behaviour by heating 1 % w/v of the compound in the corresponding solvent until fully dissolved and recording the results upon cooling.

	Compound (*n*=4 and amino acid from which derived)					
	23	**24**	**25**	**26**	**27**	**28**
Solvent	Gly	Ala	Leu	Phe	Tyr	Try
H_2O	P	P	P	P	P	P
DMSO	S	S	S	S	S	S
CH_3CN	P	P	S	S	S	P
MeOH	P	P	S	S	S	S
EtOH	P	P	S	S	S	S
Acetone	P	G	S	S	S	P
THF	P	G	S	S	S	P
DCM	P	G[a]	S	S	O	P
EtOAc	P	G	P	S	O	P
$CHCl_3$	P	G[a]	P	S	O	PG
Et_2O	I	I	P	I	O	I
Toluene	G	G[a]	P	S	O	I
Hexane	I	I	I	I	O	I

P = precipitate, S = solution, G = Gel, PG = partial gel, O = oil, I = insoluble with heating, [a] = gel unstable, breaks down over time.

In contrast to the hexylene spaced analogues **16**-**22**, butylene spaced compounds **23**-**28** showed much less prevalent, and generally weaker, gelation behaviour. Like compound **16**, the butylene-spaced glycine derived compound **23** forms gels only in toluene, although the gels are much weaker and not always stable to inversion. During heating of compound **23** in

toluene a gelatinous aggregate gradually forms in the vial which eventually dissolves upon further heating. Alanine derived **9** also behaved similarly to its hexylene-spaced analogue but with many of the gels (referenced [a]) being unstable and precipitating over time.

No gelation was observed either for leucine derived **25** or phenylalanine derived **26** despite gelation by their hexamethylene spaced analogues. Tyrosine derived compound **27** behaves similarly to **21** and formed oils in most of the solvents tested. A partial gel of tryptophan based compound **28** was observed in chloroform which was not seen for its hexamethylene spaced analogue. However, optimising this gel proved difficult and electron microscopy failed to show fibre formation so no further work was undertaken to investigate this system.

A number of other analogues with different spacer lengths were also synthesised. A valine derived gelator with two methylene units in the spacer, **29**, proved highly soluble in most solvents tested and failed to form any gels. Octylene spaced phenylalanine gelator **30** does not form gels in any of the solvents tested. It is interesting to note that the butylene- and octylene-spaced phenylalanine gelators do not form gels whilst the hexylene spaced analogue shows strong gelation in a number of solvents. The dodecylene-spaced leucine derivative **31** is also highly soluble and failed to form gels in any of the solvents tested.

2.4 Characterisation of Gel Structure

2.4.1 Crystal Structures

Single crystal X-ray structures of some of the gelator molecules provide valuable insights into the behaviour of these compounds and highlight key features in gel design. The tendency of the compounds to form highly anisotropic crystals (fine needles or plates) made obtaining suitable single crystals particularly challenging and for some systems only gels or fine precipitates were ever obtained. Crystallisations were undertaken from the full range of solvents by slow evaporation and by leaving samples in sealed vials, typically for several weeks and up to a year. In general the less strongly gelling and less flexible butylene-spaced analogues proved more crystalline and single crystals were more readily obtained.

Single crystals suitable for XRD measurements were obtained for compounds **16**, **17**, **23**, **24**, and **25** and their structures solved. Compound **23** was found to exhibit two different polymorphic modifications in the same sample which were designated forms A and B. The

other compounds also exhibit polymorphism (as discussed in section 2.4.2) but suitable crystals for single crystal XRD could not be obtained.

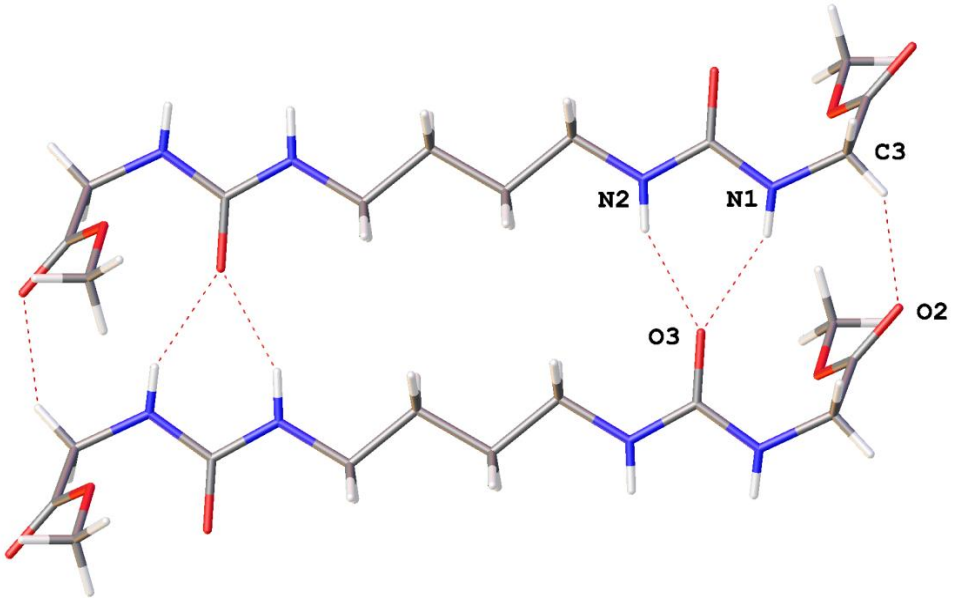

Figure 25 Antiparallel urea tape (N1···O3 distance 2.87 Å) and CH···O interactions (C3···O2 distance 3.25 Å) shown for compound **23** form A.

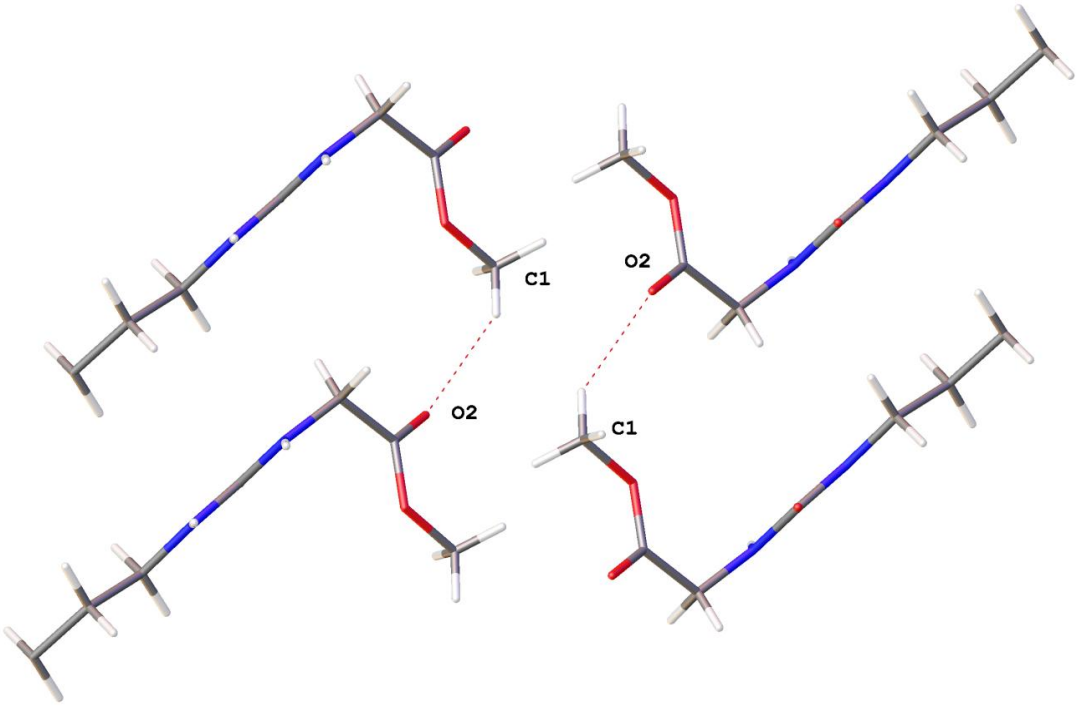

Figure 26 CH···O interactions (C1···O2 distance 3.31 Å) result in parallel C(5) tapes shown for compound **16**.

Glycine derivatives **16** and **23** form A show the same molecular conformation and crystal packing arrangement with slight differences in unit cell dimensions resulting from the difference in spacer length. The compounds crystallise in $P\bar{1}$ with half of the molecule in the

asymmetric unit. The oligomethylene chain adopts an all *trans* conformation with the carbon atoms laying in the same plane as the urea carbonyl groups. The bis-urea groups form anti-parallel $R_2^1(6)$ urea tapes typical for this class of compound (Figure 25).[38] There is an additional CH···O interaction within these stacks between the methyl ester groups and the hydrogen atom on the central (*i.e.* asymmetric or in the case of glycine derivatives prochiral) carbon atom of the amino acid (C3···O2 distance 3.25 Å, Figure 25). At the pro-chiral centre of the amino acid, the methyl ester is bent out of this plane allowing for the CH···O interaction between adjacent urea stacks. In compounds **16** and **23**, CH···O interaction takes place between methyl esters in adjacent urea stacks leading to a C(5) chain in graph set nomenclature (Figure 26).[45]

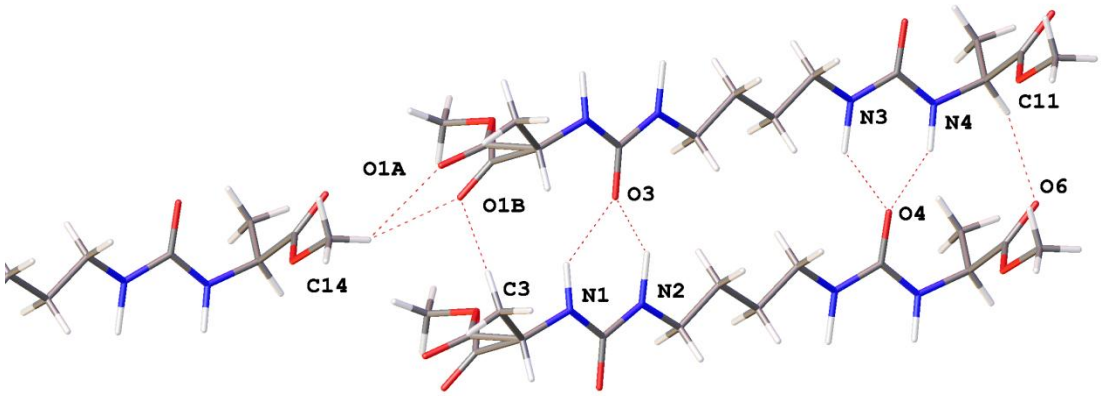

Figure 27 The methyl ester of **24** is disordered between two positions (O1A and O1B, 0.45:0.55) due to competing interactions between the methyl R-group (C3) of the molecule below in the urea stack (C3-O1B 3.24Å) and the methyl ester (C14) of a molecule in an adjacent urea stack (C14-O1A 3.23 Å). Anti parallel bis-urea tapes and CH···O interactions (C11-O6 3.23 Å) are also shown.

The presence of the methyl R-group in alanine derivative **24** breaks the symmetry of the molecule changing the space group to *P*1 with the whole molecule in the asymmetric unit consistent with the presence of the resolved chiral centre. The absolute configuration is not determined crystallographically in these light atom structures, however, as all of the compounds were synthesised from the natural *l*-amino acids the chiral centres are assumed to correspond to the S-enantiomer. The two sides of the molecule are no longer equivalent and the hydrogen atom attached to the chiral centre of the amino acid is only orientated to interact with the methyl ester of the molecule below on one side (Figure 27, C11-O6 3.23 Å). The ester group on the other side of the molecule is disordered and has been modelled with C2 and O1 occupying two positions with an occupancy which refined to 0.45:0.55 O1B:O1A

(Figure 27). The origin of this disorder appears to be competing CH···O interactions between the carbonyl oxygen (O1A) and either the methyl R-group (C3) in the same urea stack or the methyl ester (C14) of the adjacent stack.

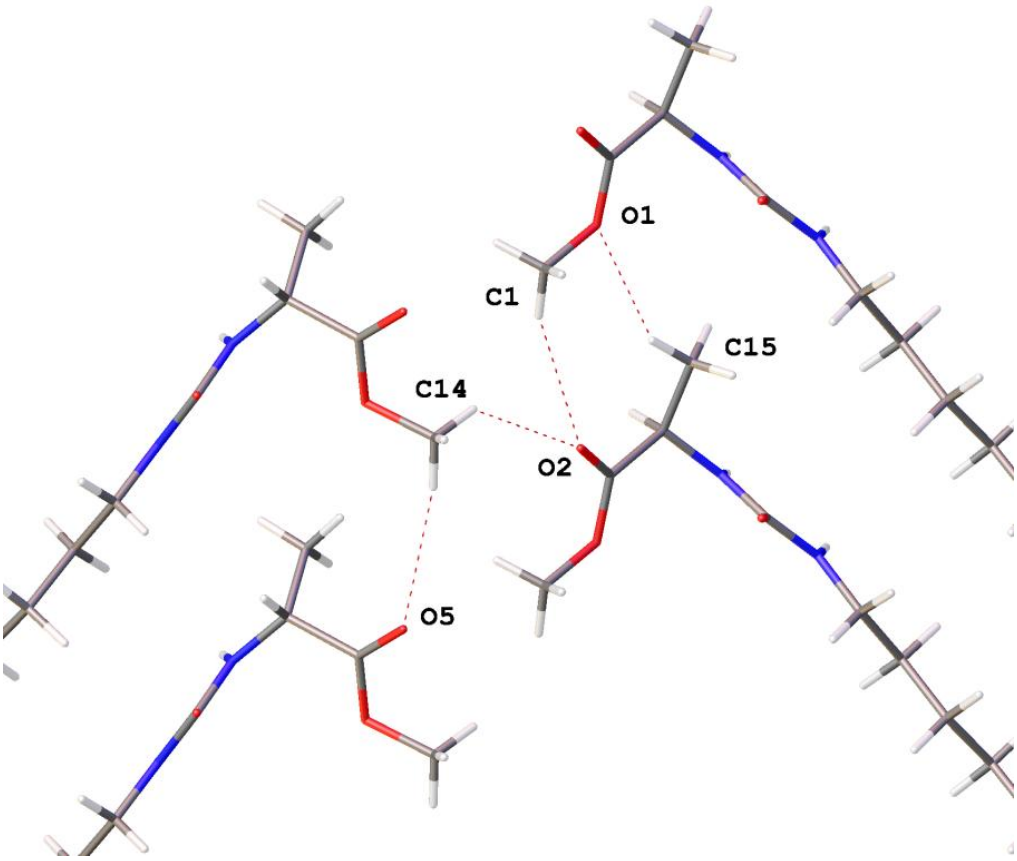

Figure 28 CH···O interactions between urea stacks of compound **17** along the *c*-axis, O5···C14 3.66 Å, C14···O2 3.52 Å, O2···C1 3.61 Å, C15···O1 3.5 Å.

The structures obtained for crystals of hexamethylene spaced alanine analogue **17** show the molecule adopts a very similar conformation to that seen for **24**. The molecules pack together through urea tapes which further align into offset sheets. However the space group is $P2_1$, not $P\bar{1}$, and adjacent sheets of urea stacks are rotated to give herringbone packing (Figure 28). The molecule is not disordered in this conformation, with **17** adopting the same packing as the major component of **24** (shown in Figure 27 as O1A). CH···O interactions take place between methyl ester groups (O5···C14 distance is 3.66 Å) at one end of the molecule and between the methyl ester and both the carbonyl and R-group at the other (C14···O2 3.52 Å, O2···C1 3.61 Å). Further interactions take place between adjacent urea stacks (C15···O1 3.5 Å). The data is of low precision due to poor crystal quality (conventional *R* value 14.2 %) but the gross molecular structure and crystal packing arrangement is unambiguous.

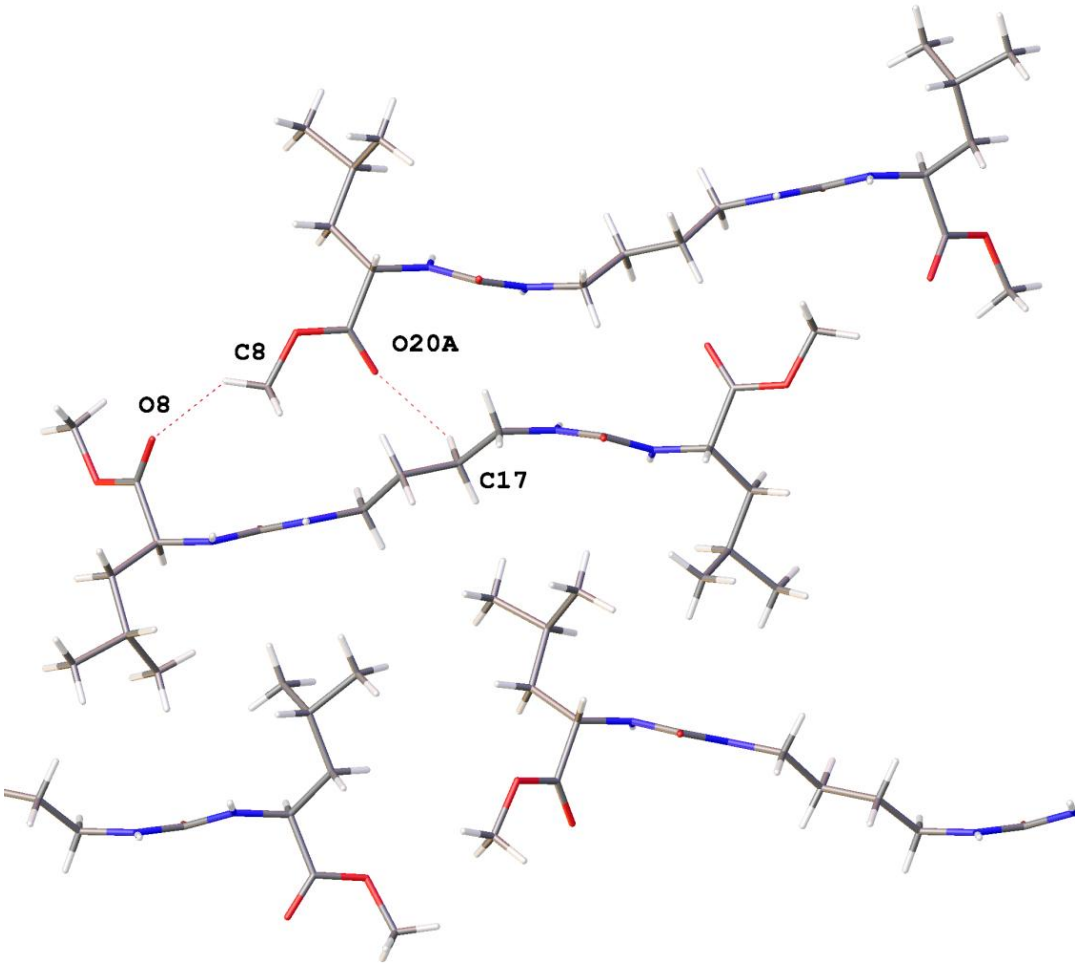

Figure 29 Compound **25** viewed along (100) showing back–to-back packing of urea stacks (O8···C8 3.23 Å, O20A···C17 3.39Å) and interdigitation of isobutyl R-groups. Only disordered component A is shown for clarity.

Leucine derived compound **25** adopts a similar conformation to those described for compounds **16**, **17**, **23a** and **24,** although the oligomethylene chain is bent out of the plane of the urea groups, presumably in order to better accommodate the bulky R-groups. Anti-parallel bis-urea tapes are formed which are arranged back-to-back to create pairs of urea tapes. This arrangement enables CH···O interactions to take place between the methyl ester groups (O8···C8, 3.23 Å) and a hydrogen atom in the butylene spacer (O20A···C17, 3.39 Å) as shown in Figure 29. The urea stacks are offset such that the CH···O interactions take place at one end of the molecule with the compound below and at the other with the compound above forming a helix. The isobutyl R-groups are positioned on the outside of the helix where they interdigitate with isobutyl groups of neighbouring spirals. The isobutyl groups at one end of the compound are disordered between two positions.

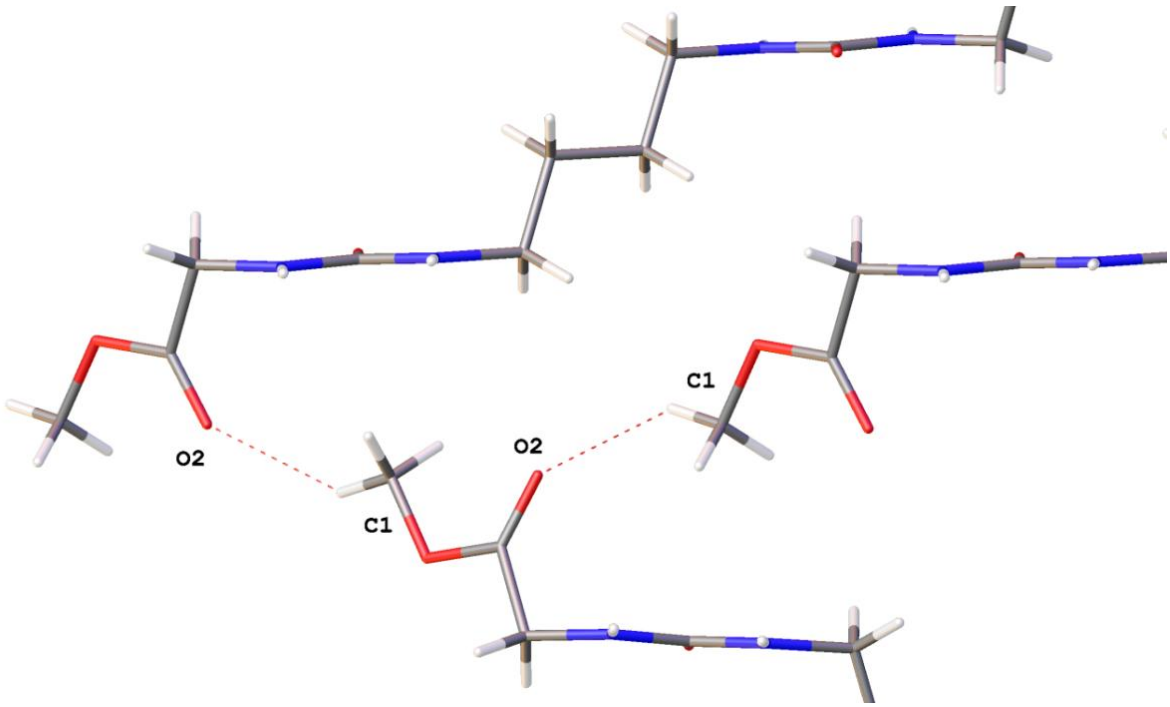

Figure 30 CH···O interactions along the 2_1 screw axis in form B of compound **23**: C1···O2 distance 3.38 Å

Compounds in the crystals described so far adopt different packing motifs as a result of different R-groups but the molecule adopts the same all *trans* oligomethylene conformation in each case. Fine needle-like crystals were found growing among the plates of **23** form A and identified as a second polymorph of **23**, form B. The compound crystallised in monoclinic space group $P2_1/n$ with half of the molecule in the asymmetric unit. In this form the antiparallel urea tape motif is conserved, however the oligomethylene spacer is *syn* to the urea groups. CH···O interactions take place between methyl ester groups along the screw axis leading to herringbone packing (Figure 30).

Compounds in this series are clearly able to pack together in variety of different ways. The steric and electronic effects of different R-groups impact upon the way the urea chains are able to pack together and a variety of CH···O interactions can take place. The oligomethylene chains are conformationally flexibile and can be either *trans* or *syn* with respect to the urea tape. Anti-parallel bis-urea stacks are conserved between all the structures reported here. However, the urea tapes are not always conserved and in crystals of the previously reported ethylene-spaced valine derivative **29** each molecule bonds via its urea groups to four different molecules resulting in two dimensional hydrogen bonded sheets.[178] It is likely that many of

the packing features observed in the known crystal forms are shared by other compounds in the series for which single crystal structures could not be obtained.

2.4.2 Solid state analysis

Studies were undertaken to investigate the molecular basis for the gelation of compounds **16-20** and **23-24** from a range of different solvents. The objective is to understand whether differences in polymorphism are responsible for gelation and non-gelation behaviour for the same compound in different solvents, and to investigate the instability observed in some of the gels.

Samples were prepared in four solvents (acetonitrile, acetone, ethyl acetate and toluene) representing a range of polarities and gelling/non-gelling behaviour by the compounds. Unless otherwise stated, samples were prepared by heating 1 % w/v of the compound in a sealed 1.75 ml vial with 1 ml of solvent until a clear solution was formed. The samples were rapidly cooled in a water bath and briefly sonicated to ensure homogeneous gel formation where applicable. Xerogels or precipitates were obtained from freshly cooled samples and the solvent was removed rapidly under vacuum to minimise the likelihood of solid form conversion during the drying process.

The solids were ground and analysed by IR, XRPD and DSC. Calculated powder patterns for the known crystal forms were matched with experimental data where possible. Different forms of a particular compound are identified as form A, B, C *etc.* but there is not necessarily any correlation between the crystal structures of different forms assigned with the same letter. A summary of the solid state forms obtained from a selection of different solvents is provided in Table 3. Solids obtained from gelling samples are highlighted in green, other samples are obtained from precipitates or solution. Where a second form is present as a minor product it is included in brackets; e.g. A(+B) means form A is the major product with form B present as a minor product. In some cases the compound converted from one form to another over time and this is indicated by an arrow, e.g. A(→B) means form A converts to form B over time.

Table 3 Solid state form obtained from samples of gelators **16**-**20** and **23**-**24** prepared from different solvents.

Solvent	Compound (corresponding amino acid and spacer length *n*)						
	16	**17**	**18**	**19**	**20**	**23**	**24**
	Gly 6	Ala 6	Val 6	Leu 6	Phe 6	Gly 4	Ala 4
Toluene	B	B	A(+B)	A	A	A	B(→A)
Ethyl acetate	A(+B)	B	A	A	A	A	B
Acetone	A	B	C (+D)	A	A	A	A
Acetonitrile	A	B	D	A	A	A	A(+B)
Water		B(→C)					

Green shading indicates sample obtained from a gel, right arrow indicates conversion of sample to a different form over time, + indicates minor form present

The non-gelling precipitates of **16** obtained from acetone and acetonitrile gave XRPD patterns which match those generated for the known crystal structure of **16**, form A. XRPD patterns for the xerogels of **16** obtained from toluene do not match those of form A and are assigned as a new form, form B. XRPD pattern for the precipitate of **16** obtained from ethyl acetate show peaks which match the patterns of both forms A and B. The relative intensities of the different peaks indicate that the ethyl acetate sample of **16** is predominantly form A, with form B as a minor component. Compound **23** shows the same XRPD pattern across all of the different solvents which match the generated XRPD pattern for the known crystal structure, **23** form A (Figure 31). Although the XRPD pattern observed is the same, gels only form in the toluene solvent system. The single crystal X-ray structures obtained for glycine derived compounds **16** and **23** form A show the gelators adopt very similar molecular conformations and crystal packing to one another. It is therefore interesting that this packing arrangement can give rise to gels for butylenes spaced compound **23** but not for hexylene spaced compound **16**.

In section 2.3.2 it was noted that heating of compound **23** in toluene produces a gelatinous material before the compound fully dissolves. XRPD patterns of this gelatinous material indicate it consists predominantly of Form B, with small amounts of form A also present. The transition is also observed in the solid state by DSC with xerogels of form A showing a melting peak at 180°C followed by recrystallization then a second melting peak at 196°C. Xerogels of form B show only one melting peak at 196°C.

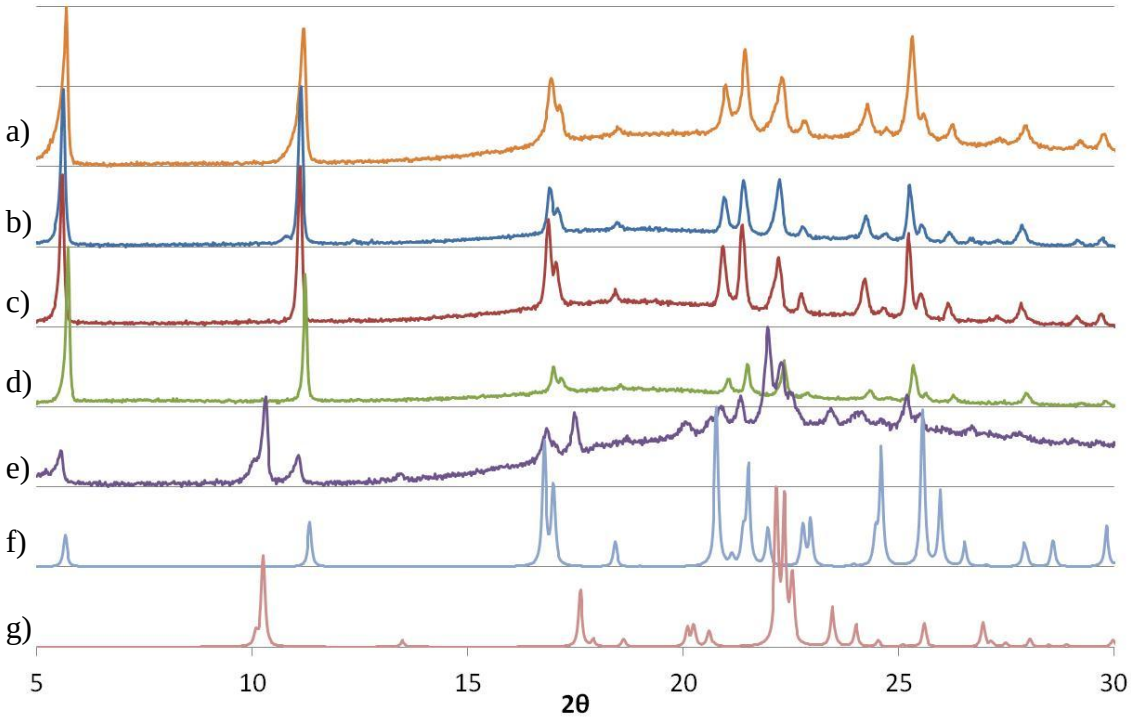

Figure 31 XRPD patterns showing recrystallisation of 1 % w/v **23** from: a) toluene- form A (orange), b) ethyl acetate- form A (blue), c) acetone- form A (red), d) acetonitrile- form A (green), e) in toluene at high temperatures- form B(+A) (purple). Calculated crystal structures of f) **23** form A (mid blue) and g) form B (pink).

Two different polymorphs of **24** appear to give rise to gelation. Xerogels obtained from acetone matched the known crystal form of **24** (form A), whilst xerogels obtained from toluene and ethyl acetate showed different XRPD patterns and were assigned as form B. The precipitate obtained from acetonitrile was found to be an approximately 1:1 mixture of forms A and B. A number of the other gels formed by this compound in DCM, $CHCl_3$ and toluene proved to be unstable over a period of hours. Toluene gels allowed to evaporate slowly over several days produced powder patterns matching those of Form A, in contrast to rapidly dried fresh samples which show patterns assigned as Form B. This indicates conversion of form B to form A over time or with drying. It is possible that conversion of form B to form A in the acetone and acetonitrile samples is responsible for the different forms observed in the xerogels.

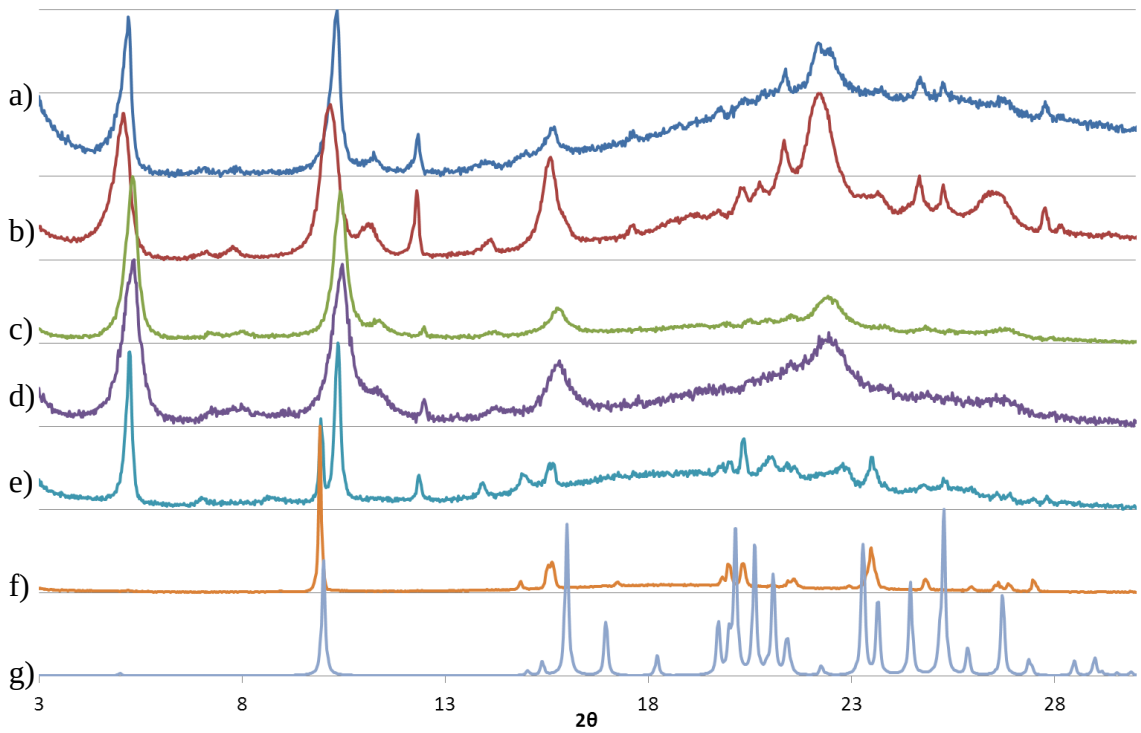

Figure 32 XRPD patterns showing recrystallisation of 1 % w/v **17** from: a) toluene- form B (blue), b) ethyl acetate- form B (red), c) acetone- form B (green), d) acetonitrile- form B (purple), e) water– form B(+C) (light blue), f) broken down gel from water- form C (orange). g) Calculated crystal structures of **17** form A (grey)

Hexylene spaced alanine gelator **17** gels all four of the solvents. The XRPD patterns for xerogels of **17** show a pattern which is different to that of the known crystal form A, so are assigned form B. The ethanol and water gels of **17** were observed to be unstable, rapidly breaking down to give precipitates. An XRPD pattern taken for a freshly formed and rapidly dried water gel showed a mixture of the gelling form B and a new form C. Samples of the precipitate formed when the water gel degraded were identified as form C. In water the gelling form B rapidly converts to a non-gelling form C. Form C shares a number of peaks (most notably at 9.5°) with the known crystal structure, Form A, but appears to be a distinct form (Figure 32).

Valine derived gelator **18** only gels ethyl acetate and the XRPD pattern of the xerogel shows a single form, designated form A. The same set of peaks are seen in the toluene xerogels by XRPD with some additional peaks of similar intensity which may be due to higher crystallinity in the sample or the presence of a second form (form B). XRPD patterns for the acetonitrile and acetone samples indicate two further forms which are assigned C and D respectively. However, some of the peaks in the acetonitrile pattern match those of form D

and a mixture of forms may be present in this sample. Repeats of the samples produced equivalent XRPD patterns with no clear changes in the ratio of peaks observed.

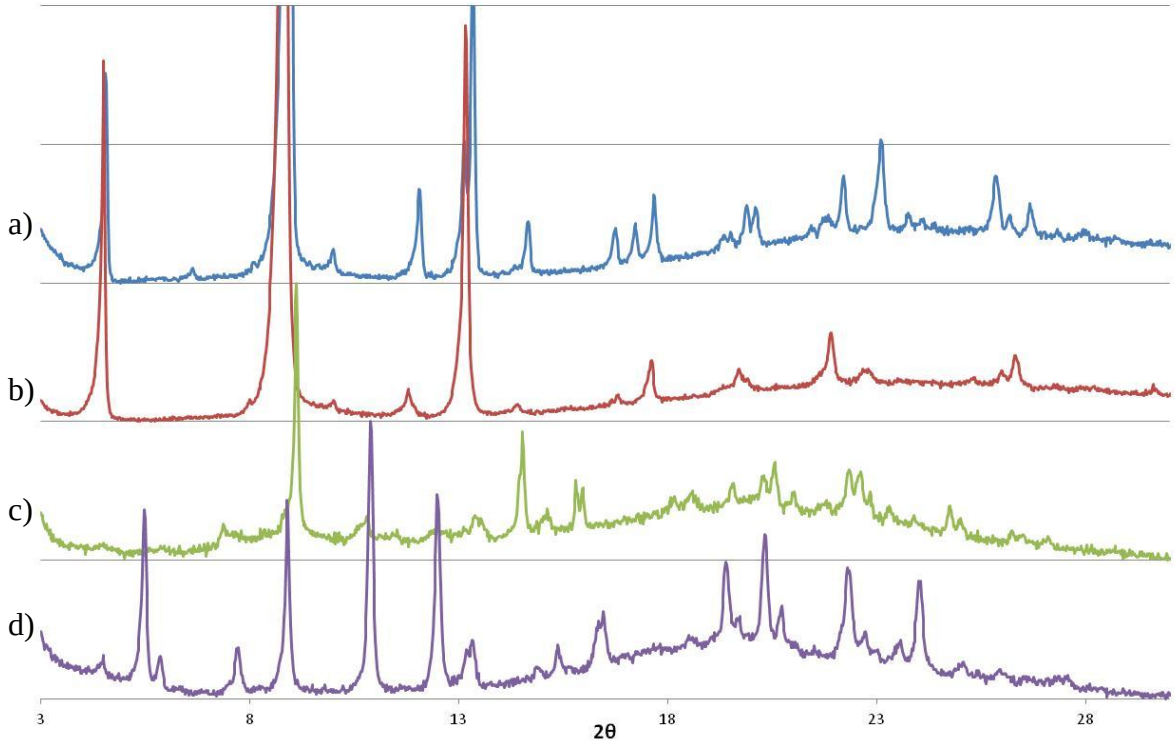

Figure 33 XRPD patterns showing recrystallisation of 1 % w/v **18** from: a) toluene- form A(+B) (blue), b) ethyl acetate- form A (red), c) acetone- form C(+D) (green), d) acetonitrile- form D (purple)

Leucine derived gelator **19** comes out of solution as the same form, designated form A, from all of the solvents but only gives rise to gels in toluene. Compound **19** was resynthesised following the same method as the original batch of gelator and shown to be of high purity by NMR spectroscopy, mass spectrometry and elemental analysis. However, when this batch of gelator was used, gels no longer formed in toluene at 1 % w/v of **19** with small amounts of precipitate forming instead. The precipitates from toluene showed the same peaks by XRPD as the other samples, but additional peaks were also observed indicating the presence of a second form, designated form B. Gels could be formed in toluene at higher concentrations of gelator (2 % w/v) or if a small amount of the original batch of gelator was added to the sample. It was suspected that a trace impurity in the new batch of gelator, possibly seeds of form B, was nucleating form B and preventing gel formation. However, all attempts to remove such an impurity by recrystallisation and filtration proved ineffective and no gels could be formed at 1 % w/v **19** from toluene using the second batch of gelator.

XRPD patterns for xerogels of **20** formed from acetonitrile and acetone closely match one another. However, the XRPD patterns for the toluene and ethyl acetate samples are weakly diffracting and an assignment could not be made on the basis of the broad, poorly defined XRPD patterns. IR spectra for all of the samples show a strong match and on this basis the xerogels are all assigned as form A (Figure 34). Xerogels produced from gels of **20** in a number of binary solvent mixtures were also investigated. DMSO:water (1:1) and THF:water (1:4) samples gave XRPD patterns which match those obtained from acetonitrile and acetone (form A), whilst xerogels formed from gels of methanol:water (3:2) gave different XRPD patterns, assigned as form B.

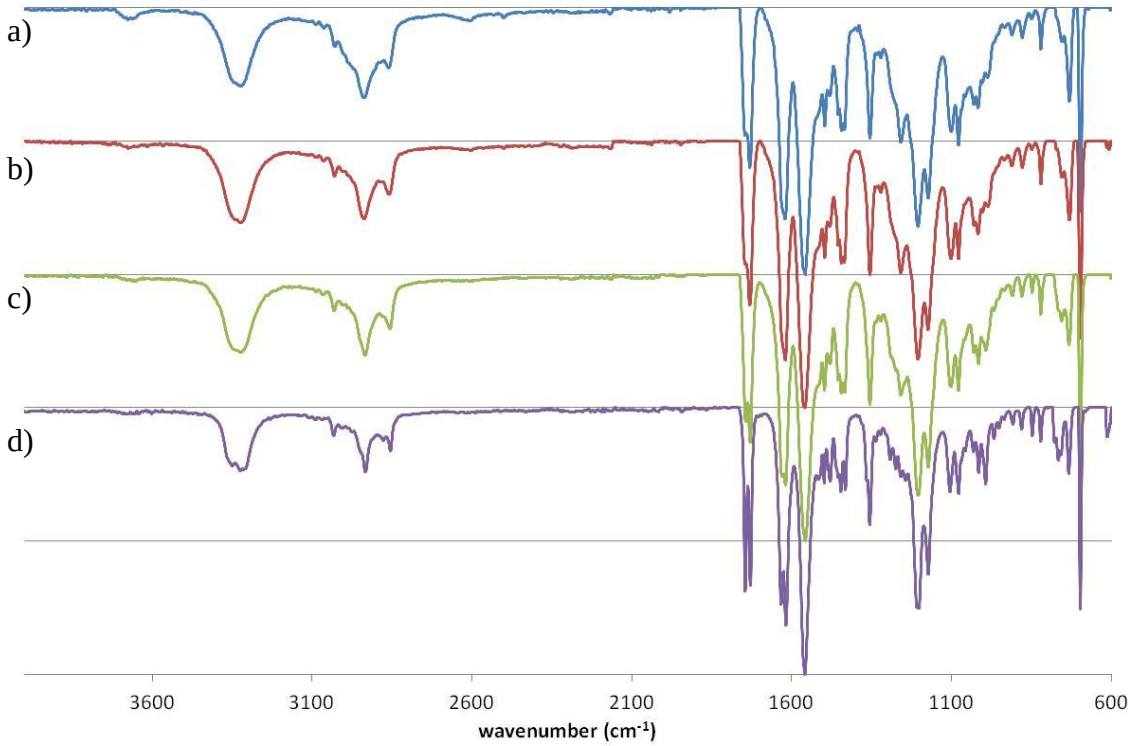

Figure 34 IR spectra showing recrystallisation of 1 wt% **20** a) from toluene (blue), b) ethylacetate (red), c) acetone (green), d) acetonitrile (purple).

This investigation highlights the extent of polymorphism displayed by this series of gelators with at least two different forms identified for each compound. Only one polymorph is associated with gel formation for all of the compounds except **24** where both forms A and B appear to give rise to gels. The gradual break down observed for toluene gels of **23** and **24** and water gels of **17** was found to be the result of a polymorphic transition in which the metastable gelling form converts to a more stable non-gelling form. Although the crystal structures obtained for compounds **16**, **17** and **23** form A showed similar conformations and packing arrangements, the behaviour of these forms in terms of their stability and ability to

form gels differed considerably. However, the formation of a particular polymorph does not guarantee gel formation, as seen for gels of **19** and **23** where the same form gives gels in some solvents but not others. The morphology of gel fibres and the way they crosslink in order to create a sample spanning structure are also important in determining gel formation.

2.4.3 Gel morphology

LMWGs can adopt a number of morphologies including fibrous, helical, ribbon-like, tubular, lamellar and vesicular structures.[24] Different morphologies can arise due to differences in molecular packing and the size and shape of fibres can be correlated with the strength and opacity of gels. Samples were prepared by applying a small amount of gel to a silicon wafer chip using a cocktail stick. The solvent evaporated rapidly under ambient conditions leaving a xerogel. The samples were placed under high vacuum and coated with 5 nm of platinum. SEM was used to image the morphology of different xerogels.

Compounds **16-19** and **23-24** all showed two dimensional, ribbon-like fibres. There was greater variation in the dimensions of the fibres within samples than between them with the thickness of the ribbons typically 10-100nm, the width between 100 nm-5 μm and lengths from 100 nm-<100 μm. The ribbons formed physically entangled networks with separate fibres weaving and wrapping around each other. The ribbons are often observed stacked on top of each other (Figure 35b) indicating attraction between the faces of the ribbons and this is thought to be the main source of crosslinking in the networks. The ribbons can also split along their length branching into two separate fibres (Figure 35c) which may provide a further means of crosslinking.

Figure 35 SEM images of xerogels formed from 1 % w/v gels of a) **17** in toluene, b) **17** in THF and c) **16** in toluene. Note the differences in scale between a) and b), stacking of ribbons in b) and splitting of ribbons in c).

The alanine gelators **17** and **24** typically exhibit a xerogel morphology comprising of smaller, less linear fibres than other gelators which corresponds to the more robust and more translucent gels observed. There was little variation in the morphology of xerogels of **17** formed from different solvents (Figure 36). The larger, more rigid plates observed for **17** in water are likely to be due to the rapid polymorphic transition (form B transforms to form C) that occurs for this system and the images are of the non-gelling precipitate.

Two distinct morphologies are observed concomitantly for samples of **23** prepared from the gelatinous aggregates formed when **23** is heated in toluene; large plate-like ribbons and smaller rod-like structures (Figure 38f). Only the larger, plate-like ribbons are seen in samples prepared from toluene gels of **23** (Figure 38g). The different morphologies are thought to correspond to the two different polymorphs of **23** with the plate-like structures form A and the rod-like structures form B.

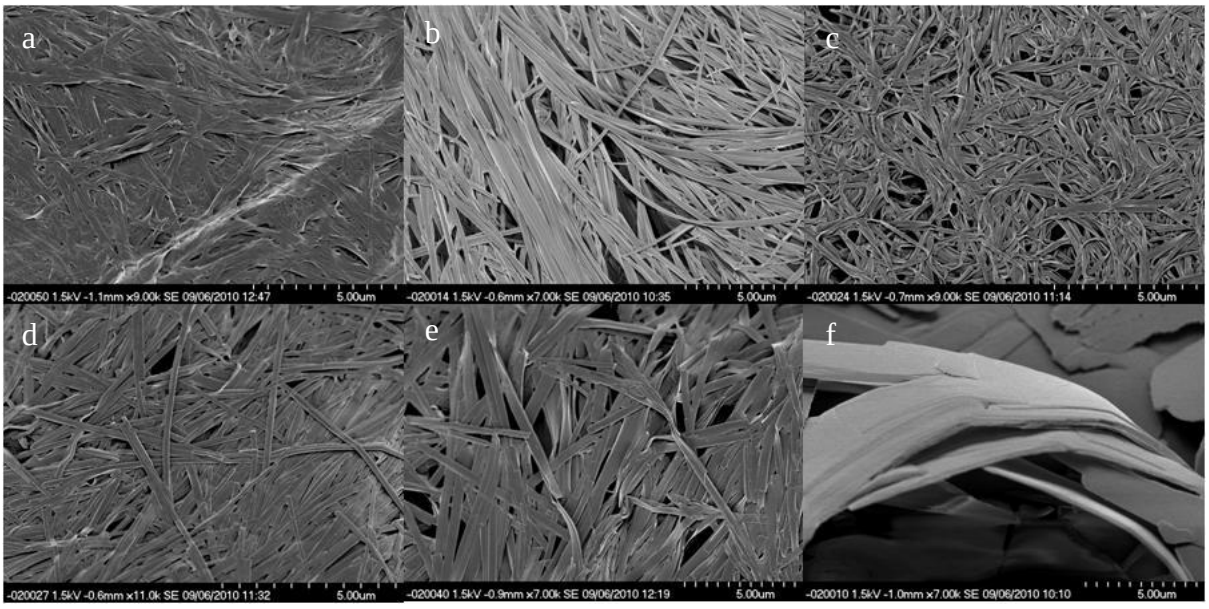

Figure 36 SEM images of 1 % w/v **17** fibres in a) toluene b) acetonitrile c) tetrahydrofuran d) chloroform e) ethyl acetate f) water.

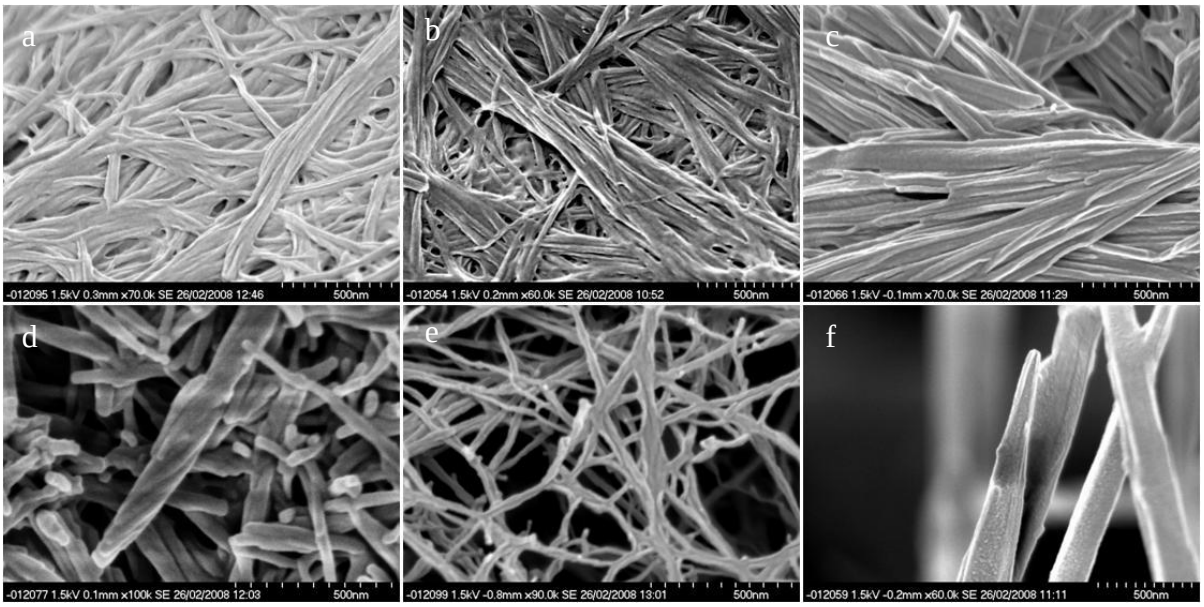

Figure 37 Xerogels formed from 1 % w/v gels of **20** in a) ethylacetate, b) acetonitrile c) acetone d) 1:4 THF:water, e) 1:1 DMSO water and f) 3:2 Methanol:water[179]

In contrast to the two dimensional structures formed by the other gelators, **20** forms randomly entangled networks of one-dimensional fibres. Individual fibrils are cylindrical and microns in length with a relatively consistent diameter of approximately 50 nm. These fibrils appear to wrap around each other in a helical manner to form larger fibres, a phenomenon often seen for chiral gelators.[174, 175, 180] There is considerable variation in the aggregation behaviour of these fibres. The fibres from toluene are more randomly orientated than the acetonitrile and acetone samples where the fibres tend to be bunched together into partially aligned clumps.

The fibrils from 1:4 THF:water mixture wrap around each other forming needle shaped structures which clearly show a helical twist. The structure of the DMSO:water gel consists of thinner fibres composed of individual fibrils which branch off and recombine with other fibres. This aligning and physical entanglement of fibrils and fibres appears to be the mechanism for crosslinking to give a sample spanning network. SEM images of the methanol:water (3:2) xerogels show significantly larger (250 nm) needle-like structures. XRPD showed the methanol:water xerogels have a different molecular packing (form B) to the other xerogels which share the same packing (form A).

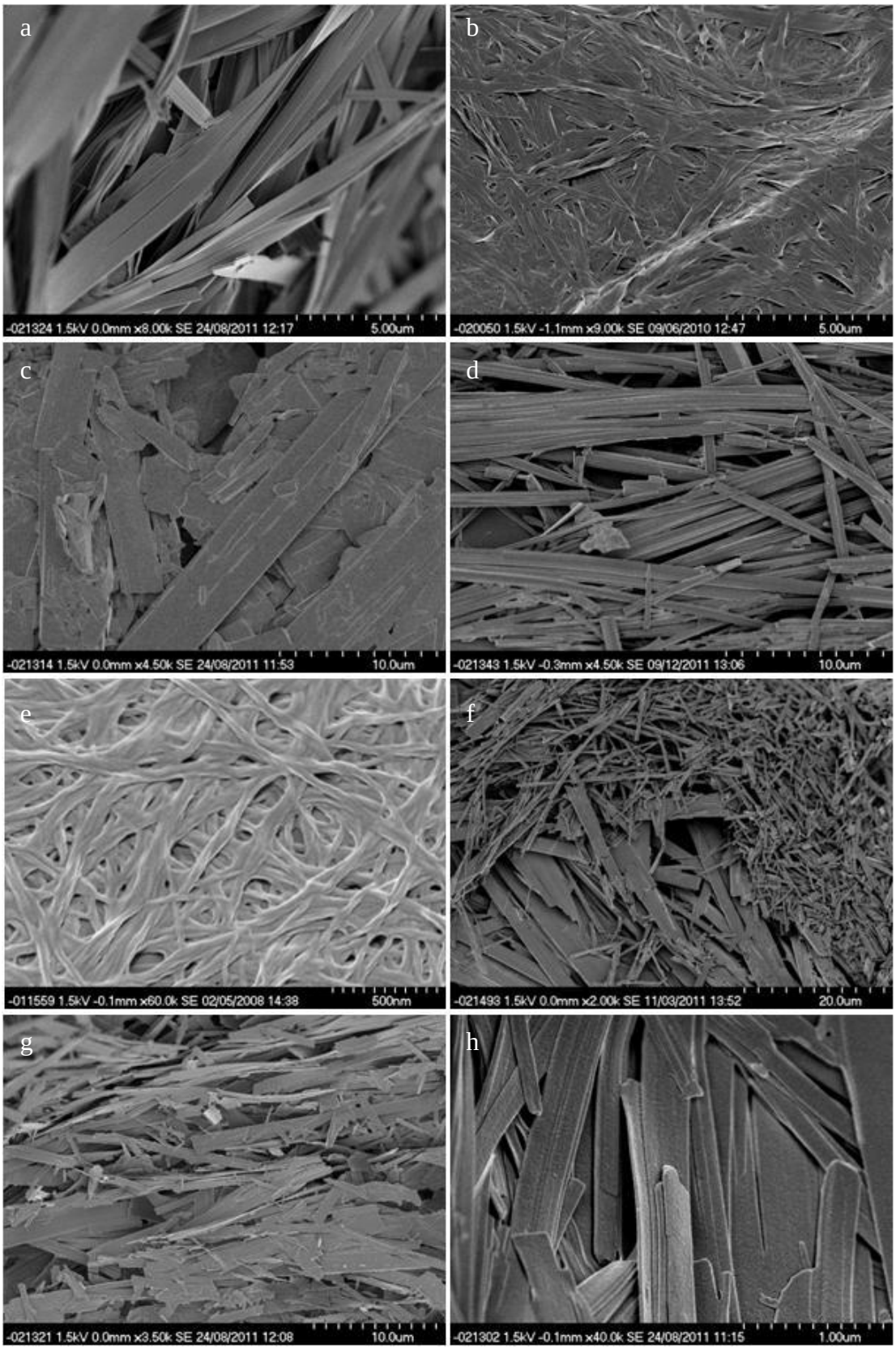

Figure 38 Xerogels of a) **16** b) **17** c) **18**, d) **19**, e) **20** f) **23** high temperature sample, g) **23** low temperature sample, h) **24**. All xerogels are formed from gels 1 % w/v in toluene except c) which is from gels of **18** in ethyl acetate.

2.5 Characterisation of Gel Properties

Within this series of compounds there are considerable differences in the properties of the gels. The strength of the gels, temperature at which they set and amount of gelator required to form a gel varies significantly with gelator and solvent. A qualitative description of some of these observations has already been reported in section 2.3; attempts to quantify some of this behaviour are reported in this section.

Toluene samples containing 1 % w/v of gelators **16**, **17**, **19, 20**, **23** and **24** were studied by rheometry. The response of the elastic (G') and loss (G'') moduli to changes in frequency, stress and strain were measured. The high temperature at which some of the gels form meant that samples had to be prepared in sealed vials and transferred using a spatula onto the rheometer which was used in a flat plate geometry. A total of 4 ml of each sample was used in each case. The gels were prepared in 7 ml vials except for compounds **16**, **17** and **24** where several smaller vials (1.75 ml) had to be combined as a build up of pressure with heating led to the escape of solvent in the larger vials. Compression of the samples between the plates resulted in loss of some solvent meaning the results may not accurately reflect a 1 % w/v gel. These limitations, along with the general challenges of getting reproducible rheometric data for LMWGs,[24] mean only general observations can be made about the behaviour of the samples.

Rheological measurements confirmed gel-like behaviour in 1 % w/v samples of **16-20** and **24** in toluene. The elastic modulus (G') is greater than the viscous modulus (G'') by approximately one order of magnitude for all samples. Application of increasing stress or strain to the samples eventually results in the gel yielding, with G'' becoming greater than G'. The general trend in gel strength and yield stress matches bench top observations, with **17** and **20** forming strong robust gels and **16**, **19** and **24** weaker more fragile gels.

As well as the regular gels of **23** in toluene**,** whose structure is assigned as Form A by XRPD, the gelatinous material formed upon heating a sample of **23** in toluene, predominantly form B with small amounts of form A present, was also tested. The form B material gives strong gels with high G' values which failed to yield at an applied stress of 300 Pa. Form A gels in contrast were much weaker readily breaking down to solutions with low applied stress (2 Pa).

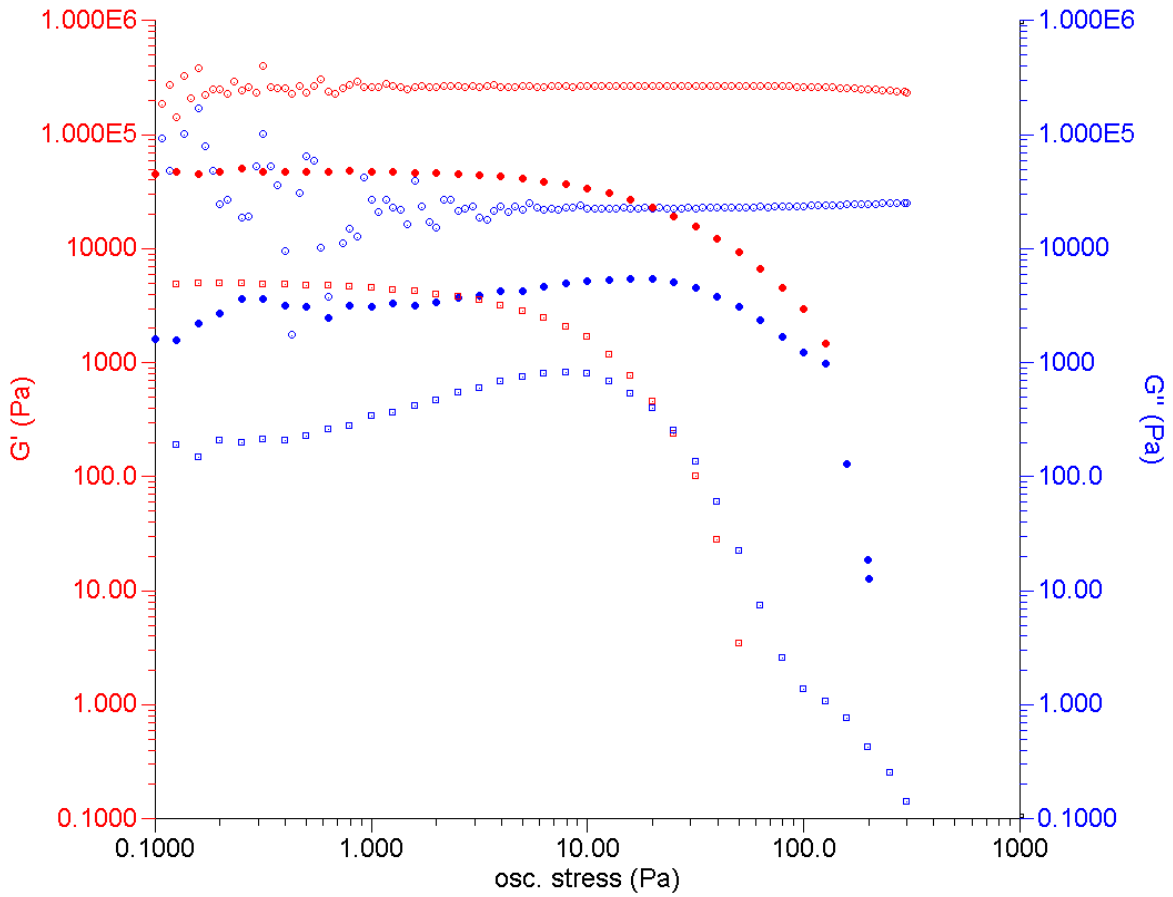

Figure 39 Oscillitory stress sweep comparing amino acid derived gelators at a constant frequency of 1 Hz.; open circles **20**, closed circles **17**, open squares **16**.

Table 4 Summary of rheometric data for 1 % w/v toluene gels of various compounds

	Compound						
Measurement	**16**	**17**	**19**	**20**	**23** form A	**23** form B	**24**
G' (Pa)	4.5×10^3	4.6×10^4	7.5×10^3	2.5×10^5	7.6×10^2	1.3×10^5	5.2×10^3
G'' (Pa)	3.4×10^2	3.1×10^3	2.3×10^3	2.1×10^4	8.9	4.6×10^3	9.9×10^2
G'/G'' (Pa)	13.3	15.2	3.3	12.2	8.6	27.7	5.3
Yield stress (Pa)	25	126	32	N/A	2	NA	20

N/A = Sample did not yield below 300 Pa

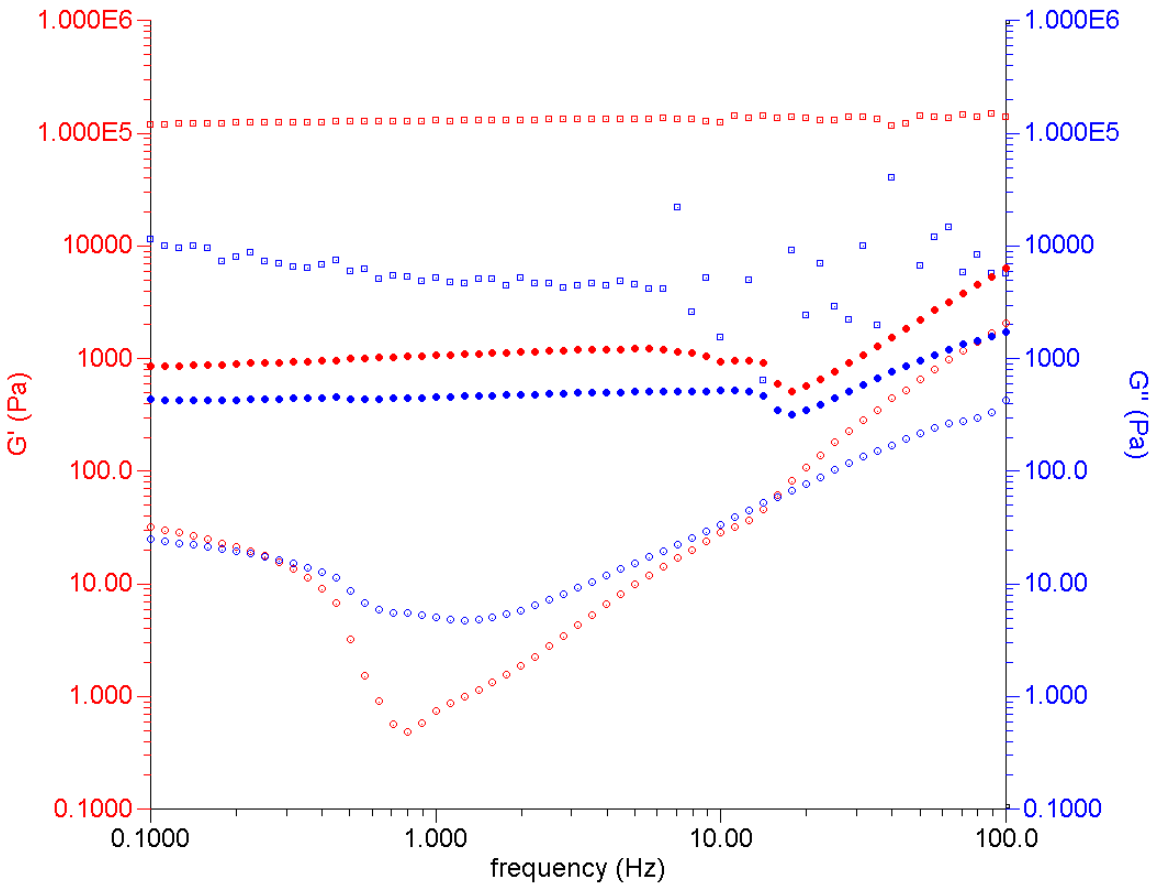

Figure 40 Frequency sweep comparing amino acid derived gelators at a constant stress of 10 Pa; 1 Hz.; open circles **23** form A, open squares **23** form B, closed circle **24**.

The *G′* and *G″* values of gels are characteristically unchanged over a wide range of frequencies. Gels of **17** and **20** showed no significant variation in *G′* or *G″* across the full range of frequencies investigated (0.1-100 Hz, 10 Pa osc. stress). Gels of **16**, **19** and **23** form B showed no variation of *G′* or *G″* in the frequency sweep up to 10 Hz after which a sudden dip then gradual increase in both values is observed. A similar dip then rise is observed much more strongly for gels of **23** form A at a much lower frequency, around 1 Hz. This non-linear behaviour is explained by the low yield stress of this gel which is below that of the applied stress.

Using the dropping ball method, toluene gels with 1 % w/v **20** was found to have a T_{gel} of 87°C with an error estimated to be ± 2°C in each case. Toluene gels with 1 % w/v of **17** measured using the dropping ball method in a sealed vial continued to support the ball bearing at temperatures of 110°C. No T_{gel} was recorded due to safety concerns regarding the build up of pressure upon heating the sample above the boiling of toluene for prolonged

periods of time. Toluene gels with 1 % w/v of **16**, **19**, **23** and **24** could not be tested using this method as they were not able to support the ball bearings. Qualitatively, toluene gels of **16**, **23** and **24** require prolonged heating with a heat gun at temperatures well above 110°C whilst toluene gels of **19** dissolve readily with moderate heating.

Compounds **17** and **20** form gels in toluene at concentrations well below the 1 % w/v of gelator used in the rheometry. The minimum amount of gelator required to form a sample stable to the inversion test, the critical gelation concentration (CGC), is 0.025 % w/v and 0.015 % w/v for compounds **17** and **20** respectively. This correlates to 330 molecules of toluene gelled for every molecule of **20** and 140 toluene molecules gelled for each molecule of **17**.

Ethyl acetate gels of **20** measured using the flat plate geometry with 8 ml of gel were found to give reproducible stress sweep curves showing strong gels which failed to break down up to oscillatory stress values of up to 1000 Pa. The effect on rheometry of the addition of anions to 1:9 acetonitrile:toluene and ethyl acetate gels of **20** and chloroform gels of **17** are reported in section 3.4.2 of Chapter 3.

2.6 Mixed Gelators

As well as gels formed by a single low molecular weight organic compound, a variety of systems in which multiple components come together to form gels have been described. Interactions with a second organic component,[14] metal ions[19] or nanoscopic materials[109] can be used to bring about gelation and the ratio of different components changed to fine tune the gel properties. Different components may interact in well defined ways with a specific stoichiometry,[42] form statistical or random co-polymers,[101] or form completely independent but interpenetrated networks.[39]

In order to further investigate the behaviour of this class of compounds, mixtures of different gelators were investigated. The crystal structures obtained for compounds **16**, **17**, **23**, **24** and **25**, and by inference those of other gelators in the series, share many similarities. Most notable is the presence of alpha urea tapes which are conserved across all of the structures and are thought to be responsible for fibre formation. The extent of polymorphism found

across the series indicates that individual gelators are able to adopt a number of low energy conformations whilst conserving the urea α-tape hydrogen bonding motif. However, small changes in substituent group can lead to subtle differences in the way the molecules pack together resulting in differences in fibre morphology, interactions between fibres and ultimately gel formation. It is therefore interesting to explore how different gelators interact with each other and the effect this has on gel structure and morphology with a view to further tuning gel properties using co-gels.

A number of binary combinations of gelators **16**, **17**, **19**, **20**, **23** and **24** with a total 1 % w/v of gelator in toluene solution were investigated by SEM and XRPD. All of the combinations investigated formed gels at all of the ratios tested. On one hand this is unremarkable in that the CGC of many of the gelators is well below 0.5 % w/v. On the other hand, given the similarities of the compounds to each other, but their differences in crystal packing arrangement, it is perhaps surprising that gel formation was not disrupted. A key question is whether phase separation occurs such that the mixed gels comprise separate networks with each gelator by itself or whether the individuals fibrils comprise of both gelators, either in an ordered, statistical or random arrangement, to give true co-gels.

As discussed in section 2.4.3, SEM images of gels formed by compound **20** show cylindrical fibres whereas ribbons are observed for other gelators. Figure 41 provides a summary of the morphology of xerogels formed from binary 1:1 mixtures of various gelators in toluene. Mixtures of butylene-spaced gelators **23** and **24** contain flat ribbon-like structures similar to those seen for the pure compounds. Mixtures of the corresponding hexylene spaced gelators, **16** and **17**, also show two-dimensional ribbons like the parent compounds. However, these ribbons adopt a marked twist not observed for the achiral gelator **16** nor observed to the same extent for chiral gelator **17**. This type of twisting is well known and often associated with chiral building blocks.[174, 181] The chiral alanine derived gelator molecules may induce a twist which is exaggerated by the achiral derived glycine gelator molecules which don't twist.

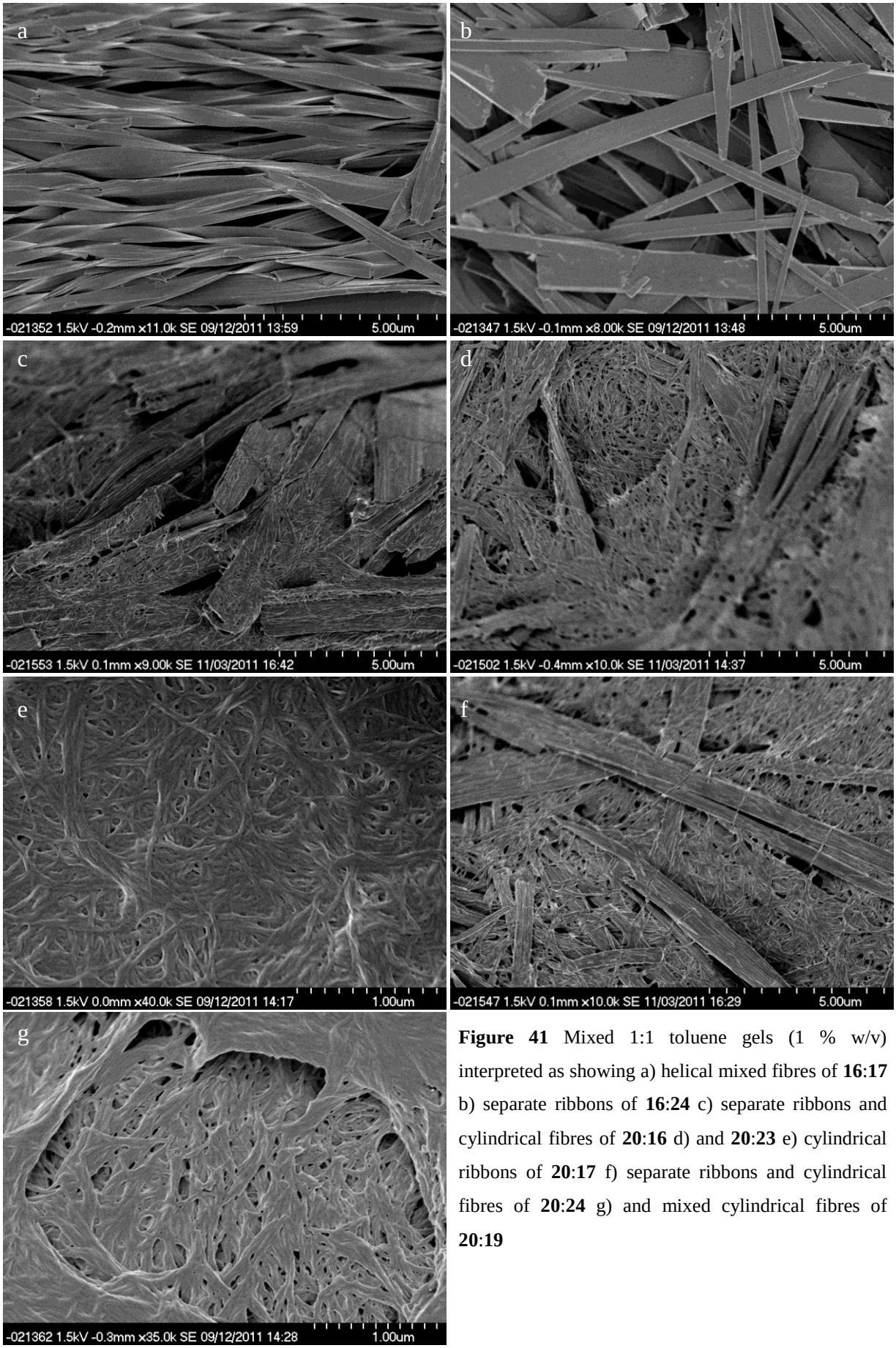

Figure 41 Mixed 1:1 toluene gels (1 % w/v) interpreted as showing a) helical mixed fibres of **16**:**17** b) separate ribbons of **16**:**24** c) separate ribbons and cylindrical fibres of **20**:**16** d) and **20**:**23** e) cylindrical ribbons of **20**:**17** f) separate ribbons and cylindrical fibres of **20**:**24** g) and mixed cylindrical fibres of **20**:**19**

SEM images of mixtures of **20** and **16** clearly show separate fibres with the distinct cylindrical and ribbon-like morphologies of **20** and **16**, respectively. In contrast, 1:1 mixtures of **20** and **17** show almost exclusively cylindrical morphology, with only the occasional ribbon-like structures observed by SEM. Predominantly cylindrical fibres are also seen for mixtures of **20** and **19**. These observations indicate compounds **17** and **19** interact strongly with **20** to produce a single morphology, whilst **16** and **20** don't interact in the same way and so produce separate fibres with the morphology of the pure compounds.

Hexylene spaced gelator **20** was also combined with butylene spaced gelators **23** and **24** to assess the impact of spacer length on co-gel formation**.** As with its hexylene analogue (**16**), glycine derivative **23** showed separate ribbon- and fibre-like structures. Separate ribbons and fibres were also clearly seen for mixtures of **20** with alanine derived gelator **24**. It is interesting to note that with the same spacer length, mixtures of **20** and **17** show a single morphology where as with different spacer lengths **20** and **24** show separate fibres and ribbons. This is readily rationalised in terms of compounds with the same spacer length being able to form bis-urea tapes more readily than those with different spacer lengths, so favouring homo-fibre formation.

In order to gain insight into molecular packing in the mixed gels, XRPD patterns were collected for xerogels formed from binary mixtures of gelators at molar ratios of 1:0 2:8, 4:6, 1:1, 6:4, 8:2 and 0:1.

The crystal structures described in section 2.4.1 for both butylene glycine gelator **23** (Form A) and alanine gelator **24** (Form A) show very similar packing motifs. The analysis in section 2.4.2 shows that this packing is observed in toluene gels of compound **23** (form A) but not toluene gels of **24** which show a second packing motif (form B). Figure 42 shows the XRPD pattern for mixtures of **23**:**24** with the ratio of **23** decreasing from top to bottom. The XRPD patterns for mixtures ranging from 1:0-2:3 **23:24** match that of the pattern for the pure glycine gelator **23** (form A). Small shifts occur in a number of peaks, most noticeably a shift in one peak from 17-15°, with increasing concentration of **24**. This indicates a co-gel is formed which adopts the packing of **23** form A with incorporation of **24** resulting in small changes in the average unit cell dimensions. At a 1:4 ratio, an additional set of peaks which matches those of **24** form B are observed in addition to those of **23** form B. This indicates

separate fibres with packing corresponding to that of **24** form B also form, but only at high concentrations of **24**.

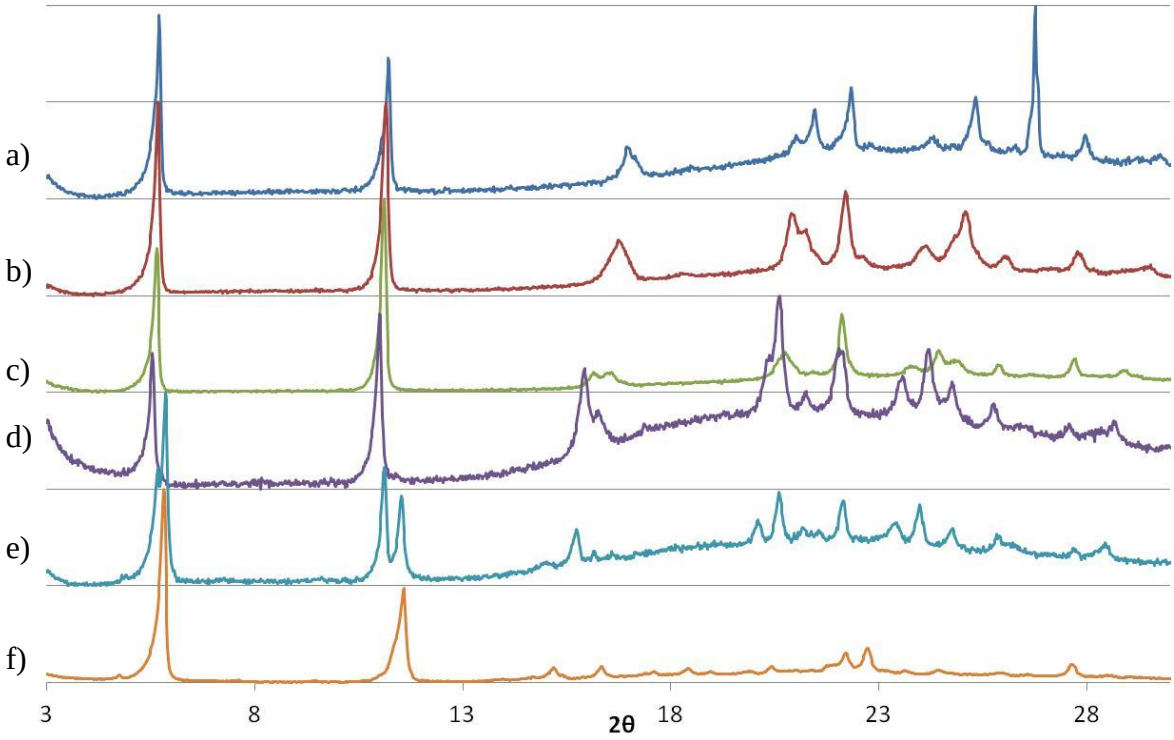

Figure 42 XRPD patterns corresponding to xerogels formed from toluene of **23**:**24** in a ratio of a) 1:0 (blue), b) 4:1 (red), c) 3:2 (green), d) 2:3 (purple), e) 1:4 (light blue), f) 0:1 (orange).

Figure 43 shows XRPD patterns for mixtures of **16**:**17** with the ratio of **16** decreasing from top to bottom. XRPD patterns for the mixed samples show a single set of peaks which do not match those of either pure **16** (form B) or **17** (form B). The positions of the peaks assigned to the new mixed phase vary significantly depending on the composition of the mixture while retaining the same basic pattern. The strong low angle peaks in the mixtures around 5° and 10° more closely resemble those of alanine gelator **17** and there is generally less correlation of the mixed phase with the pattern for **16**. However the 1:1 mixture does not follow this trend and a different pattern to other xerogels in the series. Whilst the evidence here is less clear, the behaviour is different from the butylene spaced, glycine and alanine derived co-gels (**23**:**24**) which clearly show packing similar to that of the glycine gelator. This difference in behaviour shows how small changes in the spacer length, as well as R-group, can impact upon gel structure and properties.

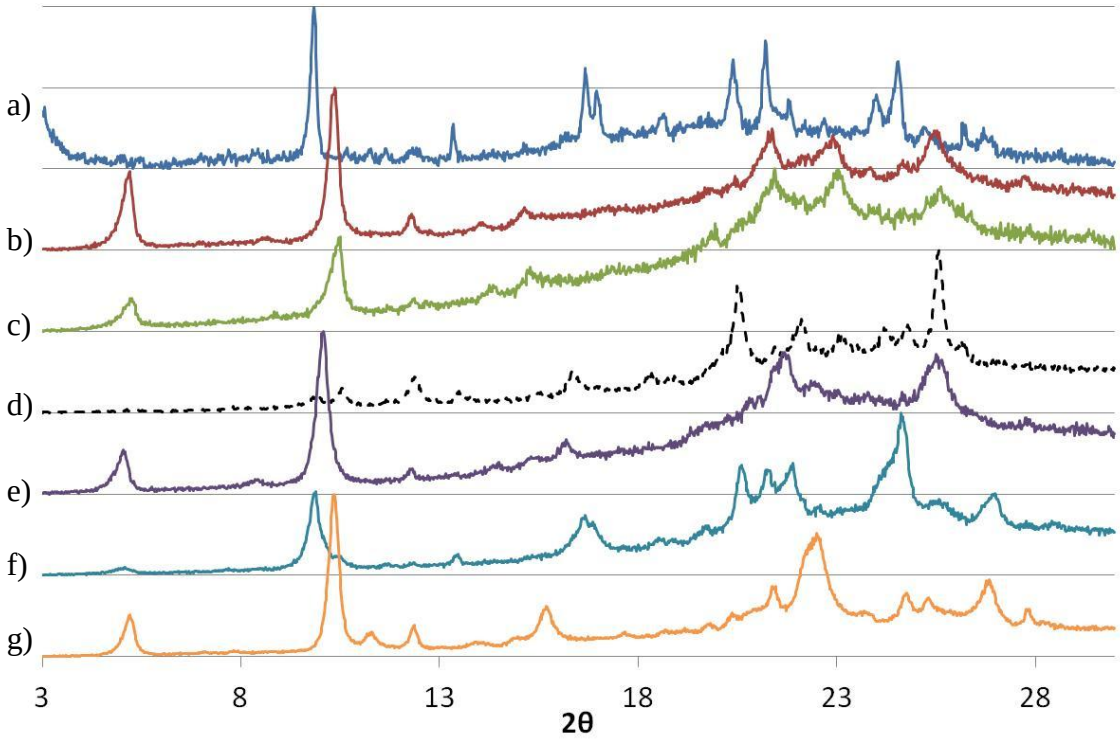

Figure 43 XRPD patterns corresponding to xerogels formed from toluene of **16**:**17** in a ratio of a) 1:0 (blue), b) 4:1 (red), c) 3:2 (green), d) 1:1 (dotted black), e) 2:3 (purple), f) 1:4 (light blue), g) 0:1 (orange).

XRPD patterns for the **17**:**20** mixtures show a gradual transition in peak shape from well resolved peaks matching compound **17** to broad peaks corresponding to the pattern of **5** (Figure 44). However, the pattern for the 4:6 mixture of **17**:**20** does not fit with this trend and shows well resolved peaks different from either parent compound. XRPD patterns for the **20**:**19** mixture show a new set of well resolved peaks which do not correspond to either parent compound indicating a new packing motif. However, experiments taken at different compositions showed almost no change in peak shape or position, apart from the 1:1 mixture where only broad peaks were observed. Further work is therefore required to understand the behaviour in these mixed gel systems and the cause of the change in morphology observed by SEM.

The SEM and XRPD results obtained indicate that different gelators in the series interact with each other in different ways. The morphology of the resulting gel fibres may be the same as that of the pure gelators, show only a single fibre type or contain new features not seen for either of the pure compounds. XRPD results indicate that one compound may become incorporated into the packing of a second compound or form completely new packing motifs. As with the pure gelators, the mixed gels may be unstable and rearrange upon drying or

consist of a mixture of different packing motifs and further work is required to fully understand these complex systems.

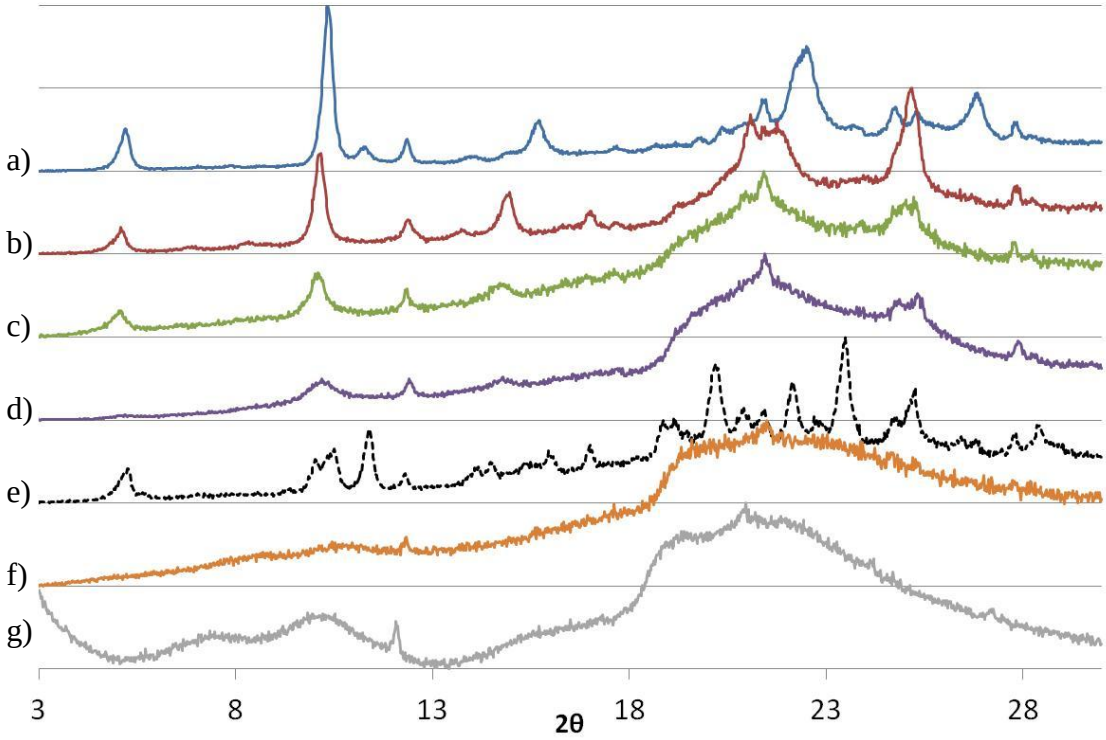

Figure 44 XRPD patterns corresponding to xerogels formed from toluene of **17**:**20** in a ratio of a) 1:0 (blue), b) 4:1 (red), c) 3:2 (green), d) 1:1 (purple), e) 2:3 (dotted black), f) 1:4 (orange) and g) 0:1 (grey).

2.7 Conclusion

A series of amino acid derived supramolecular gelators were synthesised by the reaction of methyl ester protected amino acids with alkylene spaced diisocyanates of different lengths. Many of the compounds were found to form gels, some in a wide range of solvents and at low concentrations. Subtle changes in amino acid substituent group and spacer length have a profound impact on the range of solvents gelled and the stability, strength and appearance of the gels formed. There was no overall trend in gelation behaviour with increasing size of substituent group or spacer length. Instead, a number of discrete, effective gelator structures were found with deviation from the structures detrimental to gel formation.

In X-ray crystal structures obtained for compounds **16**, **17**, **23**, **24** and **25** the basic conformational and structural features are conserved: antiparallel urea tapes, a conformation involving all-*trans* oligomethylene spacers with the methyl ester groups bent out of the plane

allowing interactions with neighbouring urea stacks. However, the introduction of increasingly bulky substituent groups subtly distorts the conformation of the molecules leading to different packing motifs. Form B of compound **23** contains a second molecular conformation with the oligomethylene spacer *syn* to the urea tape which leads to substantial differences in packing.

Solid state analysis of xerogels formed from various solvents indicates that many of the gelators exhibit polymorphism. For some compounds gel formation appears to correlate with a particular solid form; in other compounds the same packing arrangement may result in gel formation in one solvent but not another. The instability observed for gels of **17** in water can be explained by the transformation of one packing form to another. The form A crystal structures for the alanine and glycine derived gelators show very similar conformations and packing. It therefore particularly interesting that this packing motif gives rise to the gelling form of **23**, but not of compounds **16**, **17** or **24** in toluene.

Electron microscopy shows that all of the xerogels consist of entangled networks of fibres with distinct morphologies. Xerogels of **20** show fine one-dimensional fibrils twisted together into larger fibres whilst other gelators form two-dimensional ribbon-like structures. Distinct ribbon morphologies can be distinguished for the two different polymorphs of **23**. The size, thickness and flexibility of the fibres correlate well with visual observations of the opacity and robustness of the gels.

Rheometry confirmed gel-like behaviour for compounds **16**, **17**, **19**, **20**, **23** and **24** in toluene as well as **20** in ethylacetate. The stronger gels, **17** and **20,** were found to set and break-down at high temperatures and with low critical gelation concentrations. They also showed similar gelation behaviour in a number of other solvent systems.

Mixtures of compounds in this series were found to form co-gels which displayed different morphologies and packing different from those of the pure gelators. Mixtures of compounds **23** and **24** adopted the packing of glycine gelator **23**, whilst the packing in mixtures of **16** and **17** more closely matched that of alanine gelator **17**. Equally remarkably, mixtures of very similar compounds were able to self-assemble into separate fibres showing the same morphology and packing as the pure compounds. Differences in spacer length meant that

mixtures of **20** and **17** formed co-gels with a single morphology, whilst mixtures of **20** and **24** formed separate fibres with distinct morphologies.

Gelation in this series of compounds can usefully be thought of as an arrested crystallisation with entangled networks of highly anisotropic crystals resulting from differences in packing at the molecular level. The extent of polymorphism observed for this class of compounds makes them both interesting and challenging systems to study. However, gels are complex hierarchical structures and the 'right' molecular packing is insufficient to ensure gel formation. Small changes in the molecular structure, solvent composition, sample preparation or the presence of other gelators can have a profound impact upon every level of the gel structure.

2.8 Experimental Section

2.8.1 Source of compounds

Compounds **17**, **21**, **23** and **27** are novel compounds synthesised as part of this work. Compounds **20**, **26** and **30** were originally synthesised by Jonathan Foster as part of work submitted for a masters in Chemistry at the University of Durham. The photographs used in Figure 24 and SEM images used in Figure 37 relating to compound **20** were also submitted as part of the dissertation. Compound **32** was synthesised by Jenifer Cuesta Bernal, a summer student, under the direct supervision of Jonathan Foster. Compounds **16**, **18**, **19**, **22**, **23**, **25**, **28** and **31** were synthesised by MChem student Gary Cameron under the supervision of Jonathan Foster. Compound **29** was synthesised by Dr. Gareth Lloyd.[178] Methods for the production of all of the compounds are included for completeness.

2.8.2 Materials and methods

All solvents and reagents were obtained from standard commercial sources. The drying pistol was evacuated using anaspirator and heated by toluene under reflux. All NMR spectra were performed on a Varian Mercury-400 (400 MHz for 1H), Varian Inova-500 machine (500 MHz for 1H, 126 Hz for $^{13}C\{^{1}H\}$) or a Varian DD-700 (700 MHz for 1H, 176 MHz for ^{13}C) and were referenced to residual solvent. Mass spectroscopy for compounds which dissolve in methanol was undertaken using a Thermo-Finnigan LTQ FT machine running in positive electron spray (ES) mode. Insoluble compounds were measured using a Waters Xevo QTOF spectrometer equipped with an Atmospheric Solids Analysis Probe (ASAP). Elemental analysis was performed using an Exeter Analytical inc. CE-400 Elemental Analyser.

Fourier transform infrared spectra were recorded with a Perkin Elmer Spectrum 100 ATR instrument (Perkin-Elmer, Norwalk, Ct., USA). For each spectrum, 16 scans were conducted over a spectral range of 4000 to 600 cm^{-1} with a resolution of 4 cm^{-1}. Powder diffraction was performed on glass slides using a Brucker D8 or D5000 X-Ray Diffractometers using CuKα radiation at a wavelength of 1.5406 Å. Differential scanning calorimetry was undertaken on a Perkin Elmer Pyris 1 DSC or TA instruments Q1000 DSC using 1 mg of sample weighed into the centre of an aluminium pan and heated from 0-220°C at 10°C per minute.

Suitable single crystals were mounted using perflouropolyether on a thin glass fibre or preformed tip. Crystallographic measurements were carried out using a Bruker SMART 6K (6000 CCD), Oxford Diffraction Gemini or Kappa Rigaku Saturn 724+. The instruments are equipped with a graphite monochromatic Mo-Kα radiation (λ = 0.71073) or synchrotron radiation (λ = 0.68890) . The data collection temperature was maintained using by an open flow N_2 Oxford Cryostream device. Integration was carried out using SAINT, CrysAlisPro or Crystal Clear software. Data sets were corrected for Lorentz and polarization effects and for the effects of absorption. Structures were solved using direct methods (SHELXS-97)[182] and developed using alternating cycles of least-squares refinement and difference Fourier synthesis using OLEX2.[183] All non-hydrogen atoms were treated as anisotropic. Hydrogen atoms were fixed in idealised positions and allowed to ride on the parent atom to which they are attached. Hydrogen atom thermal parameters were tied to those of the parent atom. Where possible N-H and O-H hydrogen atoms were located experimentally and their position and displacement parameters refined or their position parameters constrained to ideal distances from the parent atoms. Molecular graphics were produced using the program OLEX2.

Samples prepared for SEM were applied directly to silicon wafer chips (Agar Scientific) using a cocktail stick for gels or pipettes for liquids and the solvent allowed to evaporate. Samples were stored under vacuum at $1x10^{-5}$ mbar then sputter coated with 5nm platinum in a Cressington 328 coating unit, at 40mA (density 21.09 and tooling set at 1) with rotation and a 30^0 angle of tilt. Samples were imaged using a Hitachi S-5200 field emission scanning electron microscope at 1.5kV.

Rheology experiments were performed using a TA Instruments Advanced Rheometer 2000. A 40 mm steel plate geometry was used with a gap of 500 μm and 4 ml of sample in each case. Samples were prepared by weighing 0.04 g of gelator into an 7 ml glass vial along with 4 ml of toluene (1 % w/v). The vials were sealed and heated until the gelator had fully dissolved (care must be taken due to pressure build up). The samples were rapidly cooled in a water bath and briefly sonicated at the first sign of precipitation to ensure homogeneous gel formation. The gel was transfered onto the centre of the plate of the rheometer using a spatula and the plate squashed the gel resulting in the loss of some solvent. Samples of **16**, **23** form A and **24** were prepared by combining four separate 1.7 ml vials each containing 1 ml of gel.

The high temperature form of **23,** form B, was prepared by heating the solid gelator in toluene until a patially gelling precipitate formed which was then applied to the slide using a spatula. Experiments were measured at 20°C and a solvent trap was used to reduce solvent evaporation. Frequency sweep measurements were performed over a range of 1 to 100 Hz with a constant osc. stress of 10 Pa. Oscillatory stress measurements were performed over a range of 0.01-100 % strain at a constant frequency of 1 Hz. Oscillatory stress sweep measurements were preformed over a range of 0.01-300 Pa with a constant frequency value of 1 Hz.

2.8.3 Synthesis

Methyl 2-[6-[(2-methoxy-2-oxo-ethyl)carbamoylamino]hexylcarbamoylamino]acetate (**16**) Glycine methyl ester hydrochloride (1.00 g, 7.96 mmol) was suspended in 30 ml of chloroform and an excess of triethylamine was added, whereupon the suspension dissolved. 1,6-diisocyanatohexane (0.67 g, 3.98 mmol) in 20 ml chloroform solution was added dropwise and the reaction was then left to heat under reflux for 18 hours, after which period a white suspension formed. The suspension was filtered, washed with water and methanol and dried in a heat pistol at 110°C for 1 hour. Compound **16** was isolated as a white powder (1.22 g, 3.50 mmol, 88 %): ^{1}H NMR (500MHz, DMSO-d_6, *J*/Hz): 6.15–6.08 (4H, m, C*N<u>H</u>), 3.75 (4H, d, *J* 6.0, COC<u>H</u>$_2$NH), 3.60 (6H, s, OCH$_3$), 2.96 (4H, dd, *J* 6.7, 12.8, NC<u>H</u>$_2$), 1.38-1.31 (4H, m, NCH$_2$C<u>H</u>$_2$), 1.27-1.20 (4H, m, CH$_2$CH$_2$C<u>H</u>$_2$). ^{13}C{^{1}H} NMR (126MHz, DMSO-d_6, *J*/Hz): 172.5 (s, <u>C</u>OO), 158.6 (s, N<u>C</u>O), 52.2 (s, <u>C</u>H$_3$), 42.1 (s, N<u>C</u>H$_2$), 40.7–39.7 (N<u>C</u>H$_2$CH$_2$ under DMSO residual solvent peak), 30.6 (s, NCH$_2$<u>C</u>H$_2$), 26.8 (s, CH$_2$CH$_2$<u>C</u>H$_2$). m/z (ES$^+$-MS): 347.3 ([M+H]$^+$, 40%), 369.1 ([M+Na]$^+$, 58%), 370.0 ([M+H+Na]$^+$, 100%), 715.5 ([2M+Na]$^+$, 26%). Anal. calc'd for $C_{14}H_{26}N_4O_6$: C, 48.55; H, 7.57; N, 16.17. Found: C, 48.22; H, 7.47; N, 16.00%.

Crystal data for Compound **16** form A, $C_{14}H_{26}N_4O_6$, M = 346.39, colourless plate, 0.01 × 0.008 × 0.002 mm^3 crystallised from water, triclinic space group, $P\bar{1}$ (No. 2), a = 4.635(3) Å, b = 5.659(4) Å, c = 17.929(12) Å, α = 83.189(7)°, β = 83.317(7)°, γ = 69.800(8)°, V = 436.8(5) Å^3, Z = 1, D_c = 1.3167 g/cm^3, F_{000} = 186, Kappa Rigaku Saturn724+, synchrotron radiation, λ = 0.6889 Å, T = 150.15 K, $2\theta_{max}$ = 51.0º, 3661 reflections collected, 1691 unique (R_{int} = 0.0419). Final *GooF* = 1.073, R_1 = 0.0522, wR_2 =

0.135 (all data), *R* indices based on 1243 reflections with $I \geq 2\sigma(I)$ (refinement on F^2), 160 parameters, 0 restraints. Lp and absorption corrections applied, $\mu = 0.097$ mm^{-1}.

Methyl (2S)-2-[6-[[(1S)-2-methoxy-1-methyl-2-oxo-ethyl]carbamoylamino]hexylcarbamoyl amino]propanoate (**17**)

L-alanine methyl ester hydrochloride (3.96 g, 28.5 mmol) was dissolved in 100 ml chloroform and an excess of triethylamine (3 g, 29.7 mmol) was added. 1,6-diisocyanatohexane (2.39 g, 14.25 mmol) was added dropwise then heated under reflux. After 1 hour, the solution was cooled to room temperature and the geletenous precipitate filtered and washed twice with 25 ml of DCM and then once with 25 ml diethyl ether. The resulting solid was sonicated in warm water for 30 minutes then filtered, then recrystallized from methanol, filtered and washed with diethyl ether. The compound was dried in a drying pistol for 30 minutes and the product, **17**, obtained as a white powder (4.12 g, 11.0 mmol, 77 % yield) ^{1}H NMR (700 MHz, DMSO-d$_6$, *J*/Hz): 6.16 (2 H, d, *J* 7.7, C*N<u>H</u>), 5.93 (2 H, t, *J* 5.6, N<u>H</u>CH$_2$), 4.11 (2 H, p, *J* 7.3, C*<u>H</u>), 3.58 (6 H, s, OMe), 2.99 – 2.86 (4 H, m, NHC<u>H$_2$</u>), 1.30 (4 H, d, *J* 6.4, NHCH$_2$C<u>H$_2$</u>), 1.23 – 1.17 (4 H, m, CH$_2$CH$_2$C<u>H$_2$</u>, C*CH$_3$). ^{13}C{^{1}H} NMR (176 MHz, DMSO-d$_6$, *J*/Hz) 174.75 (s, <u>C</u>OO), 157.79 (s, N<u>C</u>O), 52.09 (s, OCH$_3$), 48.55 (s, C*), 40.7–39.7 (N<u>C</u>H$_2$CH$_2$ under DMSO residual solvent peak), 30.36 (s, NCH$_2$<u>C</u>H$_2$), 26.51 (s, CH$_2$CH$_2$C<u>H$_2$</u>), 18.45 (s, C*CH$_3$). m/z (ES$^+$-MS): 375.4 ([M+H]$^+$, 20%), 397.4 ([M+Na]$^+$, 100%), 771.7 ([2M+Na]$^+$, 18%). Anal. calc'd for $C_{16}H_{30}N_4O_6$: C, 51.32; H, 8.08; N, 14.96. Found: C, 51.25; H, 8.26; N, 14.59%.

Crystal data for **17** form A, $C_{16}H_{30}N_4O_6$, M = 374.44, clear colourless plate, 0.01 × 0.008 × 0.003 mm^3 crystallised from methanol, monoclinic space group $P2_1$ (No. 4), a = 4.6814(19) Å, b = 35.331(15) Å, c = 6.149(3) Å, β = 108.562(4)°, V = 964.1(7) Å^3, Z = 2, D_c = 1.2897 g/cm^3, F_{000} = 404, Kappa Rigaku Saturn724+, synchrotron radiation, λ = 0.6889 Å, T = 150.15 K, $2\theta_{max}$ = 55.5°, 8115 reflections collected, 3855 unique (R_{int} = 0.0627). Final *GooF* = 1.758, R_1 = 0.145, wR_2 = 0.399 (all data), *R* indices based on 3504 reflections with $I \geq 2\sigma(I)$ (refinement on F^2), 244 parameters, 0 restraints. Lp and absorption corrections applied, μ = 0.093 mm^{-1}. Absolute structure parameter = -2(3)

Methyl (2S)-2-[6-[[(1S)-1-methoxycarbonyl-2-methyl-propyl]carbamoylamino] hexyl carbamoylamino]-3-methyl-butanoate (**18**)

L-valine methyl ester hydrochloride (1.00 g, 5.97 mmol) was suspended in 30ml of chloroform and an excess of triethylamine was added until the suspension dissolved. 1,6-diisocyanatohexane (0.50 g, 2.98 mmol) in 20ml chloroform solution was added dropwise and the reaction was then heated under reflux for 18 hours. The solution was washed with water and the chloroform reduced on a rotary evaporator, after which the product was isolated by the addition of a small amount of hexane. The remaining solvent was removed by rotary evaporation and then in a drying pistol. Compound **18** was isolated as a white powder (0.76 g, 1.77 mmol, 59%): ^{1}H NMR (500MHz, DMSO-d_6, *J*/Hz): 6.11 (2H, d, *J* 8.9, C*NH), 5.97 (2H, t, *J* 5.6, N<u>H</u>CH$_2$), 4.06 (2H, dt, *J* 5.5, 8.9, C<u>H</u>), 3.61 (6H, s, OCH3), 2.96 (4H, dt, *J* 6.6, 5.6, NHC<u>H</u>$_2$), 1.99–1.92 (2H, m, C<u>H</u>(CH$_3$)$_2$), 1.36–1.31 (4H, m, NHCH$_2$C<u>H</u>$_2$), 1.26–1.21 (4H, m, CH$_2$CH$_2$C<u>H</u>$_2$), 0.85 (6H, d, *J* 6.8, CH(C<u>H</u>$_3$)$_2$), 0.82 (6H, d, *J* 6.9, CH(C<u>H</u>$_3$)$_2$). ^{13}C{^{1}H} NMR (126MHz, DMSO-d_6, *J*/Hz): 174.0 (s, COO), 158.4 (s, N<u>C</u>O), 58.3 (s, <u>C</u>*), 52.2 (s, O<u>C</u>H$_3$), 40.7–39.7 (N<u>C</u>H$_2$CH$_2$ under DMSO residual solvent peak), 31.1 (s, <u>C</u>H(CH$_3$)$_2$), 30.6 (s, NHCH$_2$C<u>H</u>$_2$), 26.8 (s, CH$_2$CH$_2$C<u>H</u>$_2$), 19.7 (s, CH(<u>C</u>H$_3$)$_2$), 18.6 (s, CH(<u>C</u>H$_3$)$_2$). m/z (ES$^+$-MS): 431.3 ([M+H]$^+$, 34%), 453.4 ([M+Na]$^+$, 100%), 454.3 ([M+H+Na]$^+$, 44%), 883.6 ([2M+Na]$^+$, 44%). Anal. calc'd for $C_{20}H_{38}N_4O_6$: C, 55.79; H, 8.90; N, 13.01. Found: C, 55.58; H, 8.89; N, 12.93%.

Methyl (2S)-2-[6-[[(1S)-1-methoxycarbonyl-3-methyl-butyl]carbamoylamino]hexyl carbamoylamino]-4-methyl-pentanoate (**19**)

L-leucine methyl ester hydrochloride (1.00 g, 5.50 mmol) was dissolved in 30 ml of chloroform and an excess of triethylamine added. 1,6-diisocyanatohexane (0.46 g, 2.75 mmol) in 20ml chloroform solution was added dropwise and the reaction was then left stirring at 70°C for 18 hours. The solution was washed with water and the chloroform reduced on a rotary evaporator, after which the product was isolated by the addition of a small amount of diethyl ether. The remaining solvent was removed by rotary evaporation and then in a heat pistol. Compound **19** was isolated as a white powder (1.24g, 2.70mmol, 98%): ^{1}H NMR (500 MHz, DMSO-d_6, *J*/Hz): 6.14 (2H, d, *J* 8.0Hz, C*N<u>H</u>), 5.90 (2H, t, *J* 5.6,N<u>H</u>CH$_2$), 4.15 (2H, dt, *J* 8.0, 7.0, C*<u>H</u>), 3.60 (6H, s,OC<u>H</u>$_3$), 2.95 (4H, dd, *J* 6.6, 12.9, NHC<u>H</u>$_2$), 1.60 (2H, dp, *J* 13.3, 6.6, CH$_2$C<u>H</u>(CH$_3$)$_2$), 1.42 (4H, t, *J* 7.3, C<u>H</u>$_2$CH(CH$_3$)$_2$), 1.35–1.30 (4H, m, NHCH$_2$C<u>H</u>$_2$), 1.24–1.20 (4H, m, CH$_2$CH$_2$C<u>H</u>$_2$), 0.87 (6H, d, *J* 6.6, CH$_2$CH(C<u>H</u>$_3$)$_2$), 0.84 (6H, d, *J* 6.6, CH$_2$CH(C<u>H</u>$_3$)$_2$). ^{13}C{^{1}H} NMR (126MHz, DMSO-d_6, *J*/Hz): 175.0 (s, <u>C</u>OO), 158.3 (s, N<u>C</u>O), 52.3 (s, OC<u>H</u>3), 51.6 (s, <u>C</u>*H), 41.6 (s,

$\underline{C}H_2CH(CH_3)_2$), 40.7–39.7 ($N\underline{C}H_2CH_2$ under DMSO residual solvent peak), 30.6 (s, $NCH_2\underline{C}H_2$), 26.8 (s, $CH_2CH_2C\underline{H}_2$), 25.0 (s, $CH_2\underline{C}H(CH_3)_2$), 23.4 (s, $CH_2CH_2C\underline{H}_2$), 22.2 (s, $CH_2CH_2C\underline{H}_2$). m/z (ES^+-MS): 459.4 ($[M+H]^+$, 90%), 481.5 $[M+Na]^+$, 100%), 482.6 ($[M+H+Na]^+$, 24%), 939.7 ($[2M+Na]^+$, 14%). Anal. calc'd for $C_{22}H_{42}N_4O_6$: C, 57.62; H, 9.23; N, 12.22. Found: C, 57.55; H, 9.18; N, 12.15%.

Methyl (2S)-2-[6-[[(1S)-1-benzyl-2-methoxy-2-oxo-ethyl]carbamoylamino]hexylcarbamoyl amino]-3-phenyl-propanoate (**20**)

L-phenylalanine methyl ester dihydrochloride (1.30 g, 6 mmol) was dissolved in 150 ml chloroform by the slow addition of a slight excess of triethylamine (0.62 g, 6.1 mmol). Following heating and sonication of the mixture a hot filtration was carried out to remove un-dissolved amino acid. 1,6 di-isocynatohexane (0.50 g, 3.0 mmol) was dissolved in 50 ml chloroform and slowly added over a period of 1 hour. The solution was heat under reflux at 70˚C for 24hrs. The chloroform was reduced under vacuum and the compound washed with warm water for 1hour. The suspension was filtered, washed with ethyl acetate and dried in a heat pistol for 30minutes. A white powder (1.26 g, 2.4 mmol, 80%) was obtained and identified as **5**: ^{1}H NMR (700MHz, DMSO-d_6, *J*/Hz): 7.28 (4H, t, *J* 7.6, Ar$\underline{H}$), 7.21 (2H, t, *J* 7.6, Ar$\underline{H}$), 7.15 (4H, d, *J* 7.2, Ar$\underline{H}$), 6.12 (2H, d, *J* 8.3, C*$N\underline{H}_2$), 6.06 (2H, t, *J* 5.8, $CH_2N\underline{H}$), 4.36 (2H, td, *J* 5.5, 8.1,13.6, C*$\underline{H}$), 3.59 (6H, s, $OC\underline{H}_3$), 2.98-2.90 (6H, m, C*CH and $NHC\underline{H}_2$), 2.87 (2H, dd, *J* 8.0, 13.8, C*C$\underline{H}$'), 1.34-1.24 (4H, m,$NHCH_2C\underline{H}_2$), 1.24-1.14 (4H, m, $NHCH_2CH_2C\underline{H}_2$). $^{13}C\{^1H\}$ NMR (176 MHz, DMSO-d_6, *J*/Hz): 173.8 (s, NCO), 158.0 (s, COO), 137.8 (s, Ar$\underline{C}$), 129.9 (s, Ar$\underline{C}$), 129.0 (s, Ar$\underline{C}$), 127.3 (s, Ar$\underline{C}$), 54.7 (s, $\underline{C}$*), 52.4 (s, $O\underline{C}H_3$), 41.0-39.5 (m, DMSO +$NH\underline{C}H_2$), 38.3 (s, C*$\underline{C}H_2$), 30.6 (s, $NHCH_2\underline{C}H_2$), 26.8 (s, $NHCH_2CH_2\underline{C}H_2$). m/z ($ES^+$-MS): 527.3 ($[M+H]^+$, 78%), 549.4 ($[M+Na]^+$, 88%), 1052.6 ($[2M+H]^+$, 13%), 1074.8 ($[2M+Na]^+$, 100%). Anal. Calcd for $C_{28}H_{38}N_4O_6$: C, 63.86; H, 7.27; N, 10.64. Found: C, 63.58; H, 7.24; N, 10.77%.

Methyl (2S)-3-(4-hydroxyphenyl)-2-[6-[[(1S)-1-[(4-hydroxyphenyl)methyl]-2-methoxy-2-oxo-ethyl]carbamoylamino]hexylcarbamoylamino] (**21**)

L-tyrosine methyl ester hydrochloride (1 g, 4.31 mmol) was dissolved in 30 ml chloroform and triethylamine (0.5 g, 5 mmol) added. 1,6- diisocyanatohexane (0.36 g, 2.15 mmol) was added dropwise as a dilute solution in 10 ml chloroform and the mixture heat under reflux at 70°C. After 18 hours an immiscible oil was formed and the chloroform was poured off. The

oil was dissolved in a small volume of methanol and water was added resulting in a white precipitate. The precipitate was dried in a drying pistol and the dry product, **21**, was obtained as a clean white powder (0.5 g, 0.90 mmol) 42%) ^{1}H NMR (700MHz, DMSO-d_6, *J*/Hz): δ_H (700 MHz, dmso-d_6) 9.20 (1 H, s, OH), 6.90 (2 H, d, *J* 8.3, ArH), 6.63 (2 H, d, *J* 8.4, ArH), 6.03 (1 H, t, *J* 5.5, NHCH$_2$), 6.00 (1 H, d, *J* 8.1, C*NH), 4.28 (1 H, dd, *J* 13.7, 7.8, C*H), 3.55 (3 H, s, OCH$_3$), 2.90 (2 H, dd, *J* 12.6, 6.5, NHCH$_2$), 2.79 (1 H, dd, *J* 13.9, 5.7, ArCH$_2$), 2.73 (1 H, dd, *J* 13.7, 7.7, ArCH$_2$), 1.32 – 1.24 (2 H, m, NHCH$_2$CH$_2$CH$_2$), 1.22 – 1.13 (2 H, m, NHCH$_2$CH$_2$CH$_2$). ^{13}C{^{1}H} NMR (176 MHz, DMSO, *J*/Hz) 173.64 (s, NHCONH), 157.77 (s, COO), 156.43 (s, Ar-OH), 130.49 (s, Ar-CH$_2$), 127.42 (s, Ar-H), 115.47 (s, Ar-H), 54.68 (s, CH), 51.99 (s, OCH$_3$), 40.62 – 39.30 (m, DMSO+CH$_2$),37.32 (s,Ar-CH$_2$), 30.32 (s,CH$_2$), 26.51 (s, CH$_2$). Ms: 581.4 (100%, [M+Na]$^+$), 559.1 ([M+H]$^+$) Expected: C 60.20, H 6.86, N 10.03, Found: C 59.66, H 6.85, N 9.98; m/z (ES$^+$-MS): 581.4 ([M+Na]$^+$, 100%)

Methyl (2S)-3-(1H-indol-3-yl)-2-[6-[[(1S)-1-(1H-indol-3-ylmethyl)-2-methoxy-2-oxo-ethyl] carbamoylamino]hexylcarbamoylamino]propanoate (**22**)

L-tryptophan methyl ester hydrochloride (1.00 g, 4.19 mmol) was suspended in 30ml of chloroform and an excess of triethylamine was added, whereupon the suspension dissolved. 1,6-diisocyanatohexane (0.35 g, 2.09 mmol) in 20 ml chloroform solution was added dropwise and the reaction was then left stirring at 70°C for 18 hours. The chloroform was reduced on a rotary evaporator and hexane added to force the product out of solution. The remainder of the solvent was then removed and the product was washed thoroughly with water and dried in a heat pistol. Compound **22** was isolated as a white powder (0.82 g, 1.36mmol, 65%): ^{1}H NMR (500 MHz, DMSO-d_6, *J*/Hz): 10.89 (2H, s, ArNH), 7.44 (2H, d, *J* 7.8, ArH), 7.33 (2H, d, *J* 8.1, ArH), 7.09 (2H, d, *J* 2.2, ArH), 7.05 (2H, t, *J* 7.6, ArH), 6.97 (2H, t, *J* 7.4, ArH), 6.11 (2H, t, *J* 5.5, CH$_2$NH), 6.06 (2H, d, *J* 8.0, C*NH), 4.45 (2H, dt, *J* 7.0, 8.0, C*H), 3.55 (6H, s, OCH$_3$), 3.10–3.00 (4H, m, C*CH$_2$), 2.96–2.91 (4H, m, NHCH$_2$), 1.35–1.28 (4H, m, NHCH$_2$CH$_2$), 1.24–1.18 (4H, m, NHCH$_2$CH$_2$CH$_2$CH$_2$). ^{13}C{^{1}H} NMR (126MHz, DMSO-d_6, *J*/Hz): 174.1 (s, COO), 158.1 (s, NCO), 136.8 (s, ArC), 128.0 (s, ArC), 124.4 (s, ArC), 121.6 (s, ArC), 119.1 (s, ArC), 118.8 (s, ArC), 112.1 (s, ArC), 109.9 (s, ArC), 54.2 (s, C*), 52.3 (s,OCH$_3$), 40.7–39.7 (NHCH$_2$ under residual solvent peak), 30.6 (s, NHCH$_2$CH$_2$), 28.6 (s, C*CH$_2$), 26.8 (s, NHCH$_2$CH$_2$CH$_2$). m/z (ES$^+$-MS): 102.6 ([Et$_3$N+H]$^+$, 100%), 605.3 ([M+H]$^+$, 20%), 627.3 ([M+Na]$^+$, 10%), 706.5 ([M+Et$_3$N]$^+$, 54%), 707.4

([M+H+Et_3N]$^+$, 30%). Anal. calc'd for $C_{32}H_{40}N_6O_6$: C, 63.56; H, 6.67; N, 13.90. Found: C, 61.56; H, 7.14; N, 13.36%.

Methyl 2-[4-[(2-methoxy-2-oxo-ethyl)carbamoylamino]butylcarbamoylamino]acetate (**23**) Glycine methyl ester hydrochloride (1.00 g, 7.96 mmol) was suspended in 30 ml of chloroform and an excess of triethylamine was added, whereupon the suspension dissolved. 1,4-diisocyanatobutane (0.56 g, 3.98 mmol) in 20 ml chloroform solution was added dropwise and the reaction was then left stirring at 70°C for 18 hours, after which period a white suspension formed. The suspension was filtered, leaving a white solid which was then washed with water and dried in a heat pistol. Compound **23** was isolated as a white powder (0.96 g, 3.02 mmol, 76%): ^{1}H NMR (700MHz, DMSO-d_6): 6.13–6.08 (4H, m, NH), 3.73 (4H, d, *J* 6.0, COC$\underline{H}_2$), 3.58 (6H, s, OCH_3), 2.95–2.93 (4H, m, NHC$\underline{H}_2$), 1.32–1.30 (4H, m,$NHCH_2C\underline{H}_2$). ^{13}C{^{1}H} NMR (176MHz, DMSO-d_6): 172.1 (s, $\underline{C}OO$), 158.3 (s, N$\underline{C}O$), 51.9 (s, OC$\underline{H}_3$), 41.8 (s, CO$\underline{C}H_2$), 40.3–39.6 (NH$\underline{C}H_2$ under residual solvent peak), 27.9 (s, $NHCH_2\underline{C}H_2$). m/z (ES$^+$-MS): 102.0 ([Et_3N+H]$^+$, 50%), 319.2 ([M+H]$^+$, 10%), 341.2 ([M+Na]$^+$, 100%), 420.3 ([M+Et_3N]$^+$, 30%), 659.4 ([2M+Na]$^+$, 24%) Anal. calc'd for $C_{12}H_{22}N_4O_6$: C, 45.28; H, 6.97; N, 17.60. Found: C, 45.17; H, 6.98; N, 17.17%.

Crystal data for **23** form A: $C_{12}H_{22}N_4O_6$, *M* =318.34, colourless plate, 2.02 × 0.36 × 0.02 mm^3, oversized uncut crystal due to break up of layers on cutting, crystallised from methanol, triclinic space group $P\bar{1}$ (No. 2), *a* = 4.5954(10) Å, *b* = 5.7140(12) Å, *c* = 15.744(3) Å, α = 96.491(18)°, β = 91.594(17)°, γ = 111.21(2)°, *V* = 381.86(14) Å3, *Z* = 1, D_c = 1.384 g/cm^3, F_{000} = 170, Xcalibur, Sapphire3, Gemini ultra, Mo Kα radiation, λ = 0.7107 Å, *T* = 100.0 K, $2\theta_{max}$ = 58.2º, 5401 reflections collected, 1808 unique (R_{int} = 0.0390). Final *GooF* = 1.055, R_1 = 0.0421, wR_2 = 0.102, *R* indices based on 1492 reflections with $I \geq \sigma(I)$ (refinement on F^2), 144 parameters, 0 restraints

Crystal data for **23** form B: $C_{12}H_{22}N_4O_6$, *M* =318.34, colourless needle, 0.3 × 0.001 × 0.001 mm^3, crystallised from methanol, monoclinic space group $P2_1/n$ (No. 14), *a* = 4.554(3) Å, *b* = 17.528(13) Å, *c* = 10.104(7) Å, β = 101.686(8)°, *V* = 789.8(10) Å^3, *Z* = 2, D_c = 1.339 g/cm^3, F_{000} = 340, Kappa Rigaku Saturn724+, synchrotron radiation, λ = 0.6889 Å, *T* = 393(2) K, $2\theta_{max}$ = 48.5º, 5648 reflections collected, 1369 unique (R_{int} = 0.0869). Final *GooF* = 0.936, R_1 = 0.0665, wR_2 = 0.166, *R* indices based on 844 reflections with *I*

≥2sigma(*I*) (refinement on F^2), 101 parameters, 2 restraints. Lp and absorption corrections applied, $\mu = 0.108$ mm^{-1}.

Methyl (2S)-2-[4-[[(1S)-2-methoxy-1-methyl-2-oxo-ethyl]carbamoylamino]butylcarbamoyl amino]propanoate (**24**)

L-alanine methyl ester hydrochloride (0.94 g, 6.7 mmol) was dissolved in 50 ml chloroform to give a clear solution. An excess of triethylamine (0.7 g, 6.7 mmol) was added resulting in a cloudy suspension which remained at 70°C. 1,4-diisocyanatobutane (0.47 g, 3.3 mmol) was added dropwise. After 1 hour, the solution was cooled to room temperature and a white precipitate filtered and washed with DCM and diethyl ether. The compound was dried in a drying pistol for 30 minutes to give a white powder (0.94 g, 2.7 mmol, 81 % yield). δ H ^{1}H NMR (700 MHz, DMSO-d_6): 6.16 (1 H, d, *J* 7.6, CHN<u>H</u>), 5.94 (1 H, t, *J* 5.7, N<u>H</u>CH_2), 4.11 (1 H, p, *J* 7.3, C*<u>H</u>), 3.58 (3 H, s, OC<u>H</u>$_3$), 3.00 – 2.87 (2 H, m, NHC<u>H</u>$_2$), 1.35 – 1.26 (2 H, m, CH_2CH_2C<u>H</u>$_2$), 1.19 (3 H, d, *J* 7.3, C*C<u>H</u>$_3$). ^{13}C{^{1}H} NMR (176 MHz, DMSO-d_6) 174.74 (s, <u>C</u>OO), 157.77 (s, N<u>C</u>O), 52.10 (s, OCH_3), 48.55 (s, C<u>H</u>), 39.37 (N<u>C</u>H_2CH_2), 27.89 (s, CH_2CH_2C<u>H</u>$_2$), 18.46 (s, C*CH_3). m/z (ES$^+$-MS): 369.4([M+Na]+, 100%), 715.5([2M+Na]+, 30%), 242.4 ([fragment -2COOMe], 30%), 102.2 ([Et_3N+H]$^+$, 2%) Anal. calc'd for $C_{14}H_{26}N_4O_6$: C, 48.55; H, 7.57; N, 16.17. Found: C, 48.20; H, 7.52; N, 15.95%.

Crystal data for **24** form A: $C_{14}H_{26}N_4O_6$, M =346.39, colourless plate, 0.5 × 0.1 × 0.03 mm^3, crystallised from methanol, triclinic, space group *P*1 (No. 1), a = 4.645(2) Å, b = 6.0711(18) Å, c = 16.165(3) Å, α = 93.368(19)°, β = 95.51(2)°, γ = 109.60(3)°, V = 425.4(2) Å3, *Z* = 1, D_c = 1.352 g/cm^3, F_{000} = 186, Bruker SMART CCD 6000 area detector, MoKα radiation, λ = 0.71073 Å, *T* = 120K, $2\theta_{max}$ = 55.0º, 3525 reflections collected, 2807 unique (R_{int} = 0.0849). Final *GooF* = 0.955, R_1 = 0.0806, wR_2 = 0.213, *R* indices based on 2901 reflections with $I > 2\sigma(I)$ (refinement on F^2), 231 parameters, 27 restraints. Lp and absorption corrections applied, $\mu = 0.106$ mm^{-1}.

Methyl (2S)-2-[4-[[(1S)-1-methoxycarbonyl-3-methyl-butyl]carbamoylamino]butylcarbamoyl amino]-4-methyl-pentanoate (**25**)

L-leucine methyl ester hydrochloride (1.00 g, 5.50 mmol) was dissolved in 30 ml of chloroform and an excess of triethylamine added. 1,4-diisocyanatobutane (0.39 g, 2.75 mmol) in 20 ml chloroform solution was added dropwise and the reaction was then left stirring at

70°C for 18 hours. The solution was washed with water and the chloroform reduced on a rotary evaporator, after which the product was isolated by the addition of a small amount of hexane. The remaining solvent was removed by rotary evaporation and then in a heat pistol. Compound **25** was isolated as a white powder (0.71g, 1.65 mmol, 60%): ^{1}H NMR (700 MHz, DMSO-d_6): 6.11 (2H, d, *J* 7.7, C*N<u>H</u>), 5.89 (2H, m, CH_2N<u>H</u>), 4.13 (2H, dt, *J* 7.7, 7.7,C*<u>H</u>), 3.58 (6H, s, OCH_3), 2.93 (4H, m, NHC<u>H</u>$_2$), 1.60–1.55 (2H, m, C<u>H</u>$(CH_3)_2$), 1.40 (4H, t, *J* 7.2, C*C<u>H</u>$_2$), 1.29 (4H, s,$NHCH_2C$<u>H</u>$_2$), 0.85 (6H, d, *J* 6.6, CH(C<u>H</u>$_3)_2$), 0.82 (6H, d, *J* 6.5, CH(C<u>H</u>$_3)_2$). ^{13}C{^{1}H} NMR (176 MHz, DMSO-d_6): 174.7 (s, <u>C</u>OO), 158.0 (s, N<u>C</u>O), 52.0 (s, O<u>C</u>H_3), 51.3 (s, <u>C</u>*H), 41.3 (s, C*<u>C</u>H_2), 40.4–39.5 (NH<u>C</u>H_2 under residual solvent peak), 27.9 (s,$NHCH_2$<u>C</u>H_2), 24.7 (s, <u>C</u>H$(CH_3)_2$), 23.2 (s, CH(<u>C</u>$H_3)_2$), 22.0 (s, CH(<u>C</u>$H_3)_2$). m/z (ES$^+$-MS): 431.4 ([M+H]$^+$, 26%), 453.4 ([M+Na]$^+$, 100%), 454.3 ([M+H+Na]$^+$, 30%), 885.4 ([2M+Na]$^+$, 5%). Anal. calc'd for $C_{20}H_{38}N_4O_6$: C, 55.79; H, 8.90; N, 13.01. Found: C, 55.75; H, 8.94; N, 13.02%.

Crystal data for **25** form A: $C_{20}H_{38}N_4O_6$, *M* =430.55, colourless plate, 0.01 × 0.008 × 0.003 mm^3 crystallised from acetonitrile, orthorhombic space group $P2_12_12_1$ (no. 19), *a* = 4.724(3) Å, *b* = 19.611(11) Å, *c* = 25.402(14) Å, *V* = 424.72 2354 (2) Å^3, *Z* = 4, D_c = 1.2150 g/cm^3, F_{000} = 935.8280, Kappa Rigaku Saturn724+, synchrotron radiation, λ = 0.6889 Å, *T* = 150.15 K, $2\theta_{max}$ = 48.5º, 13222 reflections collected, 2333 unique (R_{int} = 0.0644). Final *GooF* = 1.058, R_1 = 0.0547, wR_2 = 0.149, *R* indices based on 1812 reflections with *I*>=2σ(*I*) (refinement on F^2), 349 parameters, 24 restraints. Lp and absorption corrections applied, μ = 0.084 mm^{-1}.

Methyl (2S)-2-[4-[[(1S)-1-benzyl-2-methoxy-2-oxo-ethyl]carbamoylamino]butylcarbamoyl amino]-3-phenyl-propanoate (**26**)

L-phenylalanine methyl ester dihydrochloride (0.65 g, 3.02 mmol) was dissolved in 200 ml chloroform by the slow addition of a slight excess of triethylamine (0.32 g, 3.17 mmol). The mixture was filtered to remove undissolved amino acid. 1,4 di-isocynatobutane (0.22 g, 1.58 mmol) was dissolved in 50 ml chloroform and slowly added over a period of 1 hour. The solution was heated under reflux at 70˚C for 60 h. The chloroform was reduced under vacuum and the compound washed with warm water for 1 hour. The suspension was filtered, washed with ethyl acetate and dried in a heat pistol for 30minutes. A white powder (0.58 g, 1.16 mmol, 73%) was obtained and identified as **11**. ^{1}H NMR (700MHz, DMSO-d_6, *J*/Hz):

7.25 (4H, t, *J* 7.45, ArH), 7.18 (2H, t, *J* 7.31, ArH), 7.12 (4H, d, *J* 7.31, ArH), 6.09 (2H, d, *J* 8.10, C*NH), 6.04 (2H, t, *J* 5.65, CH_2NH), 4.37 (2H, dd, *J* 7.90, 13.6, C*H), 3.56 (6H, s, OCH_3), 2.92 (2H, dd, *J* 5.5, 14.0,C*CH), 2.89 (4H, d, *J* 5.61, NHCH_2), 2.85 (2H, dd, *J* 8.0, 13.5, C*CH'), 1.25 (4H, s, NHCH$_2$CH_2). $^{13}C\{^1H\}$ NMR (700MHz, DMSO-d_6, *J*/Hz): 173.5 (s, COO), 157.7 (s, NCO), 137.6 (s, ArC), 129.6 (s, ArC), 128.7 (s, ArC), 127.0 (s, ArC), 54.4 (s, C*H), 52.0 (s, OCH_3), 39.3 (s, NHCH_2), 38.1 (s, C*CH_2, 27.8 (s, NHCH$_2$CH_2). m/z (ES^+-MS): 499.3 ($[M+H]^+$, 15%), 521.4 ($[M+Na]^+$, 100%), 996.7 ($[2M]^+$, 8%) Anal. Calcd for $C_{26}H_{36}N_4O_6$: C, 62.63; H, 6.87; N, 11.24. Found: C, 61.65; H, 6.91; N, 11.28 %.

Methyl (2S)-3-(4-hydroxyphenyl)-2-[4-[[(1S)-1-[(4-hydroxyphenyl)methyl]-2-methoxy-2-oxo-ethyl]carbamoylamino]butylcarbamoylamino]propanoate (**27**)

L-tyrosine methyl ester hydrochloride (1 g, 4.31 mmol) was dissolved in 30 ml chloroform and triethylamine (0.5 g, 5 mmol) added. 1,4- diisocyanatobutane (0.3 g, 2.15 mmol) was added dropwise as a dilute solution in 20 ml chloroform. An immiscible oil formed after 1 hour and the chloroform was poured off. Attempts to purify the oil by precipitation from methanol by the addition of water produced a gluey precipitate. This was redissolved in methanol and dried with magnesium sulphate and filtered. Addition of diethyl ether produced a white precipitate which could not be filtered. Reduction of the mixture on a rotorary evaporator at 40°C initially produced an oil and eventually a white foam which was ground and dried in a drying pistol. The product, **27**, was isolated as a white solid (0.6 g, 1.13 mmol) 53%). ^1H NMR (500MHz, DMSO-d_6, *J*/Hz): 9.24 (1 H, s, OH), 6.902 (2 H, d, *J* 8.5, ArH), 6.63 (2 H, d, *J* 8.5, ArH), 6.08 (1 H, t, *J* 5.6, NHCH_2), 6.04 (1 H, d, *J* 8.2, C*NH), 4.30 (1 H, q, *J* 4.3, C*H), 3.57 (3 H, s, OCH_3), 2.92 (2 H, d, *J* 5.7, NHCH_2), 2.78 (1 H, qd, *J* 13.8, 6.6, ArCH_2), 2.73 (1 H, dd, *J* 13.7, 7.7, ArCH_2), 1.28 (2 H, m, $NHCH_2$). $^{13}C\{^1H\}$ NMR (176 MHz, DMSO, *J*/Hz) 173.91 (s, NHCONH), 158.01 (s, COO), 156.70 (s, Ar-OH), 130.75 (s, Ar-CH_2), 127.66 (s, Ar-H), 115.74 (s, Ar-H), 54.94 (s, CH), 52.27 (s, OCH_3), 40.62 – 39.30 (m, DMSO+CH_2), 37.59 (s,Ar-CH_2), 28.09 (s,CH_2). m/z (ES^+-MS): 531.4($[M+H]^+$, 15%) 553.4 ($[M+Na]^+$, 100%), 569.3 ($[M+K]^+$, 15%). Anal. calc'd for $C_{26}H_{34}N_4O_8$: C, 58.86; H, 6.46; N, 10.56%. Found: C, 58.17; H, 6.54; N, 10.45%.

Methyl (2S)-3-(1H-indol-3-yl)-2-[4-[[(1S)-1-(1H-indol-3-ylmethyl)-2-methoxy-2-oxo-ethyl] carbamoylamino]butylcarbamoylamino]propanoate (**28**)

L- tryptophan methyl ester hydrochloride (1.00 g, 4.19 mmol) was suspended in 30 ml of chloroform and an excess of triethylamine was added, whereupon the suspension dissolved. 1,4-diisocyanatobutane (0.29 g, 2.09 mmol) in 20 ml chloroform solution was added dropwise and the reaction left overnight at ambient temperature. The chloroform was reduced on a rotary evaporator and the solid product was isolated by the addition of hexane. The remaining solvent was removed by rotary evaporation and the solid washed thoroughly with water before drying in a heat pistol. **28** was isolated as an off-white powder (0.75 g, 1.30 mmol, 62%): ^{1}H NMR (500MHz, DMSO-d_6): 10.88 (2H, s, ArH), 7.44 (2H, d, *J* 8.0, ArH), 7.33 (2H, d, *J* 8.1, ArH), 7.09 (2H, d, *J* 2.3, ArH), 7.06 (2H, t, *J* 7.1, ArH), 6.97 (2H, t, *J* 7.4, ArH), 6.12 (2H, t, *J* 7.4, CH_2NH), 6.07 (2H, d, *J* 8.1, C*NH), 4.45 (2H, dt, *J* 6.7, 8.1, C*H), 3.55 (6H, s, OCH_3), 3.05 (4H, m, C*CH_2), 2.94 (4H, d, *J* 5.5, NHCH_2), 1.30 (4H, m, NHCH$_2$CH_2). ^{13}C{^{1}H} NMR (126MHz, DMSO-d_6): 174.1 (s, COO), 158.1 (s, NCO), 136.8 (s, ArC), 127.9 (s, ArC), 124.4 (s, ArC), 121.6 (s, ArC), 119.1 (s, ArC), 118.8 (s, ArC), 112.1 (s, ArC), 109.9 (s, ArC), 54.1 (s, C*H), 52.3 (s, OCH_3), 40.7–39.6 (NHCH_2 under residual solvent peak), 28.6 (s, C*CH_2), 28.2 (s, NHCH$_2$CH_2). m/z (ES$^+$-MS): 599.3 ([M+Na]$^+$, 100%). Anal. calc'd for: $C_{30}H_{36}N_6O_6$: C, 62.49; H, 6.29; N, 14.57. Found: C, 61.09; H, 6.40; N, 14.20%.

Methyl (2S)-2-[6-[[(1S)-1-methoxycarbonyl-2-methyl-propyl]carbamoylamino]ethyl carbamoylamino]-3-methyl-butanoate (**29**)[178]

Methyl (2S)-2-[4-[[(1S)-1-benzyl-2-methoxy-2-oxo-ethyl]carbamoylamino]octylcarbamoyl amino]-3-phenyl-propanoate (**30**)

L-phenylalanine methyl ester dihydrochloride (1.099 g, 5.1 mmol) was dissolved in 150ml chloroform by the slow addition of a slight excess of triethylamine (0.515g, 5.1mmol). Following heating and sonication of the mixture, a hot filtration was carried out to remove un-dissolved amino acid. 1,6 di-isocynatohexane (0.50 g, 2.6 mmol) was dissolved in 50ml chloroform and slowly added over a period of 1 hour. The solution was heated under reflux at 70˚C for 24 h. The chloroform was reduced under vacuum and the compound washed with warm water for 1hour. The suspension was filtered, washed with ethyl acetate and dried in a heat pistol for 30 minutes. A white powder (1.12 g, 2.0 mmol, 77%) was obtained and identified as **30**: ^{1}H NMR (700MHz, DMSO-d_6, *J*/Hz): 7.27 (4H, t, *J* 7.2, ArH), 7.20 (2H, t, *J* 7.2, ArH), 7.14 (4H, d, *J* 7.3, ArH), 6.10 (2H, d, *J* 8.1, C*NH), 6.04 (2H, t, *J* 5.4, CH_2NH),

4.38 (2H, dd, *J* 7.9, 13.6, C*H), 3.58 (6H, s, OCH_3), 2.97-2.86 (6H, m, C*CH and NHCH_2), 2.86 (2H, dd, *J* 8.1, 13.6, C*CH'), 1.33-1.24 (4H, m, NHCH_2CH_2), 1.24-1.13 (8H, m, NHCH_2CH_2CH_2 and NHCH_2CH_2CH_2CH_2). $^{13}C\{^1H\}$ NMR (700MHz, DMSO-d_6, *J*/Hz): 173.8 (s, COO), 158.0 (s, NCO), 137.9 (s, ArC), 129.8 (s, ArC), 128.9 (s,ArC), 127.2 (s, ArC), 54.7 (s, C*H), 52.4 (s, OCH_3), 40.8-39.8 (m, DMSO + NCH_2), 38.3 (s, C*CH_2), 30.6 (s, NHCH_2CH_2), 29.5 (s, NHCH_2CH_2CH_2), 27.0 (s, NHCH_2CH_2CH_2CH_2). m/z (ES^+-MS): 555.4 ($[M+H]^+$, 21%), 577.4 ($[M+Na]^+$, 100%), 1130.9 ($[2M+Na-2H]^+$, 68%). Anal. Calcd for $C_{28}H_{38}N_4O_6$: C, 64.96; H, 7.63; N, 10.10. Found: C, 64.73; H, 7.60; N, 9.93 %.

Methyl 2-[6-[(1-methoxycarbonyl-3-methyl-butyl)carbamoylamino]dodecylcarbamoylamino] -4-methyl-pentanoate (**31**)

L-leucine methyl ester hydrochloride (1.00g, 5.50mmol) was dissolved in 30 ml of chloroform and an excess of triethylamine added. 1,12-diisocyanatododecane (0.69 g, 2.75 mmol) in 20 ml chloroform solution was added dropwise and the reaction was then left stirring at 70°C for 18 hours. The solution was washed with water and the chloroform reduced on a rotary evaporator, after which the product was isolated by the addition of a small amount of hexane. The remaining solvent was removed by rotary evaporation and then in a heat pistol. Compound **31** was isolated as a white powder (0.74 g, 1.36 mmol, 50%): ^1H NMR (700 MHz, DMSO-d_6): 6.09 (2H, d, *J* 7.7, C*NH), 5.86 (2H, t, J=5.6, CH_2NH), 4.13 (2H, dt, *J* 7.9, 7.7,C*H), 3.57 (6H, s, OCH_3), 2.96–2.89 (4H, m, NHCH_2), 1.61–1.55 (2H, m, CH(CH_3)$_2$), 1.40 (4H, t, *J* 7.3, C*CH_2), 1.33–1.28 (4H, m, NHCH_2CH_2), 1.22–1.20 (16H, s, -CH_2-), 0.85 (6H, d, *J* 6.7, CH(CH_3)$_2$), 0.82 (6H, d, *J* 6.7, CH(CH_3)$_2$). $^{13}C\{^1H\}$ NMR (176MHz, DMSO-d_6): 174.7 (s, COO), 158.0 (s, NCO), 52.0 (s, OCH_3), 51.3 (s, C*H), 41.3 (s,C*CH_2), 40.3–39.6 (NHCH_2 under solvent residual peak), 30.4 (s, -CH_2-), 29.5 (s, -CH_2-), 29.2 (s, -CH_2-), 26.8 (s, -CH_2-), 24.7 (s, -CH_2-), 23.2 (s, CH(CH_3)$_2$), 22.0 (s, CH(CH_3)$_2$). m/z (ES^+-MS): 543.6 ($[M+H]^+$, 100%), 566.5 ($[M+Na]^+$, 10%). Anal. calc'd for $C_{28}H_{54}N_4O_6$: C, 61.96; H, 10.03; N, 10.32. Found: C, 61.50; H, 9.92; N, 10.09%.

Methyl (2S)-2-[[4-[[3,5-diethyl-4-[[(1S)-1-methoxycarbonyl-3-methyl-butyl]carbamoyl amino]phenyl]methyl]-2,6-diethyl-phenyl]carbamoylamino]-4-methyl-pentanoate (**32**)

N_ε-Boc-*l*-lysine methyl ester hydrochloride (0.5 g, 1.7 mmol) was dissolved in 75 ml chloroform by the slow addition of a slight excess of triethylamine (0.182 g, 1.80 mmol). To the clear solution was added 1,6 di-isocyanatohexane (0.135 g, 0.80 mmol) in 25 ml

chloroform and the resulting solution was heated under reflux for 18 hours. A solution was obtained which was washed with water (5 ml, twice), dried with $MgSO_4$ and filtered. The chloroform was removed under vacuum and a yellow oil obtained. The oil was partially dissolved in DCM and diethyl ether added resulting in a cloudy suspension which rapidly gelled. The mixture of solvents was reduced under vacuum and a white powder was recovered (0.39 g, 0.56 mmol, yield: 67 %) and identified as the product **32**: ^{1}H NMR (700MHz, DMSO-d_6, J/Hz): 6.73 (1H, t, *J* 5.2, N<u>H</u>Boc), 6.14 (1H, d, *J* 8.3, CHN<u>H</u>), 5.93 (1H, t, *J* 5.2, N<u>H</u>CH_2), 4.02 (1H, dd, *J* 6.8, 13.0, C<u>H</u>), 3.14 (3H, s, OCH_3), 2.91 (2H, dd, *J* 8.0, 13.2 , NHC<u>H</u>$_2$), 2.82 (2H, dd, *J* 6.8, 13.0, C<u>H</u>$_2$NHBoc), 1.55 (2H, m, CHC<u>H</u>$_2$),1.54 (9H, s, C(C<u>H</u>$_3$)$_3$), 1.46 (2H, m, -CH_2-), 1.32 (2H, m, -CH_2-), 1.30 (2H, m, NHCH$_2$C<u>H</u>$_2$), 1.19 (2H, m,$CH_2CH_2CH_2$). m/z (ES$^+$ MS): 711,4 ([M+Na$^+$], 100%), 689,4 ([M], 20%). Anal. Cal for: $C_{32}H_{61}N_6O_{10}$: C 55,80; H 8,78; N 12,20. Found: C 54,83; H 9.00; N 12.01

Chapter 3: The use of 1- and 2-pyrenylalanine derived gelators as fluorescent probes in anion responsive supramolecular gels

3.1 Introduction

Incorporating fluorescent functionality into supramolecular gels has been used to gain insights into gel structure and formation and has led to a number of novel applications.[10, 85, 109, 126, 184-189] Aggregation of molecules from solution into the gel state can bring about changes in fluorescence such as a decrease,[190] increase [191, 192] or shifts in the wavelength of particular bands observed in the emission spectrum.[184] Fluorescent gelators have been utilised in a variety of sensing applications,[10, 85, 185, 186] for light harvesting,[187] in re-writable materials for fluorescence imaging[126] and as models for drug delivery.[193]

Pyrene derivatives have been used extensively as fluorophores in a variety of applications ranging from monitoring oxygen levels[194] and DNA charge transfer [195] in biological systems[196] to uses in organic light emitting diodes (OLEDs) and organic field effect transistors (OFETs).[197] The high sensitivity of the vibronic fine structure of pyrene and its derivatives to changes in chemical environment (the Ham effect),[198] their long-lived fluorescence and the formation of fluorescent excimers via π-π interactions make pyrene particularly useful as a fluorescent probe. Extended aromatic ring systems such as pyrene have also been used to drive gel formation through π-stacking interactions.[188, 189]

Pyrene is usually functionalised at the 1-, 3-, 6- or 8- positions where the maximum contributions of the HOMO lie making it most amenable to electrophilic aromatic substitution. Substitution of pyrene at the 2- or 7-carbon atoms is synthetically challenging as a nodal plane in both the HOMO and LUMO passes through these positions. However, by derivatising at these nodal positions, substituents interact less strongly with the pyrene orbitals than at other positions leading to more 'pyrene-like' fluorescence.[199]

Chapter 2 describes the gelation behaviour of a series of oligo-methylene spaced bis-urea gelators functionalised with a number of amino acid derivatives. In this chapter we extend this series of natural amino-acids to include synthetic 1- and 2-pyrenylalanine derivatives, **35** and **36**. It was anticipated that use of the same bis-urea oligomethylene core would mean the pyrenyl derivatives would become incorporated into the urea backbone of the other gelators

to give mixed gels.[39, 51, 101, 200, 201] The fluorescent pyrene functionality can then be used to provide additional information about the structure, properties and response to anions of the different mixed gels.

3.2 1- and 2- Pyrenylalanine gelators

3.2.1 Synthesis of gelators

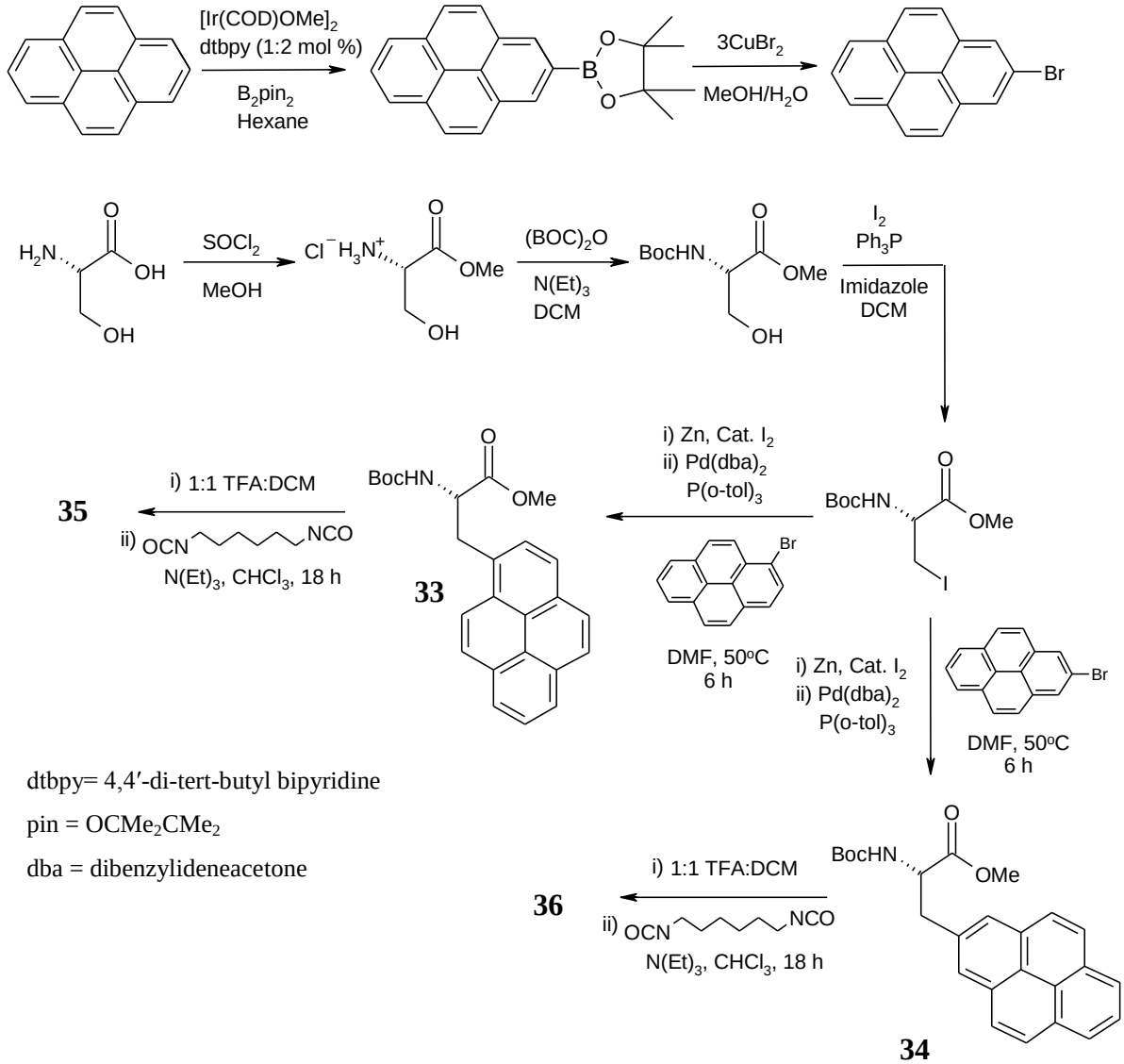

Scheme 2 Synthesis of a) 2-bromo pyrene b) 1- and 2- pyrenylalanine derived amino acids **33** and **34** and gelators **35** and **36**.

The 2-bromo pyrene was synthesised by Dr. Andrew Crawford using an iridium catalysed borylation.[202, 203] Selectivity for the 2-position was achieved due to the sterically crowded five-coordinate fac-tris(boryl)species. 1-Bromo pyrene was synthesised using aqueous

hydrobromic acid and hydrogen peroxide.[204] The 1- and 2- pyrenylalanine methyl esters **33** and **34** were synthesised by Dr. Neil Colgin using a versatile strategy for the synthesis of artificial amino acids (Scheme 2). The *l*-iodoalanine precursor is prepared in four steps starting from *l*-serine. A Negishi coupling reaction[205-207] is then used to connect *l*-iodoalanine to either 1- or 2- bromo pyrene.

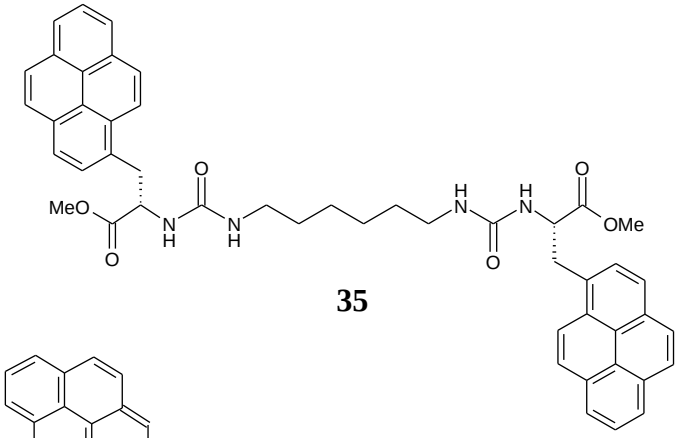

35

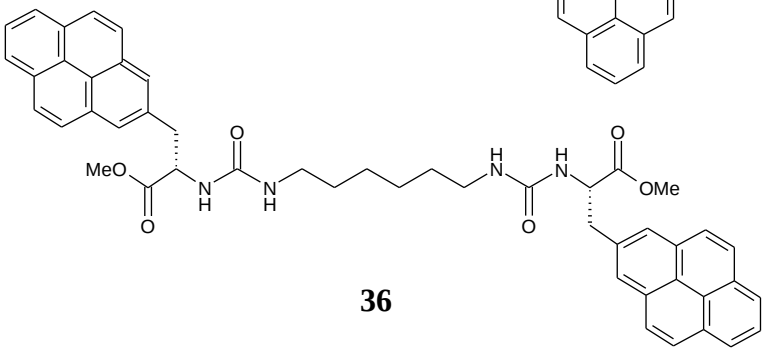

36

Compounds **35** and **36** were synthesised from the corresponding 1- and 2- pyrenylalanine methylester BOC-protected amino acids. The BOC-groups are readily removed by dissolving **33** or **34** in 1:1 DCM:trifluoracetic acid and stirring at room temperature for 30 minutes. Following removal of the solvent and neutralisation with triethylamine, the deprotected amine then reacts in a 2:1 ratio with 1,6-diisocyanatohexane to give compounds **35** and **36**. The resulting products are insoluble and are filtered from the reaction mixture and washed with water. The products were isolated as beige solids, dried in a heating pistol and ground before use. Less than 100 mg of each compound was synthesised due to the difficulty in producing the pyrenylalanine amino acids.

3.2.2 Gelation behaviour

The gelation behaviour of **35** and **36** was investigated at 1 % w/v in a range of solvents. Samples were tested using 0.2 ml of solvent in 1.75 ml vials owing to the small amount of **35** and **36** available. The compounds were generally poorly soluble in most of the solvents tested and required high temperatures and sonication to fully dissolve. Once dissolved, samples were cooled rapidly and briefly sonicated to aid homogeneous gel formation. The results are summarised in Table 5 and compared with those obtained for glycine, alanine and phenylalanine derived gelators **16**, **17** and **20** discussed in detail in Chapter 2.

Table 5 Phase upon cooling of hot 1 % w/v solutions of **16**, **17, 20, 35** and **36** in a range of solvents

Solvent	**Compound** (*n*=6 and amino acid from which derived)				
	16	**17**	**20**	**35**	**36**
	Gly	Ala	Phe	1-Pyr	2-Pyr
Water	P	G[a]	I	I	I
DMSO	S	S	S	S	S
Acetonitrile	P	G	G	G	G
Methanol	P	S	S	PG	G
Ethanol	P	G[a]	S	G	G
Acetone	P	G	G	G	I
THF	P	G	S	G	G
DCM	P	PG	S	G	I
Ethylacetate	P	G	G	PG	I
Chloroform	P	G	S	G	G
Diethylether	I	I	I	I	I
Toluene	G	G	G	G	P
Hexane	I	I	I	I	I

P = precipitate, S = solution, G = gel, PG = partial gel, O = oil, I = insoluble with heating, superscript a = gel unstable, breaks down over time.

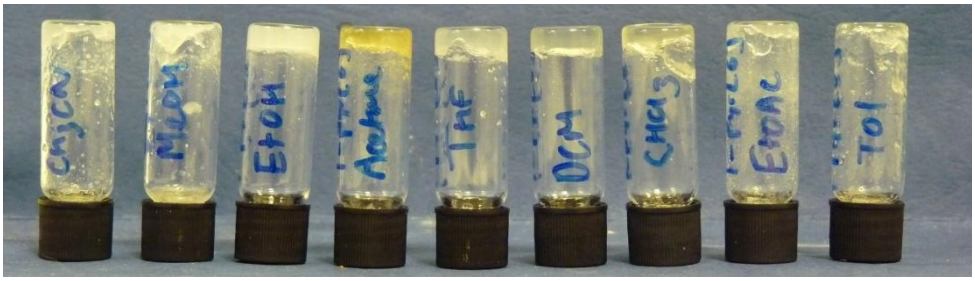

Figure 45 Gels containing 1 % w/v **35** in (left to right): acetonitrile, methanol, ethanol, acetone, tetrahydrofuran, dichloromethane, chloroform, ethyl acetate and toluene.

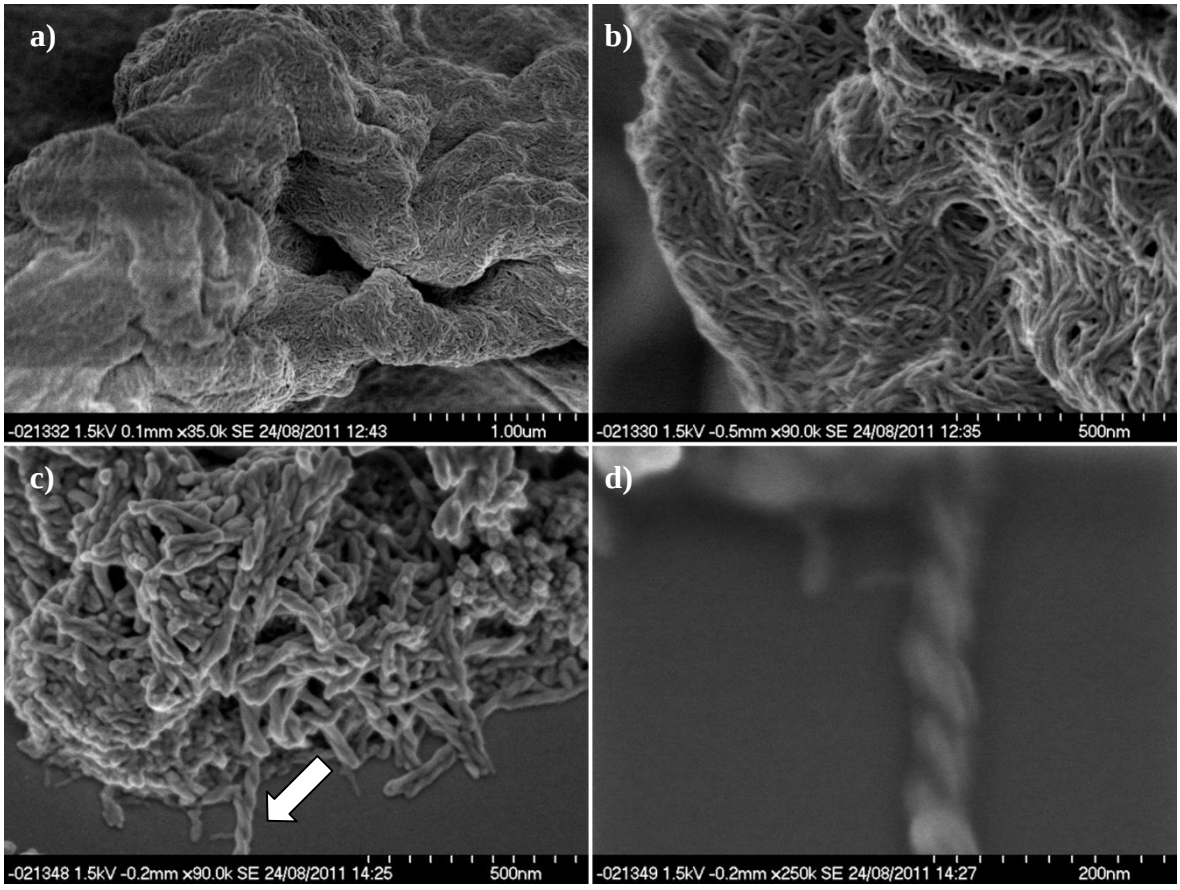

Figure 46 SEM images showing the morphology of 1 % w/v xerogels of **35** shown at various magnifications produced from : a) acetonitrile b) chloroform c) methanol, d) methanol. Arrow indicates position of twisted fibre seen in image d) in image c).

The 1-pyrenylalanine derived gelator **35** formed gels in a wide range of solvents across the polarity spectrum. The gels were translucent with a light yellow colour which was more intense in the acetone sample. Some of the gels (acetonitrile, ethanol, acetone, THF, DCM, $CHCl_3$) were robust, formed readily and were stable over a period of several weeks. Other gels, particularly methanol and ethyl acetate formed only weak, partial gels. SEM revealed a morphology consisting of an entangled network of fine, flexible fibres approximately 50nm in width (Figure 46). The fibres take the form of left handed helices, an effect attributed to the chirality of the molecules.[52, 174, 181] The morphology is consistent across the range of solvents investigated.

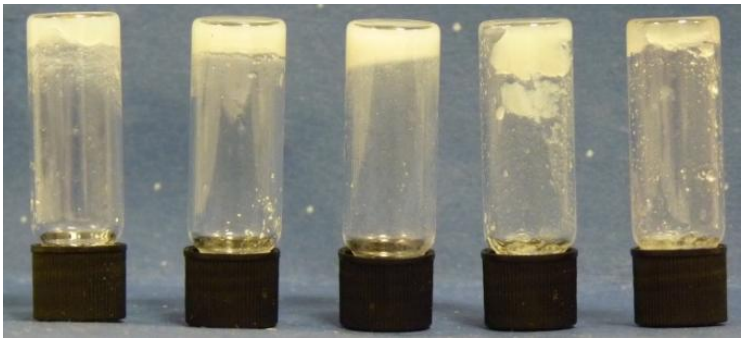

Figure 47 Gels of **36** at 1 % w/v in (left to right): acetonitrile, methanol, ethanol, tetrahydrofuran, chloroform

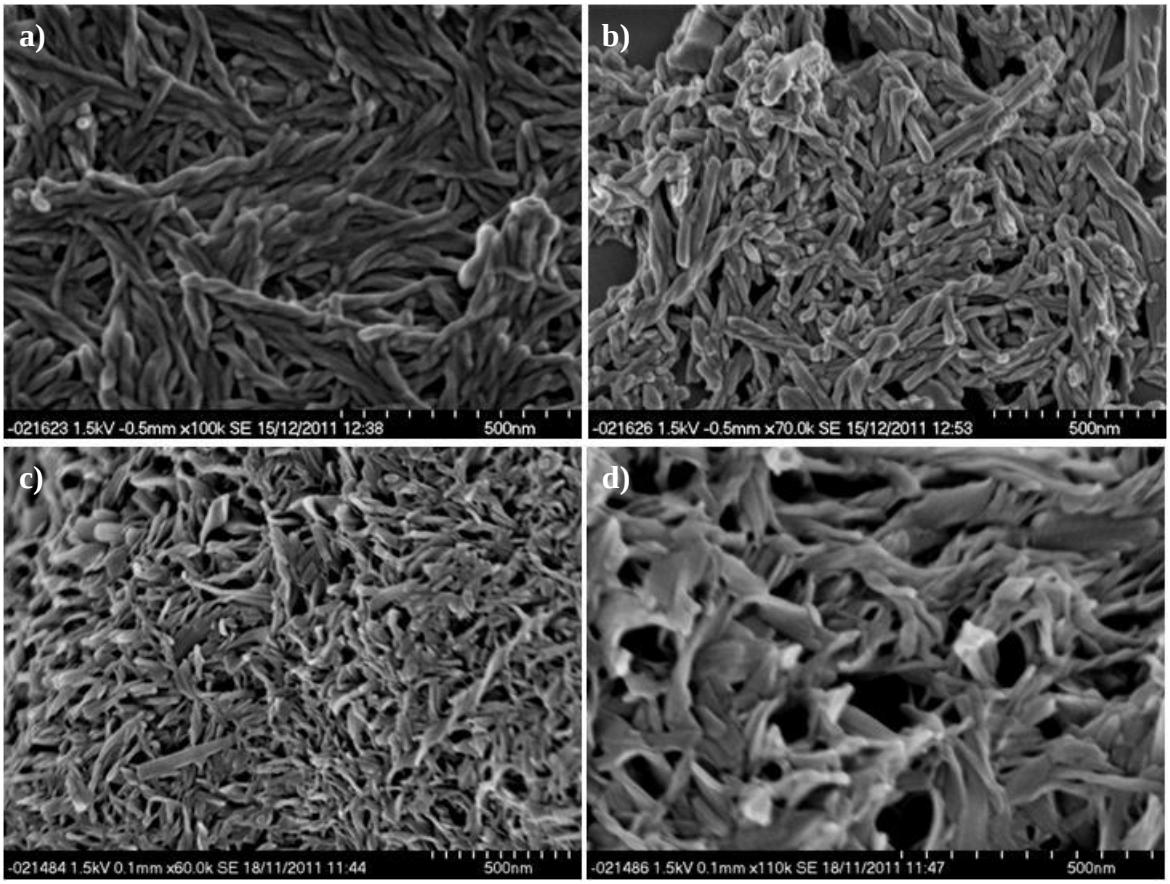

Figure 48 SEM images showing the morphology of 1 % w/v xerogels of **36** shown at various magnifications produced from: a) and b) toluene c) acetonitrile d) methanol

The 2-pyrenylalanine derived gelator **36** also formed gels across a range of solvents. The compound is generally poorly soluble and there were difficulties dissolving the compound, particularly in volatile solvents such as acetone, DCM and ethyl acetate. It may be possible to form gels in acetone, DCM and ethylacetate if the method was scaled up as the large volume of the vials (1.7 ml) relative to the volume of solvent (0.2 ml) means that much of the solvent is in the gas phase. However, repeated attempts to form gels of **36** on a larger scale in toluene

were unsuccessful. Electron microscopy revealed fine helical cylinders in xerogels of **36** formed from acetonitrile, chloroform and methanol, similar to those observed in gels of **35** (Figure 48). Fine fibres are also identifiable in SEM images of the non-gelling precipitate of **36** formed in toluene, however they have a flatter, less well-defined shape (Figure 48a and b). It is interesting to note that a small difference in the orientation of the pyrene group between the two isomers translates into a difference in gelation behaviour and fibre morphology.

3.2.3 Fluorescence of 1- and 2- pyrenylalanine gelators

Pyrene shows a number of photophysical features which make it ideal as a fluorescent probe. The pyrene monomer shows vibrational fine structure with five characteristic vibronic bands: I = 373 nm, II = 379 nm, III = 383 nm, IV = 389 nm, V = 393 nm.[208] The first band (I) belongs to a forbidden transition which can be enhanced in more polar solvent environments due to interactions between the excited single state and the solvent dipole, a phenomenon known as the Ham effect.[198] By referencing the intensity of band I against a strong transition, such as band III, the III/I ratio can be used to give an indication of the polarity of the pyrene environment. For example, the III/I ratio of a dilute pyrene solution in hexane is 1.65 whilst in acetonitrile it is 0.54.[208] Interactions between pyrene moieties can result in excimer formation which is observed as a broad structureless emission band centred at *ca.* 480-500 nm.[209] Excimer formation can occur at concentrations of pyrene above 10^{-5} mol dm^{-3} or when two pyrene derived moieties are less than approximately 10 Å away from each other.[210] Overlap of different components of the spectra and broadening of bands due to interactions with other molecules complicates the interpretation of these different phenomena.[211]

The emission spectra of the BOC-protected pyrenylalanine amino acids (**33** and **34**) in dilute toluene solution (green spectra in Figure 49) show monomer emission with vibrational fine structure. A slight bathochromic shift in band I of 3 nm (214 cm^{-1}) is observed in the emission spectra for both the 1- and 2- substituted compounds compared to those expected for pyrene.[208] The five characteristic vibronic bands are labelled for compound **33** in Figure 49a (I = 376 nm, II= 382 nm, III= 388 nm, IV = 395 nm, V= 397 nm). The position of these bands is conserved across all of the emission spectra measured for compounds **31**-**34**.

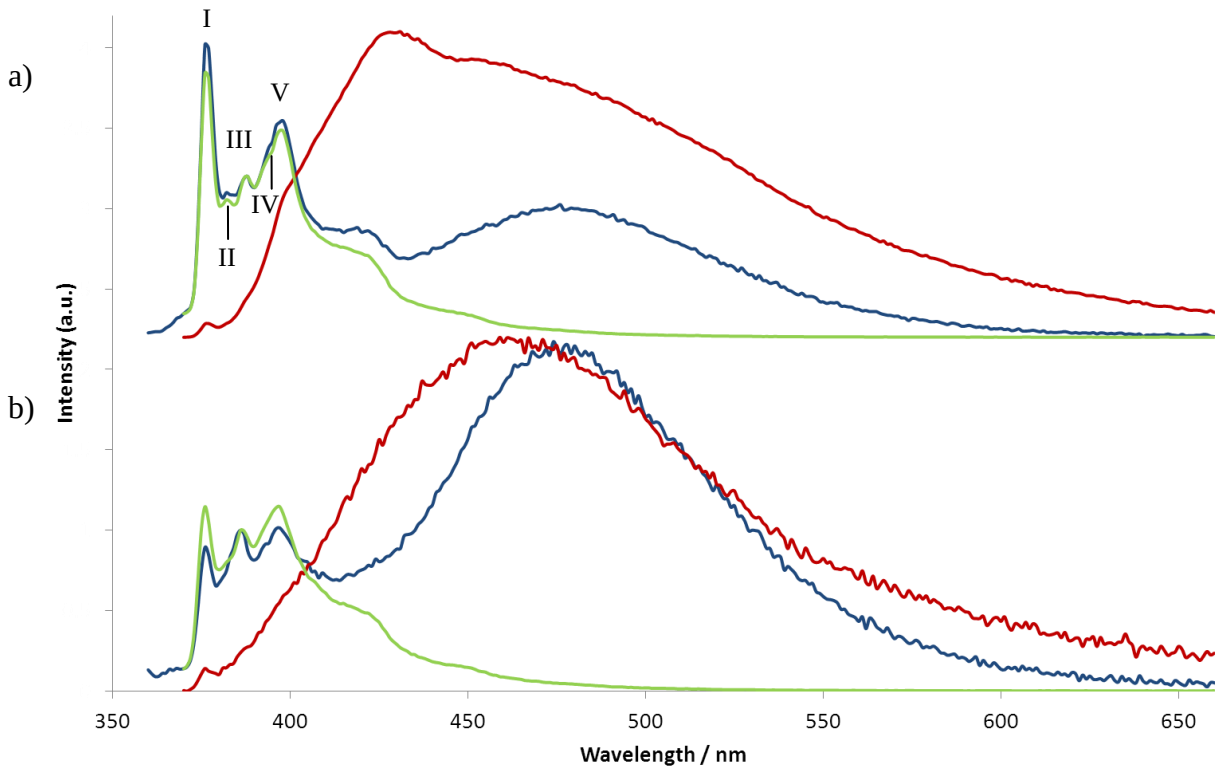

Figure 49 Overlaid normalised emission spectra for (a) 1-pyrenylalanine amino acid **33** in dilute toluene solution (green), 1-pyrenylalanine gelator **35** in dilute solution (blue) and **35** as a 1 % w/v gel. Bands I-V are labelled. (b) 2-pyrenylalanine amino acid **34** in dilute toluene solution (green), 2-pyrenylalanine gelator **36** in dilute solution (blue) and **36** as a 1 % w/v precipitate. λ_{ex} = 345 nm, spectra normalised to band III (386 nm) apart from the 1 % w/v samples of **35** and **36** which are adjusted to allow comparison between the spectra.

In addition to monomer emission, a broad, featureless excimer band with a maximum around 476 nm is observed in the emission spectrum of **35** as a dilute solution (blue spectra in Figure 49a). As the excimer is observed in the dilute solution of the gelator **35**, but not the starting amino-acid **33**, this is thought to be due to intramolecular interactions between the pyrenyl-moieties at either end of the compound.[211] The hexamethylene spacer tethers the two pyrene functionalities together and must be flexible enough for the pyrene groups to mutally interact resulting in excimer formation. The same features are observed for **36** but with stronger excimer emission relative to monomer emission. This is thought to be due to the longer-lived excited state of the 2-pyrenylalanine allowing more time for excimer formation to take place.[199] Geometrical considerations may also play a role with the more symmetric 2-pyrenyl groups achieving better overlap than the 1-pyrenyl analogues.

Compound **35** forms robust gels in toluene at 1 % w/v whilst **36** forms fibrous precipitates which fail to gel. The emission spectra are dominated by a strong excimer band where only

the first vibrational band of the monomer emission is distinguishable. For **36**, the excimer maximum is located at 466 nm, significantly blue shifted compared to the intramolecular excimer emission seen in dilute solution (476 nm). As fibre formation occurs in this system, the excimer band is thought to correspond to intermolecular excimer emission resulting from interactions between adjacent pyrene groups within urea hydrogen bonded stacks. The excimer emission band for the 1-pyrenyl alanine derivative **35** in the gel state is much weaker than for precipitates of **36**. Taking into account overlap with monomer emission, the intermolecular-excimer emission maximum of **35** is estimated to be around 466 nm. It is interesting to note that gel formation by other pyrene derivatives has previously been found to quench[190] as well as induce excimer formation.[192]

3.3 Mixed Gels

3.3.1 Fluorescence studies

Compounds **16**, **17** and **20** belong to a series of compounds whose behaviour, structure and properties are discussed extensively in Chapter 2. The three gelators adopt different molecular packing motifs in the gel state: glycine and alanine derivatives **16** and **17** show ribbon-like nanoscopic morphologies whilst phenylalanine derivative **20** shows fibre like architectures. All three compounds reliably form robust gels in toluene. Mixtures of the different gelators can produce gels with different packing and morphology to those of the pure compounds as discussed in section 2.6. Given the structural similarity of **35** and **36** to this class of compounds the formation of mixed gels with **16**, **17** and **20** was undertaken. The fluorescent properties of **35** and **36** allow information about the behaviour and environment of different mixed gels to be monitored and compared.

Gels were formed in toluene with 1 % w/v of a 1:9 binary mixture of gelators **35** or **36** with either **16**, **17** or **20** (*e.g.* 1ml Toluene, 1mg **35**, 9 mg **16**). The samples were heated and sonicated until fully dissolved with gels forming upon cooling to room temperature. Compounds **35** and **36** were difficult to dissolve completely and a number of heating and cooling cycles were undertaken to ensure complete dissolution and homogenisation occurred.

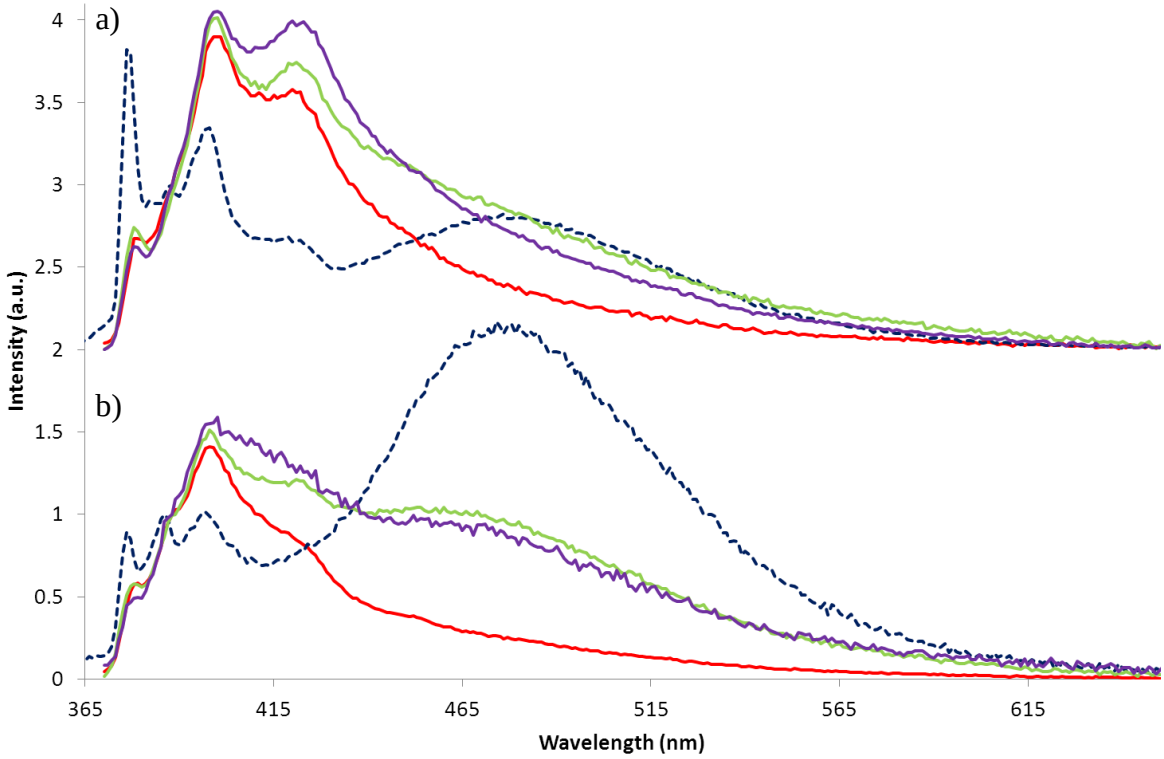

Figure 50 Overlaid normalised spectra for (a) **35** (b) **36** in 1:9 mixed gels with **16** (green), **17** (purple) **20** (red) and as a dilute toluene solution (dotted blue). λ_{ex} = 345 nm, spectra normalised to band III (386 nm).

The emission spectra show considerably lower intensity excimer bands in the mixed gels compared to solution (Figure 50). This is thought to arise due to incorporation of the pyrenyl gelators into bis-urea tapes of the co-gelator. X-ray crystallographic studies in Chapter 2 show that molecules in this series adopt an extended conformation as part of a bis urea hydrogen bonded stack. This conformation would prevent the pyrenyl molecule folding over to produce intramolecular excimers. Pyrenylalanine derived gelator molecules which happen to be adjacent in a urea stack may still be able to form intermolecular excimers, however since the fluorescent gelator is relatively dilute the number of adjacent fluorophores is likely to be relatively low.

The excimer maximum at 463 nm in the 1:9 **36:16** mixed gels is in good agreement with the intermolecular excimer observed for the 1 % w/v fibrous precipitate of **36** from toluene (466 nm). This suggests the excimer present is due to intermolecular, rather than intramolecular excimer formation. Overlap with the monomer emission makes identifying the maximum for the excimer band of **35**:**16** difficult although the band appears substantially blue shifted relative to the intramolecular excimer of the solution sample. Decreasing the concentration of

35 relative to **20** in the mixed gel results in a decrease in the intensity of the excimer band (Figure 51). This provides further evidence that the excimer band is due to intermolecular interactions between pyrene molecules with a lower probability of two pyrenyl molecules being adjacent in the fibres at lower concentrations.

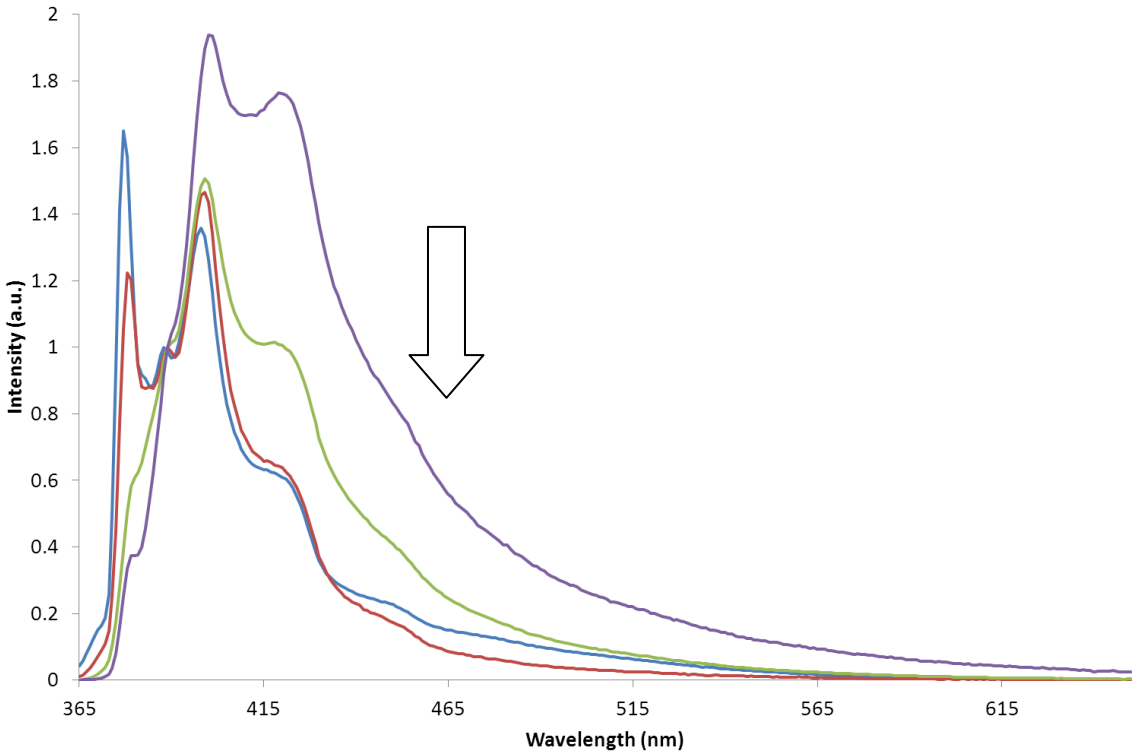

Figure 51 Mixed 1 % w/v toluene gels with of **35**:**20** at different ratios: 1:9 (purple), 1:19 (green), 1:99 (red), saturated solution of **35** in 1 % w/v gel of **20** (blue). Arrow shows effect of decreasing ratio of **35** relative to **20** on excimer band. λ_{ex} = 345 nm, spectra normalised to band III (386 nm).

The intensity of the first vibronic band is much lower in intensity relative to band III in the mixed gels than it is for the pyrenyl gelators in toluene solution. Band I appears to increase relative to band III with decreasing concentration of gelator from 2.7 in a 1:9 mixture of **35**:**20** to 0.8 in a 1:99 mixture. This corresponds to an enormous change in the environment of the pyrene moieties upon incorporation into the gel phase, with the observed ratio of 2.7 much greater than the ratio of 1.65 seen in hexane.[208] However, interpretation of the III/I ratio is complicated by overlap with the excimer band which overlaps band III more than band I. The same changes in III/I ratio would be expected solely on the basis of increased excimer formation with a higher concentrations of **35**. The difficulty in deconvoluting the contributions of different effects from the emission spectra makes it difficult to draw any firm conclusions about the gel environment. Further experiments examining the effects of

different solvent environments on the emission spectra of dilute solutions of amino acid derivatives **33** and **34**, where no intermolecular excimer formation takes place, would help establish the extent to which the Ham effect is responsible for the differences observed in the intensity of band I between spectra.

3.3.2 Effects of sample preparation on mixed gelator emission spectra

Sample preparation was found to have a significant influence on the emission spectra of the resulting mixed gels. All mixed gel samples were heated with a heat gun until a clear solution was formed. Two different cooling protocols were then adopted: a fast cooling method in which the samples were imersed in a cool water bath at approximately 16°C and briefly sonicated for approximately 1 s, and a slow cooling method where the samples were simply placed on a wooden bench top and allowed to cool. Fast cooled samples generally formed gels in under a minute whilst slow cooled samples took up to 10 minutes for the gels to fully form. Repeats were carried out using the same samples with the gel reformed each time according to either the fast or slow cooling procedures. Heating of the samples took place in sealed vials as the temperature required to dissolve gelators **16** and **17** is greater than that of the boiling point of the solvent (toluene 110°C). It was found that a heat gun, rather than a thermostatically controlled heating block, allowed the gelator to be rapidly dissolved without damaging the plastic caps of the vials. Consequently, the temperature to which each sample is heated will differ slightly for each repeat which may explain the variation seen within the results from each protocol. The resulting emission spectra are shown in Figure 52 with fast cooled samples shown in blue and slow cooled samples in red.

In the mixed gels of **35** and **36** with **17**, fast cooling consistently results in a less intense excimer band than slow cooling. The opposite behaviour is seen for both mixed gels of **16** where a consistently more intense excimer band is seen for the fast cooled samples compared to the slow cooled ones. The excimer band is thought to be the result of intermolecular interactions between pyrene groups on adjacent molecules. Slow cooling must therefore lead to more adjacent pyrene groups in the alanine system (*i.e.* a more phase separated sample) but fewer in the glycine system.

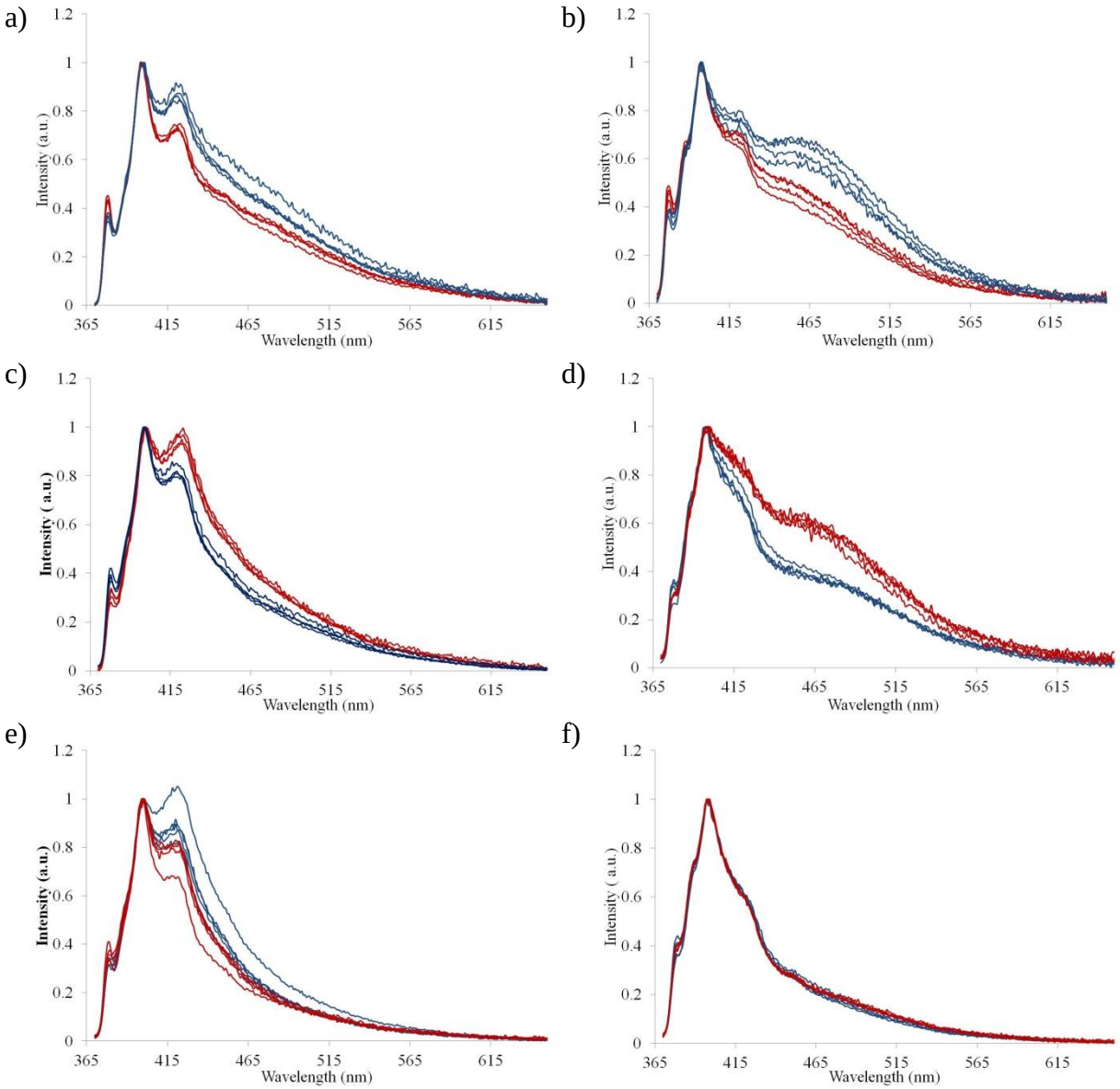

Figure 52 Overlaid fluorescence emissions spectra for fast (blue) and slow (red) cooled 1 % w/v 1:9 toluene gels of: a) **25**:**16** b) **36**:**16** c) **35**: **17** d) **36**:**17** e) **35**:**20** f) **36**:**20**. λ_{ex} = 345 nm, spectra normalised to band V (399 nm).

In 1:9 **35**:**20** mixed gel samples, fast cooling leads to slightly more excimer emission than slow cooling but the difference is less pronounced than for the other systems. No difference is observed with preparation method for the 1:9 **36**:**20** samples. This indicates that the pyrenylalanine gel incorporates readily into the phenylalanine structure with the 2-pyrenylalanine isomer incorporating more easily than the 1-pyrenylalanine analogue. As well as the extent of incorporation, it may be that the packing of the molecules in the phenylalanine gelators does not allow for intermolecular excimer formation by **35** and **36** as easily as in the alanine and glycine mixed gels.

Mixed gels of 1:9 **35**:**20** and **36**:**17** appear to be homogeneous with no significant differences observed in emission spectra taken of different sides of the same sample. The samples were also tested for stability over time. One week old samples showed greater III/I ratios than freshly prepared samples but typically similar excimer emissions. Measurements over shorter time periods showed variations in some samples, but no particular trends could be established and the differences were within those seen between repeats carried out using the fast and slow cooling methods.

3.3.3 Stuctural Studies

The decrease in the excimer band observed in the emission spectra of the mixed gels compared with solution is taken to indicate the incorporation of **35** and **36** into the gel fibres of **16**, **17** and **20** preventing intramolecular excimer formation. However, the variations observed in the extent of intermolecular excimer formation with gel composition and preparation indicate mixing of the different gelators is not uniform. Scanning electron microscopy and X-ray powder diffraction were used to examine the mixed gel structures and gain insights into the observations made by fluorescence spectroscopy.

SEM was used to image the morphology of xerogels formed from 1:9 mixed toluene gels of **35** or **36** with **16**, **17** and **20** formed by both the fast and slow cooling methods. Fast cooled mixed gel samples were further investigated by XRPD and compared with patterns obtained for the pure gelators under the same conditions. XRPD patterns of both the pure 1- and 2-pyrenylalanine xerogels showed broad, poorly defined peaks consistent with the small fibre size observed by SEM. Further details about the morphology and packing of gelators **16**, **17** and **20** can be found in Chapter 2.

Fine cylindrical fibres were seen in SEM images of the 1:9 mixed gels of phenylalanine derived gelator **20** with **35** which are similar to those seen for xerogels of both pure compounds (Figure 53). The same morphology is also observed for 1:9 mixed gels of **20** and **36** with no evidence of the irregular ribbons observed in the toluene precipitates of **36**. Both pyrenylalanine mixed gels with **20** showed broad, poorly defined XPRD patterns with similar shapes to each other (Figure 54). The shape of the pattern for the mixed gels most closely resembles that of the major component, **20**. However, separate fibres of **20** and **35** or **36**

cannot be ruled out by either SEM or XRPD due to the similarities in xerogel morphology and poor crystallinity of the gel fibres.

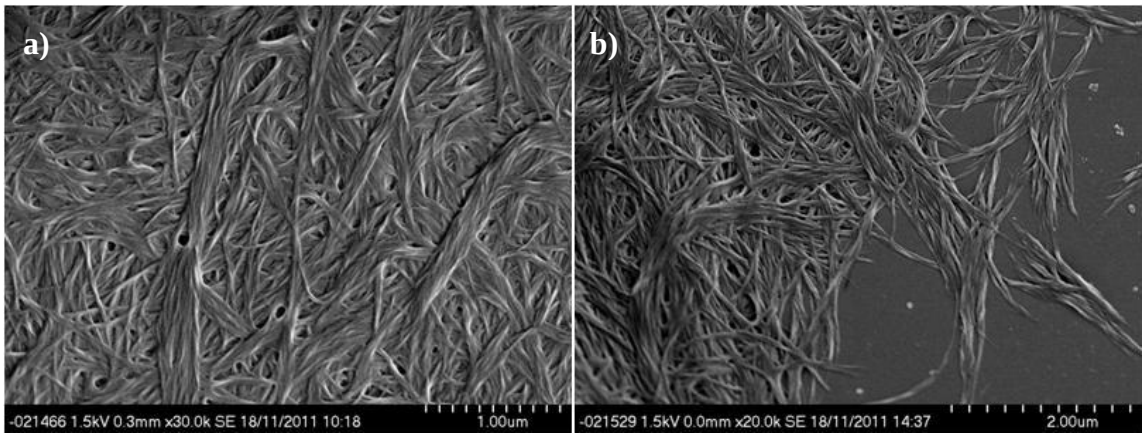

Figure 53 SEM images of xerogels formed from a total of 1 % w/v mixed gels in toluene with a ratio of a) 1:9 **35**:**20** slow cooled, b)1:9 **36**:**20** fast cooled.

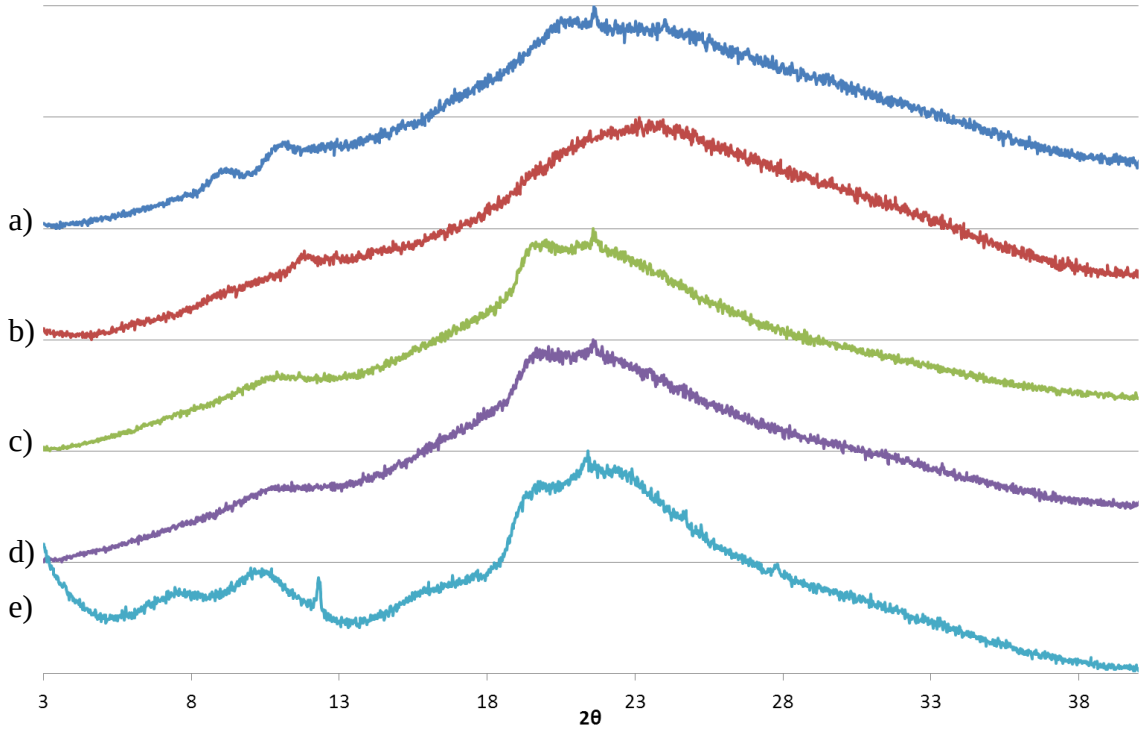

Figure 54 XRPD patterns for xerogels prepared from fast cooled toluene gels with 1 % w/v: a) **35** (dark blue), b) **36** (red)**,** c) 1:9 **35**:**20** (green), d) 1:9 **36**:**20** (purple), e) **20** (light blue).

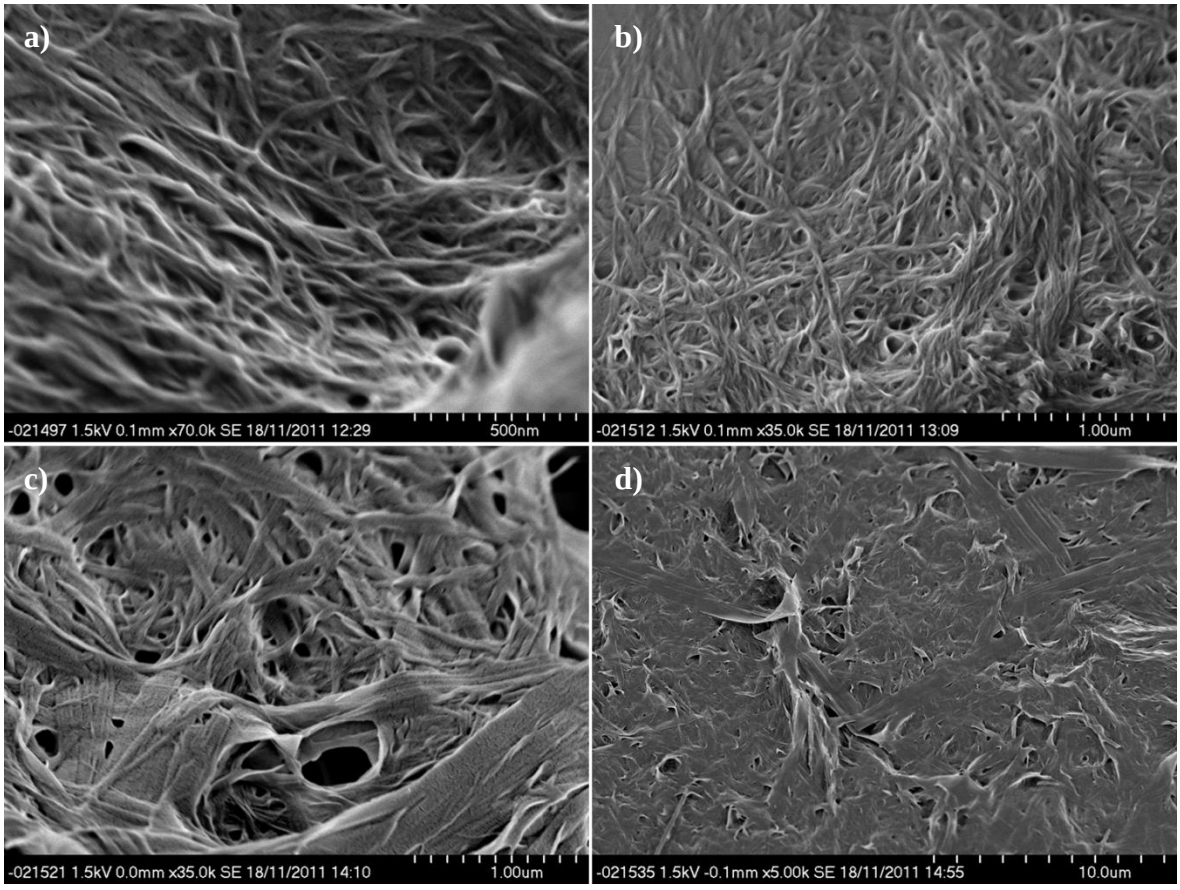

Figure 55 SEM images of xerogels formed 1 % w/v 1:9 mixed gels from a) slow cooled **35**:**17** b) slow cooled **36**:**17** c) slow cooled **35**:**17** d) slow cooled **36**:**17**.

Alanine-derived gelator **17** forms two-dimensional ribbons in toluene. However, in slow cooled mixed gels of **17** with **35** or **36,** much smaller ribbons are observed which are similar in size to those of the pyrenylalanine gels (Figure 55). Only occasional larger ribbons comparable with those observed for **17** are seen in the SEM images. In the fast cooled samples the same smaller fibres are observed alongside larger flat ribbons similar to those seen for pure **17**. The ribbons and fibres appear to merge into and branch off from each other with a large variation in widths observed. The samples are inhomogeneous with areas dominated by different morphologies. In a sample prepared using less than 0.1mg/ml **36** in **17**, the majority of the sample consists of ribbons, however large regions of fibres are also observed. This indicates that even very small amounts of **35** or **36** can have a significant effect on the morphology of gels of **17**.

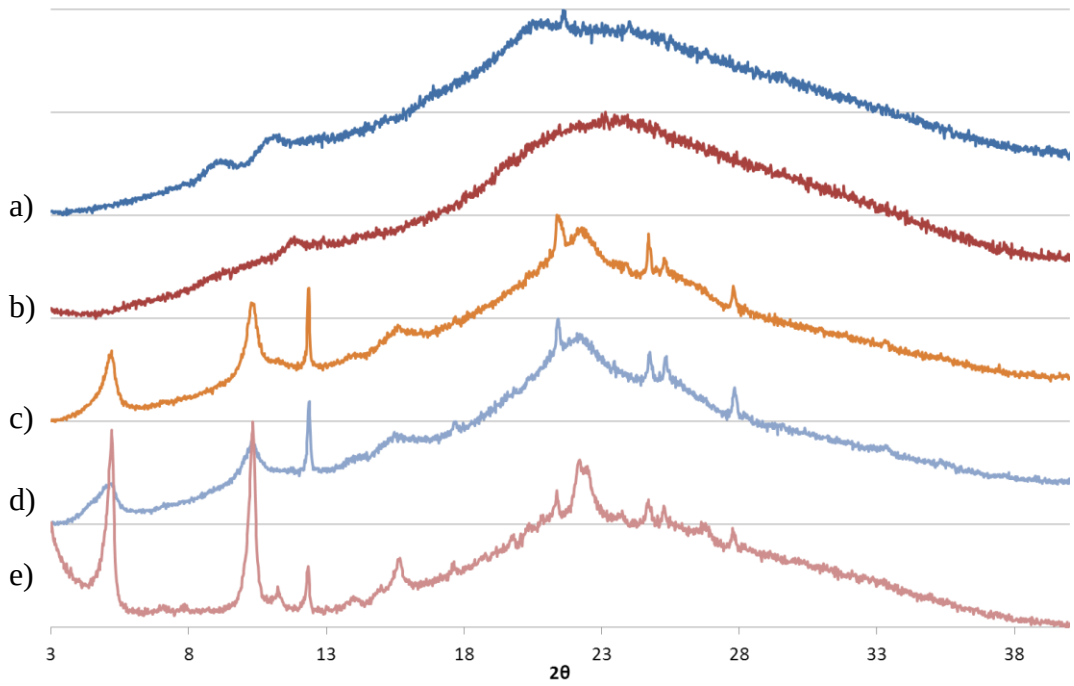

Figure 56 XRPD patterns for xerogels prepared from fast cooled toluene gels with 1 % w/v: a) **35** (dark blue), b) **36** (red), c) 1:9 **35**:**17** (orange), d) 1:9 **36**:**17** (light blue), e) **17** (pink).

XRPD patterns for both fast cooled mixed gels of **17** show a number of well resolved peaks which closely match those found in the pattern for pure gelator **17** (Figure 56). This indicates that although a dramatically different fibre morphology is seen, the underlying packing still resembles that of the alanine gelator. Broadening of peaks at 2θ angles of 5.2° and 10.0° but not at 12.3° may be due to the bulky pyrenyl groups varying the spacing in the urea tapes.

Xerogels of **16** from toluene adopt straight, ribbon-shaped structures. Three different morphologies are observed in the mixed gels of **35** and **16**. The majority of the material is in the form of straight ribbons, similar to those seen for **16**. Attached to these ribbons are isolated clumps of fine cylindrical fibres, similar to those seen for xerogels of **35**. There are also ribbons of a similar size to the straight ones, but with a clear left handed twist not seen in the straight ribbons. Compound **16** is achiral and as this type of microscopic twisting is normally associated with chiral molecules, it is likely that the twisting is induced by the incorporation of the chiral *l*-pyrenylalanine derived gelators. The same effect is observed in mixed gels of **16** and **17** as discussed in Chapter 2 section 2.6. In the mixed gels of **36**:**16**, the majority of the ribbons appear to be twisted and there are fewer clumps of fine fibres compared to the **35**:**16** gels. This implies fibres containing a mixture of gelators are more easily formed by **16** with **36** than **35**.

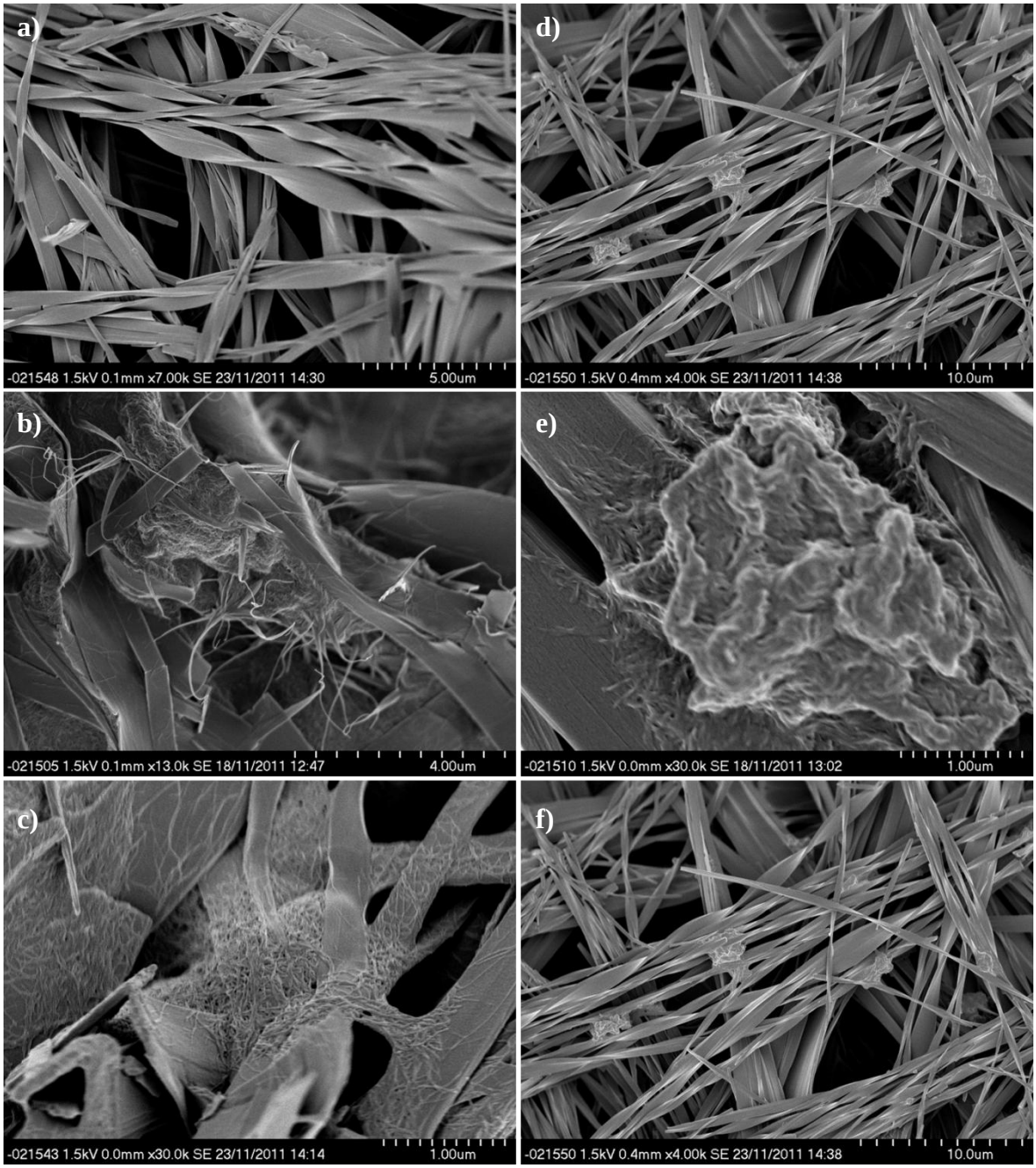

Figure 57 SEM images of xerogels formed from 1 % w/v 1:9 mixed toluene gels of a) and b) slow cooled **35**:**16**, c) fast cooled **35**:**16**, d) and e) slow cooled **36**:**16** f) fast cooled **36**:**16**

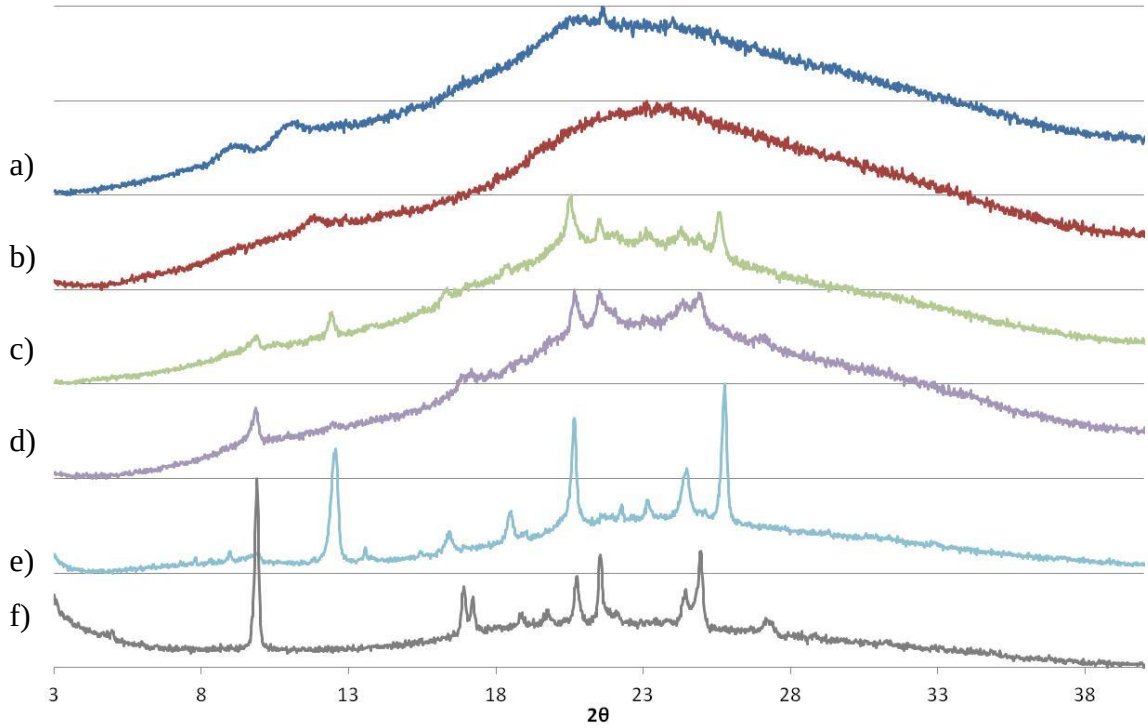

Figure 58 XRPD patterns for xerogels prepared from fast cooled toluene gels with 1 % w/v: a) **35** (dark blue), b) **36** (red), c) 1:9 **35**:**16** (green), d) 1:9 **36**:**16** (purple), e) **16** form B (light blue). f) Pattern for non-gel forming precipitate from acetonitrile of **16**, form A (grey).

Hexamethylene spaced glycine derived compound **16** has two known crystal forms, the gelling form B which is produced in toluene and non-gelling form A which is observed from other solvents including acetonitrile (Table 3, Chapter 2). A number of peaks are resolved for XRPD patterns of **16**:**35** and **16**:**36** mixed gels which do not match the patterns of gels of **16** formed from toluene (form B). A closer match is found with the non-gelling form A of **16** obtained from acetonitrile (Figure 58). Some additional peaks matching those of **16** form B are observed in the mixed gels with **35** and more weakly with **36**. It is likely that the different morphologies observed by SEM contain different packing motifs; straight ribbons of **16** form B, fine fibres of **35** or **36** and twisted ribbons of mixed composition with packing similar to that of **16** form A.

3.4 Anion modification of gel rheology

The hydrogen bonding functionality of ureas allows them to interact strongly with anions and ureas have been utilised in a variety of anion sensors.[212, 213] In Chapter 2, gelators in this series were shown to stack together through hydrogen bonds between urea-moieties to form α-urea tapes. The addition of anions can be used to disrupt these urea-urea interactions weakening, and ultimately preventing gel formation. Controlled addition of anions to gels has therefore received considerable interest as a means of tuning the rheometry of gels.[19, 60, 214]

A number of studies were undertaken to investigate the effect of anions on gel formation and structure. Solution based NMR spectroscopy is used to establish the interaction of individual gelator molecules with anions whilst rheometry is used to examine the macroscopic effects of anions on gel properties. These investigations are complemented by exploiting the fluorescent properties of **35** and **36** to gain greater understanding of the gel-sol transition upon the addition of anions. Acetate was selected for investigation as it has previously been shown to bind strongly to urea functionalities due to its high basicity. Tetrafluoroborate was selected as a reference anion as it is only weakly interacting with ureas. The anions were used as tetra-n-butyl ammonium (TBA) salts due to the cation's weakly co-ordinating properties and high solubility in organic solvents.[51, 215]

3.4.1 Solution studies

In order to establish and quantify the interactions between the different gelators and anions, solution based NMR spectroscopic titration studies were undertaken. As anion binding is rapidly reversible on the NMR spectroscopic time scale, the observed chemical shift of the urea NH protons change with the addition of increasing concentrations of anions reflecting an average of the chemical shifts for the bound and unbound states (Figure 59). These chemical shift changes can be analysed to provide binding constants and determine the ratio in which the components bind (Figure 60).[66, 212, 216, 217] Studies are undertaken in DMSO, a relatively competitive solvent, due to the poor solubility of the gelators in other solvents. A summary of the findings are given in Table 6.

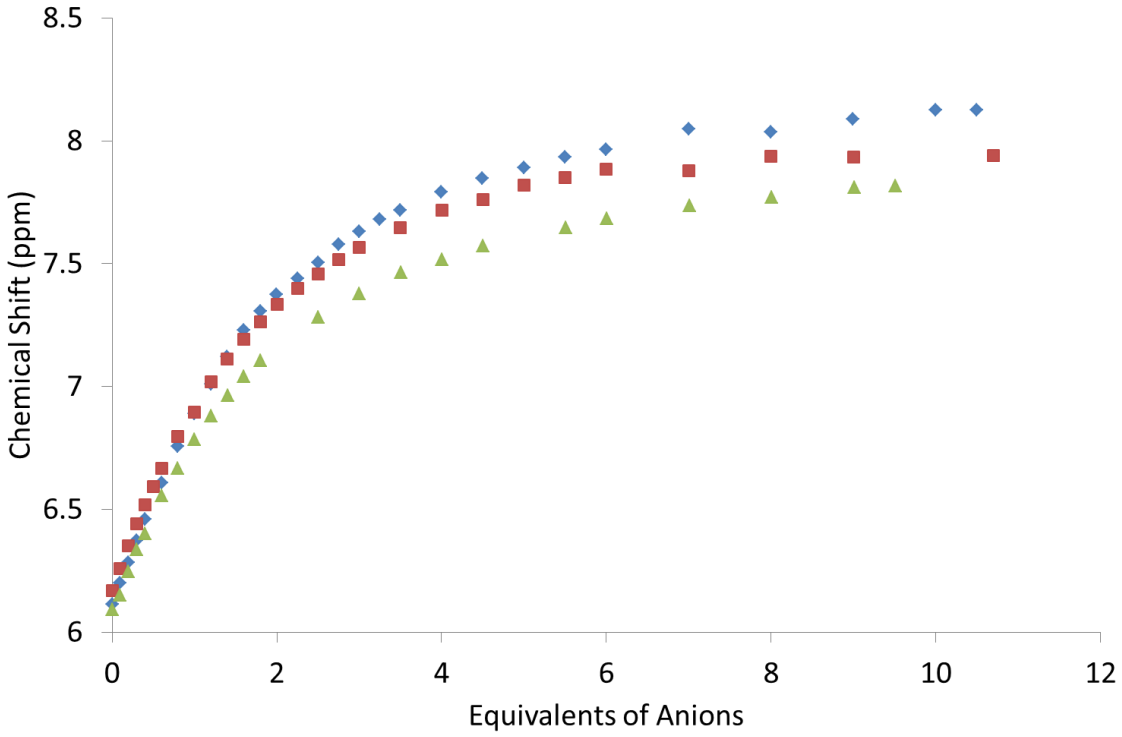

Figure 59 NMR titration data for TBA-acetate with gelators **16** (blue diamond), **17** (red square) and **20** (green triangle) in DMSO-d_6.

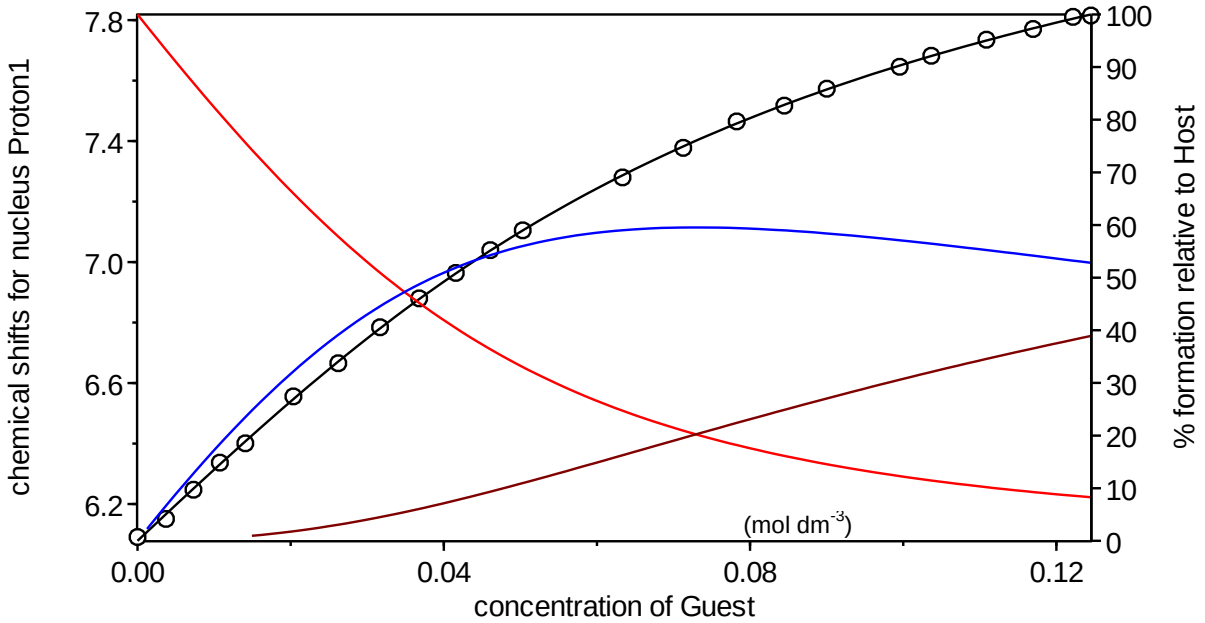

Figure 60 Speciation plot showing experimental data for ^{1}H NMR spectroscopy titrations for the binding of TBA acetate by **16** in DMSO fitted using a 1:1 and 1:2 host guest binding model: black circles- experimental measurements, black line- fit of model to data, red line- free host in solution, blue line- 1:1 host:guest binding, brown line- 1:2 host:guest binding.

Table 6 Binding constants determined by ^{1}H NMR spectroscopic titrations in DMSO-d_6

Compound	Log β_{11}	Log β_{12}
16	1.96(2)	2.91(2)
17	1.30(6)	2.53(4)
20	1.77(4)	2.61(5)

The anion binding titrations indicate weak 1:1 binding is dominant with additional contributions from 1:2 gelator:anion binding interactions (Table 6). The binding constants are broadly comparable between the different compounds with **16** showing the strongest binding and **17** the weakest. Equivalent titrations with the addition of BF_4^- showed no shift in the urea protons by NMR spectroscopy with the addition of anion.

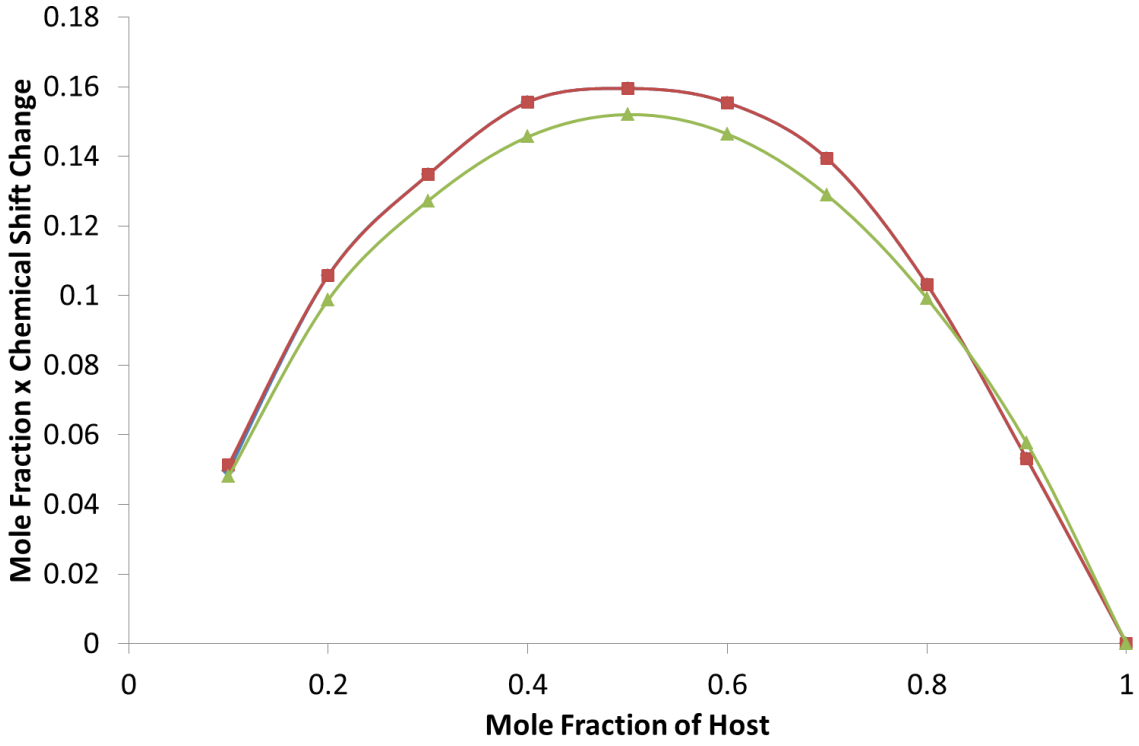

Figure 61 Job plot showing the addition of TBA-acetate to a solution of **20** in DMSO-d6

Job plots[66, 216, 217] for compound **20** (Figure 61) show a maximum around 0.5 suggesting that the 1:1 species is predominant. The 2:1 complex is not observed in the Job plot as the weak binding means very little 2:1 complex formation takes place, particularly under the dilute concentrations used in the Job plot (about 2 mmol dm^{-3}). NMR spectra obtained for compounds **16** and **17** showed peak broadening and splitting on addition of acetate which varied unpredictably across the series and it was not possible to produce a meaningful plot. The shape of the peaks were reproducible when the samples were remade with the same stock

solutions whilst a repeat using higher concentrations of **17** only showed line broadening with the addition of acetate. The origin of the line broadening and splitting is thought to be due to host self-aggregation effects or other more complex behaviour, and requires further investigation.

Due to the small amount of material available, analogous NMR measurements were not carried out on **35** and **36**. Instead the effect of anions on the fluorescence of solutions of **35** and **36** were investigated. The experiments were carried out in DMF due to the narrow absorption window of DMSO and the low solubility of the compounds in other solvents. Solutions of TBA-acetate or TBA-tetrafluoroborate in DMF (1.3 $x10^{-4}$ mol dm^{-3}) were gradually added to a solution of gelators **35** or **36** in DMF (2.6 $x10^{-8}$ mol dm^{-3}) and the emission spectra recorded.

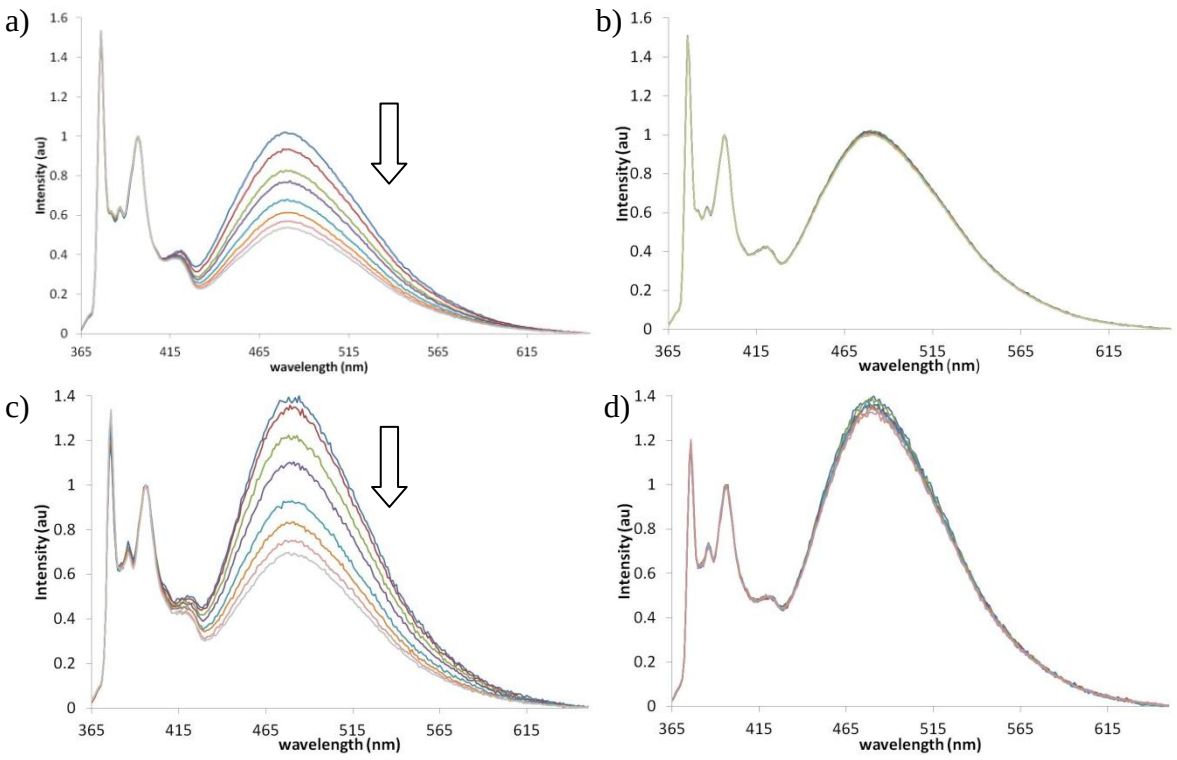

Figure 62 Emission spectra for a solution of (a and b) **35** or (c and d) **36** in DMF (2.6 $x10^{-8}$ mol dm^{-3}) to which increasing equivalents of (a and c) TBA-OAc or (b and d) TBA-BF_4 solution (1.3 $x10^{-4}$ mol dm^{-3}) are added: 0 eq. (blue), 50 eq. (red) 250 eq. (green) 500 eq. (purple) 1000 eq. (light blue) 1500 eq (orange) 2000 eq. (pink) 2500 eq. (grey). Arrow shows effect of the addition of increasing equivalents of anions on excimer band. λ_{ex} = 345 nm, spectra normalised to band V (398 nm).

The solution phase emission spectra in DMF shows enhanced excimer emission relative to the comparable toluene solutions. Addition of TBA acetate results in a drop in the intensity of

the excimer band with no change in the relative intensities of the monomer bands (Figure 62). The decrease in the intensity of the excimer emission is thought to be due to conformational changes in the gelator upon binding to the anions preventing the pyrene groups associating to form an intramolecular excimer. Because binding is weak in a competitive solvent such as DMF, and the concentration of gelator is very low, a large number of equivalents of anions are required to bring about this change (2500 eq.). Dilution of the final samples with DMF resulted in an increase in excimer emission intensity which is attributed to the reduced proportion of bound bis(urea)due to the decrease in anion concentration. Addition of non-binding BF_4^- anions results in no change in the fluorescence emission over the same concentration range.

3.4.2 Rheometric studies

Varying equivalents of TBA-acetate were added to 1 % w/v of gels of **20** in 1:9 acetonitrile:toluene mixtures in a concentric cylinder couette apparatus. In the absence of anions, strong gel-like behaviour was seen with G' values an order of magnitude higher than G'', an effect which persists even at high oscillatory stresses of 300 Pa. Gels formed in the presence of increasing equivalents of TBA-acetate showed a lower value of G' and a smaller difference in magnitude between G' and G'' (Figure 63). The stress with which the gels broke down to give liquid-like behaviour, the yield stress, also decreased with increasing concentrations of anion. With 1.5 equivalents of TBA acetate, the gel fails to form and the viscous modulus G'' becomes greater than the elastic modulus G'. Interestingly G' is slightly higher in the 1:9 acetonitrile:toluene gel than for the pure toluene gel (10,000 Pa) of **20** when measured under the same conditions.

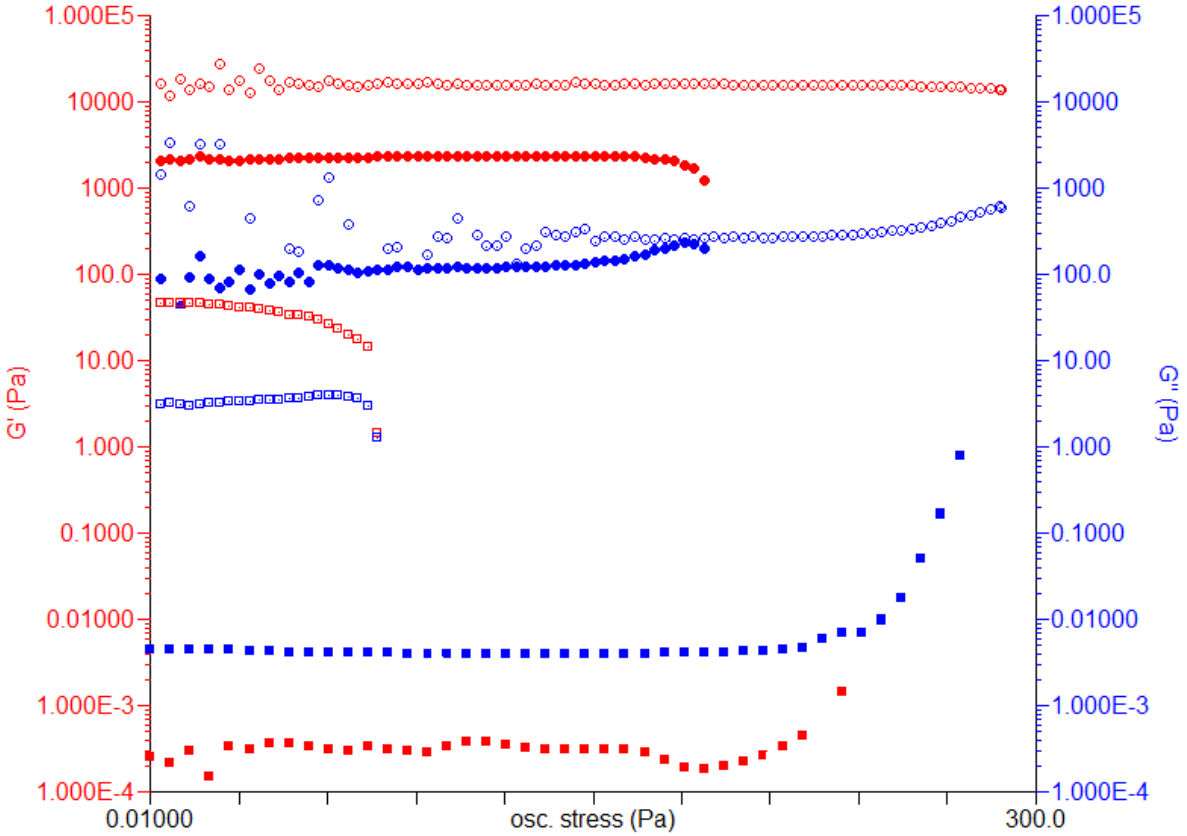

Figure 63 Oscillatory stress sweep for 1 % w/v **20** in 1:9 CH_3CN:toluene at increasing concentrations of TBA-acetate: 0 equiv. (open circle) 0.5 equiv. (closed circle) 1 equiv. (open squares) 1.5 equiv (closed square) at frequency of 1Hz. Data curtailed after yield stress for clarity.

The same trends are observed for 1 % w/v **20** in ethyl acetate and results are shown in Figure 64. The gels have similar G' and G'' values to the acetonitrile:toluene system and increased anion concentration results in lower G' values and yield stresses. Only 0.8 equivalents of TBA-acetate are required to prevent gel formation indicating stronger acetate binding to the gelator in ethyl acetate than the toluene:acetonitrile mixture or weaker gelator-gelator interactions.

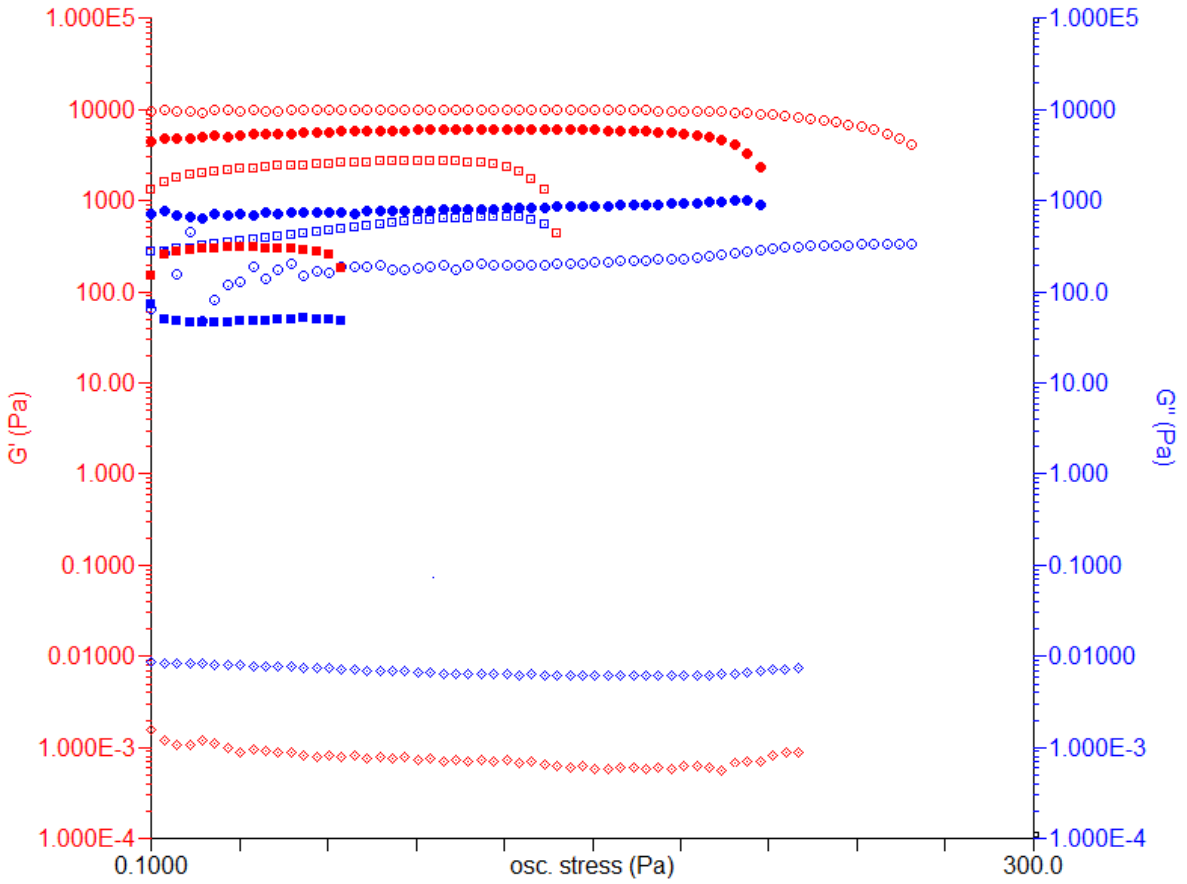

Figure 64 Plot of rheometric study showing *G′* (red) and *G″* (blue) values for 1% w/v ethyl acetate gels of **20** at various oscillatory stresses with varying equivalents of anions: 0 (open circles), 0.2 (closed circles), 0.4 (open squares), 0.6 (closed squares), 0.8 (open diamonds). Data curtailed after yield stress for clarity.

The temperature at which gels of **16** and **17** form in toluene and ethyl acetate is greater than the boiling point of the solvents meaning it was not possible to transfer a sol from a sealed vial into the rheometer cup. Studies were therefore undertaken for **17** in chloroform where the compound is generally more soluble and gel formation slower and weaker. These observations were reflected in the rheometry with *G′* values an order of magnitude lower than for the phenylalanine gels. The presence of increasing concentrations of anions resulted in the same decrease in *G′* and yield stress observed for gels of **20** (Figure 65). As **16** only forms gels in toluene it was not possible to undertake studies on this compound.

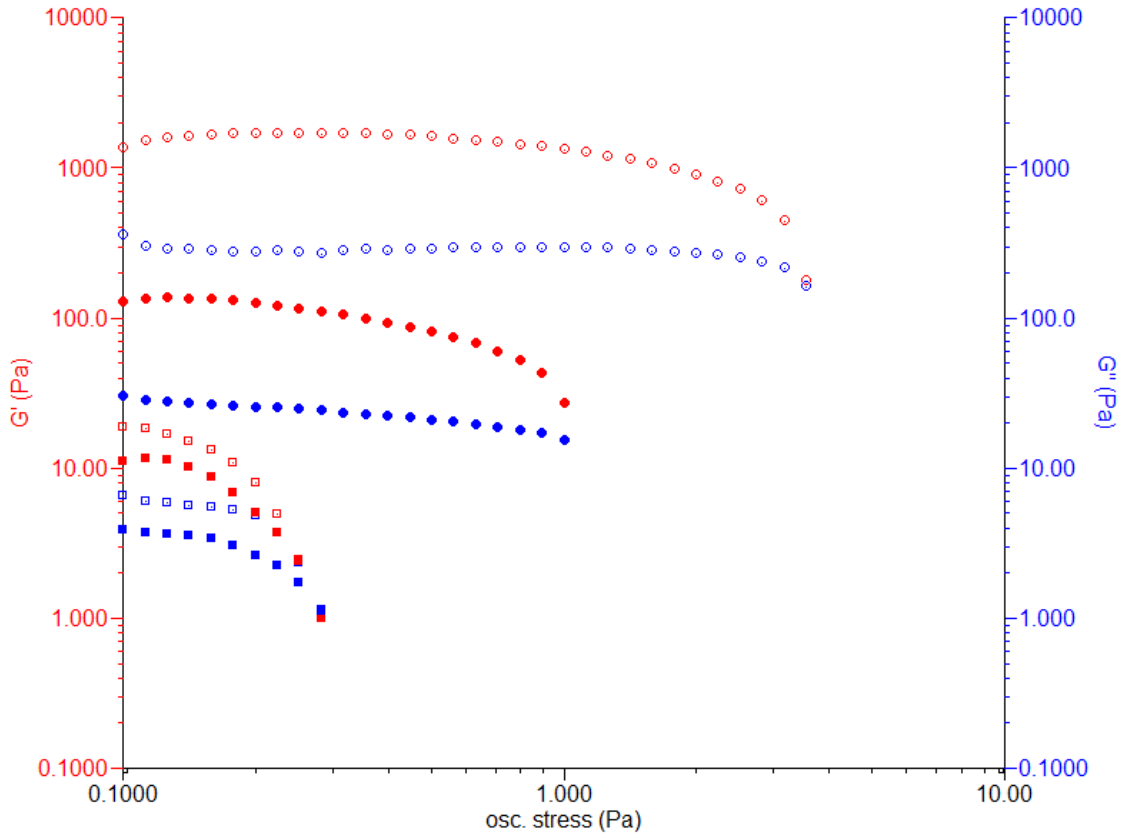

Figure 65 Plot of rhometric study showing G' (red) and G'' (blue) values for 1% w/v chloroform gels of **17** at various oscillatory stresses with varying equivalents of anions; 0 (open circles), 0.1 (closed circles), 0.2 (open squares), 0.3 (closed squares), 0.4 (open diamonds), 0.5 (closed diamonds). Data curtailed after yield stress for clarity.

3.4.3 Mixed gel fluorescence studies

The NMR spectroscopic and fluorescent studies in section 3.3.1 provide information about the solution phase interactions of isolated gelator molecules with anions whilst the rheometric measurements of section 3.4.2 describe the effect of anions on the macroscopic structure of the gel. In this section the fluorescent properties of **35** and **36** are exploited to probe the influence of anions on the gel structure at a molecular level. Rheometry indicates that at 1.5 equivalents of TBA-acetate gels of **20** fail to form in toluene. However, rheometry gives a measurement of the macroscopic integrity of the gel therefore it would be interesting to probe the gel-sol transition on a molecular level. It would also be interesting to monitor the effects of anions on aggregation in the gelator mixtures once the gels appear to have fully dissolved.

Toluene was selected because compounds **16**, **17** and **20** all form strong gels in this solvent. Low concentrations of the pyrenylalanine gelators were used in order to minimise intermolecular excimer formation and simplify interpretation of the resulting spectra. Compounds **35** and **36** are only sparingly soluble in toluene at room temperature. Saturated solutions at room temperature were therefore used with a concentration estimated to be <0.01 mg/ml (1.3×10^{-5} mol dm^{-3}). However, anions are poorly soluble in toluene so a second solvent is required to ensure the anions remain in solution. Acetonitrile was selected as the co-solvent because TBA-acetate and tetrafluoroborate are highly soluble in this solvent so relatively small volumes can be added. Concentrated solutions of anion were made such that 0.02 ml of solution contained 1 mole equivalents of anion relative to **20** in a 1 % w/v gel. Preliminary tests indicated that toluene gels of **16**, **17** and **20** still formed in the presence of low concentrations of acetonitrile.

Stock solutions of toluene saturated with either **35** or **36** at room temperature were used to prepare 1 % w/v of gels of **16**, **17** or **20**. The samples were heated and sonicated repeatedly with a heat gun until all solids were fully dissolved. All gels were formed using the fast cooling procedure described in section 3.3.1. TBA-acetate or TBA-BF_4 was added as a solution in acetonitrile (0.95 mmol dm^{-3}) using a micro-syringe. Samples were redissolved following the addition of anion and the gels reformed before a new measurement was taken. All samples were reheated regardless of whether gel formation was apparent. The phases of the samples at the time of measurement are recorded in Table 7.

Reference experiments using dilute solutions of **35** and **36** in toluene without co-gelator (Figure 66) showed the addition of acetate results in a decrease in the intensity of the excimer band (λ_{max} = 470 nm). This is consistent with the behaviour observed in DMF solution and is thought to be due to conformational changes upon binding of the gelator to the anion inhibiting intramolecular excimer formation. The loss of excimer is more pronounced in toluene than in DMF with only two equivalents of anion required to extinguish excimer emission. No loss of excimer band intensity is observed with the addition of the tetrafluoroborate solution consistent with the weaker binding of the gelators to this anion. Indeed, a small increase in the intensity of the excimer band occurs presumably due to the change in solvent composition favouring excimer formation. The position of the excimer band is also shifted significantly from 457 nm to 471 nm with the addition of 0.1 ml of the

BF_4^- solution, presumably due to the change in solvent environment. These competing factors complicate interpretation of the spectra for the mixed gels.

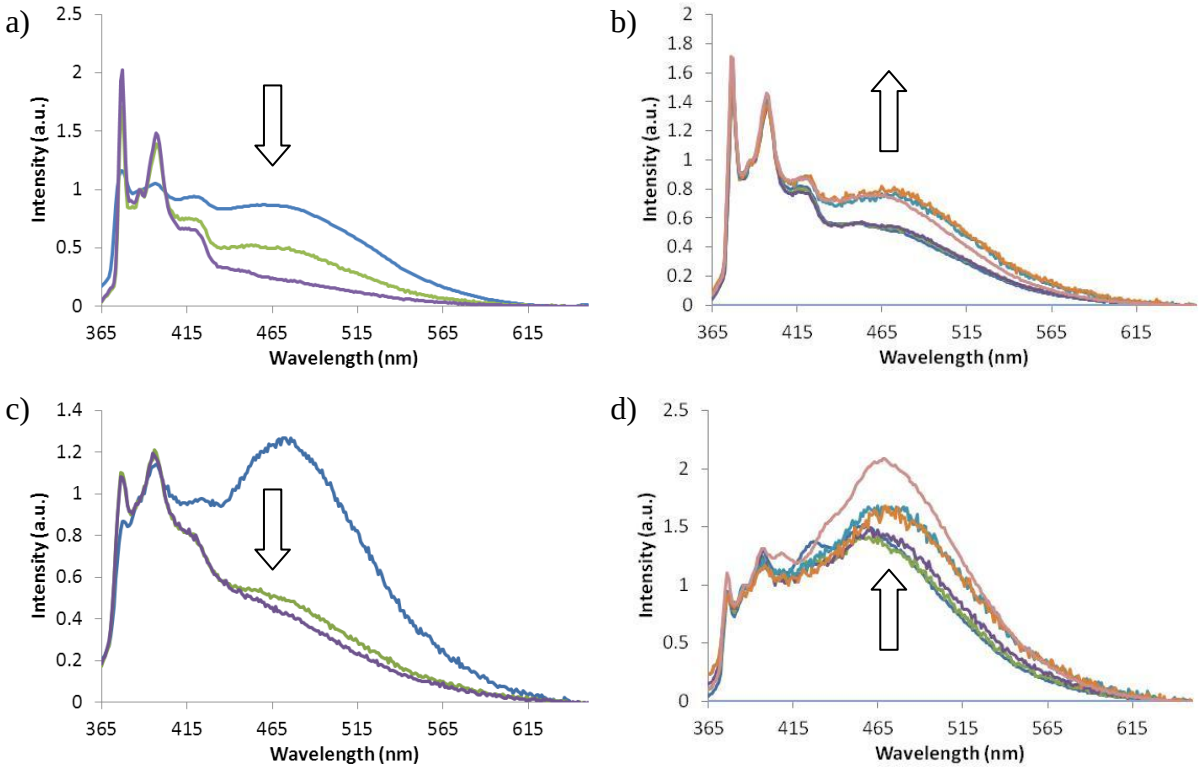

Figure 66 Fluorescence emission spectra recorded for saturated toluene solutions of (a and b) **35** (c and d) **36** upon the addition of (a and c) TBA-Acetate solution or (b and d) TBA-tetrafluoroborate solution (0.95 mmol dm^{-3}): 0 ml (blue), 0.02 ml (green), 0.04 ml (purple). Further additions of BF_4 solution were made: 0.01 ml (turquoise), 0.1 ml (orange), 0.2 ml (light blue), 0.4 ml (pink). Arrows show the effect of increasing concentration of anion solution on excimer band intensity. λex = 345 nm, spectra normalised to band III (386 nm).

Table 7 Phase of mixed gels upon the addition of increasing equivalents of TBA-acetate.

Mixed Gel 1:9		Anion	TBA-Acetate solution							
			0	0.5	1	1.5	2	5	10	20
35	**16**	AcO^-	G	G	WG	S	S	S	S	-
		BF_4	G	G	G	G	G	PG	PG	PG
	17	AcO^-	G	G	WG	S	S	S	S	-
		BF_4	G	G	G	G	G	G	G	WG
	20	AcO^-	G	G	WG	S	S	S	S	-
		BF_4	G	G	G	G	G	G	G	WG
36	**16**	AcO^-	G	G	WG	S	S	S	S	S
		BF_4	G	G	G	G	G	PG	PG	PG
	17	AcO^-	G	G	WG	S	S	S	S	S
		BF_4	G	G	G	G	G	G	G	WG
	20	AcO^-	G	G	WG	S	S	S	S	S
		BF_4	G	G	G	G	G	G	G	WG

G= gel, WG= weak gel, PG= partial gel, S= solution.

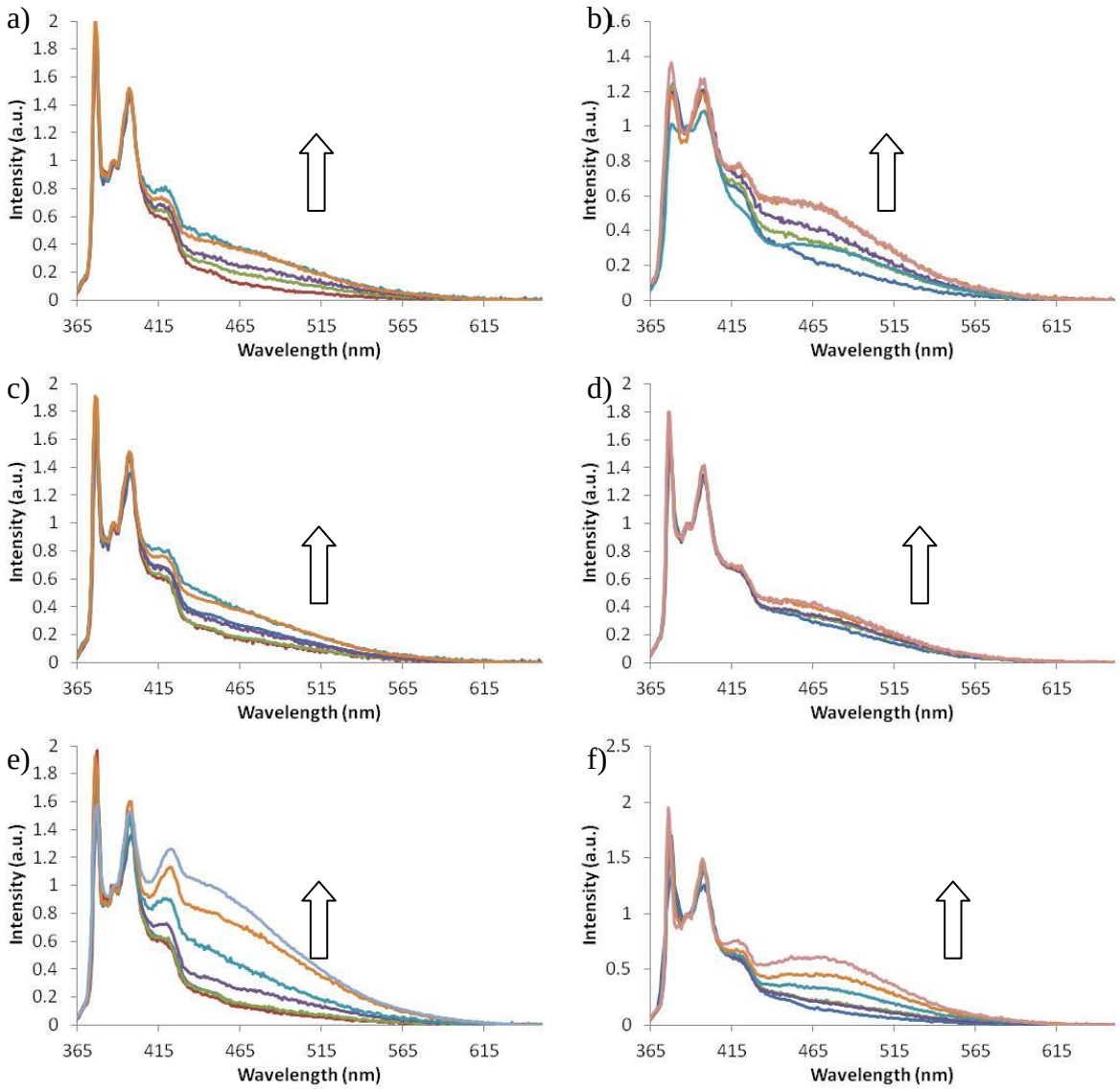

Figure 67 Emission spectra showing the addition of anion solutions to 1 % w/v 1:9 mixed gels of **35** with a) **16**+AcO^-, b) **16**+BF_4^-, c) **17**+AcO^- , d) **17**+BF_4^-, e) **20**+AcO^-, f) **20**+BF_4^-: 0 eq. (blue), 0.5 eq (red), 1 eq. (green), 2 eq. (purple), 5 eq. (turquoise), 10 eq (orange), 15 ml (light grey), 20 eq (pink). Arrows shows the effect of increasing concentration of anion solution on the excimer band. λ_{ex} = 345 nm, spectra normalised to band III (386 nm).

Only monomer emission is observed in the mixed gels of **16**, **17** and **20** with **35** and **36** before the addition of anions (Figure 67 and Figure 68). This indicates that **35** and **36** are incorporated into gel fibres preventing intramolecular excimer formation whilst the dilute conditions prevent intermolecular excimer formation. The addition of increasing concentrations of TBA acetate results in the breakdown of the gels (Table 7) and a gradual increase in the excimer emission bands. By inhibiting fibre formation, the anions release the pyrenylalanine gelators to undergo intramolecular excimer formation. This effect is in competition with binding of the acetate anions to the pyrenylalanine gelator in solution and

hence prevention of intramolecular excimer formation, as observed in the solution anion complexation experiments. However, there is a large excess of non-fluorescent gelators (**16**, **17** or **20**) which can also bind and effectively sequester the acetate, limiting the amount of acetate available to bind to the released pyrenyl derived gelators.

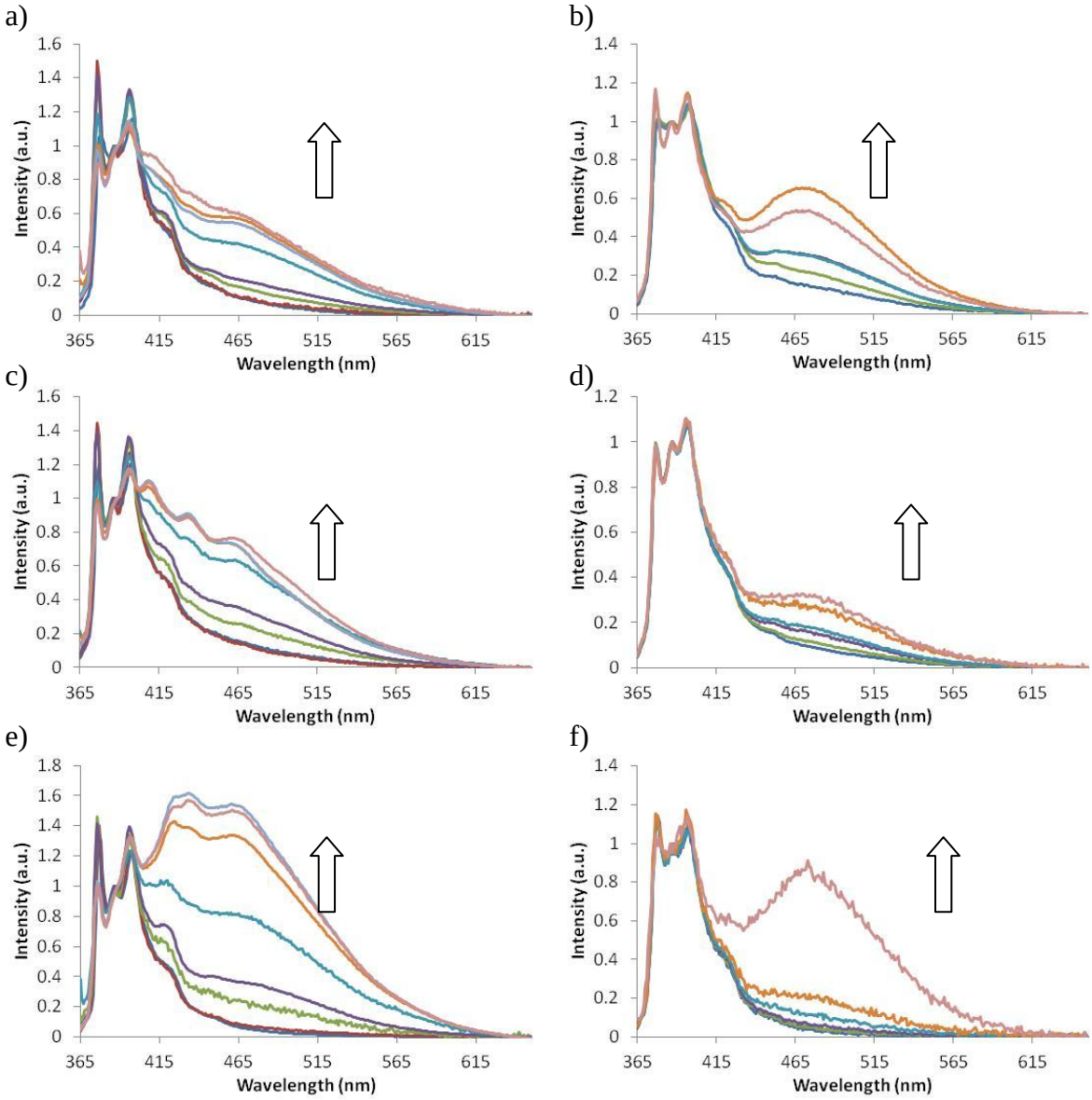

Figure 68 Emission spectra showing the addition of anion solutions to 1 % w/v 1:9 mixed gels of **36** with a) **16**+AcO^-, b) **16**+BF_4^-, c) **17**+AcO^- , d) **17**+BF_4^-, e) **20**+AcO^-, f) **20**+BF_4^-: 0 eq. (blue), 0.5 eq (red), 1 eq. (green), 2 eq. (purple), 5 eq. (turquoise), 10 eq (orange), 15 ml (light grey), 20 eq (pink). Arrows shows the effect of increasing concentration of anion solution on the excimer band. λ_{ex} = 345 nm, spectra normalised to band III (386 nm).

Below one equivalent of acetate there is relatively little change in the excimer band compared to the absence of anion. Above 1-2 equivalents of acetate the excimer emission increases substantially with the addition of further equivalents of anion. This corresponds well with the break-down of the gels which occurs around 1.5 equivalents of TBA-acetate for all of the mixed gels. It is interesting that excimer emission continues to increase with further additions of anions long after the gel has broken down. This indicates that acetate continue to disrupt aggregation which must still be taking place even after the three-dimensional gel structure has broken down. Much greater increases in the intensity of the excimer emission are observed for the mixed gels containing **36** compared to those with **35**, consistent with the longer lived excited state of this isomer.[199] Excimer emission is also more intense relative to monomer emission in mixed gels of **20** than those of **16** or **17** indicating greater dissolution of the gels of **20** by acetate. In some cases, for example the 1:9 gel of **16**:**36** (Figure 68a), the increase in excimer levels off at higher concentrations of acetate, presumably as a result of complete disaggregation, and hence full dissolution of the pyrenyl gelators.

An increase in the intensity of the excimer band is also seen with the addition of TBA-tetrafluoroborate solution. For most of the mixed gel systems, the increase in the excimer is much larger with the addition of acetate than tetrafluoroborate solution. However, gels of **35** with **1** show stronger excimer emission with the addition of BF_4^- than AcO^-. Gel formation is seen in the mixed samples of **35** or **36** with **17** or **20**, even with 20 equivalents of BF_4^- as shown in Table 7. However, the rate of gel formation is noticeably slower, and the gels formed weaker, the higher the concentration of BF_4^- solution. As the solution studies show little binding to TBA-BF_4, this is attributed to higher solubility of the gelators in the toluene:acetonitrile mixtures. In contrast, mixed gels of **35** or **36** with **16** begin to precipitate above five equivalents of tetrafluoroborate solution and only partial gels are formed. This may be because **16** forms a non-gelling precipitate in acetonitrile (form A) with a different XRPD pattern to its gelling form in toluene (form B) whilst compounds **17** and **20** both form gels in acetonitrile with the same XRPD patterns as the corresponding toluene gels. In either case, the change in solvent composition disrupts the gel resulting in an increase in excimer formation.

Table 8 Summary of the competing effects of different components on gel formation and excimer emission

Species	TBA acetate	Acetonitrile	TBA tetrafluoroborate
16/**17**/**20**	- Disrupts gel formation	- Increases solubility of gelators - Favours non-gelling form A in **16**	- No effect
35/**36**	- Releases gelator to undergo intramolecular excimer formation - Binding of gelator to acetate quenches excimer	- Solubilises gelator to undergo intramolecular excimer formation	- No effect

The increase in the intensity of the excimer band with the addition of anion is not always consistent and in some cases spectra corresponding to higher concentrations of anion have lower intensity excimer bands than the previous measurement. This may be in part due to the stochastic nature of gel formation and small differences in sample preparation. However, the emission spectra of the final samples were re-measured after one day and in several cases a considerable decrease in excimer emission bands was observed. This indicates that the gel systems were not fully equilibrated after the approximately 5 minute cooling period allowed between measurements. A longer equilibration period between experiments may therefore be required, particularly with higher concentrations of anion where gel formation is considerably slowed.

Disruption of the gel by the change in solvent composition makes it difficult to isolate the effect of acetate on excimer formation and the experiment would be greatly simplified by keeping the solvent composition constant. Analysis is further complicated by binding of the pyrenyl gels to acetate, but not tetrafluoroborate, inhibiting excimer formation. Nevertheless, the general explanation that the addition of acetate leads to the gradual breakdown of gel fibres releasing trapped pyrenyl co-gelators to undergo excimer formation is still thought to hold true. The results indicate that even when acetate prevents the formation of a macroscopic gel, aggregation still occurs which traps the pyrenylalanine gelators and limits excimer formation. Addition of higher equivalents of anion therefore further breakdown these aggregates releasing more fluorescent gelators and causing an increase in excimer emission intensity.

3.5 Conclusion

In general the synthetic 1- and 2-pyrenylalanine gelators behave similarly to the other amino acid derivatives in the series. Both compounds form gels by themselves and as mixed gels with other amino acid derived gelators. Differences in the range of solvents gelled, fibre morphology and XRPD patterns indicate that conformational differences between the pyrenylalanine isomers impacts upon the structure of the gel fibres they form. The general trends in fluorescence emission exhibited by both the 1- and 2-pyrenylalanine derived gelators are the same. However, stronger excimer emission is observed for the 2-pyrenylalanine gelator (**35**) which is attributed to its longer lived excited state.[199]

In free solution, the two pyrenyl ends of gelators **35** and **36** are able to mutually interact in their excited state to form an intramolecular excimer. In mixed gels with compounds **16**, **17** and **20**, intramolecular excimer formation is prevented as the pyrenyl gelators become incorporated into bis-urea tapes. As the proportion of pyrenylalanine gelator is increased, a new intermolecular excimer band forms due to association between adjacent pyrenylalanine gelators. The emission spectra of the 1:9 mixed gels are sensitive to the method of gel preparation. Rapid gel formation results in a decrease in intermolecular excimer emission for 1:9 mixtures of **35** or **36** with **17** but an increase in excimer emission with **16** compared with slow cooled samples.

Compounds **35** and **36** appear to incorporate well into the gel structure of **20**, resulting in little excimer formation and no observable differences in gel morphology or XRPD patterns compared to pure gels of **20**. However, the presence of **35** or **36** changes the morphology of the normally large ribbon-like strands of **17** to give much smaller, narrower ribbons. Mixtures of the two morphologies are seen in different samples with increasing concentration of **36** producing a higher proportion of the smaller ribbons. However, XRPD data indicates that despite the change in morphology there is no change in the underlying packing which is similar to that of pure **17**. Three different microscale morphologies are observed for **16** with **35** or **36** which XRPD indicates correspond to three different packing arrangements. In addition to the straight ribbons and fine fibres attributed to the pure gelators, twisted fibres are also seen which are thought to correspond to mixed gels with packing similar to form A of **16**. The differences observed in the intensity of the excimer band with sample preparation

are likely to be the result of changes in the ratio of these different components as a result of differences in sample cooling rate.

Compounds **17** and **20** display gel-like rheology which weakens with the addition of TBA-acetate until liquid-like behaviour is observed. NMR studies show TBA-acetate undergoes weak 1:1 and 2:1 binding with the urea functionalities of compounds **16**, **17** and **20**. Binding of acetate to **35** and **36** in DMF or toluene solution results in a loss of intramolecular excimer emission, thought to result from conformational changes in the gelators upon binding to the anions preventing association of the pyrenyl end groups. Addition of acetate to mixed gels of compounds **16**, **17** and **20** breaks down the gels, releasing the pyrenylalanine gelators to undergo intramolecular excimer emission. Little increase in the intensity of the excimer band is seen until the gel is observed to breakdown at 1.5 equivalents. Excimer emission continues to grow with the addition of higher equivalents of acetate indicating that the aggregation of the gelators continues to be disrupted at anion concentrations well above those required to prevent macroscopic gel formation. However, an increase in excimer emission is also observed with the addition of TBA-BF_4 which is attributed to disruption of the gels by the addition of acetonitrile.

The approach taken of incorporating a fluorescent functionality into a known gelator motif and forming mixed gels with related gelators allows valuable insights to be gained into gel formation and dissolution. However, differences in molecular packing and morphology induced in some of the gel systems indicate that the pyrenylalanine gels are not simply passive probes. This work highlights the sensitivity of the gel state to apparently small differences in gelator structure, sample preparation and solvent composition.

3.6 Experimental Section

3.6.1 Materials and Methods

The syntheses of compounds **16**, **17** and **20** are reported in section 2.8. 1- and 2-pyrenylalanine gelators **35** and **36** were synthesised from their corresponding BOC-protected amino acids which were supplied by Dr. Neil Colgin (Durham University). 2-Bromo pyrene was synthesised by Dr. Andrew Crawford and Robert Edkins (Durham University).[202] Commercial reagents were used as supplied without further purification. Instrumentation and procedures for the characterisation of compounds and gels are as described in the experimental section of Chapter 2.

3.6.2 Synthesis

Methyl (2S)-2-[6-[[(1S)-2-methoxy-2-oxo-1-(pyren-1-ylmethyl)ethyl]carbamoylamino] hexylcarbamoylamino]-3-pyren-1-yl-propanoate (**35**)

BOC-protected 1-pyrenylalanine methylester, **33,** (0.07 g, 0.17 mmol) was stirred at room temperature in 4 ml 1:1 dry TFA:DCM. NMR indicated deprotection occurred after 1 hour and the solvent was removed under vacuum and the product re-suspended in chloroform (10ml). Triethylamine was added dropwise to produce a neutral solution, as monitored using indicator paper. 1,6-diisocyanatohexane (0.013 g, 0.08 mmol) was added dropwise and the solution was heated under reflux for 18hours. The mixture was cooled and the fine precipitate filtered and washed with cold chloroform then diethylether. The precipitate was sonicated as a suspension in 5ml of distilled water, filtered and dried in a heating pistol for 30minutes. The product was obtained as a cream solid (Yield 0.039 g, 0.05 mmol, 30 %) ^{1}H NMR (700MHz, DMSO-d_6): 8.39 (2 H, d, *J* 9.2, Ar-H), 8.32 (4 H, t, *J* 8.6, Ar-H), 8.26 (4 H, dd, *J* 17.1, 8.5, Ar-H), 8.18 (4 H, s, Ar-H), 8.11 (2 H, t, *J* 7.5, Ar-H), 7.92 (2 H, d, *J* 7.8, Ar-H), 6.38 (2 H, d, *J* 8.2, C*NH), 6.07 (2 H, t, *J* 5.3, NHCH$_2$), 4.70 (4 H, dd, *J* 15.0, 7.6, C*H), 3.79 (2 H, dd, *J* 14.1, 6.2, C*CH), 3.67 (2 H, dd, *J* 13.8, 7.9, C*CH'), 3.67 (6 H, s, OCH$_3$), 2.94 (4 H, dd, *J* 13.1, 6.5, NHCH$_2$), 1.32 – 1.24 (4 H, m, NHCH$_2$CH$_2$), 1.20 – 1.11 (4 H, m, CH$_2$CH$_2$CH$_2$). ^{13}C{^{1}H} NMR (700MHz, DMSO-d6, *J*/Hz): 173.8 (s, COO), 158.1 (S, NCO), 138.4 (s, ArC), 131.6 (s, ArC), 131.1 (s, ArC), 130.6 (s, ArC), 129.5 (s, ArC), 129.1(s, ArC), 128.2 (s, ArC), 128.1 (s, ArC), 127.6 (s, ArC), 126.9 (s, ArC), 125.9 (s, ArC), 125.7 (s, ArC), 125.4 (s, ArC), 124.9 (s, ArC), 124.8 (s, ArC), (s, ArC), 123.9 (s, ArC), 55.1 (s, C*), 52.5 (s, OCH$_3$), 40.3 (s, NCH$_2$ under DMSO peak), 36.1 (s, C*CH$_2$), 30.6 (s, NCH$_2$CH$_2$), 26.8 (s, NCH$_2$CH$_2$CH$_2$).

m/z (ASAP+, 650°C): 215.1 ($[PyCH_2]^+$, 100%), 710.3 ($[M\text{-}2H_2O]^+$, 55%) Anal. calc'd for $C_{48}H_{46}N_4O_6$: C, 74.40; H, 5.98; N, 7.23 Found: C, 72.98; H, 5.94; N, 7.11%.

Methyl (2S)-2-[6-[[(1S)-2-methoxy-2-oxo-1-(pyren-2-ylmethyl)ethyl]carbamoylamino] hexylcarbamoylamino]-3-pyren-2-yl-propanoate (**36**)

BOC-protected 2-pyrenylalanine methylester, **34**, (0.12 g, 0.296 mmol) was stirred at room temperature in 4 ml dry 1:1 TFA:$CDCl_3$. NMR spectroscopy indicated deprotection had occurred after 1 hour and the solvent was removed under vacuum and the product re-suspended in chloroform (10ml). Triethylamine was added dropwise to produce a neutral solution, monitored using indicator paper. 1,6-diisocyanatohexane (0.025 g, 0.148 mmol) was added dropwise and was heated under reflux at 70°C for 18 h. The mixture was cooled and the precipitate filtered and washed with cold chloroform then diethylether. The product was obtained as a creamy precipitate (Yield 0.072 g, 0.093 mmol, 31%) ^{1}H NMR (700MHz, DMSO-d_6): 8.28 (4 H, d, *J* 7.5, Ar-H), 8.17 (4 H, d, *J* 7.5, Ar-H), 8.12 (4 H, d, *J* 7.5, Ar-H), 8.10 (4 H, s, Ar-H), 8.05 (2 H, t, *J* 7.5, Ar-H), 6.26 (2 H, d, *J* 8.2, C*NH), 6.03 (1 H, t, *J* 5.4, NHCH$_2$), 4.67 (2 H, dd, *J* 13.8, 8.1, C*H), 3.64 (6 H, s, OCH$_3$), 3.44 (2 H, dd, *J* 13.8, 5.5, C*CH), 3.34 (2 H under H_2O solvent peak, C*CH') 2.87 (4 H, dd, *J* 12.9, 6.5, NHCH$_2$), 1.23 – 1.19 (4 H, m, NHCH$_2$CH$_2$), 1.10 – 1.08 (3 H, m, CH$_2$CH$_2$CH$_2$). ^{13}C{^{1}H} NMR (700MHz, DMSO-d6, J/Hz): 173.8 (s, COO), 158.0 (s, NCO), 136.0 (s, ArC), 131.2 (s, ArC), 131.1 (s, ArC), 128.1 (s, ArC), 127.8 (s, ArC), 126.6 (s, ArC), 126.5 (s, ArC), 125.7 (s, ArC), 124.3 (s, ArC), 123.3 (s, ArC), 55.1 (s, C*), 52.4 (s, OCH$_3$), 46.4 (s, NCH$_2$), 38.9 (s, C*CH$_2$), 30.5 (s, NCH$_2$CH$_2$), 26.6 (s, NCH$_2$CH$_2$CH$_2$). m/z (ASAP+, 550°C): 215.1 ($[PyCH_2]^+$, 100%), 439.2 ($[M\text{-}C_{20}H_{17}NO_2\text{-}H_2O]^+$, 35%), 710.3 ($[M\text{-}2H_2O]^+$, 5%) Anal. calc'd for $C_{48}H_{46}N_4O_6$: C, 74.40; H, 5.98; N, 7.23. Found: C, 69.88; H, 5.79; N, 6.68%.

3.6.3 Experimental procedures

3.6.3.1 ^{1}H NMR spectroscopic titrations

NMR spectra were performed on a Varian Mercury-400 (400 MHz for ^{1}H). All chemical shifts are reported in ppm and referenced to the residual protic solvent. A solution of the host species of known concentration, typically 0.02–0.03 mM, was made up in an NMR tube using DMSO-d_6 (0.5 ml). Solutions of TBA Acetate (1 ml) were made ten times the concentration of the host solution. The guest solution was typically added in 10 µl aliquots, representing 0.2 equivalents of the guest with respect to the host. Larger aliquots were used above 2 equivalents of guest. Spectra were recorded after each addition. Results were analysed using the curve-fitting program HypNMR 2006.[218]

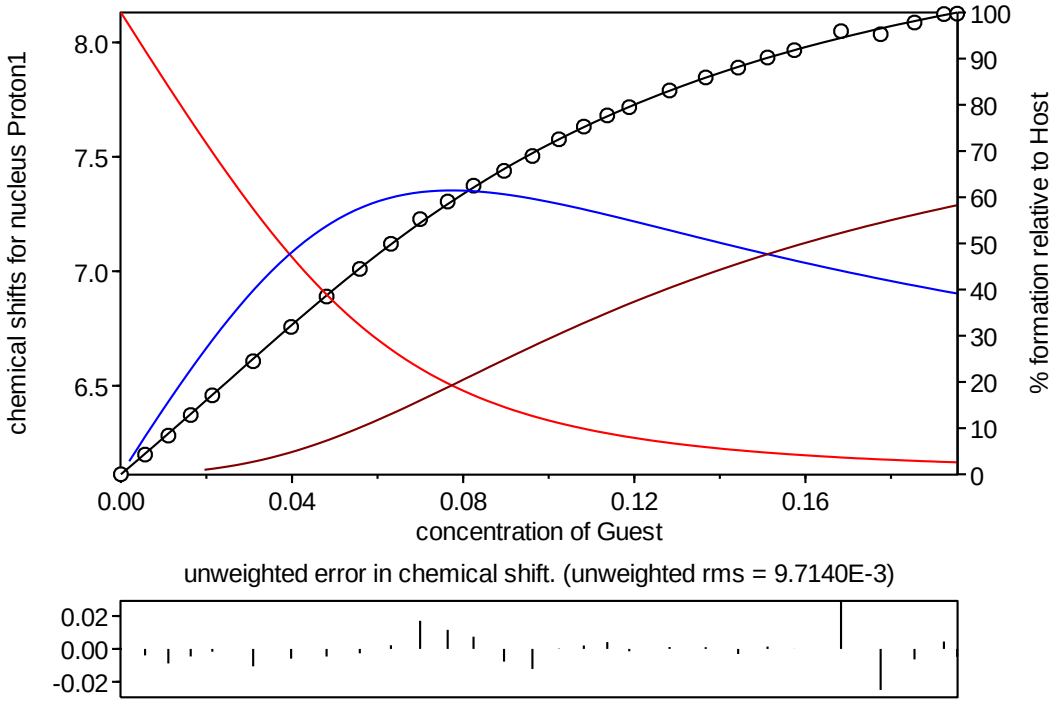

Figure 69 NMR titration data and fit for binding of TBA acetate by **16** in DMSO: black circles- experiemental measurements, black line- fit of model to data, red line- free host in solution, blue line- 1:1 host:guest binding, brown line- 1:2 host:guest binding.

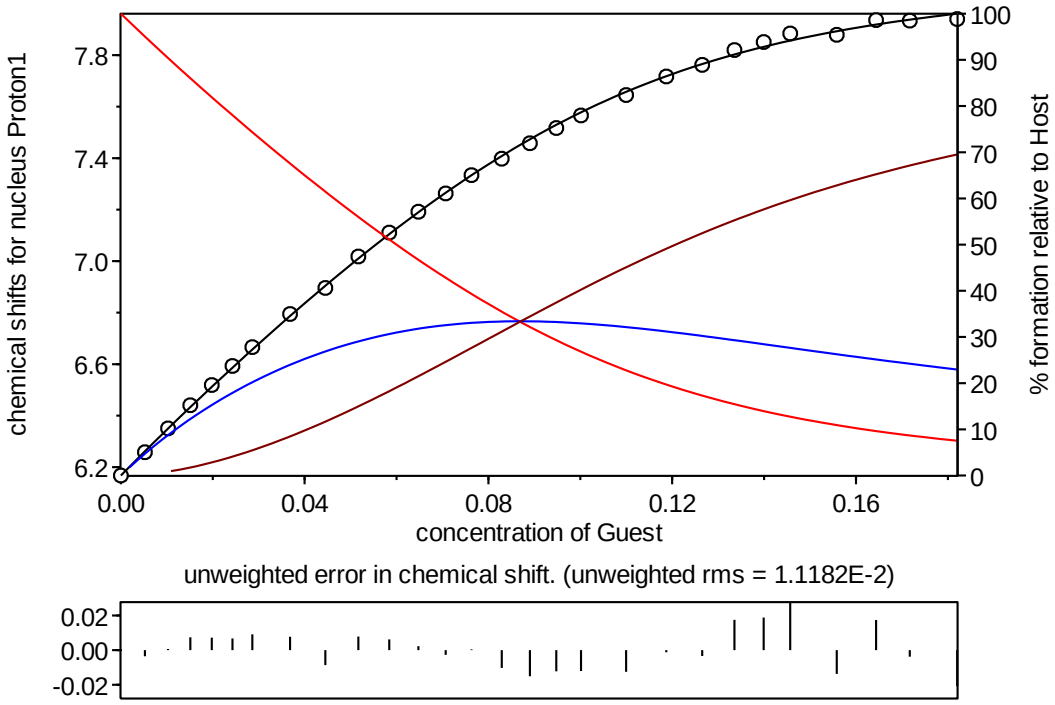

Figure 70 NMR titration data and fit for binding of TBA acetate by **17** in DMSO: black circles- experiemental measurements, black line- fit of model to data, red line- free host in solution, blue line- 1:1 host:guest binding, brown line- 1:2 host:guest binding.

3.6.3.2 Job plots

Stock solutions of **20** (0.0255 g in 5 ml DMSO-d_6) and TBA-acetate (0.0146 g in 5 ml DMSO) were prepared in glass vials. The solutions were added to separate NMR tubes to give samples with the same total volume (0.8 ml) but different mole fractions of **20**:TBA-acetate ranging from 0.9-0.1 **20**. Results were analysed in Microsoft Excel.

3.6.3.3 Rheometric studies

Rheology experiments were performed using a TA Instruments Advanced Rheometer 2000. A concentric cylinder couette geometry with a gap of 1000 μm and 10 ml of sample was used in each case. Samples were prepared by weighing 0.1 g of gelator into a 15 ml glass vial along with the appropriate molar equivalents of TBA-acetate and 10 ml of solvent mixture. The vials were sealed and carefully heated until the gelator had fully dissolved (care must be taken due to pressure build up). The hot gelator solution was transferred into the pre-heated concentric cylinders using a preheated glass pipette. Gels of **20** in 1:9 toluene to acetonitrile mixtures were cooled from 90-20°C whilst ethyl acetate gels of **20** and chloroform gels of **17** were cooled from 50-20°C. Oscillatory stress sweep measurements were preformed over a range of 0.01-300 Pa with a constant frequency value of 1 Hz.

3.6.4 Fluorescence studies

UV-vis absorption spectra were obtained on a Hewlett-Packard 8453 diode array spectrophotometer using standard 1 cm width quartz cells. All emission spectra were produced with an excitation wavelength of 345 nm which corresponds to a maximum in the UV-vis absorption spectra for both **35** and **36** in dilute toluene solution. Emission spectra were obtained using a Jobin-Yvon Horiba Fluorolog 3-22 Tau-3 spectrofluorimeter and were corrected for the spectral response of the instrument. Solution based spectra were recorded with a right angle illumination and collection method using a standard quartz cell with a path length of 1 cm. Gel samples were measured in front-facing geometry in 1.75 ml screw top vial. Slit widths were varied with samples ranging from 1.5 to 8 nm depending on concentration and intensity of sample emission.

Analytical grade solvents were used without drying or degassing procedures. No emission is observed for gelators **16** or **17** and negligibly weak fluorescence was observed for concentrated gels of phenylalanine derived gelator **20**. Dilute toluene solutions were produced by heating and sonicating 1 mg of **35** or **36** in 10 ml of solvent and to create a saturated solution at room temperature. The samples were then filtered through cotton wool to remove excess solid and the concentration was estimated to be in the order of 1×10^{-7} mol dm^{-3}.

3.6.4.1 Co-gelation studies

1:9 mixed gel samples were prepared by weighing 0.0010 g of **35** or **36** and 0.0090 g of **16**, **17** or **20** into glass screw top vials and adding 1 ml of solvent. Samples were repeatedly heated with a heat gun and sonicated to ensure complete dissolution and homogeneous gel formation. Slow cooled samples were prepared by placing the vial on a wooden bench top and allowing to cool to room temperature. Fast cooled samples were prepared by heating the sample with a heat gun until fully dissolved. The sample was then rapidly immersed in a water bath (16°C) and at the first sign of phase separation (approximately 10 seconds) briefly sonicated (approximately 1 second). If the sample is sonicated well above the T_{gel} the sample remains in solution whilst prolonged sonication disrupts gels which have already formed. Differences in the temperature to which samples are heated and the stochastic nature of gel nucleation can mean there is some variation in the time taken for gels to form.

3.6.4.2 Anion addition to 35 and 36 in dilute DMF solution

Concentrated stock solutions were prepared by dissolving **35** or **36** (0.001 g) in DMF (1 ml). Samples were made by diluting 0.02 ml of stock solution with 2 ml of DMF in a quartz cuvette. Stock solutions of anion were formed by dissolving TBA actetate (0.0390 g) or TBA tetrafluoroborate (0.0425 g) in 1 ml of DMF. Anion solutions were added to the cuvette using a microsyringe and shaken, but not heated, between measurements.

3.6.4.3 Anion addition to 35 and 36 in toluene mixed gels

Stock solutions were prepared by heating and sonicating 1 mg of **35** o **36** in 10 ml of toluene for 5 minutes then allowing the sample to cool to room temperature. Saturated solutions were formed by passing the solution through a pipette containing cotton wool to remove the undissolved material. Mixed gel samples were prepared by weighing 10 mg of gelators **16**, **17** and **20** into 1.75 ml vials and adding 1 ml of the toluene stock solution containing **35** or **36**. The samples were heated until all material was fully dissolved then rapidly cooled in a water bath with brief sonication in accordance with the fast cooling method. Stock solutions of anion were prepared by dissolving 0.172 g of TBA-acetate or 0.187 g of TBA-tetrafluoroborate in 0.6 ml of acetonitrile. Gels were reformed following the addition of each aliquot of anions and emission spectra recorded after a 5 minute cooling period.

Chapter 4: Using Gel Morphology to Control Pore Shape

4.1 Introduction

A variety of low molecular weight gelators (LMWGs) have been found to self assemble into supramolecular structures capable of immobilising solvent to form a gel.[24, 72, 171] These gels adopt a number of nanoscopic morphologies including fibrous, helical, ribbon-like, tubular, lamellar and vesicular structures.[121] Such frameworks have been used as scaffolds to template the formation of rigid nanoscopically structured materials for applications such as filtration, catalysis, tissue repair, drug delivery and rewritable materials.[126, 131, 219] The soft template of the gels can be 'fixed' in a variety of ways such as by depositing an inorganic material on the inner or outer surface of the template or using LMWGs which can themselves be polymerised to give a rigid structure.[61, 121, 122] LMWGs able to gel polymer precursors such as styrene or methyl methacrylate which can be subsequently polymerised have been used to give composite materials.[125, 126] The supramolecular nature of the gel matrix means it can be removed by washing or chemical treatment of the composites to leave an imprint of the gel structure in the polymer. A number of fibrillar,[128-130] helical,[131, 132] tubular and macroporous structures[133] have been imprinted in this way.

The present study utilises two hexylene spaced bis-urea gelators functionalised with alanine or phenylalanine end groups, namely **17** and **20**, respectively. The compounds gel a variety of solvents[170] including a 1:1 mixture of polymer precursor methyl methacrylate (MMA) and cross-linker ethylene glycol dimethacrylate (EDGMA). Electron microscopy revealed the nanoscopic morphology of the gels was different for the two compounds with xerogels of **20** showing small cylindrical fibres whilst **17** consists of two-dimensional ribbon-like structures. The present study compares the structure and porosity of methylmethacrylate polymers templated with the two different gelators.

4.2 Sample preparation

Gels are formed by heating a set amount of gelator (0, 1, 5, 10 or 20 % w/v) in 1 ml of 1:1 MMA:EGDMA in a sealed vial to give a clear solution. A high concentration of cross-linker was chosen to minimise rearrangement upon washing.[128] Gelation occurs rapidly upon cooling to room temperature. Samples were initially prepared using 1,1′-azobis(cyclohexane carbonitrile) as a polymerisation initiator. This initiator is thermally sensitive so has to be

diffused into the gel once formed. This is achieved by layering a concentrated solution of the initiator on top of a preformed gel and allowing it to diffuse for 18 hours. Later samples used a blend of diphenyl(2, 4, 6-trimethylbenzyl)phosphine oxide and 2-hydroxy-2-methylpropiophenone as the initiator which is thermally stable and can be heated along with the gelator ensuring a more even distribution of initiator.

Polymerisation was induced by irradiating the samples with UV light for a further 24 hours. The gelator was then removed by washing the samples with hot methanol in a Soxhlet apparatus for up to three days. Removal of the gelator was confirmed by both chemical analysis which showed no nitrogen in the washed samples, and by NMR spectroscopy of the solvent from polymer samples immersed in DMSO-d_6 which showed no signals corresponding to gelator. Samples were dried under vacuum to remove residual solvent.

The transparency of the gels and corresponding polymers decreases with increasing gelator concentration and there is a further increase in the opacity of the polymers following washing. The polymers templated by **20** allow more light to pass through than those formed with the corresponding concentration of **17**. Samples of the polymers were prepared for SEM by shattering the brittle polymers and attaching the fragments to carbon tape mounted on silicon wafers. The samples were placed under high vacuum and coated with 5 nm of platinum prior to imaging.

4.3 SEM Studies

Electron microscopy images of xerogels of **17** formed from the un-polymerised 1:1 MMA:EGDMA gel samples revealed ribbon-like structures (Figure 71). The ribbons appear to have a consistent thickness of ~25 nm, but exhibit considerable variation in the width ranging from hundreds of nanometres to several micrometres. In contrast, SEM images of **20** prepared in the same way indicate a tangled network of one-dimensional fibrous strands. The diameter of individual fibres is relatively uniform (~50 nm) though they are often tangled together into larger bunches. A helical twist is evident in some fibres indicating they may be composed of smaller fibrils twisted together. Increasing the concentration of gelator has little effect on the dimensions of the fibres. The difference in morphology between the two gelators is thought to be due to differences in the underlying packing of the molecules in the gel, as discussed in Chapter 2.

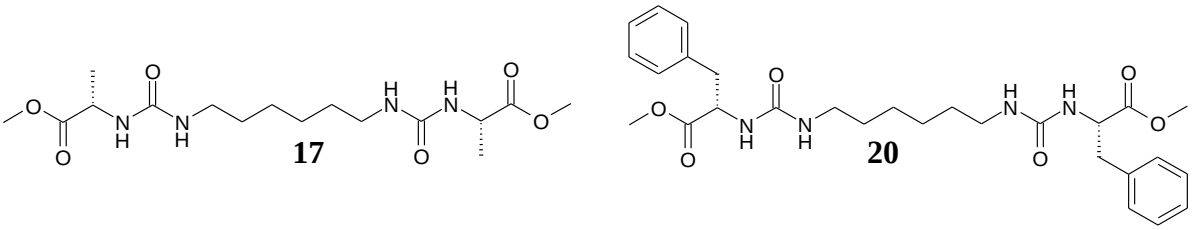

17

20

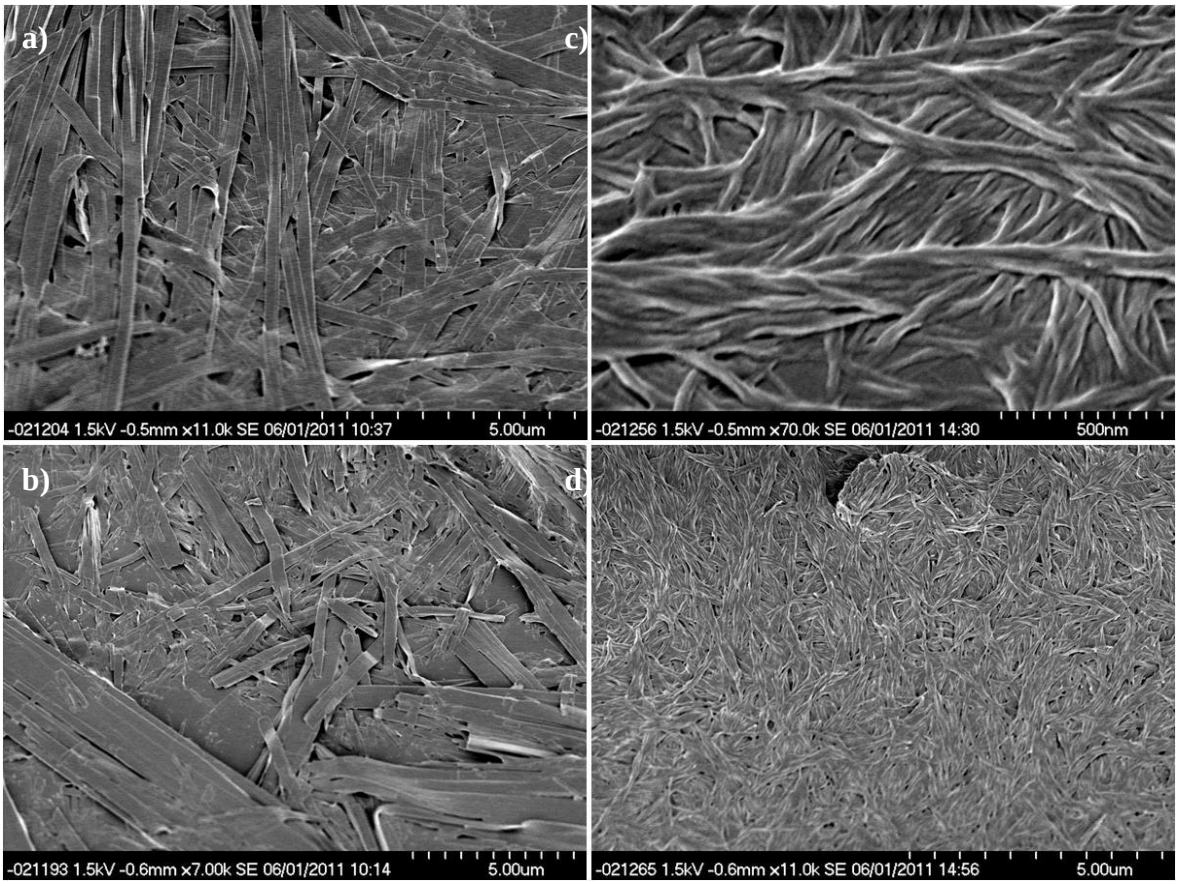

Figure 71 SEM images showing xerogels formed from 1:1 MMA:EDGMA with a) 5 % w/v **17** b) 20 % w/v **17** c) 2 % w/v **20** d) 5 % w/v **20**

Evidence of the gel fibres could be seen in the unwashed gel-polymer composites, particularly of **2** where ribbons protruding from, and running along the surface of the polymer can be clearly seen. Some contraction of the polymer or gelator appears to have taken place with gaps between the gel ribbons and surrounding polymers evident. Less direct evidence of the fibres of **5** were observed in the composites, possibly due to their smaller size making them difficult to distinguish from the polymer surface.

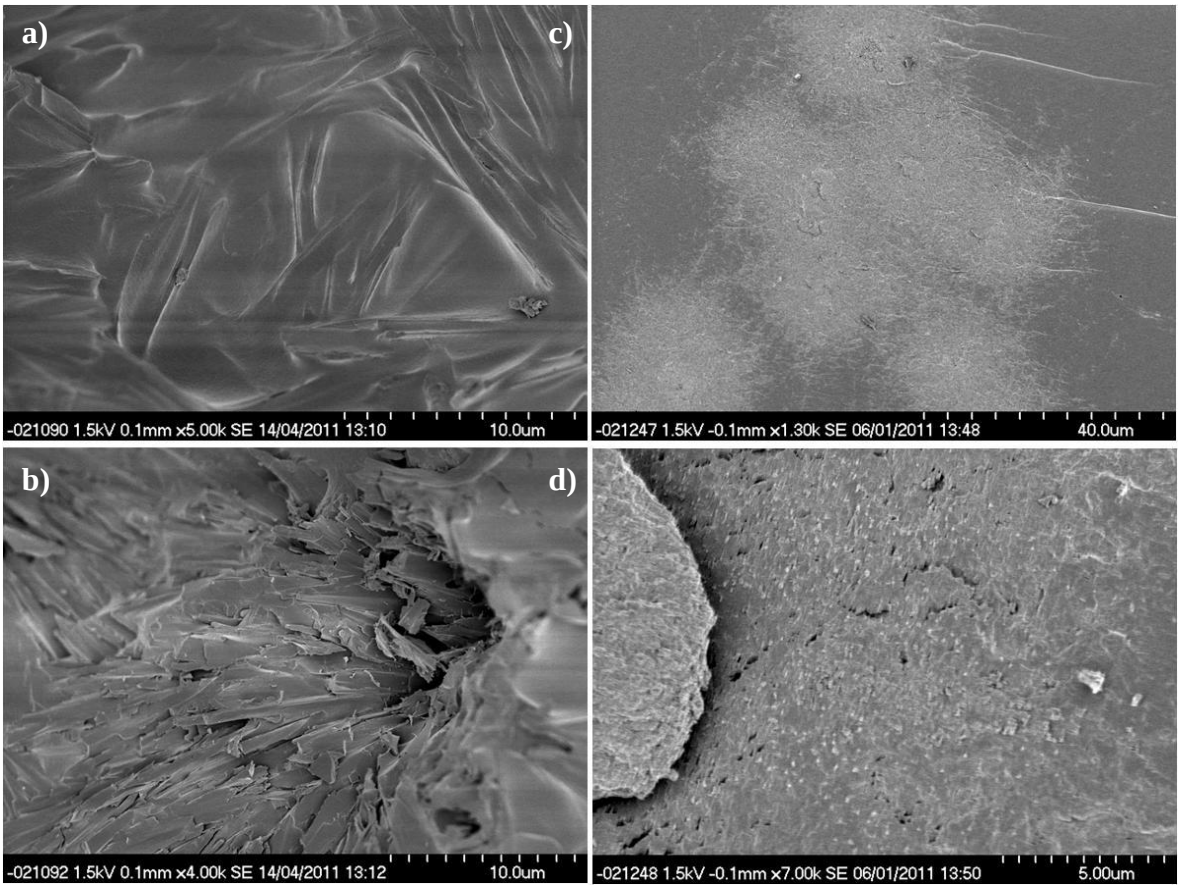

Figure 72 Unwashed polymer composed of 1:1 PMMA:EGDMA formed with (a and b) 10 % w/v **17**, (c and d) 5 % w/v **20**

Washing the polymerised gels with methanol to remove the gelator produced polymers with a variety of features consistent with the imprinting of gel fibres. Gelator **17** left slits and ribbon-like grooves in the polymer surface with dimensions consistent with those seen for the xerogels. These features tend to be in isolated patches at lower concentrations whilst at high concentrations less well defined, macro-porous materials are formed. Polymers formed by **20** showed fibre-like imprints and cylindrical pores, again consistent with the gel morphology. The shape of individual pores tends to be poorly defined, presumably due to bunching of fibres and differences in the angle at which the fibre intersects the surface.

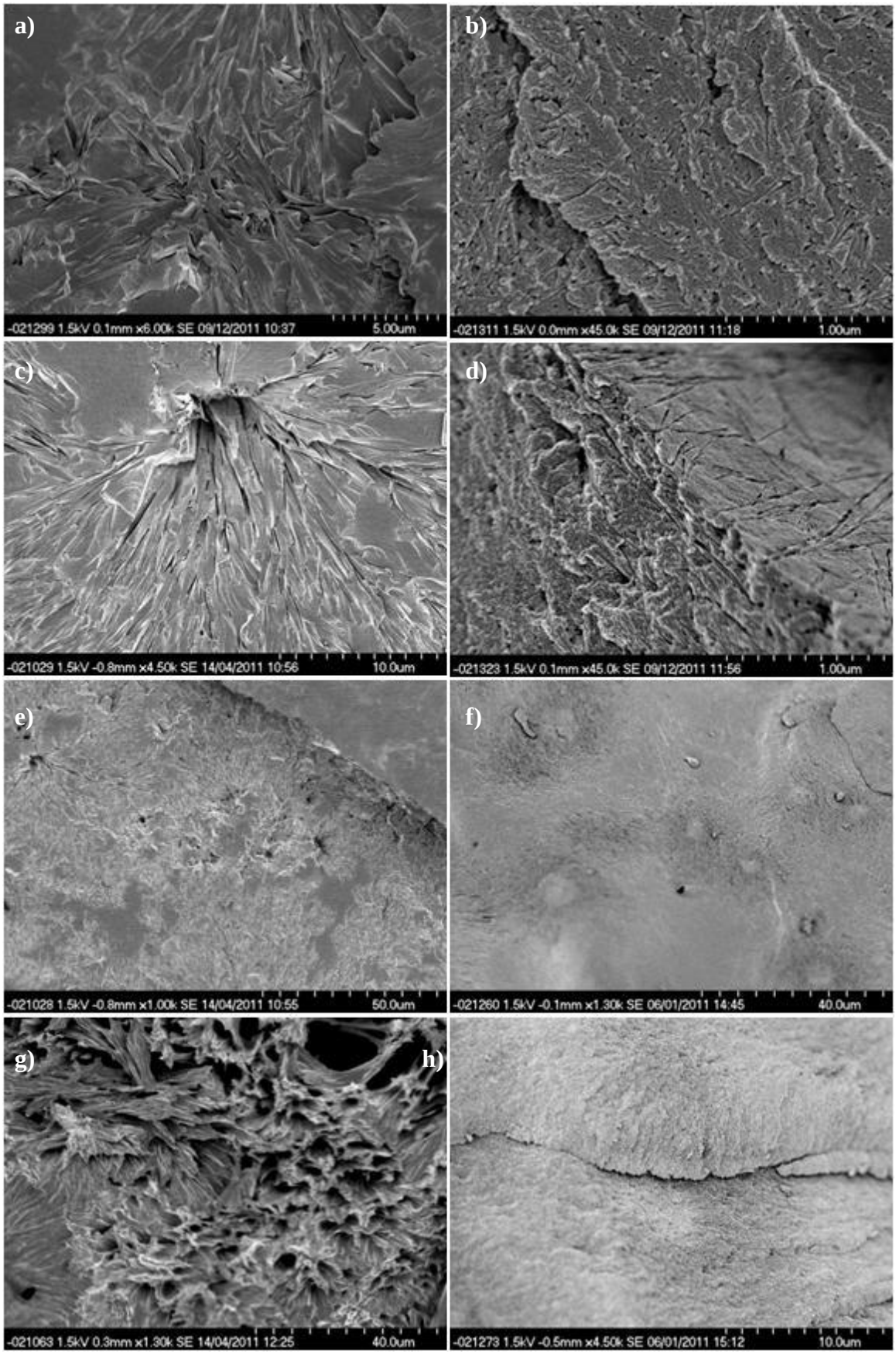

Figure 73 SEM images of nano-porous polymers formed by a) 1 % w/v **17**, b) 1 % w/v **20**, c) 5 % w/v **17**, d) 5 % w/v **20**, e) 5 % w/v **17**, f) 10 % w/v **20**, g) 20 % w/v **17**, h) 20 % w/v **20**.

Interestingly, for polymers formed by both **17** and **20** the porous features are not evenly distributed throughout the sample (see Figure 73e and f) but tend to be bunched together, separated by patches of smooth polymer. In some cases the direction of the fibres appears to have been aligned. This presumably reflects bunching and entanglement of the fibres in the gel phase. This inhomogeneity and aligning is often seen in SEM images of collapsed xerogels and their presence in the polymers indicates that this is a real property of the gels rather than a result of the drying process.

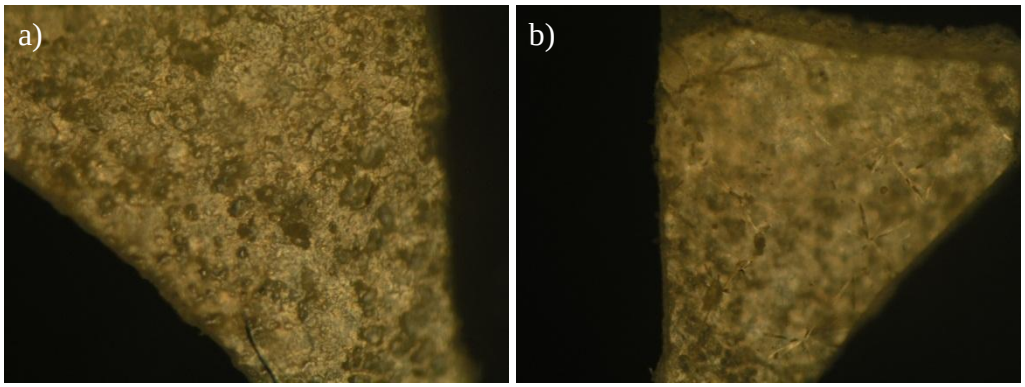

Figure 74 Optical microscopy images showing different faces of polymer sample a) rough face, b) smooth face

In general the polymers proved relatively inhomogeneous with different fragments displaying a variety of different surface textures, some of which contain no evidence of imprinting. It is thought that the smooth fragments represent portions of the polymer resting against the glass sides of the vial or at the gel surface, as observed by optical microscopy in Figure 74. 1:1 PMMA:EGDMA reference samples, formed using the same processes but without gelator, showed a number of different textured surfaces and occasional holes (Figure 75). However, none of the features described for any of the imprinted polymers were observed in the reference samples.

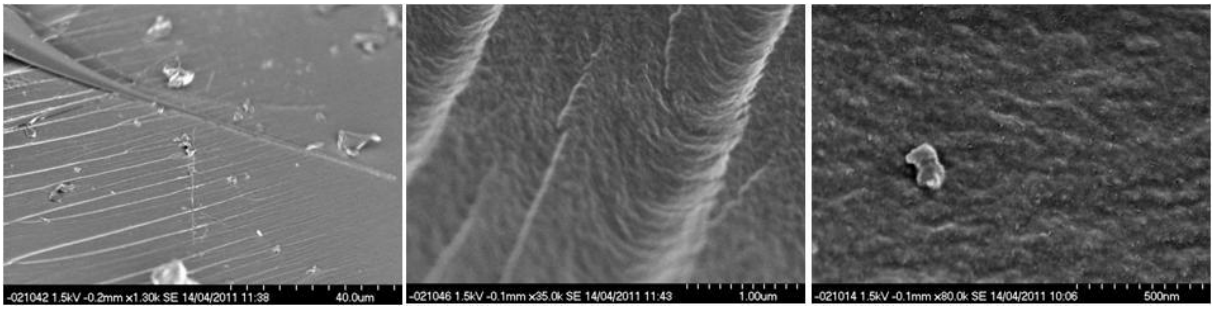

Figure 75 SEM images of control polymer formed from 1:1 MMA:EGDMA without gelator

4.4 Imprinted Polymer Gas Porosity Measurements

The porosity of samples of polymers with 1, 5 and 10 % w/v **17** or **20** was measured by gas adsorption studies which confirmed the formation of microporous structures by both gelators. Results are summarised in Table 9 and the isotherms are shown in Figure 76. Densities were measured by gas pycnometry and found to be approximately constant across all samples ranging between 1.22-1.28 g/cm^3. No correlation between density and concentration of gelator was observed indicating an open pore structure.

Table 9 Summary of nitrogen gas adsorption data for washed polymers templated with various concentrations of compounds **17** and **20**.

	Composition of gelator template					
Gelator	**17**			**20**		
Concentration	1 % w/v	5 % w/v	10 % w/v	1 % w/v	5 % w/v	10 % w/v
Density (g/cm^3)	1.2675 ±0.0019	1.2816±0.0067	1.2605±0.0011	1.2695±0.0019	1.2233±0.0020	1.2458±0.0019
BET Surface Area (m²/g)	0.5425 ± 0.0074	0.2487 ± 0.0099	4.818 ± 0.027	1.209 ±0.011	12.974 ±0.049	29.70 ±0.14
BET constant, C:	66.58	31.32	80.87	70.01	87.97	97.94
Correlation Coefficient:	0.9992	0.9935	0.9998	0.9996	0.9999	0.9999
BJH average pore diameter (nm)	17.10	36.03	22.94	8.66	8.71	8.84

BET surface area measurements show the polymers produced by **17** have substantially lower surface areas (0.2-4.8 m^{2}g^{-1}) than those templated by **20** (1.2-30.0 m^{2}g^{-1}). It is worth noting that whilst the absolute surface areas for both polymer types are low compared to materials such as charcoal (400 m^{2}g^{-1})[220] or zeolites (50-1250 m^{2}g^{-1}),[221] this is unsurprising given the low porosity of the materials (<10%). The surface areas are high when compared with polyHIPEs (3 m^{2}g^{-1}, 74% nominal porosity)[222] which have micron sized pores and porosities of >74%. The surface areas increase with the concentration of **20** as expected. The trend is less clear for polymers of **17** with the 5 % w/v sample showing an unexpectedly low surface area compared to the other samples.

The BET constant, C, is related exponentially to the enthalpy of adsorption in the first adsorbed layer and provides an indication of the magnitude of the adsorbant-adsorbate interaction.[223] High C-values (~100) are associated with a sharp knee in the low pressure region allowing the precise pressure at which monolayer formation is complete to be determined. If the C-value is low (typically less than 20), a specific plateau cannot be

determined whilst C-values greater than 200 typically indicate microporosity. The C-values obtained for the polymers templated by **20** have values in the range 70-98 which provide a good fit to the BET model. The **17** series has comparatively low C-values (31-80), but is still large enough to allow a good fit to be made, as reinforced by the strong correlation coefficients. As the polymer is the same in each case, and the C-values are obtained in the low pressure region of the isotherm so will be unaffected by pore size and shape, it is difficult to explain the extent of variation in C-value between samples. The variation may indicate incomplete removal of gelator or differences in cross-linker efficiency. However, as the BET model does not account for surface energies and the correlation coefficients indicate a good fit to the model, this variation is not thought to have broader implications.

Gas adsorption isotherms have been classified based on empirical observations about the shape of isotherms and hysteresis loops obtained from different materials.[223] Both series of materials show type IV isotherms with characteristic hysteresis loops associated with condensation taking place in mesopores. The series of gels templated with **20** reach a plateau at high pressure and show hysteresis over a broad pressure range. The hysteresis loop shape matches that of an H2 material which is characteristic of relatively disordered porous material. [223] The sudden increase in the gradient of the desorption curve at relative pressures of 0.4-0.5 is attributed to the phenomena of forced closing and indicates channels of varying diameter. Other 'kinks' in the curves are thought to represent inhomogeneity either in the surface chemistry or pore structure. The sudden increase in adsorption at high pressure in the 1 % w/v **20** sample was also observed when the measurements were repeated.

In polymers templated by **17** a plateau is rapidly reached at low pressures associated with completion of the nitrogen monolayer. This is followed by the unrestricted adsorption of nitrogen at higher pressures with no saturation occurring. The hysteresis loop shape matches that of a H3 type material which is characteristic of materials with narrow, slit-like pores such as those which are observed when plate-like materials agglomerate.[223] No forced closing is seen at 0.4-0.45 relative pressure which indicates a consistent pore diameter.

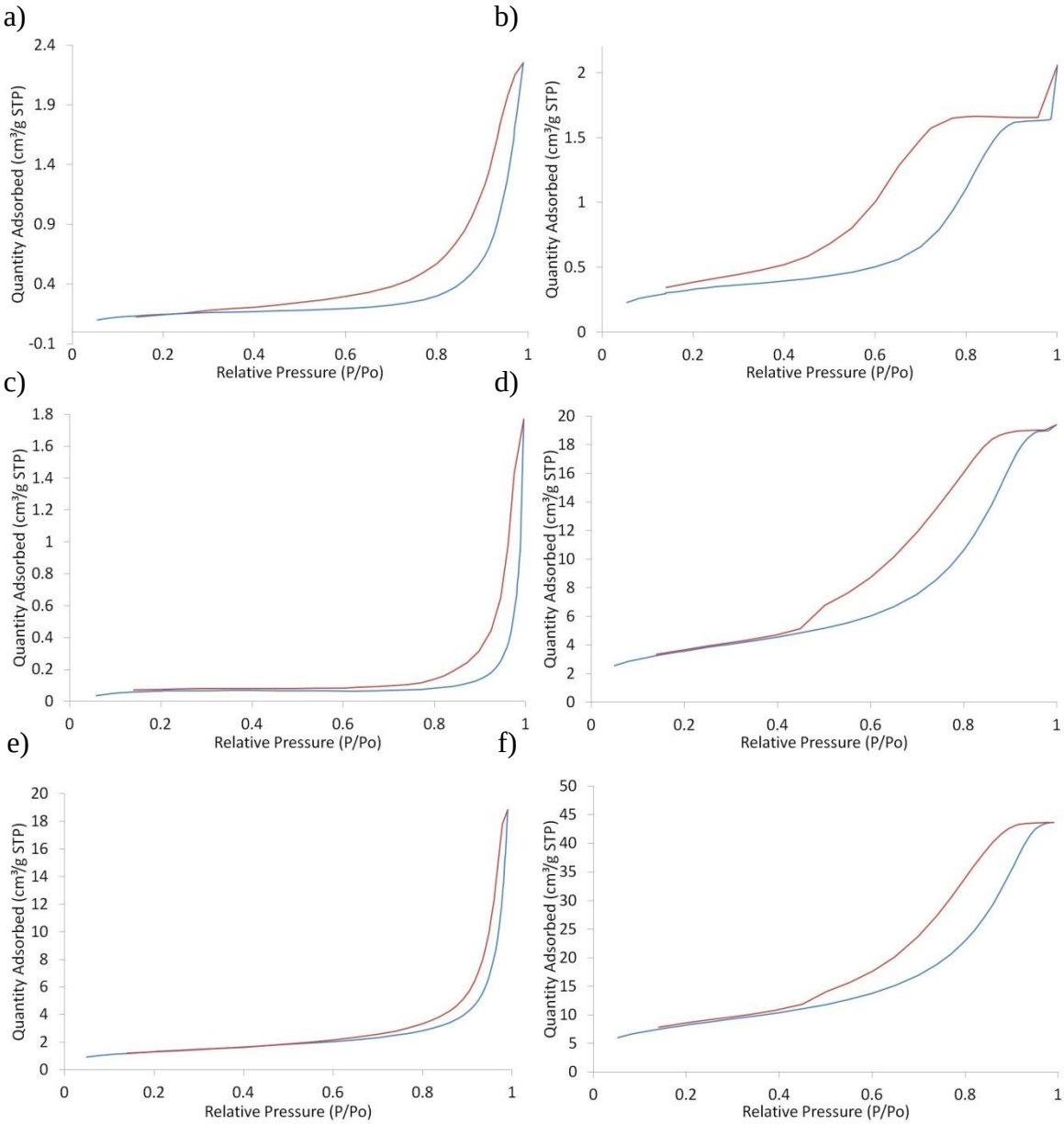

Figure 76 BET isotherms showing adsorption (blue) desorption (red) curves for washed polymer samples formed from a) 1 % w/v **17** b) 1 % w/v **20** c) 5 % w/v **17** d) 5 % w/v **20** e) 10 % w/v **17** f) 10 % w/v **20**

4.5 Pore size distribution

The pressure at which an adsorptive will spontaneously condense (and evaporate) in a cylindrical pore size can be calculated using the Kelvin equation. However, condensation occurs in pores that already have multilayers on the walls. The pore size distribution is therefore calculated using the BJH model which modifies the Kelvin equation to take this into account.[224] The average pore diameters for the templated polymers are given in Table 9 and the pore size distribution is shown in Figure 77 and Figure 78. The data for the **20** series is calculated from the adsorption curves to avoid complications due to forced closing in the

desorption isotherms.[224] Pore diameter is shown plotted against pore volume. Plots of pore diameter against pore surface area show the same patterns but with the distributions skewed slightly towards lower pore diameters.

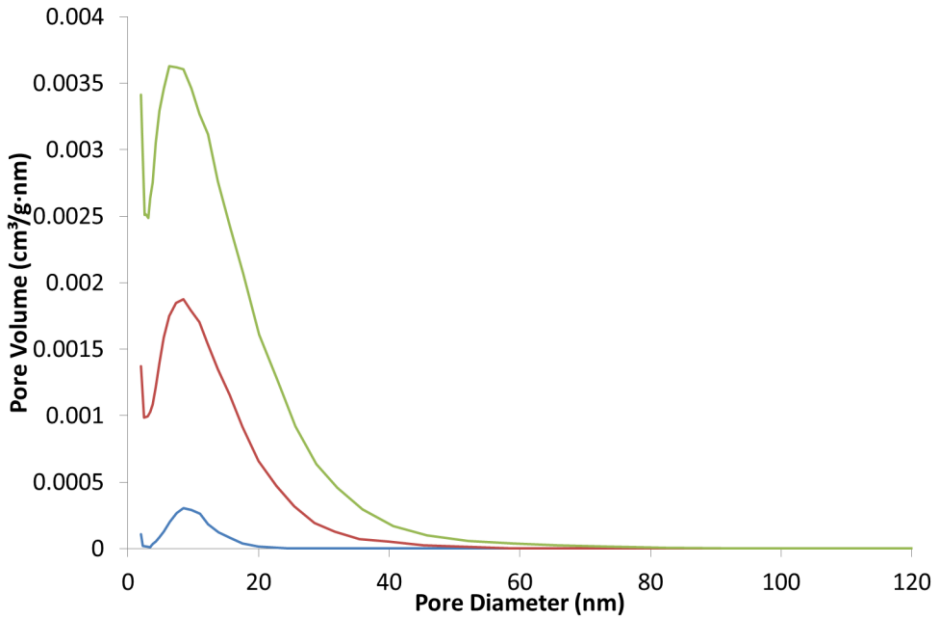

Figure 77 Pore size distribution calculated from the adsorption isotherm measured for washed polymer samples templated with **20**: 1 % w/v (blue), 5 % w/v (red), 10 % w/v (green),

The average pore diameter is 8-9 nm in polymers templated with **20** and there is a narrow distribution of pore sizes centred around the average. The pore volume increases with the concentration of gelator and the range of pore diameters increases from an upper limit of 25 nm in the 1 % w/v sample to around 80 nm in the 10 % w/v sample. This is consistent with the observation by SEM that the size of the fibrils stays approximately constant but with increased bunching at higher concentrations of gelator. However, the average pore size is smaller than might be expected based upon the SEM images and indicates that in solution individual fibrils are less aggregated than they appear in the dried xerogel images.

The average pore size is slightly larger in the **17** templated series, ranging between 19-36 nm, and there is a much broader pore size distribution pattern (Figure 78). The shape of the distribution for 5 % w/v **17** is poorly defined and with lower pore volume than for the samples formed with both higher and lower concentrations of gelator. The 1 % w/v data sample ranges in pore size up to 80 nm increasing to 120 nm for the 10 % w/v sample. This greater range in pore diameters reflects the broad range of ribbon widths observed by SEM.

Further experiments will be undertaken by Dr. David Johnson using mercury porosimetry to examine the macroporosity of these materials.

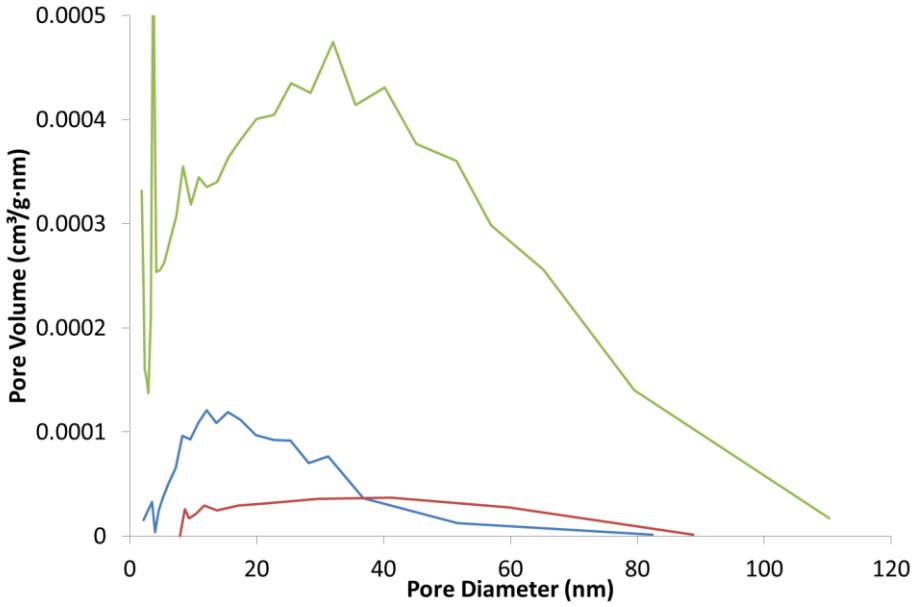

Figure 78 Pore size distribution calculated from the desorption isotherm measured for washed polymer samples templated with **2**: 1 % w/v (blue), 5 % w/v (red), 10 % w/v (green),

4.6 Conclusion

By making small changes to the molecular structure of a LMWG and hence gel morphology, polymeric materials with very different pore shapes, sizes and adsorption characteristics can be created. The entangled networks of cylindrical fibres observed in xerogels of **20** produce polymers with corresponding circular pores and fibrous imprints. Gas adsorption measurements are indicative of a mesoporous material with a random pore structure. The pores formed by **20** have a relatively well defined average pore diameter of 8-9 nm and the total volume increases linearly with the concentration of gelator. In contrast the larger ribbon-like xerogels of **17** give polymers with slit shaped pores and a gas adsorption profile indicative of plate-like aggregates. The average pore diameter is larger and there is a broader pore size distribution reflecting the variable width of the ribbons of **17**. Supramolecular gels provide a ready means of creating porous polymers with very different architectures and properties which can be tuned by varying the concentration of template.

4.7 Experimental Section

All solvents and reagents were obtained from standard commercial sources and used without further purification. Details for the preparation of compounds **17** and **20** are provided in the experimental section of Chapter 2. Elemental analysis of the polymers was performed using an Exeter Analytical inc. CE-400 Elemental Analyser and NMR experiments using a Varian Mercury-400 (400 MHz for 1H).

4.7.1 Preparation of polymers

Method 1

0, 5, 25, 50 and 100 mgs of gelators **17** and **20** were weighed into separate 2 ml screw top glass vials. 0.5 ml of a 1:1 by weight methylmethacrylate (MMA): ethylene glycol dimethacrylate (EDGMA) (Aldrich refs) stock solution was added to each vial. The sealed sample was heated until the gelator was fully dissolved and gelation took place rapidly upon cooling. 0.05 ml of a 1:1 MMA:EDGMA solution containing 5 mg (1 % w/v) of 1,1'-azobis(cyclohexane carbonitrile) was layered on top of the sample and allowed to diffuse overnight. The samples were irradiated with 254 nm UV radiation using a UVGL-58 handheld UV lamp for 48 hours at a distance of 5 cm. The samples were washed with hot methanol in a soxhlet for 36 hours. The samples were dried overnight under vacuum in a desiccator. CHN analysis of the polymers showed no nitrogen was present in the polymers indicating removal of the gelator.

Method 2

0, 10, 20, 100 and 200 mgs of gelators **17** and **20** were weighed into separate 10 screw top glass vials. To each vial was added 2 ml of a 1:1 by weight MMA:EDGMA stock solution containing 1 % w/v blend of diphenyl(2, 4, 6-trimethylbenzyl)phosphine oxide and 2-hydroxy-2-methylpropiophenone (Aldrich 405663). The sealed sample was heated until the gelator was fully dissolved then rapidly cooled and sonicated to ensure homogeneous gel formation. The samples were irradiated with 254 nm UV radiation using a UVGL-58 handheld UV lamp for 48 hours at a distance of 5 cm. The samples were washed with hot methanol in a soxhlet for at least 72 hours. The samples were dried overnight under vacuum in a desiccator. CHN analysis of the polymers showed no nitrogen was present in the polymers indicating removal of the gelator. Suspension of samples of the polymer in d_6-DMSO showed no indication of gelator by NMR spectroscopy.

4.7.2 Scanning electron microscopy

Samples were applied directly to silicon wafer chips (Agar Scientific) using a cocktail stick for gels or a pipette for liquids. Solid samples of polymer were stuck onto the wafers using carbon conductive adhesive tape. Samples were stored under vacuum at $1x10^{-5}$ mbar then sputter coated with 5nm platinum in a Cressington 328 coating unit, at 40 mA (density 21.09 and tooling set at 1) with rotation and a 30^0 angle of tilt. Samples were imaged using a Hitachi S-5200 field emission scanning electron microscope at 1.5 kV.

4.7.3 Gas pycnometry

The sample density was measured using an AccuPyc II Micromeitics He pycnometer. The material was then weighed (0.8-1.5 g) into the sample cup (10 cm^3) and placed in the instrument. The sample was then allowed to reach thermal equilibrium with the instrument for 5 to 10 min. The material was then purged 20 times ($He_{(g)}$, 19.5000 psig). The material was then placed under pressure ($He_{(g)}$, 19.5000 psig) and the volume measurements taken once an equilibrium pressure was reached (0.0050 psi min^{-1}). The final density measurement is taken as an average of the 20 repeats and reported with a standard deviation.

4.7.4 Gas adsorption isotherms

The sample was added to a sample tube (1 inch diameter) and then degassed on the instrument (20^oC) until a constant pressure was reached. The sample was then weighed (0.8-1.5 g) into the sample tube which was then fitted with a filler rod and isothermal jacket. Nitrogen sorption was then measured under isothermal conditions (77 K) between P/P_0 of 0.0500 to 0.9990 and desorption between 0.999 and 0.140.

BET and Langmuir plots were obtained from measurements at $0.050< P/P_0 <0.2500$; BJH adsorption and desorption plots were obtained at $0.1400< P/P_0 <0.990$. Pore size distributions were obtained using the Faas modified BJH model with a Halsey thickness curve used for the **20** series and the Harkins Jura thickness curve used for the **17** series.

Chapter 5: Supramolecular gels: a new medium for crystallisation

5.1 Introduction

Gel media have been utilized for over a century for the growth of inorganic, organic and protein crystals.[148-150, 157, 162, 225, 226] The improved physical characteristics of the resulting crystals (better optical quality, larger size and fewer defects) are usually ascribed to the suppression of convection currents, sedimentation and nucleation afforded by the viscous gel environment.[147, 164] The majority of crystal growth in gels to date has focused on inorganic systems grown from aqueous gels. In many instances the gel is thought to act as an inert matrix within which crystal growth occurs, however in some recent cases, the gel structure has been shown to influence the polymorphism,[154] enantiomorphism[164] and habit of crystals.[157] Occasionally, gel fibres may become incorporated into the crystals, giving rise to composite materials.[227]

Conventional gels are formed using polymeric or clay-like materials such as gelatine, agarose, polyacrylamide or silica.[150, 228] More recently, a new class of low molecular weight gelators (LMWGs) has emerged which self assemble into supramolecular networks capable of forming gels.[24, 25, 60, 62, 229-231] The supramolecular nature of such systems gives them a potential inherent advantage in that their formation is readily reversible. This sol-gel transition can be triggered in response to a range of stimuli such as changes in temperature, pH, sonication, irradiation with light or, as in the present work, addition of a chemical trigger in the form of anions.[62, 72, 85, 87, 100, 186, 214, 232, 233] Moreover, the chemically diverse nature of supramolecular gels means that almost any solvent can be gelled. A broad range of chemical species have been shown to form gels including surfactants, sugars, fatty acids, amino acids, bis(ureas), and many others, in a variety of solvent systems.[24, 62] However, the potential of LMWGs as a medium for crystal growth remains largely unexplored,[165-167] with the exception of some elegant work on the use of LMWGs for the growth of calcium carbonate[25] and other inorganic minerals[169], as part of studies on biomineralisation.

The reversible nature of supramolecular gels can be utilized to allow easy recovery of crystals whilst the diverse array of chemical functionalities that can be introduced allows for tuning of interactions between the gel and growing crystal. LMWGs are generally readily synthesised, so depending on the system, are relatively inexpensive, particularly if required on a large

scale. This investigation aims to show proof of principle for the growth and recovery of organic crystals from anion-triggered supramolecular gels, and to explore the potential of this medium for influencing crystal growth, particularly in active pharmaceutical ingredients (APIs) for which crystal habit and polymorphism is a key economic and formulation problem.[234, 235]

5.2 Development of Methodology

As well as opportunities, the gel phase poses a number of additional challenges to the growth, recovery and characterisation of crystals compared with solution. With little precedent for the growth of organic molecules from supramolecular gels, a brief outline explaining the reasoning behind the approach taken will be provided in the following section. More specific problems and adaptations encountered will be detailed along with specific experiments in subsequent sections (5.3 and 5.4) and in Chapters 6 and 7.

5.2.1 Gelators

Most common polymeric and clay based gelators used for crystallisation are hydrogelators and the majority of studies involve the crystallisation of inorganic salts from aqueous gels. Many pharmaceutical compounds are relatively hydrophobic in order to permeate cell membranes and can be poorly soluble in water. Crystallisation studies of pharmaceutical compounds typically involve using a wide range of solvents in order to access as many different polymorphs as possible. Pharmaceutical compounds contain a wide variety of functional groups which must not disrupt the supramolecular interactions required for gel formation. The opacity of gels varies from clear to opaque and identifying whether crystallisation has taken place in an opaque gel is more difficult than in a transparent one. Sonication, which can encourage homogeneous gelation for this class of gelator, would also affect the crystallisation of the compounds so was deemed unsuitable for use in gel phase crystallisation. The ideal gelator will therefore reliably form robust, transparent gels without sonication in a wide variety of solvents in the presence of a wide range of chemical functionalities.

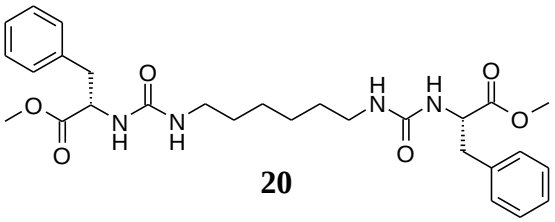

20

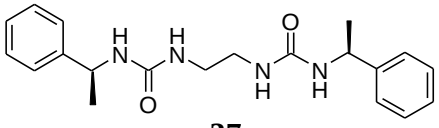

37

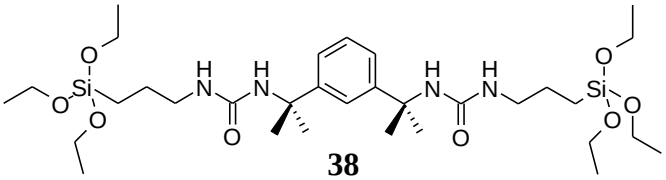

38

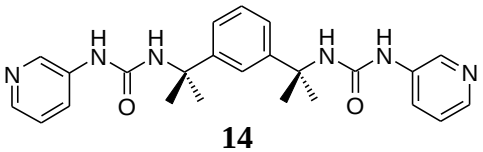

14

	H_2O	MeOH	ETOH	DMSO	THF	CH_3CN	Acetone	$CHCl_3$	DCM	EtOAc	Toluene	Cychex	Hexane	Et_2O
20		G[a]	G[a]	G[a]	G[a]	G	G			G	G			
37		G[a]	G[a]	G[a]	G	G	G	G			G[b]			
38											G	G	G	G
14		G[c]												

Table 10 showing gel formation, G, by compounds **20, 37, 38** and **14** in various solvents. [a] Gels formed upon addition of varying amounts of H_2O [b] Gel formed in toluene/DMSO mixtures [c] in presence of 0.5 eq. $CuBr_2$ or $CuCl_2$.

Preliminary experiments were carried out in order to assess the gelators in terms of the robustness and reliability of gel formation, which solvents they formed gels in, at what concentrations and the opacity of the resultant gels. Early studies used number of gelators previously developed within the group by myself (**20)** and others (**37**,[52] **38**,[63] **14**[71]**)**. Gelators **20**, **37** and **38** were chosen because they reliably form gels in a number of solvents ranging from aqueous systems to toluene, whilst **14** is a metallogelator which forms blue coloured gels with substoichiometric amounts of $CuCl_2$ in methanol.[19] Between them the gelators are able to gel a range of solvents (Table 10), at different temperatures (T_{gel}), and with a different critical gelator concentration (CGC). This class of compound has the potential to form the basis of a library of gelators which will allow the selection of gel properties and specific functionalities to match the compound and crystallisation conditions of interest.

5.2.2 Reversibility

The viscous nature of the gel state means the use of solution phase techniques, such as filtration, to recover crystals are difficult therefore mechanical means are generally used to

separate individual crystals from polymeric gels. Whilst this is possible for large single crystals, it is inconvenient for microcrystalline samples or large scale experiments. The supramolecular nature of LMWGs means that they can readily be dissolved, potentially allowing for recovery of crystals by solution phase techniques such as filtration. LMWGs have been developed which respond to a wide range of stimuli.[62, 72, 85, 87, 100, 186, 214, 232, 233] The use of anions as a means of bringing about dissolution of supramolecular gels has been developed within the Steed group and by others.[19, 178] The presence of anions has been shown to disrupt the urea tape hydrogen bonding motifs which are central to the formation of the one dimensional fibres which give rise to the gel state (Figure 79).

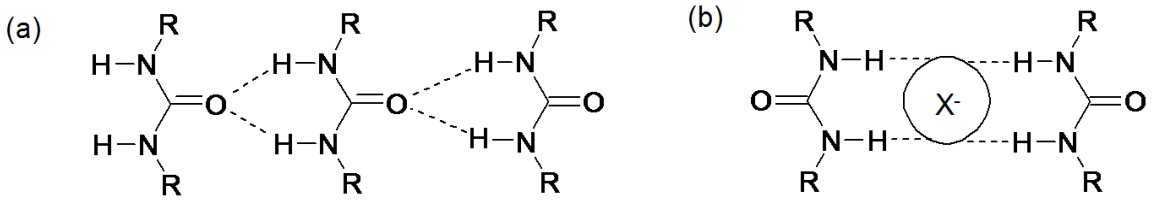

Figure 79 a) urea tape hydrogen bonding motif which gives rise to long fibres b) hydrogen bonding motif adopted by ureas in the presence of anions resulting in breakdown of gel fibres.

Preliminary studies using gelator **20** mirrored findings from more detailed studies[52] on similar compounds which showed tetrabutylammonium (TBA) acetate have the most pronounced effect on gel strength. Other anions such as HSO_4^- and F^- have much less effect, even at higher concentrations. The choice of solvent is a key limiting factor in the use of anions to disrupt gelation. In apolar solvents such as toluene the anions would not dissolve whilst in aqueous solutions solvation of the anions prevented disruption of the urea motifs. Mixtures of solvents such as 1:9 CH_3CN:toluene or 1:9 $CHCl_3$:toluene proved ideal compromises providing apolar environments where anion-urea interactions were strong whilst allowing sufficient anion to dissolve (Figure 80).

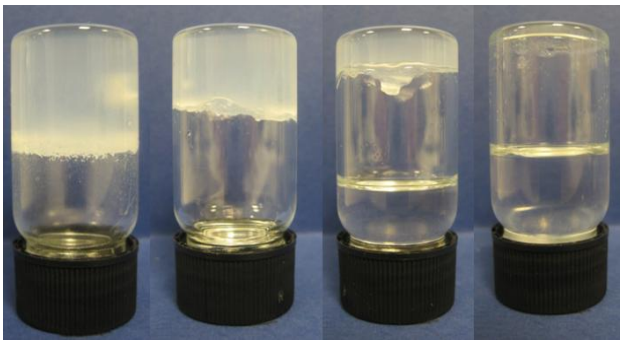

Figure 80 Images showing the effect of the addition of one equivalent of TBA-acetate in 500 µl of acetonitrile on a gel of 1 % w/v **20** in 4 ml of toluene over a period of 10minutes.

In Chapter 3, rheometric studies examining the breakdown of 1 % w/v gels of **20** in 1:9 acetonitrile:toluene and ethylacetate found 1.5 and 0.8 equivalents of acetate were required to disrupt gel formation. However, in these experiments the gels are formed from hot solutions in the presence of increasing concentrations of anion. For the purposes of recovering crystals from the gels, the anions must be added to the pre-formed gel structure. This presents a kinetic barrier to the anions interacting with the urea groups which may be buried in the centre of large fibres with sterically inhibiting or hydrophibic end groups. It is also desirable not simply to break down the gel structure, but to fully dissolve the gel matrix which the fluorescence studies in Chapter 3 show can take as many as 10 equivalents of anion in acetonitrile:toluene mixtures. The anions can be added either as a solid on top of the gel, or as a solution dissolved in a suitable solvent such as acetonitrile or chloroform.

5.2.3 Crystal growth

Crystallisation can be achieved using a variety of approaches including fast and slow cooling, evaporation of solvent, addition of anti-solvent, vapour diffusion, sublimation, grinding and crystallisation from the melt. Evaporation is unsuitable for gel phase crystal growth as are non-solvent based methods. Preliminary investigations using non-drug compounds were undertaken into the use of layering or vapour diffusion of an antisolvent to induce crystallisation. For example, 0.5 ml of cyclohexane layered on top of a 1 % w/v gel of **20** in toluene containing 1 % w/v of 2-hydroxybenzylalcohol (2HBA) induced crystallisation of 2HBA without disruption of the gel. The same result was also observed in a gel of the same composition sealed inside a larger vial containing a small amount of cyclohexane. However, the presence of a second solvent was an additional complication and the slower rates of crystal growth of little advantage to the already slow rates of crystallisation from the gels.

Table 11 Crystallisation of organic molecules from 1 % w/v gels of compound **20** and **38** in various solvents.

Compound	Gelator	Solvent	Control	Gel	Cryst
i) 2-methoxybenzaldehyde 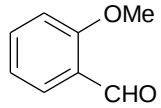	**20**	$DMSO:H_2O$	S	P	-
		EtAc	S	G	- [b]
		Toluene	S	G	-
	38	Et_2O		PG	C[a]
		Hexane		G	C[a]
		Cyclohexane		PG	-
		Toluene	S	G	
ii) Triphenylamine 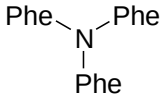	**20**	$DMSO:H_2O$	S	G	- [b]
		EtAc	S	G	-
		Toluene	S	G	-
	38	Et_2O		G	-
		Hexane		G	-
		Cyclohexane		PG	C[a]
		Toluene	S	G	C[a]
iii) Biphenyl-2-methanol 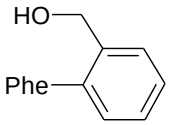	**20**	$DMSO:H_2O$	S	G	-
		EtAc	S	G	-
		Toluene	S	G	-
	38	Et_2O		G	C[a]
		Hexane		PG	-
		Cyclohexane		G	C[a]
		Toluene	S	G	C[a]
iv) 2-hydroxybenzyl alcohol 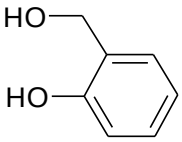	**20**	$DMSO:H_2O$	S	G	C[a]
		EtAc	S	G	C
		Toluene	C	G	C
	38	Et_2O		G	- [b]
		Hexane		P	C
		Cyclohexane		P	C
		Toluene	C	P	C
v) Napthylamine 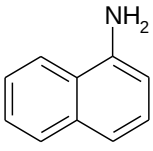	**20**	$DMSO:H_2O$		P	-
		EtAc		G	-
		Toluene	C	P	-
	38	Et_2O		PG	C
		Hexane		G	C[a]
		Cyclohexane		PG	-
		Toluene	C	G	-

G= gel formation, PG= partial gelation, P= precipitation, S= solution, C= crystal, [a] crystal growth on bottom of the vial [b] opaque gel- no crystals observed

Cooling induced supersaturation was identified as the best method for bringing about crystallisation. All of the gels used are thermally reversible and form rapidly upon cooling from a hot solution. Initially the approach was to weigh both the compound (1-5 % w/v) and the gelator (0.1-1 % w/v) into the same vial, add solvent and heat until complete dissolution was observed. Upon cooling the gels form rapidly over a period of minutes and the crystals

grow slowly over a period of hours to weeks. This approach has the advantages that individual samples are quick to prepare and the technique requires little knowledge of the compound's solubility. However, the problem with this approach is that solubility varies considerably between different compounds and solvents. The 'hit' rate for achieving good crystallisation conditions is therefore very low with too much compound not fully dissolving upon heating and too little compound remaining in solution upon cooling. In a preliminary study (Table 10) the concentration was set at 10 mg/ml across six different solvents and five compounds. Crystallisation was observed in only ten out of the seventy samples with all the hits corresponding to just two of the compounds investigated: 2-hydroxbenzyl alcohol and napthylamine.

A second approach was developed which was used in the screen of pharmaceutical compounds described in section 5.4. An appropriate degree of supersaturation for each sample was achieved empirically by gradually adjusting the ratio of compound and solvent until the desired rate of crystallisation was achieved. The optimised hot solution was then added to the pre-weighed gel in a vial before everything was reheated and cooled to form the gel. This process ensured crystallisation was observed in the majority of samples (76/80).

A final approach to generating saturated solutions is to slurry the compound in a particular solvent at a set temperature (e.g. 60°C), then to perform a hot filtration to remove any un-dissolved material. This approach requires less manual adjustment but proved more time consuming and inefficient for producing lots of different small-scale samples. The use of specialist slurrying and filtration equipment overcame these problems during the studies conducted at GSK (Chapter 7).

The rate of cooling is one variable which was not well controlled during these experiments. High temperatures (>150°C) are often required to fully dissolve the gelators and large variations in dissolution temperatures exist between different compounds, gelators and solvent systems. Studies were undertaken at GSK using specialist temperature controlled crystallisation equipment. However, the limited heating range (≤140°C) was insufficient to fully dissolve the gelator in all solvents and the slow cooling rates (≥5 °C min^{-1}) were detrimental to gel formation. This equipment was also unavailable in the Steed lab making it impractical for the majority of studies. Heating was therefore carried out to an arbitrary

temperature using a heat gun with the mixture being heated and sonicated as required to ensure complete dissolution. The samples were then removed from the heat and allowed to cool to room temperature on the bench with gels forming over a period of minutes and crystallisation first observed after several hours or days. Although it is not possible to observe the time or temperature at which the nm-size critical nuclei form, it is likely given the high T_{gel} of many of the gelators used that nucleation takes place once the gels have formed. As the polymorph obtained is locked in at the nucleation stage, controlling nucleation via supersaturation of the system, as well gel fibre chemistry, is likely to be key in selectively crystallising a particular polymorph.

5.2.4 Crystal characterisation

After growing crystals in the gels, the crystal habit and form were identified in order to understand the effect of the gel media on crystal growth. Where the transparency of the gel allowed, a photographic record of shape and position of the crystal was made along with a detailed description. Observations about the habit of crystals from opaque gels were made once the crystals had been extracted. These observations were later simplified to broad categories (block/plate/needle etc.) as records of subtler variations between samples were found to add little value due to their complexity.

The presence of gelator in the sample vial can complicate the characterisation of compounds. Adding anions to dissolve the gel allows crystals to be filtered and washed, separating the gelator (as well as solvent and anions) from the compound. However, recovery by this method can only be used in a limited range of solvents and in some cases the addition of anions resulted in the dissolution of the crystals. It was therefore necessary to identify crystal forms in the presence of the gelator. In cases where the crystals were large or clumped together they could be isolated from the gel by hand using a spatula. Where crystals were more dispersed, the whole gel-sample was filtered and submitted for analysis. The typically low concentrations of gel compared to product, and low crystallinity of the gel fibres, meant that identifying crystal forms by XRPD was generally unproblematic provided there was sufficient sample for analysis. IR spectra were more affected by the presence of the gels with the additional component making the fingerprint region difficult to interpret. This was not a problem for compounds where there are characteristic bands for particular polymorphs which do not overlap with those of the gelator. Determination of unit cells from representative

single crystals also proved a useful method for identifying crystal form. During studies at GSK, *in situ* characterisation of the crystals inside the gels was possible by Raman spectroscopy as discussed in Chapter 7.

Because sedimentation is prevented in gels, crystal growth occurs in the environment in which the crystal nucleates. In some cases crystal growth occurred in the centre of gels, but often it occurred either at the gel surface or from the walls of the vials. Care was taken to preserve as much detail about individual crystallisation events as possible although each sample was unique and it was not always possible to establish trends. In a number of cases, concomitant crystallisation of more than one form occurred in the same gel. Where possible, crystals with clearly different habits were isolated separately and tested for polymorphism using the techniques described above. It should be noted that the effects of solvent and gel environment on the rate of growth of different faces mean crystals of the same polymorph may have very different crystal habits or those of different forms have similar ones. Assignment of crystal forms on the basis of morphology alone is therefore unreliable and should be used in conjunction with other characterisation techniques such as XRPD, IR or XRD.

5.3 Proof of principle for crystal growth in LMWGs

5.3.1 The polymorphism of carbamazepine

Carbamazepine (CBZ), an anticonvulsant, serves as a model compound for many groups engaged in the study of crystal polymorphism.[236-241] There are four known polymorphs of CBZ as well as a dihydrate, several solvates and a number of co-crystals. Recently the fourth form was grown using a polymer heteronucleus[237, 242] and a fifth form using seed crystals of the closely related 10,11-dihydrocarbamazepine (DHC) form II.[243] There is some confusion across the literature over the nomenclature of these forms as summarised by Grzesiak *et al*.[236] Details of the forms relevant to this report are shown in Table 12. The well-defined crystal habits of different common polymorphs of carbamazepine, block shaped form III and needle shaped form II, make it an ideal system to study as initial characterisation can be made from the morphology.

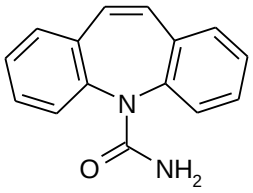

Carbamazepine
(CBZ)

Table 12 Solvent-free polymorphs and selected solvated forms of CBZ.

Form	Space group	Habit	Stability order	Crystallisation method
I	Triclinic, $P\bar{1}$	Needle	2	Melt
II	Trigonal, $R\bar{3}$	Needle	5	Rapid cooling (5ºC) from EtOH
III	Monoclinic $P2_1/c$	Block	1	Slow cooling (25ºC) from EtOH
IV	Monoclinic $C2/c$	Prism	4	Heteronucleation
V	Orthohrombic *Pbca*	Plate	3	Heteronucleation
Dihydrate	Monoclinic $P2_1/c$	Needle	n/a	Recrystallisation from wet ethanol
Acetone/ DMSO solvate	Triclinic, $P\bar{1}$	n/a	n/a	Evaporation from solvent

5.3.2 The effect of gelator 1 on the crystallisation behaviour of CBZ

The crystallisation behaviour of carbamazepine was investigated from gels of **20** in various solvents and at a range of different concentrations and was compared with crystallisation from solution and other gels. Preliminary investigations indicated little disruption of gels of **20** in the presence of even high concentrations of CBZ and large crystals grew readily in some of the samples. A systematic investigation into the polymorphic behaviour of CBZ when crystallised from various solutions and gels of **20** at different concentrations is reported in Table 13.

Table 13 Comparison of gel (1 % w/v **20**) and solution phase crystallisation from various solvent systems at different concentrations of CBZ

Solvent system and phase		**Concentration of CBZ mg/ml**				
		5	**10**	**15**	**20**	**25**
1:9 CH_3CN:Tol	G	G	G	G	G	G
		-	-	-	Blocks	Blocks
	S	-	-	Blocks	Blocks	Blocks
1:9 $CHCl_3$:Tol	G	G	G	G	PG	PG
		-	Blocks	Blocks	Blocks	Blocks + Needles
	S	-	Blocks	Blocks	Needles + Blocks	Blocks
EtOAc	G	G	G	PG	PG	PG
		-	-	Needle growth	Needle growth	Blocks
	S	-	-	Needles + Blocks	Needles	Needles

Solvent system and phase		**Concentration of CBZ mg/ml**				
		10	**20**	**30**	**40**	**50**
1:1 DMSO:H_2O	G	G	G	G	G	G
		-	Block	Clumps	Clumps	Opaque gel
	S	-	-	Needles	PG of needles	G of needles

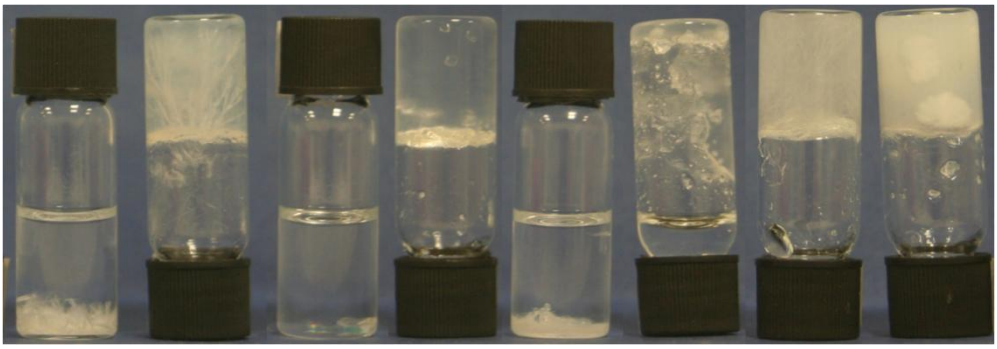

Figure 81 Photographs of 20mg CBZ crystallised from solutions then gels of **20**. left to right: form II grown from ethylacetate solution then gel, form III grown from acetonitrile:toluene solution then gel, hydrate grown from form DMSO:water solution and clumps of form I grown from DMSO:water gel.

The toluene gels of **20** resulted in a mixture of needles of form II and blocks of form III. By adjusting the concentration of CBZ it proved possible to grow either form. Higher concentrations of CBZ result in needles of form II whilst lower concentrations produce blocks of form III. Varying the ratio of co-solvent to toluene had a similar effect with more $CHCl_3$ requiring higher concentrations of CBZ to induce crystal growth and growth of form II. Conversion of form II to form III was observed in 1:9 v/v chloroform:toluene solutions and also more slowly in the corresponding gels. In 1:9 v/v acetonitrile:toluene mixtures, only

blocks of form III were observed with slightly higher concentrations of CBZ required to induce crystal growth in the gel samples of **20** (>20mg/ml) compared with solution (>15mg/ml). However, a repeat of this study showed a mixture of needles and blocks formed at higher concentrations (>25mg/ml) and no crystallisation was observed from either sample at 15 mg/ml of solvent. In ethylacetate gels of **20** form II was also produced with nucleation appearing to occur on the glass near the gel surface with crystals growing down into the gel (Figure 81). No evidence of conversion to form III was observed in the ethylacetate gel even after several months.

TBA acetate can be used to breakdown each of the anhydrous gels of **20** without dissolving the carbamazepine crystals. Figure 82 shows an example of the use of TBA-acetate, added as a solid, to recover a single large crystal of CBZ form III grown in a 1:9 $CHCl_3$:toluene gel of **20**. In this example, disruption of the gel occurred over approximately 20 minutes with only small amounts of fibrous material remaining. The crystals were extracted by filtration and washed with hexane to remove any remaining gelator. No visible degradation to the carbamazepine crystal was evident.

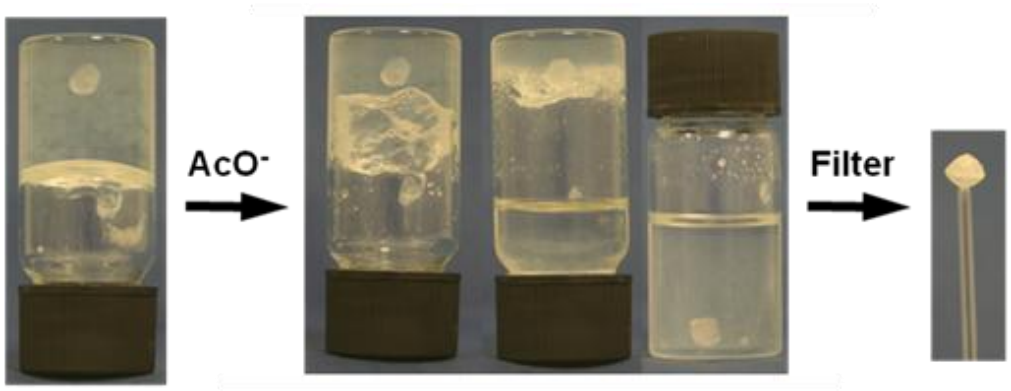

Figure 82 Recovery of a single crystal of CBZ form III by the addition of a spatula tip of TBA-acetate to a 1 % w/v gel of **20** in 1:9 $CHCl_3$:toluene.

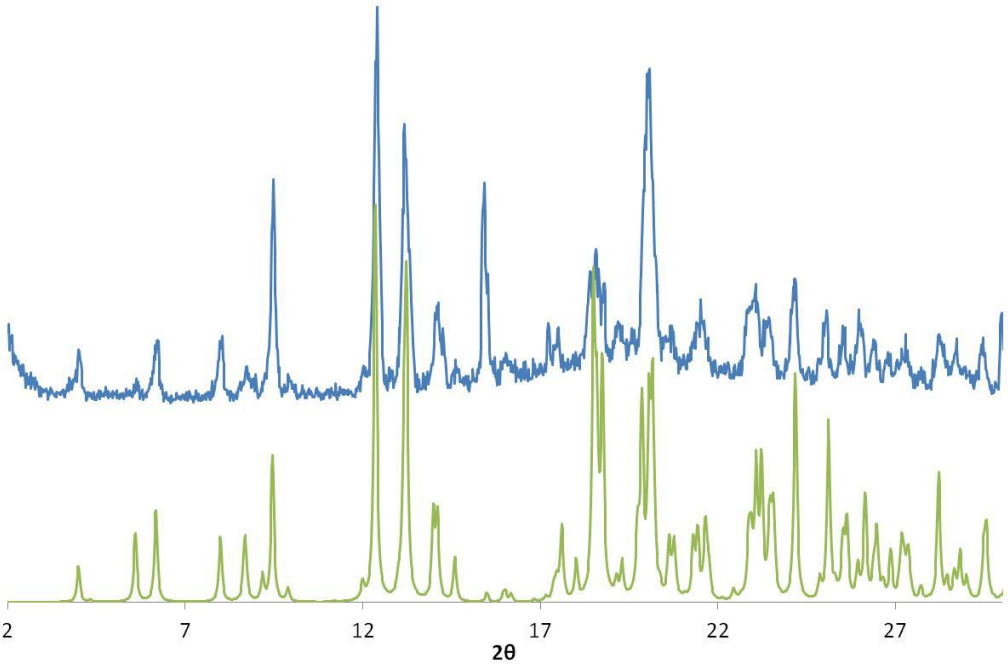

Figure 83 Comparison of crystals of CBZ obtained from 40 mg CBZ in a 1 % w/v **20** gel of 1:1 DMSO:H_2O (top-blue) with calculated pattern for CBZ form 1, CSD ref CBMZPN13 (bottom-green).[244]

In DMSO:water solution in the absence of gel, CBZ formed long, needle-like crystals (at concentrations of 40 g/ml) which were shown to be a mixture of carbamazepine dihydrate and form 3 by XRPD. At low CBZ concentrations no crystal growth was observed in the gels. However, at higher concentrations clumps of very fine crystals formed inside the gel of **20** exhibiting a powder diffraction pattern corresponding to the relatively unusual CBZ form I (Figure 83). Form I is the high temperature form of CBZ and is normally produced from the melt at 170 ºC. It has also been shown that dehydration of the dihydrate can lead to form I under conditions of low humidity.[245] However, IR spectroscopic experiments carried out on the wet samples confirmed that a pure form I rather than the dihydrate is formed in the gel phase. The formation of form I in the gel under the same conditions that give the dihydrate from solution is a surprising result and suggests that the LMWG can have a significant effect on crystal form.

5.3.3 Comparing the effect of different gelators

Parallel investigations were carried out by other people from the group into the crystallisation behaviour of CBZ in gels of compounds **37** and **38** and the results, along with those for **20**, are summarised in Table 14. A number of interesting observations emerged from the study which give insights into crystallisation from supramolecular gels. Whilst needle shaped

crystals of form II grown from toluene solutions gradually convert to thermodynamically stable blocks of form III, needles produced in toluene gels of **38** remain as needles over many months. In contrast to ethylacetate gels of **20** where form II readily forms, ethyl acetate gels of **37** always give thermodynamic form III even at high concentrations of CBZ (>50mg/ml). Other forms of carbamazepine are also encountered. Acetone gels of **37** containing 50 mg of CBZ form the acetone solvate whilst parallel experiments in acetone solution did not produce any crystals.[246, 247] In this case, the gel induces crystallisation at a lower level of super saturation than the level required for crystallisation from the pure solvent.

Table 14 Crystallisation of CBZ in gels of **20**, **37** and **38**.

Solvent[a]	Crystal forms in pure solvent[b]	Crystal forms from gel **20**[b]	Crystal forms from gel **37**[b]	Crystal forms from gel **38**[b]
Toluene[c]	II and/or III	II and/or III	II and/or III	II transform to III
CH_3CN:Toluene	II and/or III	II and/or III	III	n/a[e]
$CHCl_3$:Toluene	II and/or III	II and/or III	n/a[f]	II transform to III
Ethyl Acetate	II	II	III	n/a[e]
Acetone	No crystals[d]	n/a[e]	Acetone solvate	n/a[e]
MeOH:H_2O[c]	Dihydrate	n/a[e]	Dihydrate	n/a[e]
DMSO:H_2O[c]	Dihydrate	I	n/a[e]	n/a[e]

[a] Crystallization performed at the same concentration, heating and cooling rates for samples of gel and pure solvent. [b] Gels of **20** and **38** are 1 % w/v whilst gels of **37** are 0.1 % w/v[c] Crystals could not be retrieved by dissolving the gel with anions [d] Crystallization of the acetone solvate structure occurs upon further super-saturation by evaporation or addition of more CBZ [e] no gelation in this solvent. [f] CBZ retards gelation.

One further result which provides a good illustration of the potential of this type of system for influencing the properties of growing crystals is a study carried out by Dr Marc Piepenbrock into the crystallisation of CBZ from hydrogels of metallogelator **14**. The crystal form was found to be the hydrate in each case however clear differences in morphology were seen between crystals grown in the gel and solution phases. Moreover, by varying the concentration of copper ions in the gel (0.3-0.7 equivalents) it was possible to 'tune' the morphology of the crystals as shown in Figure 84.

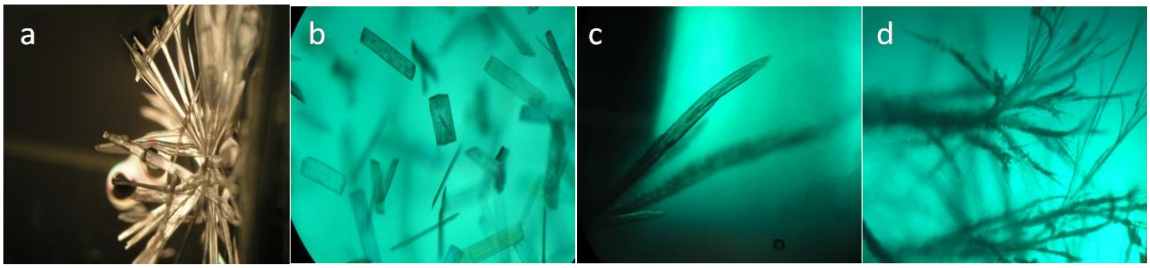

Figure 84 Optical microscopy of CBZ (1 weight%) grown in (a) 1:1 MeOH:water solution, in metallogels of **14** / $CuCl_2$ with (b) 0.4, (c) 0.5, (d) 0.7 equivalents of $CuCl_2$.

5.3.4 Monitoring gel drug interactions

We sought to understand the interactions between gelator and drug molecule in order to monitor the influence of the drug on the gel structure and conversely the gel on the drug crystallisation. Rheological observations on toluene gels of **38** showed that carbamazepine had essentially no effect on the magnitude of the storage and loss moduli of the gel. However, in the presence of CBZ (1 % w/v) a marked increase by approximately one order of magnitude was observed in the yield stress.[170] This effect is in direct contrast to anion binding by bis(urea) gels, in which the competition between anion binding and gelator self-association results in marked anion-dependent decreases in gel strength and yield stress.[52] The gel-sol transition temperature was also found to be lowered by the presence of CBZ. [170]

Nuclear magnetic resonance spectroscopy (NMR) was used to probe this relationship further. NMR spectroscopic titration experiments showed only very weak apparent binding of CBZ to **38** with log K_{11} = 0.84(8) in $CDCl_3$ and a similar (albeit less precise) value in toluene above the T_{gel} at 70°C. Variable-temperature (VT) NMR spectroscopic experiments show that the gelator has a marked effect on the chemical shift of CBZ, which is probably linked to the disruption of CBZ dimer formation[236] in solution (Figure 85). Because of its gelation ability, the host itself is also likely to undergo significant self-association and hence the competition between both gelator and CBZ aggregation and gelator–CBZ binding results in a low overall apparent binding constant. It was therefore concluded that the increased yield stress may not be a result of specific binding of the CBZ to the gelator, but could arise from the physical support of the gel by solid CBZ crystals.

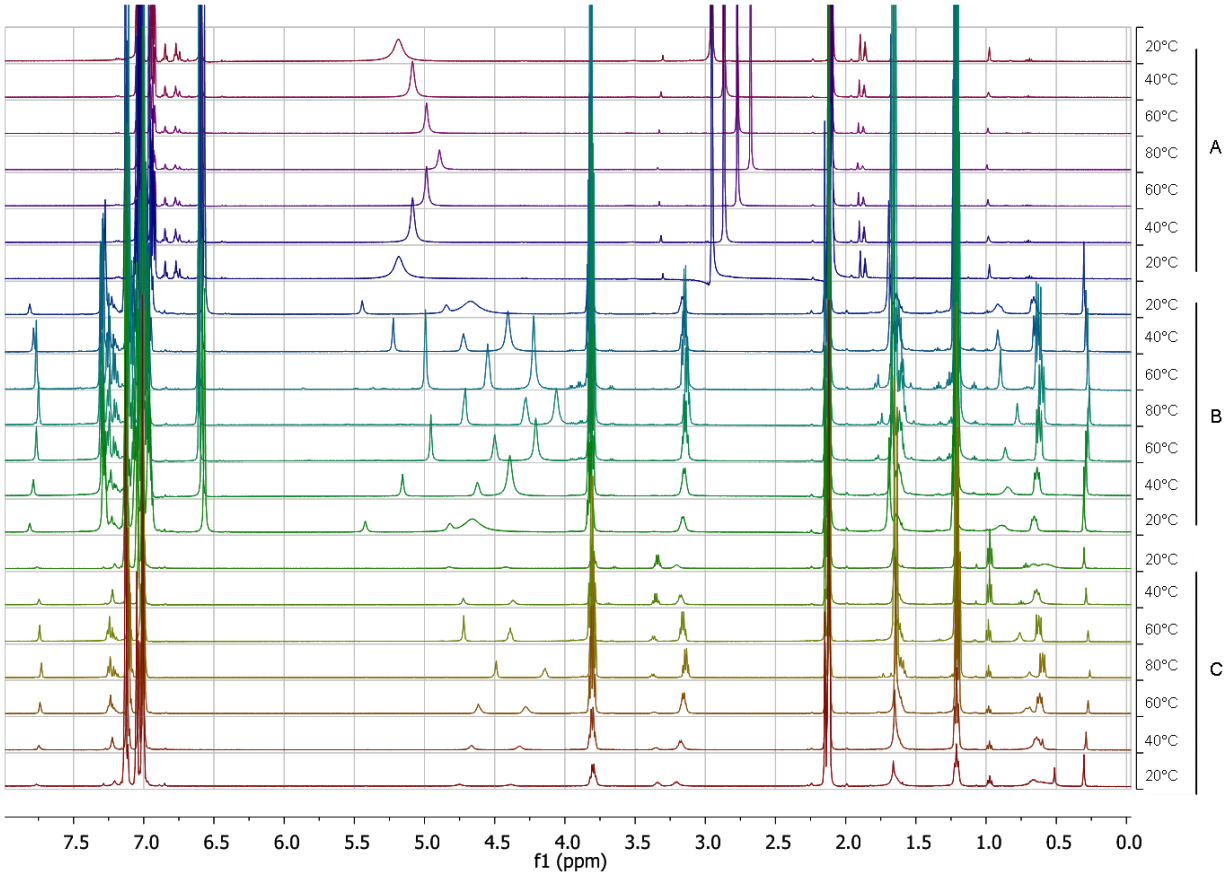

Figure 85 Variable temperature ^{1}H NMR spectra 20 – 80^{o}C in toluene (a) 0.5 % w/v CBZ, (b) mixture of **20** and CBZ and (c) 1 % w/v gelator **20**

5.4 Demonstrating the versatility of API crystal growth in LMWGs

5.4.1 Methodology and objectives

In addition to the more detailed study carried out into the polymorphism of carbamazepine under a wide range of gelators and concentrations, a broader study was undertaken to establish the scope of supramolecular gels as a medium for the crystallisation of pharmaceutical compounds. During preliminary investigations it was found that a number of compounds appeared to completely disrupt gel formation. If this technique is to be widely applicable for use in the pharmaceutical industry for the screening of drug compounds it needs to be shown to be broadly applicable to a variety of APIs.

Compound **20** was selected for use in these studies as it reliably forms gels in a number of different solvent systems. Gel-phase and parallel solution phase crystallisations were carried out for the following pharmaceutical or related compounds: Piroxicam (PIX), Sulindac

(SUL), Indomethacin (IND), Sparfloxacin (SPF), Theophylline (THE), Caffeine (CAF), Acetaminophen (ACP) and Ibuprofen sodium salt (IBU). Experiments were carried out under empirically determined conditions designed to bring about crystallisation in the following solvents: 1:9 CH_3CN:toluene, 1:9 $CHCl_3$:toluene, ethyl acetate, 1:1 DMSO:H_2O and 3:2 MeOH:H_2O. All of these solvent mixtures form thermoreversible gels with **20**, and the first three can be broken down upon the addition of acetate anion. The substrates were chosen as commonly available drug substances or model bioactive compounds that represent a wide range of structures and functional group types and are either polymorphic, form hydrates or otherwise exhibit interesting crystal packing.

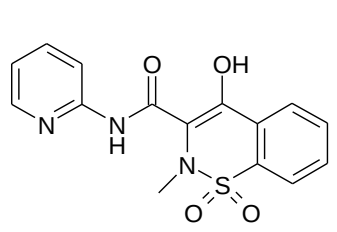

Piroxicam (PIX)

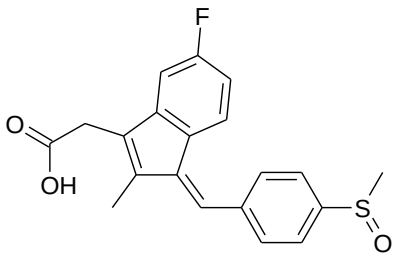

Sulindac (SUL)

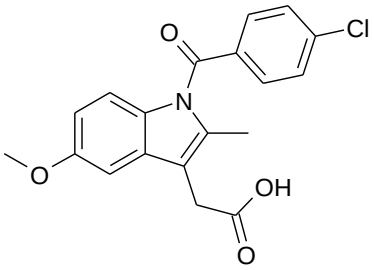

Indometacin (IND)

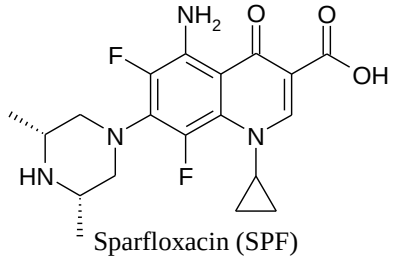

Sparfloxacin (SPF)

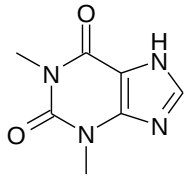

Theophylline (THE)

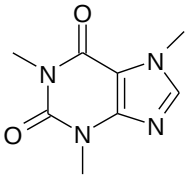

Caffeine (CAF)

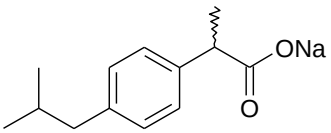

Ibuprofen Sodium Salt (IBU)

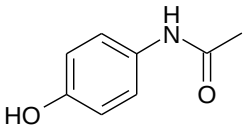

Acetaminophen (ACP)

An appropriate degree of supersaturation for each sample was determined empirically by gradually adjusting the ratio of compound and solvent until the desired rate of crystallisation was achieved. The hot stock solution was then split into two vials, one containing 1 wt% of gelator, and both vials were sealed and heated until all solids were fully dissolved. Gels formed rapidly over a period of minutes whilst crystallisation took place over a period of hours to weeks. Because this approach only tests one set of crystal growth conditions for each sample it is not as thorough as carrying out separate crystallisations at different temperatures as was done for CBZ. However, it does provide a valuable snapshot into the crystallisation

behaviour of each compound and gives a broad overview of the effect of the gel environment on the crystallisation behaviour of a wide range of chemically different APIs.

One problem encountered with a number of the APIs (e.g. PIX) was that the addition of anions resulted in the dissolution of the crystals. This is assumed to be due to disruptive interactions of the anions with bonding motifs in the crystals in a similar way as brings about the dissolution of the gels. Anion addition followed by filtration was therefore not used to separate the gels from the crystals and characterisation took place in the presence of gelator as discussed in section 5.2.4. It should be noted that characterisation of compounds was carried out on samples dried under ambient conditions and the possibility that metastable or solvated forms convert to more stable forms once removed from the mother liquor cannot be ruled out.

5.4.2 Results

A summary of the results is given in Table 15 and evidence for the assignments is provided in the experimental section 5.6. Compound **20** is used as the gelator at 1 % w/v gelator in each case. A reference system to identify different combinations of compound, phase and solvent is set out in Table 15 and is used to aid the discussion. Different compounds are labelled with a three letter acronym, whilst solvents are labelled A-E with gel and solution phases denoted G and S respectively. These are combined to give a unique representation for each experiment, for example PIX-A-G refers to the crystallisation of Piroxicam from a 1:9 acetonitrile:toluene gel.

The anti-inflammatory drug Piroxicam (PIX) has three anhydrous forms and a hydrate which are readily distinguished by IR.[248] Crystallisation of piroxicam from 1:9 acetonitrile:toluene gels produced fast growing, needle-like form II in the gel and large block shaped crystals of slow growing form I. In 1:9 chloroform:toluene gels a clump of piroxicam form II was obtained from solution and at the gel surface, whilst blocks of form I were obtained from the bulk of the gel. In ethylacetate the gel was partially disrupted by the growth of several clumps of form II. In DMSO:water, yellow blocks corresponding to the hydrate were identified from solution whilst the kinetic form II was recovered from the gel. In methanol:water, small yellow blocks of the piroxicam hydrate were seen dispersed throughout the gel systems and on the bottom of the corresponding solution phase vial.

Table 15 Table summarising gel formation, crystal habit and crystal form for compounds 1-8 under solvent systems A-E in the gel (G) and solution (S) phases.

		1:9 CH_3CN:Tol **A**	1:9 $CHCl_3$:Tol **B**	EtOAc **C**	1:1 DMSO:H_2O **D**	3:2 MeOH:H_2O **E**
Piroxicam PIX	**G**	G Needles II	G Blocks + needles I + II	PG Needles II	G Irregular blocks II	G Irregular blocks Hydrate
	S	Blocks I	Needles II	Long needles II	Irregular blocks Hydrate	Irregular blocks Hydrate
Sulindac SUL	**G**	G Powder clumps Orthorhombic[1]	G Powder clumps Orthorhombic[1]	PG -	G -	P Needles Orthorhombic[1]
	S	Powder clumps Orthorhombic[1]	Powder clumps Orthorhombic[1]	-	-	-
Indometacin IND	**G**	PG -	G -	PG Plates γ	P Needles UA	G Needles α
	S	Fibres ?	Plate γ	Plates γ	needles α	needles α
Sparfloxacin SPF	**G**	PG Plates[2] UA	G Small plates -	P Needles[3] UA	G Small plates ?	G Small plates -
	S	Plates -	Plates -	Plates UA	Large plates -	Small plates -
Theophylline THE	**G**	PG Plates Anhydrous	G Blocks Anhydrous	PG -	G -	G -
	S	Plates Anhydrous	Plates Anhydrous	Plates Anhydrous	Large plates -	Needles -
Caffeine CAF	**G**	PG Spherulites β	PG Needles[3] β	PG Needles -	G Needles β	G Fine needles Monohydrate[6]
	S	Needles β	Needles β	-	Gel of fibres[4] β	Gel of fibres[4] β
Ibuprofen Sodium salt IBU	**G**	PG Clumps needles s-Na- dihydrate	PG Clumps needles -	PG Clumps needles s-Na- dihydrate	Viscous liquid -	C Block of plates s-Na- dehydrate
	S	Precipitate s-Na- dihydrate	Precipitate -	Needles s-Na- dihydrate	-	Block of plates[5] s-Na- dehydrate
Acetaminophen ACP	**G**	PG Fibres -	G Clusters I	PG -	P Large block I	G Large block I
	S	Plates I	Needles I	-	Large block I	Large block I

For each sample the phase (G= Gel, PG= partial gelation, S= solution, P= precipitate), a description of crystal habit and form (colour indicates method of identification IR, XRPD, XRD. UA- in colour indicates assignment inconclusive) are given. [1] XRPD and IR patterns match DOHREX in CSD variously assigned as form I or II in different papers, [2] reported for repeat at 4ml scale, [3] crystals growth occurred on vial walls above solvent/gel, [4] solvent retained upon inversion, [5] took much longer to form than solution sample. [6] Some evidence of other forms present.

Sulindac (SUL) is a non-steroidal anti-inflammatory drug of which at least three polymorphs and three solvates are known.[249, 250] Crystallisation occurred in both sets of toluene samples and in some of the aqueous samples, but in neither of the ethylacetate samples. In all the anhydrous gels and solutions dense clumps of needles formed except in SUL-B-G where dispersed needles were seen; both were assigned as the orthorhombic form by IR and XRPD. In the methanol:water case the gel failed to form and crystals of Sulindac were isolated, whilst no crystals were obtained from the corresponding solution. In DMSO water mixtures the gel formed, but no crystals were obtained from either the gel or solution. XRPD analysis identified the clumps of crystals in SUL-A-G and -S as corresponding to the orthorhombic structure DOHREX in the CSD. IR spectra of all crystals correlated strongly and matched assignments for form II whose XRPD pattern matches that of DOHREX[249] although this is assigned as form I in other papers.[250]

Indomethacin (IND) is used as an anti-inflammatory agent amongst other applications and the γ and metastable α forms have been characterised.[251] Crystal growth appeared completely inhibited in both of the toluene based gels but was observed in the corresponding solutions. Plate-like single crystals isolated from IND-B-S were identified as the γ form from a XRD unit cell determination. Long fibres were grown from IND-A-S but the XRPD pattern did not match any of the structures in the CSD. Single crystals grew from both the ethyl acetate gel and solution and were identified as the γ form by their unit cell. Gel formation was impeded in the DMSO:water gel sample but initially formed in the methanol-water sample before gradually breaking down over a period of weeks. Large aggregates of fine white needles were observed in both aqueous solution samples which were shown by XRPD to be the α-form. Spherulitic arrangements of fine needles were found in the gels but could not be identified by XRPD due to weak diffraction. IR showed strong correlation in the finger print region of the α-form with IND-E-G, but poor correlation with IND-D-G.

Sparfloxacin (SPF) is a third-generation fluoroquinolone antibiotic used to treat a variety of diseases and has one anhydrous and a trihydrate form.[252] Growth in the toluene gels was considerably slowed and small yellow blocks dispersed throughout the gel were observed whilst larger flat plates were grown from solution. The experiment was repeated on a larger scale (4ml) and a root-like network of plates was observed. In ethylacetate gel formation was again partially disrupted with needles growing on the walls of the vial above the solution. Comparison of XRPD patterns for these two samples (SPF-A-G and SPF-C-G) show overlap

of major peaks with neither sample matching the reported anhydrous form (JEKMOB) or hydrated forms. Small plates were observed in both the aqueous gels and the corresponding solutions although plates tended to be aggregated into clusters in solution and dispersed in the gel. The XRPD pattern of SPF-D-S was different again from the other experimental and reported patterns. Small amounts of sample make these results inconclusive but potentially of future interest.

Theophylline (THE) is used as a muscle relaxant or vasodilator in the treatment of asthma and has one stable anhydrous form[253] and a monohydrate[254] as well as several solvates including DMSO. A metastable anhydrous phase[255] has also been identified which forms upon drying in air of the monohydrate at relatively low temperatures (40-50ºC).[256] Gels formed in all solvents in the presence of theophylline but were disrupted in the case of the ethyl acetate system. The three anhydrous gel samples showed a largely amorphous background by XRPD and the solution phase samples showed strong preferred orientation and a tentative assignment of the expected anhydrous form (CSD ref BAPLOT01)[253] is made. In the aqueous samples, crystallisation occurred from solution but no crystallisation was observed in the gel samples.

Caffeine (CAF) has two anhydrous forms; the β-phase is stable at room temperature but converts to the α-phase at ~141ºC.[257] A 4/5 hydrate is stable at room temperature but only under elevated relative humidies and rapidly dehydrates to the β-form under atmospheric conditions.[258] Gel formation was partially disrupted in the acetonitrile-toluene and ethylacetate samples but formed in the remaining systems. In samples CAF-B-G and CAF-C-G growth of needles in feather-like arrangements occurred above the sample and in CAF-A-S and CAF-B-S feather-like growth occurred in solution. In CAF-A-G spherulitic growth of needles were seen whilst no crystal growth was observed in CAF-C-S. In the aqueous solutions CAF-D-S and CAF-E-S, crystallisation resulted in fibre-like networks which retained solvent upon inversion, a crude definition of a gel. The growth of these fibres was impeded in the gels and more needle-like structures were observed in CAF-D-G and CAF-E-G. XRPD analysis indicated that all samples measured contained the stable anhydrous β form. The exception was CAF-E-G where the strongest match for was with the hydrate (CAFINE01) although some additional peaks can be accounted for by partial conversion to the β-form.

Ibuprofen (IBU) is a widely used non-steroidal anti-inflammatory drug which is normally administered as a racemic mixture and can be made more soluble as a sodium salt. Two anhydrous forms of racemic ibuprofen and one of the *S*-enantiomer are known as well as two ibuprofen sodium dihydrates, one containing the *S*-enantiomer and one a racemic mixture.[259] [260] The sodium dihydrate is stable under ambient conditions up to 44ºC. Gels formed in the three anhydrous systems but did not completely gel the sample. The growth of clumps of needles were observed in all three non-aqueous gel systems, fine precipitates were observed in the two toluene solutions and larger crystalline structures were observed in the ethlyacetate solution. Despite differences in morphology, XRPD for all the samples gave the best match for the simulated spectra for KATNOJ, the sodium dihydrate containing only one enantiomeric form. A viscous liquid formed in the IBU-D-G and IBU-D-S remained as a solution. A large crystal formed after a week in IBU-E-G and over a month in IBU-E-S. Despite their size, the crystals formed were composed of fine layers and could not be indexed by XRD. XRPD analysis again gave a match for the sodium dihydrate of the single enantiomeric form.

Acetaminophen (ACP) has two well characterised forms, the commercially distributed monoclinic form I and a less thermodynamically stable orthorhombic form II.[261] Recently a study of the effect of polymer heteronuclei on the polymorphism of acetaminophen found that relatively non-polar side chains tended to lead to the formation of the orthorhombic polymorphs whilst more polar side chains led to a mixture of both polymorphs.[262] A number of hydrates have been formed under more unusual conditions: a trihydrate is reported to form by crystallisation from aqueous solutions at 0ºC,[263] a monohydrate at 150K[264] and a dihydrate has been formed at high pressures (1.1 GPa)[265] as has a methanol:water solvate.[266] All hydrated forms are unstable with respect to the monoclinic form under ambient conditions. Gels formed in methanol/water and toluene/chloroform systems, were largely disrupted in acetonitrile/toluene and ethylacetate and there was no evidence of gel formation in the DMSO:water system. Unit cell determinations of crystals grown from ACP-A-S and ACP-D-G were found to be the thermodynamically favourable monoclinic form I (HAXCAN01). XRPD was used to characterise the remaining crystals which were also found to be form I.

5.4.3 Discussion of results

Gel formation proved to be compatible with a wide range of substituents and of the 40 combinations tested, gel formation was observed in all but 7 cases. In many cases the presence of the API had no impact on gel formation (17 gels). In some cases the gels appeared weaker, leaked solvent or appeared disrupted by the gel sample (16 partial gels). The ethylacetate gel appeared to be the least robust gel and was either disrupted or failed to form in the presence of any of the compounds. The high solubility of many of the compounds meant that often the concentration of drug molecules was equivalent to, or considerably greater than, that of the gelator. The highest concentrations of compound were methanol:water systems with 41 mg/ml of ibuprofen or 40 mg/ml caffeine, four times that of the gelator. The smaller molecules (Theophyline, Caffeine, Ibuprofen and Acetaminophen) appeared to be more disruptive than the larger more complex ones although it is difficult to draw conclusions about the effect of any particular functionalities on gel formation.

After several months, no evidence of crystallisation was seen in four of the systems and higher concentrations of API are required. Crystallisation was found to occur in solution but not the gel in five instances and in the gel but not solution in one instance (SUL-E-G). This indicates that the gel phase tends to suppress nucleation with presumably higher concentrations of compound required to induce crystallisation, as observed for CBZ. Other phenomena such as the crystallisation of compounds on the sides of the vials and above the gel were also observed (e.g. SPF-C-G).

Considerable differences in crystal habit were observed in compounds grown from the gel phase compared with solution. A selection of images is given in Figure 86 and a full set can viewed in the experimental section 5.7.2. In some instances differences are due to the growth of different polymorphs, such as for sparfloxacin in PIX-A-G and PIX-A-S. In cases where the underlying polymorphism is the same, differences must therefore be due to effects of the gel environment. In a number of instances where long needles grew in solution, they were shorter in the gel phase ACP-B-G/S, CAF-A-G/S. The lack of sedimentation in the gel environment also affected the aggregation of crystals accounting for further differences in appearance e.g. THE-A-G/S.

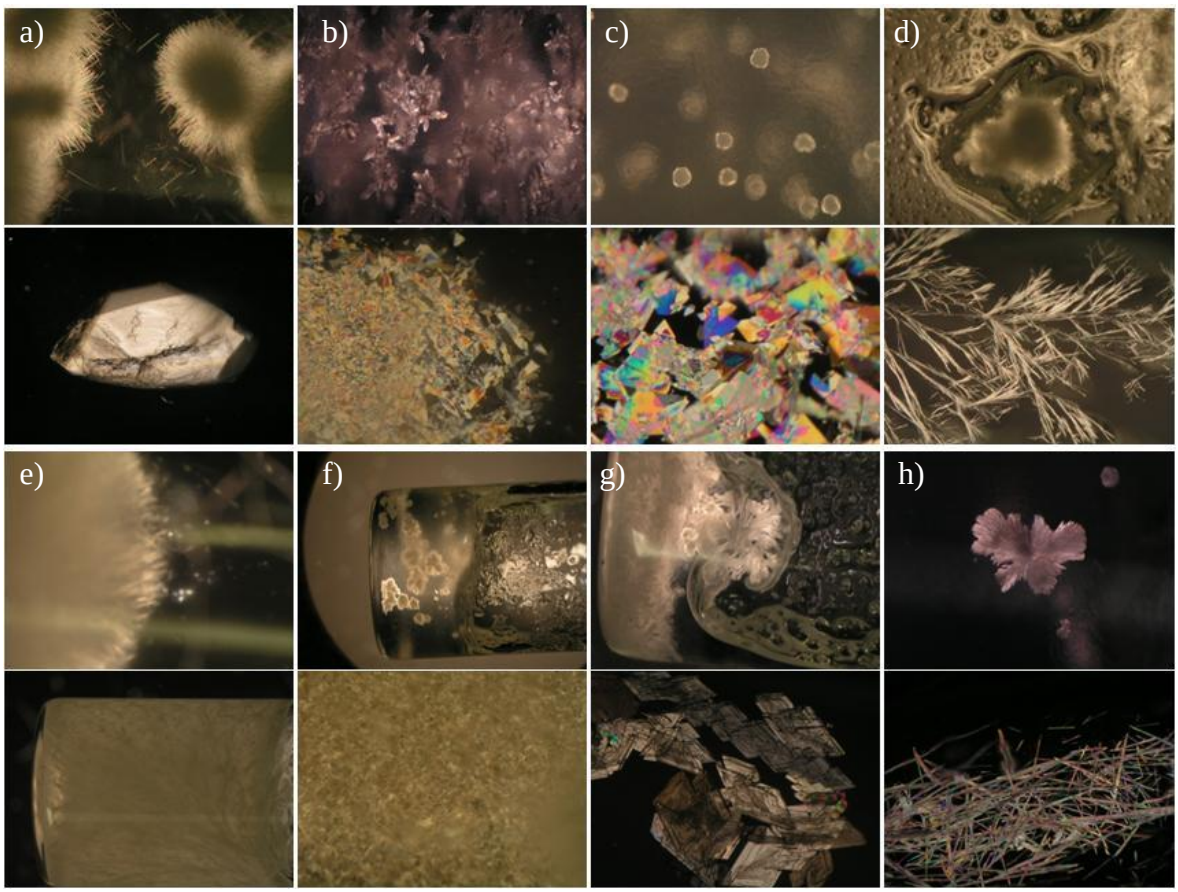

Figure 86 Pairs of images comparing crystal growth in the gel (top) and solution (bottom) of: a) PIX- A-G/S, b) THE-A-G/S. c) THE-B-G/S. d) CAF-A-G/S. e) CAF-D-G/S. f) IBU-A-G/S, g) ACP-A-G/S. h) ACP-B-G/S.

Differences were seen in polymorphism between crystals grown from the solution and gel phases. This was most pronounced in Piroxicam where needles of kinetic form II were seen in PIX-A-G whilst blocks of form I were seen in the corresponding solution. This is the opposite behaviour to that observed for carbamazepine where there was a tendency for the thermodynamic form to grow from gels of **20** and the kinetic form to grow from solution. The kinetic form was also found in PIX-D-G whereas the hydrate grew from solution. This may indicate that the gel is encouraging rapid nucleation giving rise to the kinetic form. However, the presence of both forms I and II in PIX-B-G and of the hydrate in PIX-E-G indicate that more work needs to be done to establish the crystallisation behaviour of PIX from gels of **20**. Differences in polymorphism were also seen for the crystallisation of Caffeine from methanol:water systems where the monohydrate was seen in the gel and the β-form from solution.

Preliminary experiments have also been carried out on various other compounds which were not used for a variety of reasons. Cafradroxil and Ampicilin decomposed upon heating which

is a limitation of the high temperatures required to fully dissolve the gelator using this method. Mebendazole was tested but proved insoluble in the solvents tested. Cytosine and Diatrizoic Acid were soluble in aqueous systems only whilst 2- and 3-hydroxybenzyl alcohol were soluble only in non-aqueous solvents. Preliminary screens were carried out on a ligand developed within the group designated NPU and showed a promising range of polymorphic behaviour but was put aside as it is not an API.

5.5 Industrial compounds

In addition to these 'model' pharmaceutical systems which were selected for their reliable and well characterised crystallisation behaviour, two further pharmaceutical compounds were supplied by industrial sponsors GlaxoSmithKline (GSK). For commercial reasons the compounds will be reffered to only as **GSK-A** and **GSK-B**. Only limited characterisation was undertaken of these systems. Preliminary experiments indicate **GSK-A** and **-B** can be crystallised from gels of **20** using the same procedure and range of solvents as used in section 5.4. Disruption of the ethylacetate gel occurred in the presence of **GSK-A** whilst only the toluene gels were stable in the presence of **GSK-B**. No significant differences were observed in the polymorphism of the compounds crystallised from the solution and gel states.

One interesting observation is depicted in Figure 87. **GSK B** initially crystallised as fine needles from both the 1:9 acetonitrile:toluene gel and solution samples. However, in solution over a period of months the needles gradually converted into large blocks which were solved by single crystal X-ray diffraction and identified as the thermodynamically stable form II. In contrast, no change in morphology was observed over the 2 month period in the gel phase samples and the needles were isolated and identified as form I by XRPD. The same stabilisation of form I was observed in the 3:2 methanol:water gel samples, with conversion to form II occurring in solution. However, in this case gelation was disrupted by the presence of GSKB and the stabilisation occurred in the presence of a precipitate. This may indicate compound **20**, rather than the gel phase is stabilising form I of GSK B.

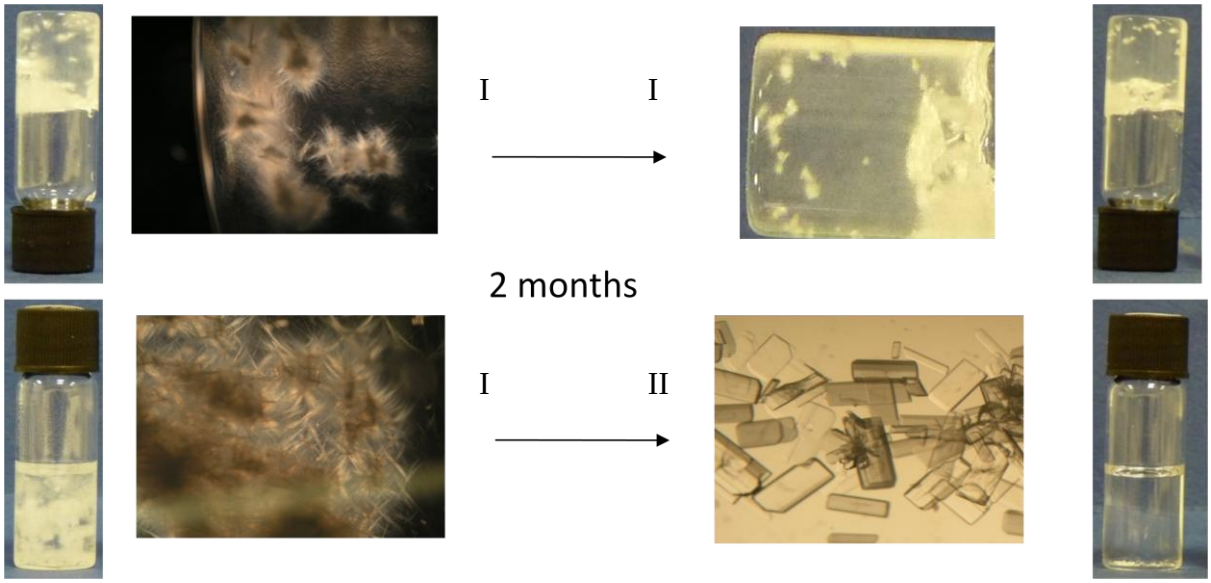

Figure 87 Images showing kinetic form I of drug compound GSKB was stable in the gel sample (1 % w/v 1:9 acetonitrile:toluene) after several months where it had converted to the thermodynamic form in solution.

5.6 Conclusion

The work outlined in this chapter demonstrates the use of LMWGs as a medium for organic crystal growth. The supramolecular nature of these gels allows for the facile recovery of crystals upon the addition of acetate anion without damage to the crystals. Although the effectiveness of anion-triggered reversal of gel formation is limited by the solvent and the ability of the crystalline substrate itself to interact with the anion, gelators can be designed that respond to a variety of external stimuli. The ability of LMWGs to gel a wide range of solvents allows for detailed screening of compounds. Gel formation was found to be compatible with a wide variety of drug compounds although instances where gels failed to form in the presence of particular compounds were observed. The vast body of literature on supramolecular gels provides a library of gelators that can be chosen to match the crystallisation conditions and compound of interest.

LMWGs may act as an inert matrix, slowing down crystallisation and leading to larger, more uniform crystals, and inhibiting the conversion of metastable polymorphs. In some cases crystallisation was found to occur in the gel but not in solution, whereas in others nucleation required higher levels of supersaturation in the gel phase. Clear differences in crystal habit have been seen in the gel phase when compared with solution, and in some cases the gel-phase crystallisation results in the formation of different polymorphs when compared to the

parallel solution-phase experiments. No gelator-substrate cocrystals were observed, suggesting effective phase separation between the rapidly forming gel and the slower growing substrate crystals. This important observation indicates the general applicability of these systems.

The high-quality single crystals that result from gel-phase crystallisations are of great potential use in macromolecular crystallography, where crystal quality, particularly in synchrotron work on small samples, is of paramount importance. The diversity of this class of gelator potentially allows for tuning of interactions between gel and solute, an idea developed in Chapter 6. Supramolecular gels could find an application as an important tool within the context of the polymorph screening methodologies that are routinely applied at several stages in the drug development pipeline. Interest from the pharmaceutical industry in developing this approach led to a collaboration with GlaxoSmithKline (GSK) and details of this work are discussed in Chapter 7.

5.7 Experimental section

5.7.1 General procedures

Details for the synthesis of gelator **20** can be found in Chapter 2. Compounds **37**,[52] **38**[63, 170] and **14**[71] were prepared by Dr Gareth Lloyd and Dr Mark Piepenbrock. Drug compounds were purchased from Sigma Aldrich and were used with no further purification. All solvents used were analytical reagent grade.

Variable temperature NMR spectra were performed on a Varian Inova-500 machine (500 MHz for ^{1}H, 126 Hz for ^{13}C) and were referenced to residual solvent. Binding constants were determined using the non-linear least squares fitting program HypNMR 2006.[218] Powder diffraction was performed on glass or silicon slides using a Siemens D5000 X-Ray Diffractometer using CuKα radiation at a wavelength of 1.5406 Å. Other instrumentation and general experimental procedures used are described in Chapter 2.

5.7.1.1 Sample preparation

In Section 5.3 gel phase crystallisations were carried out by weighing the appropriate amount of substrate (1-5 % w/v) and gelator (0.1-1 % w/v) in a vial and adding a suitable solvent from a stock solution. The sealed vial was then heated until both solids were fully dissolved and the mixture was then allowed to cool to room temperature. In each case the gel is formed over a period of a few minutes whilst crystallisation takes place over tens of minutes to weeks.

In section 5.4 for a typical experiment, a known mass of compound was added to a large vial along with a known volume of solvent. This was then heated until everything was dissolved and allowed to cool. If the compound did not fully dissolve, or crashed out of solution rapidly upon cooling, more solvent was added to the vial and it was reheated. If the compound dissolved very easily or did not come out of solution upon refrigeration or after several days, more compound was added. A number of iterations of this process were carried out until each sample gradually crystallised from solution over a period of hours to days. The solution was heated, then divided between a smaller vial containing a weighed concentration of gelator and a reference vial with no gelator. The samples were then heated and allowed to sit at room temperature for a period of a week.

5.7.1.2 Sample analysis

Where possible, recovery of the crystals was achieved by adding a measured amount of acetate as the tetrabutylammonium (TBA) salt to break down the gels, followed by filtration of the resulting solution and washing with water or diethyl ether. Polymorphs were identified by comparing experimental X-ray powder diffraction patterns (D5000) with those calculated from the known single crystal coordinates in the CSD, from their solid state IR spectra (PE Spectrum 100), or where crystal size permitted, from the unit cell dimensions of a number of representative single crystals (Bruker 6000).

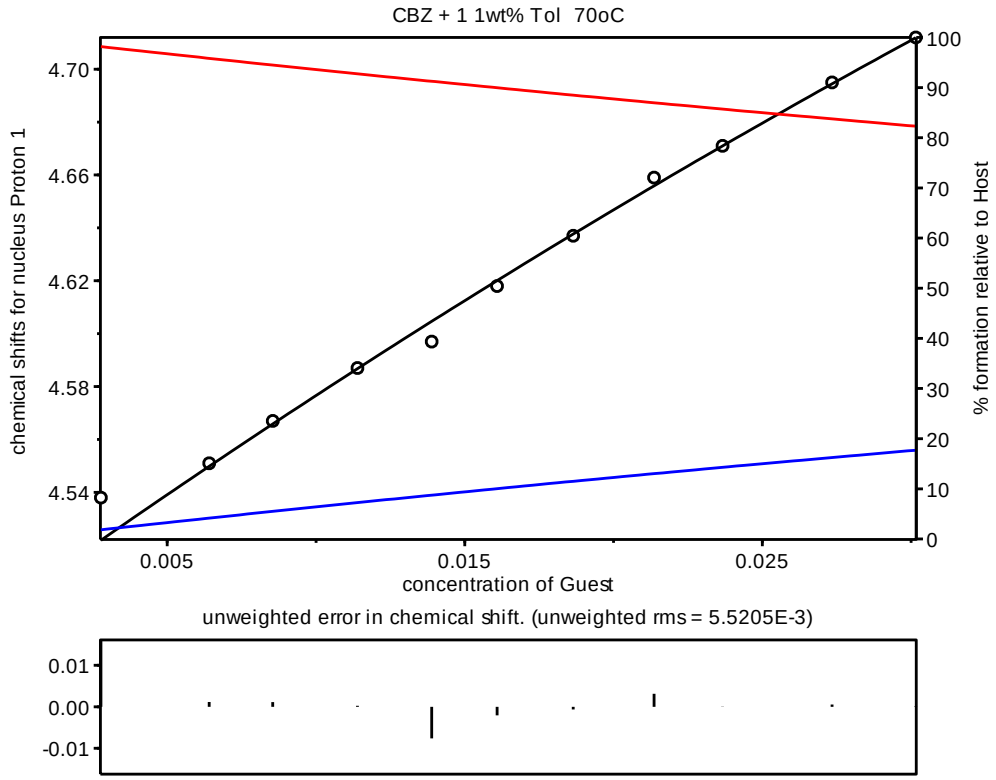

Figure 88 NMR titration data and fit for binding of CBZ by gelator **20** in toluene at 70 °C; above T_{gel}; log K_{11} = 0.87(27)

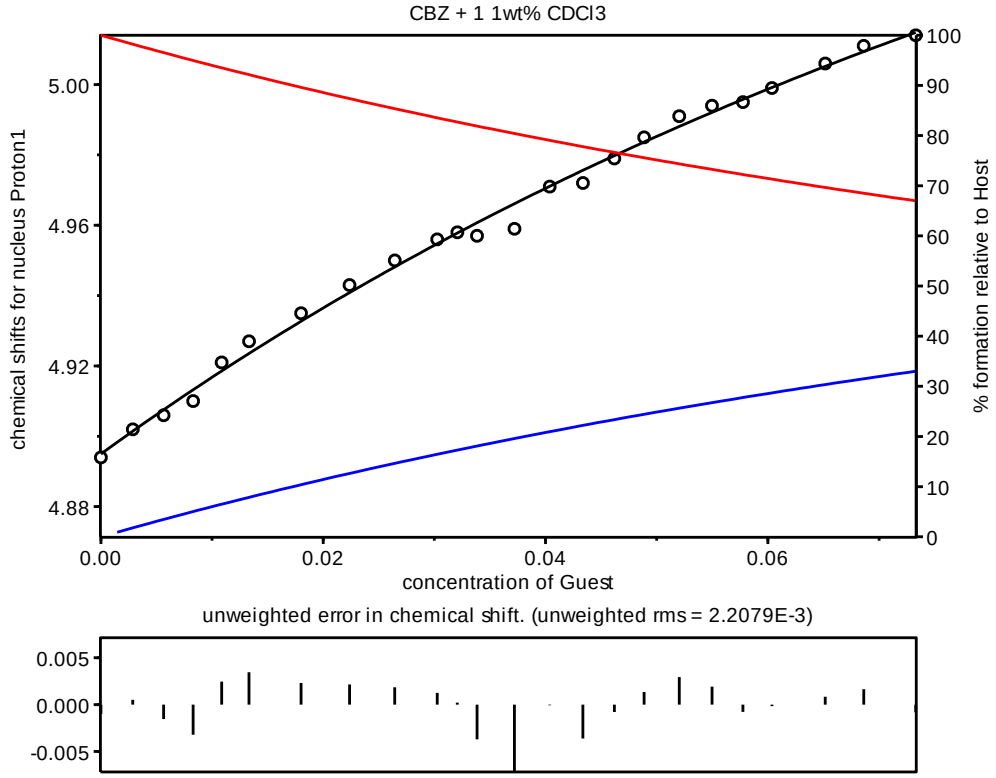

Figure 89 NMR titration data and fit for binding of CBZ by gelator **20** in $CDCl_3$ at 20 °C; log K_{11} = 0.84(8)

5.7.2 Screen of pharmaceutical compounds

5.7.2.1 Piroxicam (PIX)

a)

b)

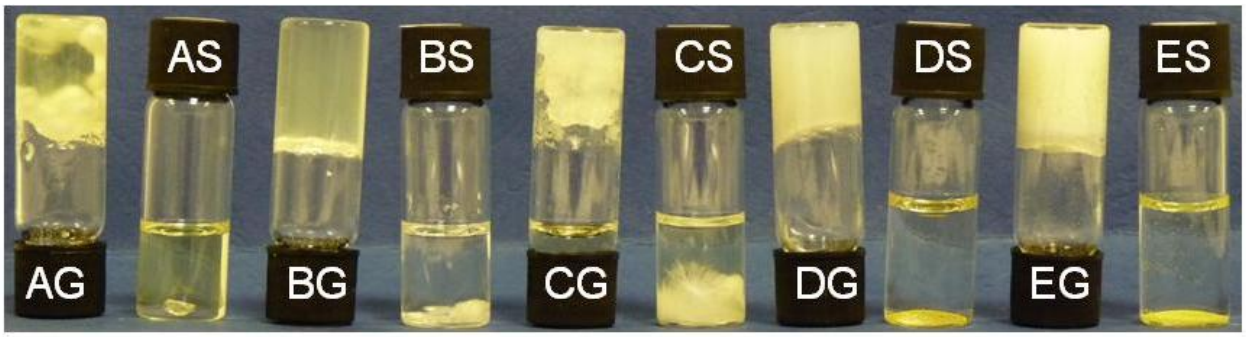

c)

	A) CH_3CN:Tol	B) $CHCl_3$:Tol	C) EtOAc	D) DMSO:H_2O	E) MeOH:H_2O
Gel formation	PG	G	PG	G	G
Crystal from gel	Needles II	Block + needles I + II	Needles II	Yellow bits II	Yellow bits Hydrate?
Crystal from sol	Block I	Needle II	Long needles II	Irregular blocks Hydrate?	Irregular blocks Hydrate?

d)

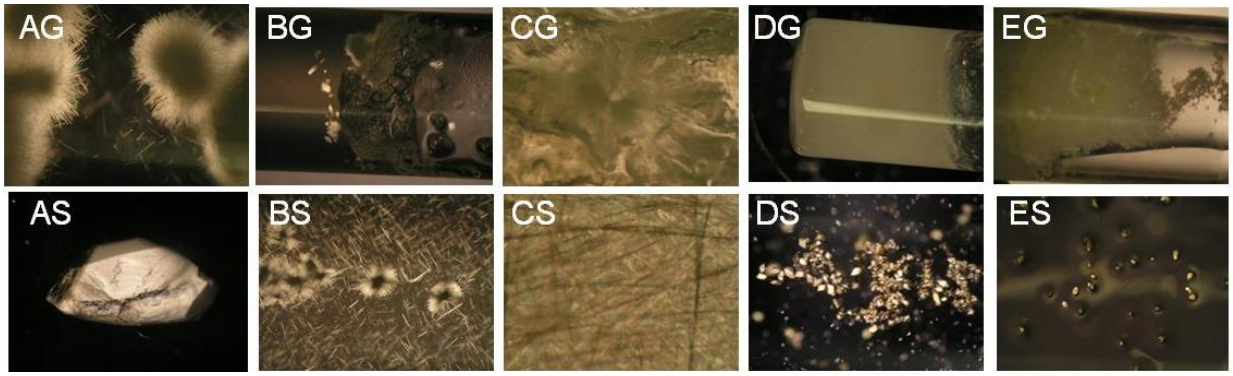

Figure 90 a) Structure of Piroxicam b) photographs of PIX crystallised from different solvent combinations with and without gelator c) table showing gel and crystal formation in different samples d) selected microscopy images of crystal structures from corresponding samples.

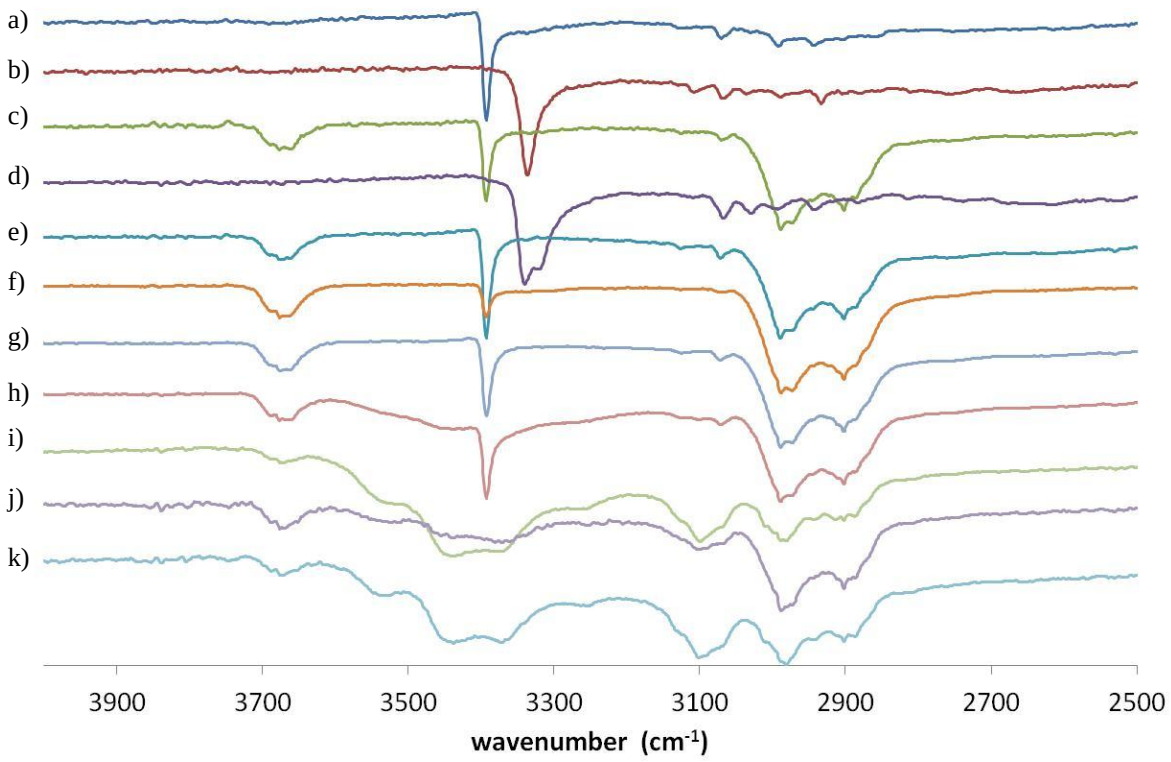

Figure 91 Infrared spectrum showing assignments[248] of crystal forms for Piroxicam (PIX): a) G-A form II (blue), b) S-A form I (red), c) G-B needle form II (green), d) G-B block form I (purple), e) S-B form II (mid blue), f) G-C form II (orange), g) S-C form II (light blue), h) G-D form II (light red), i) S-D hydrate (light green), j) G-E hydrate (light purple), k) S-E hydrate (sky blue).

5.7.2.2 Sulindac (SUL)

a)

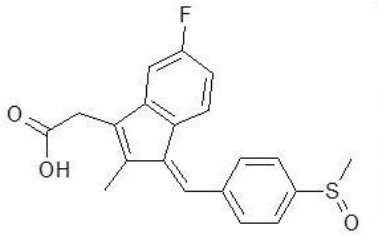

b)

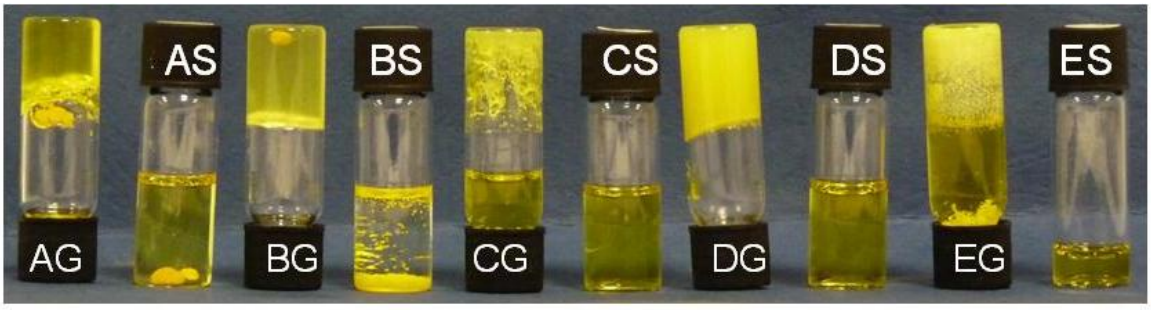

c)

	A) CH_3CN:Tol	B) $CHCl_3$:Tol	C) EtOAc	D) DMSO:H_2O	E) MeOH:H_2O
Gel formation	G	G	PG	G	X
Crystal from gel	Powder	Powder	X	X	Needles
Crystal from sol	Powder	Powder	X	X	X

d)

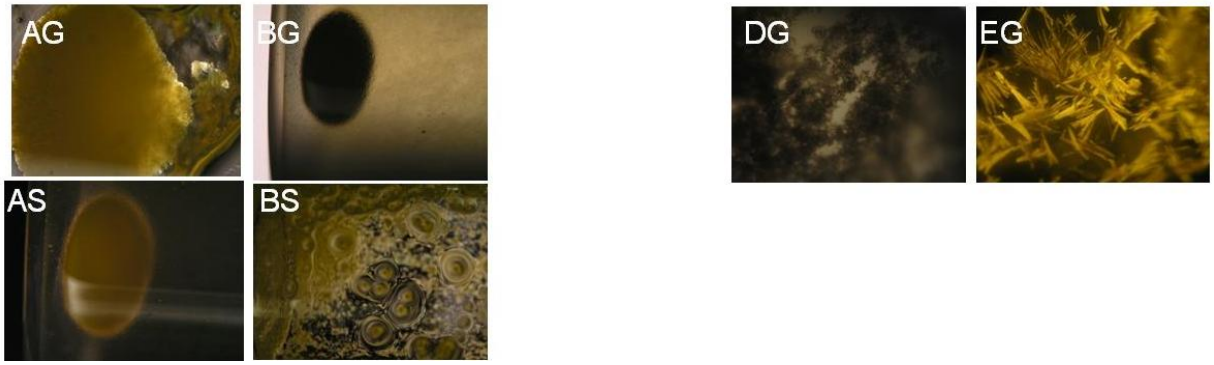

Figure 92 a) Structure of Sulindac b) photographs of SUL crystallised from different solvent combinations with and without gelator c) table showing gel and crystal formation in different samples d) selected microscopy images of crystal structures from corresponding samples.

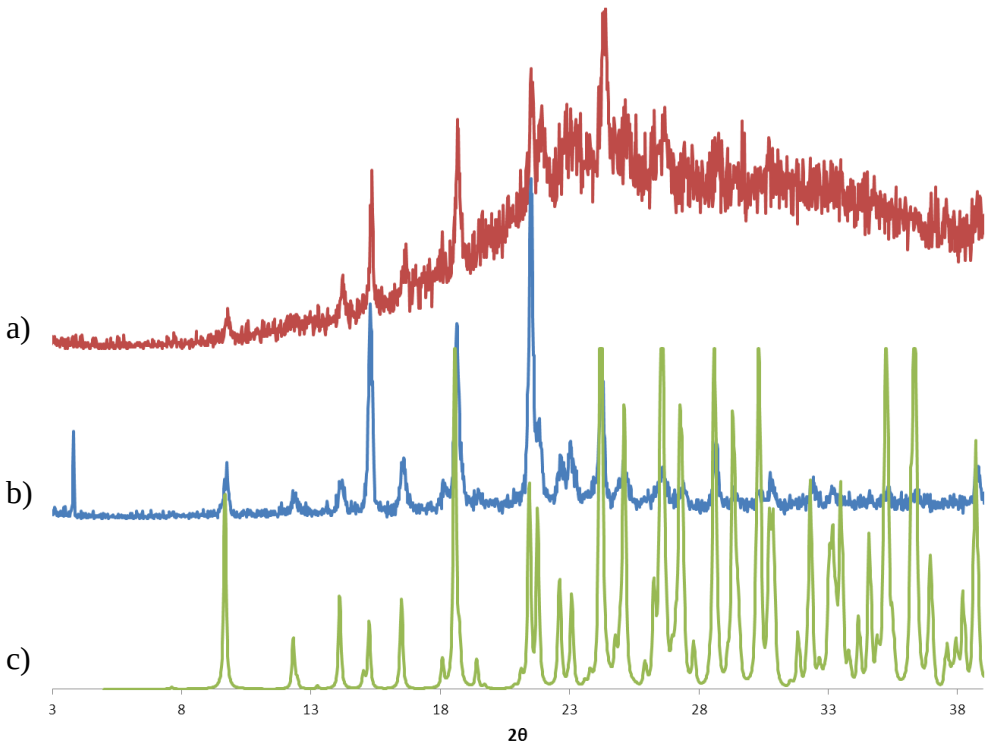

Figure 93 XRPD pattern comparing patterns for a) SUL-A-S (red) and b) SUL-A-G (blue) with c) pattern for orthorhombic form II of sulindac (green) generated using CSD reference DOHREX in Mercury.

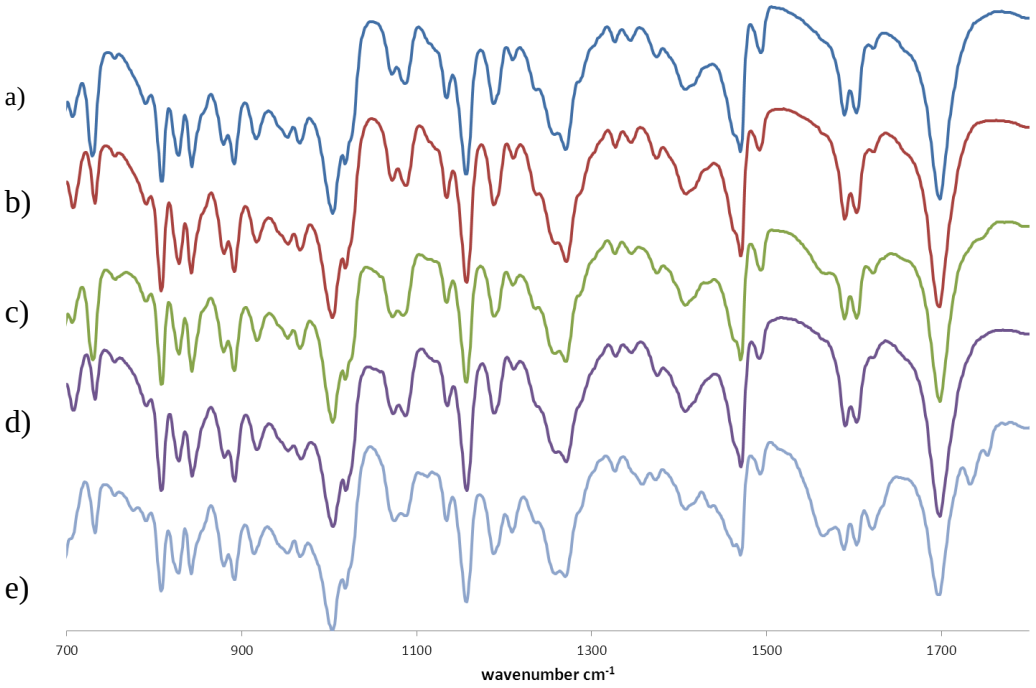

Figure 94 IR spectra for samples of Sulindac: SUL-A-G (blue), SUL-A-S (red), SUL-B-G (green), SUL-B-S (purple), SUL-E-G (light blue)

5.7.2.3 Indomethacin (IND)

a)

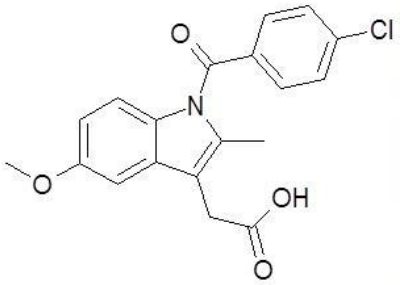

b)

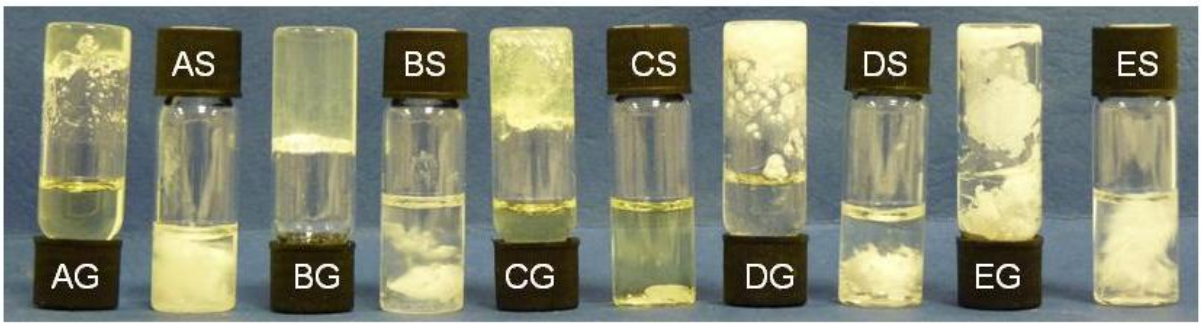

c)

	CH_3CN:Tol A	$CHCl_3$:Tol B	EtOAc C	DMSO:H_2O D	MeOH:H_2O E
Gel formation	PG	G	PG	X	G
Crystal from gel	X	X	X	Balls of needles	Stars of needles
Crystal from sol	PG fibres	C	X	Clump of needles	Clump of needles

d)

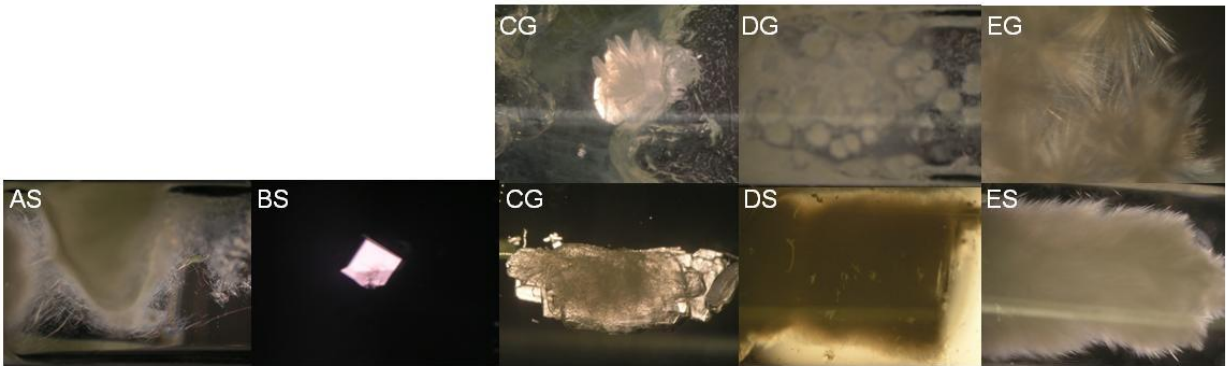

Figure 95 a) Structure of Indomethacin b) photographs of IND crystallised from different solvent combinations with and without gelator c) table showing gel and crystal formation in different samples d) selected microscopy images of crystal structures from corresponding samples.

Table 16 Comparison of experimental unit cell data and CSD reference INDMET03

	A	**B**	**C**	**α**	**β**	**γ**	**V**
3SB	9.22(3)	9.67(3)	10.87(3)	70.3(2)	87.7(3)	70.5(3)	857(5)
3GC	9.226(1)	9.6064(9)	10.860(1)	69.937(7)	87.24(1)	69.497(8)	844.0(2)
3SC	9.268(3)	9.699(6)	10.920(2)	69.70(3)	87.29(2)	69.14(4)	857.1(7)
INDMET03	9.236	9.62	10.887	69.897	87.328	69.501	847.865

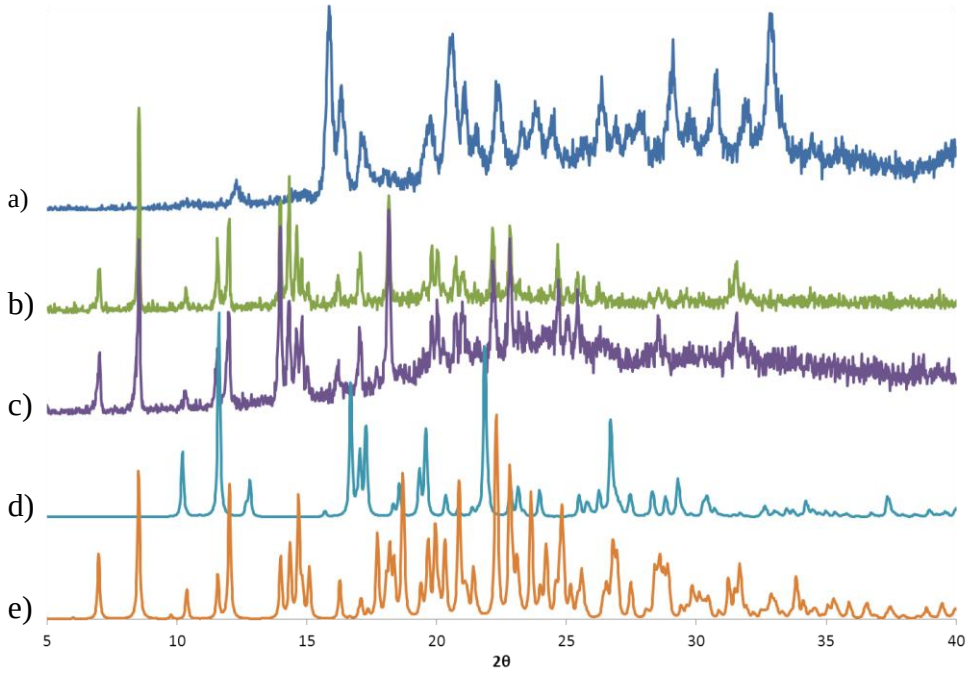

Figure 96 XRPD pattern comparing experimental data with CSD references for known forms of indomethacin: a) IND-A-S (blue), b) IND-D-S (green), c) IND-E-S (purple), d) IND01 (light blue) e) IND02 (orange).

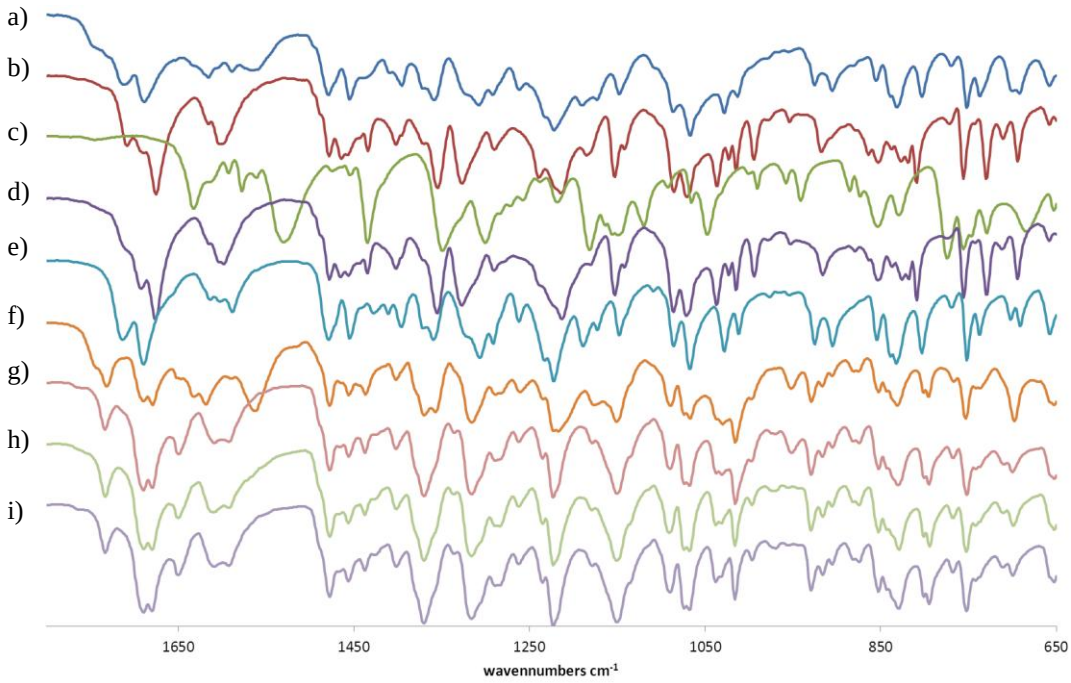

Figure 97 IR spectrum showing IR patterns for samples of indomethacin, the presence of gelator complicates spectra making interpretation difficult: a) IND-A-G, b) IND-A-S, c) IND-B-G, d) IND-B-S, e) IND-C-S, f) IND-D-G, g) IND-D-S, h) IND-E-G, i) IND-E-S.

5.7.2.4 Sparfloxacin (SPF)

a)

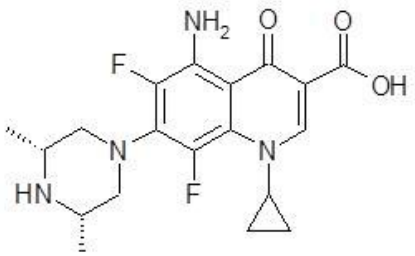

b)

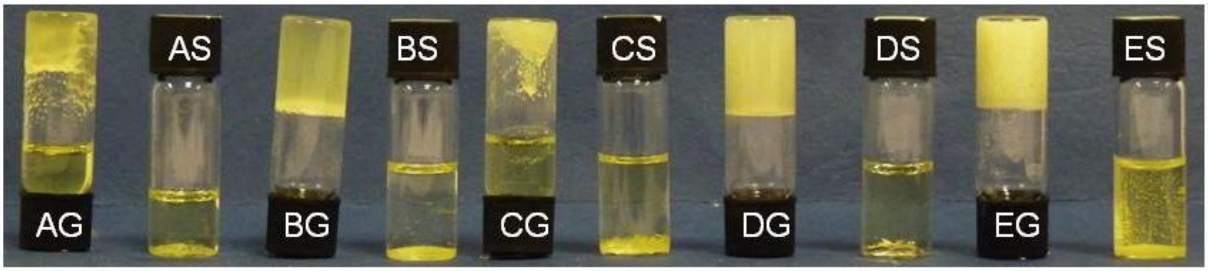

c)

	CH_3CN:Tol A	$CHCl_3$:Tol B	EtOAc C	DMSO:H_2O D	MeOH:H_2O E
Gel formation	G	G	X	G	G
Crystal from gel	Small blocks	Small blocks	*Needles Above solvent*	Small plates	Small plates
Crystal from sol	Plates	Plates	Flat plates	Large plates	Small plates

d)

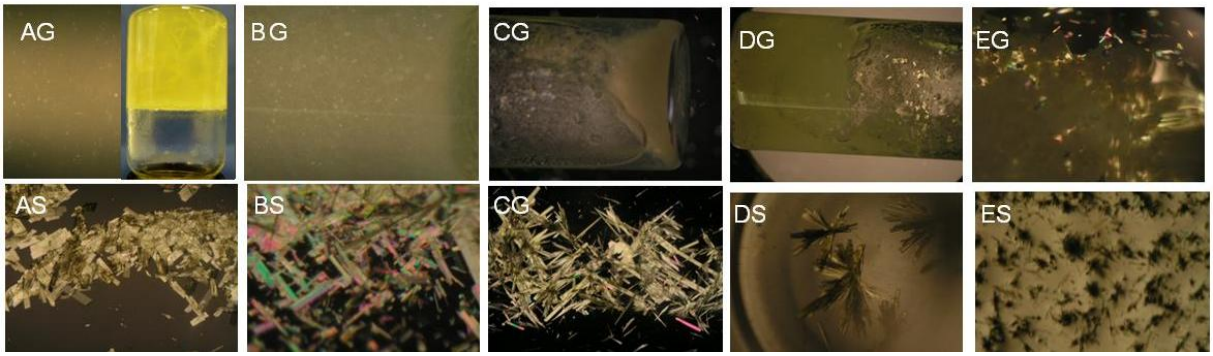

Figure 98 a) Structure of Sparfloxacin b) photographs of SPF crystallised from different solvent combinations with and without gelator c) table showing gel and crystal formation in different samples d) selected microscopy images of crystal structures from corresponding samples.

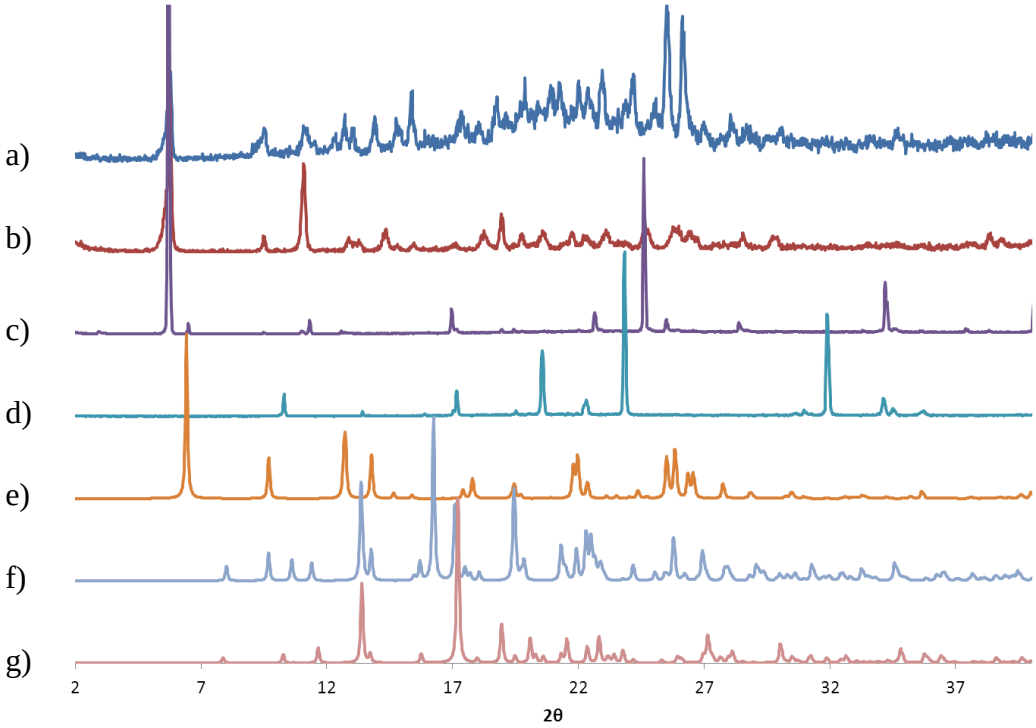

Figure 99 XRPD pattern comparing experimental data with CSD references for known forms of Sparfloxacin: a) SPF-A-G (blue), b) SPF-C-G (red), c) SPF-C-S (purple), d) SPF-D-S (light blue) e) JEKMOB (orange) f) COQWOU (grey) g) COQWOU01 (pink)

5.7.2.5 Theophylline (THE)

a)

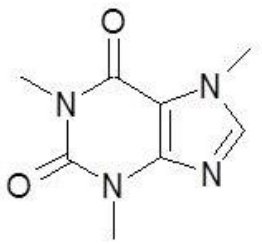

b)

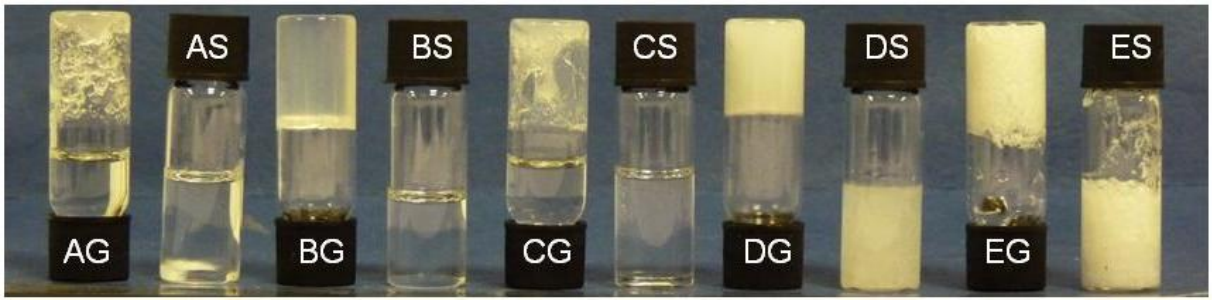

c)

	CH_3CN:Tol A	$CHCl_3$:Tol B	EtOAc C	DMSO:H_2O D	MeOH:H_2O E
Gel formation	PG	*G*	PG	G	G
Crystal from gel	Spherulites	*Needles above gel*	Needles	Fine needles	V. fine needles
Crystal from sol	Feather of Needles	Needles	X	Gel	Gel

d)

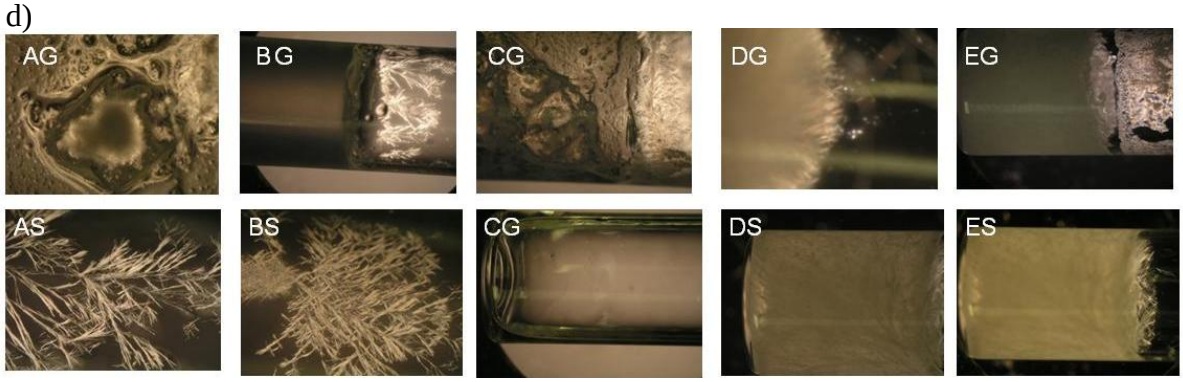

Figure 100 a) Structure of Theophylline b) photographs of THE crystallised from different solvent combinations with and without gelator c) table showing gel and crystal formation in different samples d) selected microscopy images of crystal structures from corresponding samples.

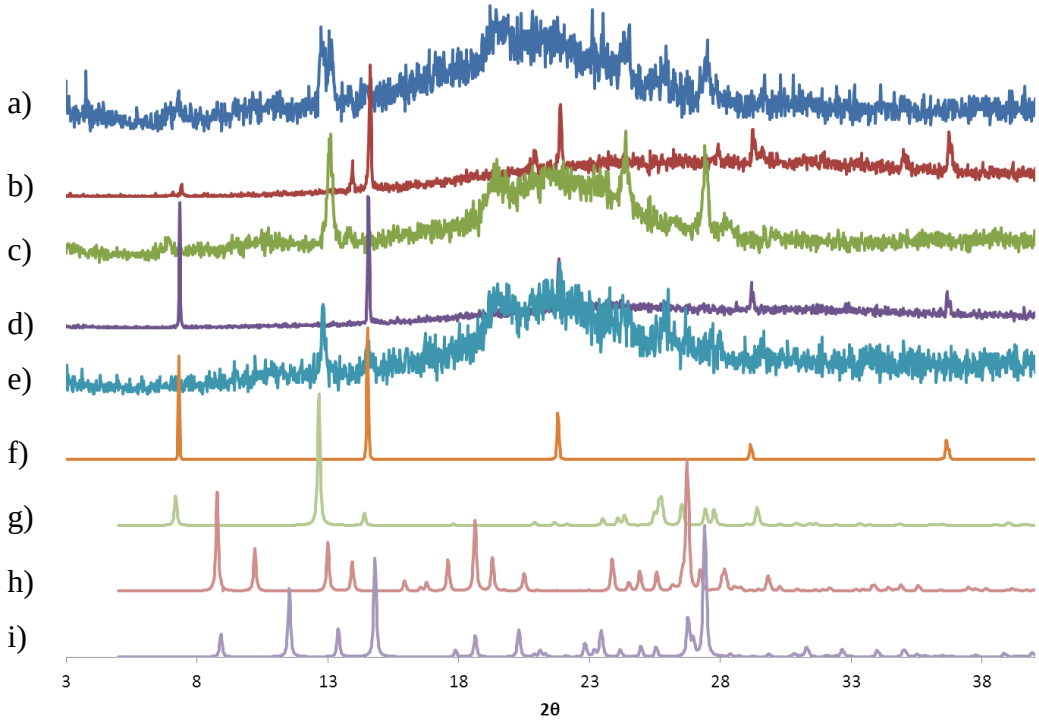

Figure 101 XRPD pattern comparing experimental data with CSD references for known forms of Theophylline: a) THE-A-G (blue), b) THE-A-S (red), c) THE-B-G (green), d) THE-B-S (purple), e) THE-C-G (light blue), f) THE-C-S (orange) g) BAPLOT01 (green) h) RIGYEM (red) i) THEOPH01 (violet)

5.7.2.6 Caffeine (CAF)

a)

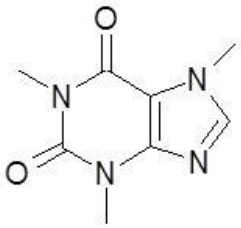

b)

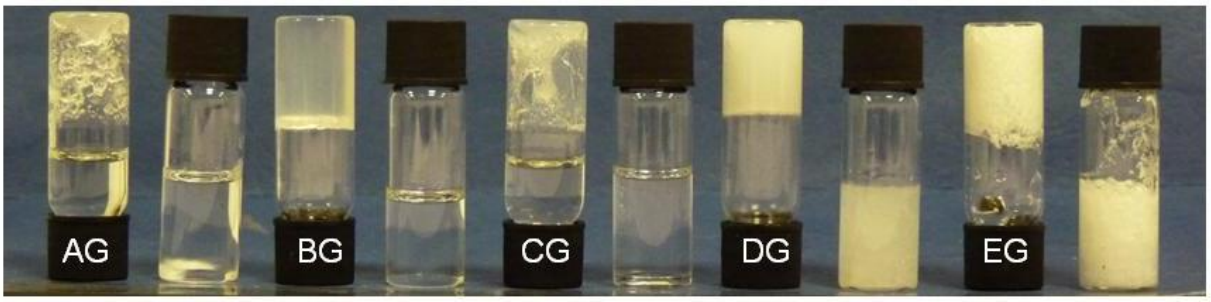

c)

	CH_3CN:Tol A	$CHCl_3$:Tol B	EtOAc C	DMSO:H_2O D	MeOH:H_2O E
Gel formation	PG	*G*	PG	G	G
Crystal from gel	Spherulites	*Needles above gel*	Needles	Fine needles	V. fine needles
Crystal from sol	Feather of Needles	Needles	X	Gel	Gel

d)

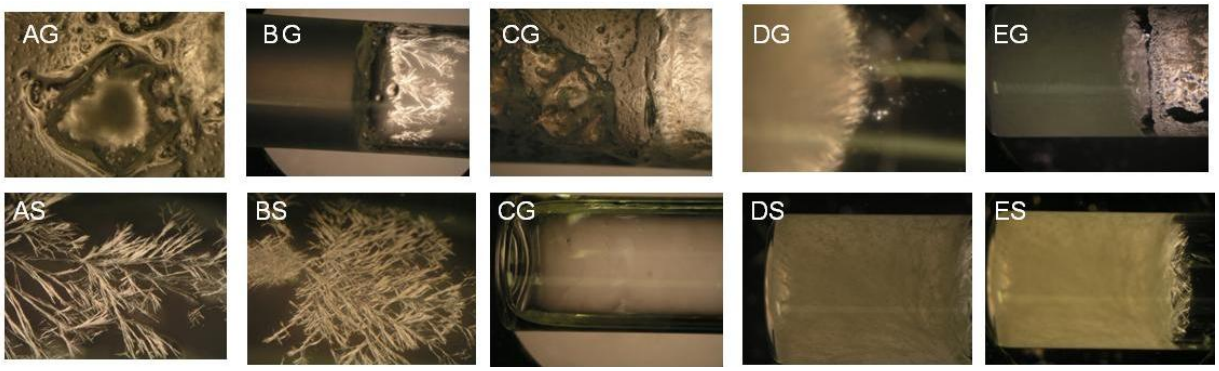

Figure 102 a) Structure of Caffeine b) photographs of CAF crystallised from different solvent combinations with and without gelator c) table showing gel and crystal formation in different samples d) selected microscopy images of crystal structures from corresponding samples.

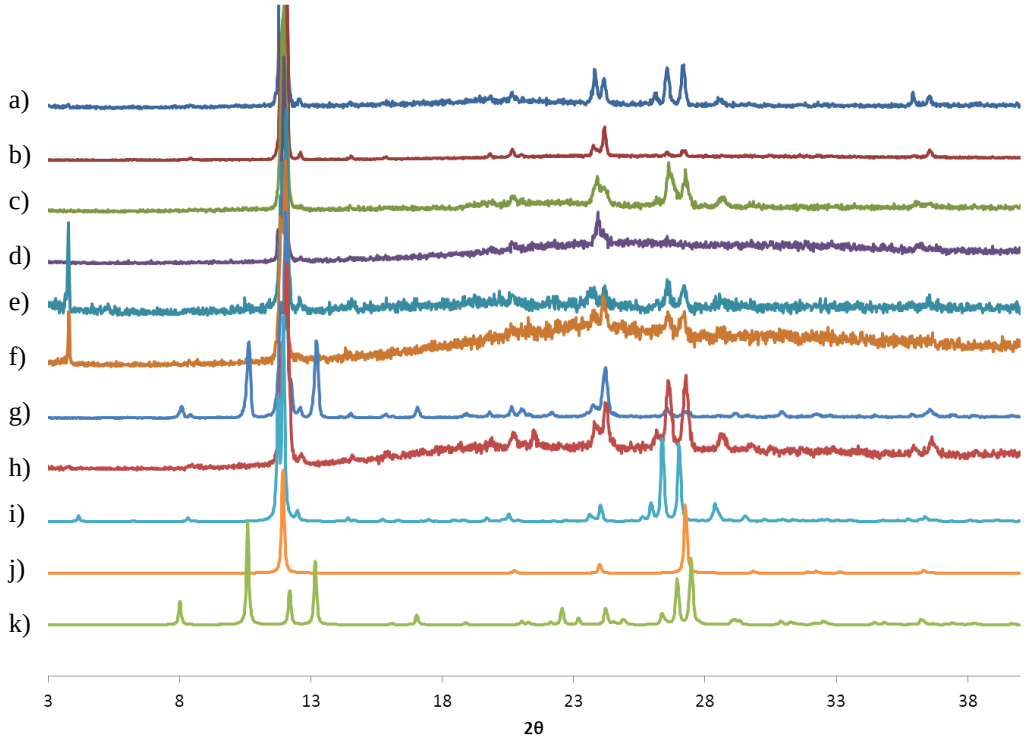

Figure 103 XRPD pattern comparing experimental data (Table 5) with CSD references for known forms of Caffeine: a) CAF-A-G (blue) b) CAF-A-S (red), c) CAF-B-G (green) d) CAF-B-S (purple), e) CAF-D-G (blue), f) CAF-D-S (orange), g) CAF-E-G (blue), h) CAF-E-S (red), i) NIWFEE03 (light blue), j) NIWFEE04 (orange), k) CAFINE (green)

5.7.2.7 Ibuprofen (IBU)

a)

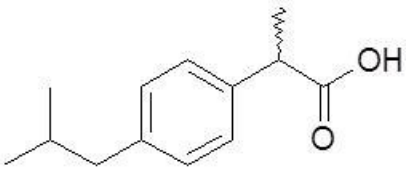

b)

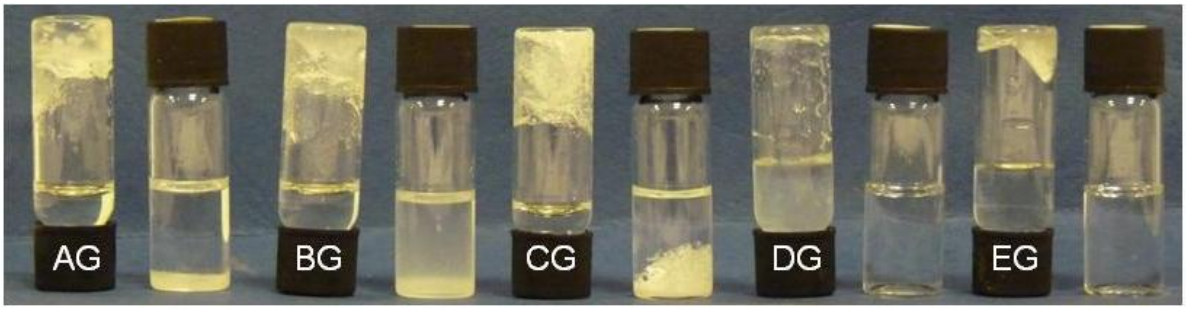

c)

	CH_3CN:Tol A	$CHCl_3$:Tol B	EtOAc C	DMSO:H_2O D	MeOH:H_2O E
Gel formation	PG	PG	PG	Viscous liquid	X
Crystal from gel	Needles	Needles	Spherelites + needles	X	Large crystal
Crystal from sol	Tiny needles	Tiny needles	Needles	X	X

d)

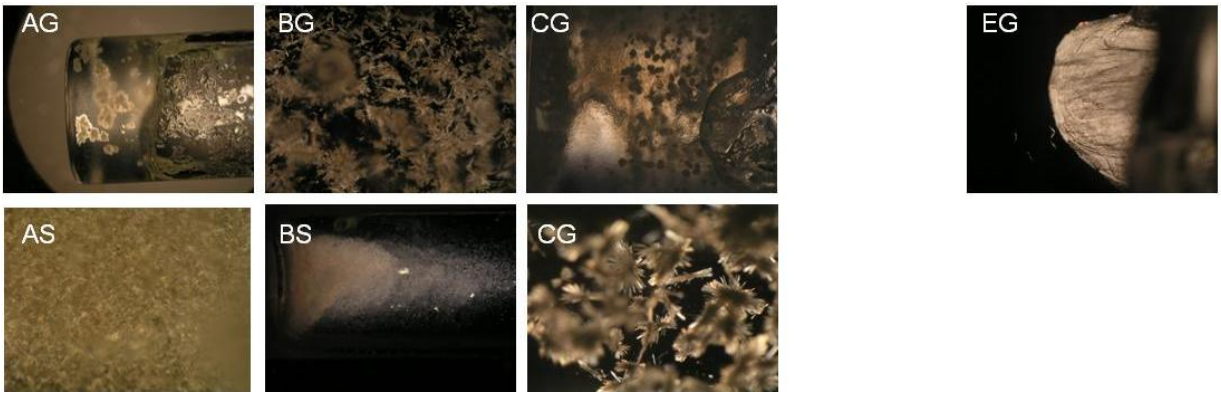

Figure 104 a) Structure of Ibuprofen b) photographs of IBU crystallised from different solvent combinations with and without gelator c) table showing gel and crystal formation in different samples d) selected microscopy images of crystal structures from corresponding samples.

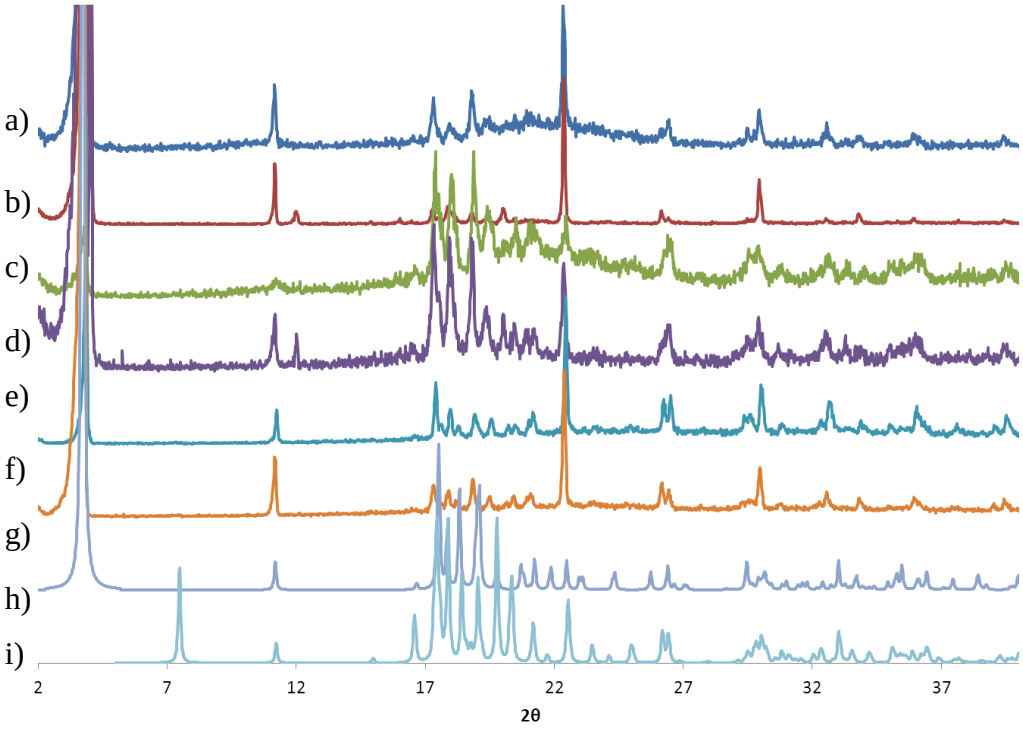

Figure 105 XRPD pattern comparing experimental data with CSD references for known forms of Ibuprofen: a) IBU-A-G (blue), b) IBU-A-S (red), c) IBU-C-G (green), d) IBU-C-S (purple), e) IBU-E-G (blue), f) IBU-E-S, g) IBU-E-S (orange), h) KATNOJ2 (mid blue), i) KASVEG (light blue).

5.7.2.8 Acetaminophen (ACP)

a)

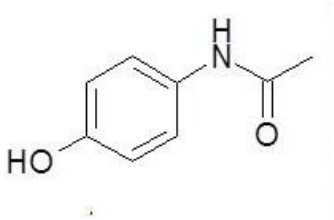

b)

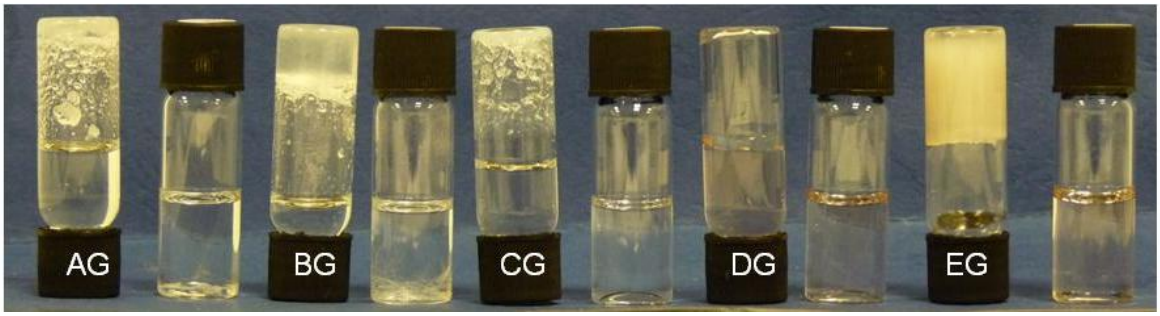

c)

	CH_3CN:Tol A	$CHCl_3$:Tol B	EtOAc C	DMSO:H_2O D	MeOH:H_2O E
Gel formation	PG	PG	PG	S-P	G
Crystal from gel	Fibres	Fibres	X	C	X
Crystal from sol	Plates	Needles	X	C	X

d)

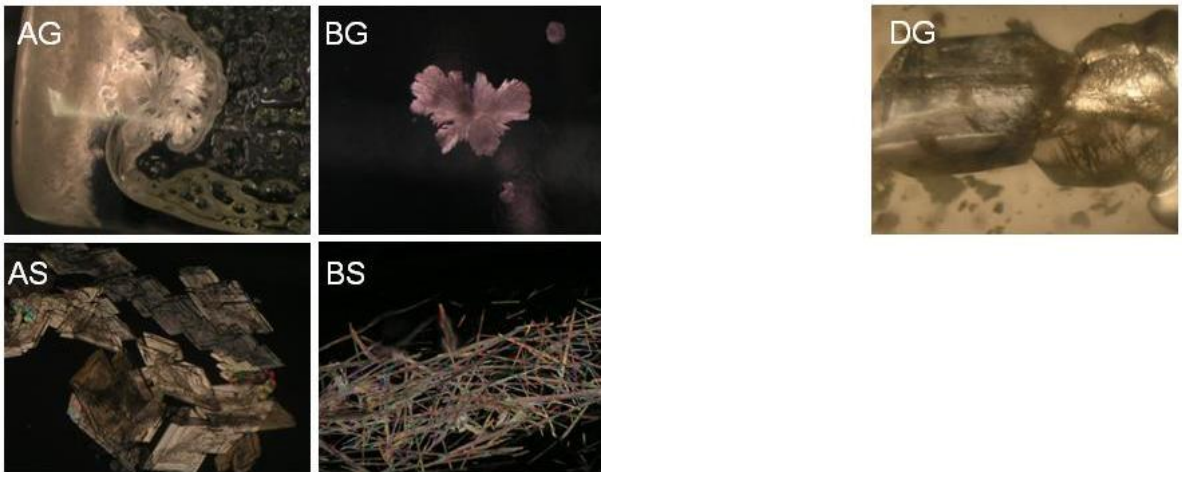

Figure 106 a) Structure of Acetaminophen b) photographs of ACP crystallised from different solvent combinations with and without gelator c) table showing gel and crystal formation in different samples d) selected microscopy images of crystal structures from corresponding samples.

Table 17 Comparison of experimental unit cell data and CSD reference HAXCAN01

	A	B	C	α	β	γ	V
8SA	7.095(2)	9.322(2)	11.678(3)	89.96(2)	97.54(1)	90.04(2)	785.7(3)
8GD	7.0972	9.3141	11.6844	90.003	97.588	90.008	765.62
HAXCAN01	7.1	9.4	11.72158	90	97.1165	7.1	776

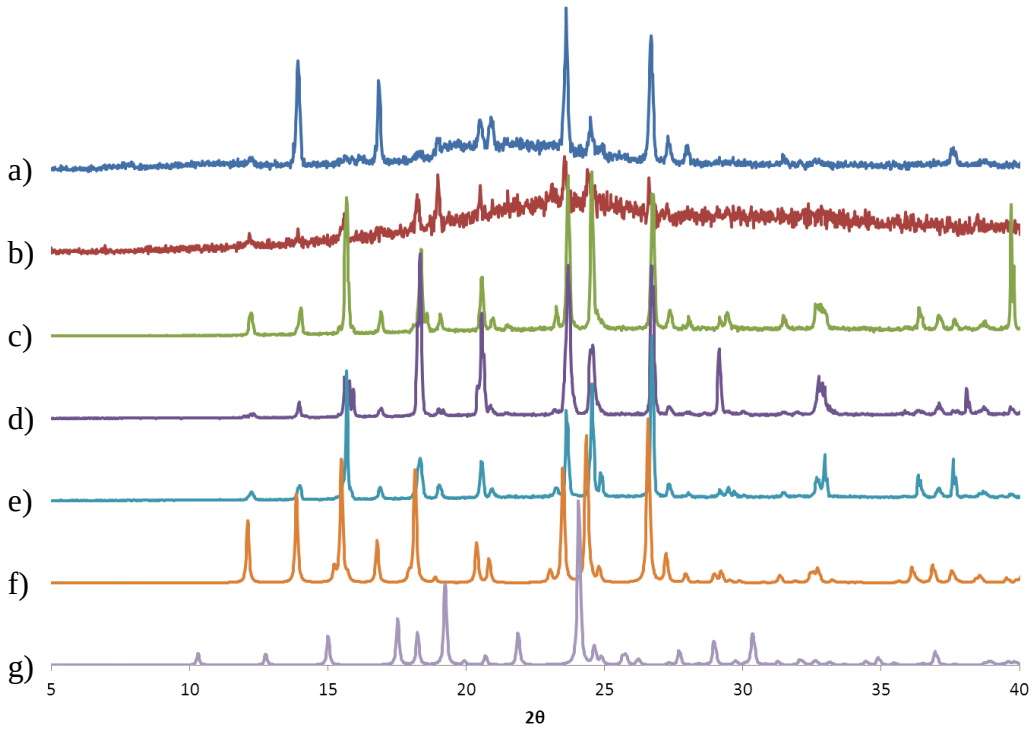

Figure 107 XRPD pattern comparing experimental data with CSD references for known forms of Acetaminophen: a) ACP-B-G (blue), b) ACP-B-S (red), c) ACP-D-S (green), d) ACP-E-G (purple), e) ACP-E-S (light blue), f) HAXCAN01 (orange), h) HAXCAN (purple).

Chapter 6: Tailored Gelators for the Crystallisation of Pharmaceutical Compounds

6.1 Designer gelators incorporating specific functionalities

6.1.1 Background and approach

The gel matrix is often considered to provide an inert environment with crystal growth taking place within the macropores between gel fibres. The nature of the gel structure is such that both solvent and growing crystals are 'trapped' by the gel matrix, preventing convection and sedimentation. The decreased mobility and flux of material delivered during crystal growth in gels leads to higher quality crystals of enhanced stability.[267] The habit of crystals grown from gels can be different to those grown from solution as crystal growth is diffusion limited and not inhibited by contact with the vessel walls or other crystals.[158] In an inert gel environment, homogeneous nucleation tends to dominate allowing higher levels of supersaturation to be achieved than in solution and allowing access to single crystals of metastable phases.[153]

As well as providing a benign environment for crystallisation, interactions between the compound being crystallised and the gel fibres may occur. Heteronucleation on gel fibres may template the nucleation of particular crystal forms or stabilise metastable forms which would otherwise convert or redissolve.[154, 155] Interactions between fibres and the different faces of growing crystals may influence the rate of growth of different faces leading to differences in habit for crystals grown from different gels.[157, 158] Helical gel fibres have also been found to produce an enantiomeric excess of one enantiomorph of sodium chlorate where a racemic mixture is obtained from solution.[164]

The approach taken in Chapter 5 is to combine an existing gelator with an available pharmaceutical compound. This combinatorial approach has revealed a number of differences in crystal habit, form and stability between crystals grown from the gel and solution phases.[170] The wide variety of LMWGs reported in the literature means there is enormous scope for observing the effect of other gelators on pharmaceutical systems. However, any differences observed by this approach are unpredictable and are due to fortuitous matches between the gel and crystal structures.

One potential advantage of supramolecular gelators is the relative ease with which different chemical functionalities can be deliberately incorporated into a gelator's structure. Rather than relying on chance complementarity between gelator and API, this chapter reports attempts to design LMWGs incorporating chemical functionalities tailored to mimic those of the compound under investigation. The idea is that gels displaying functionalities which complement those of the compound under investigation are more likely to interact with nucleating or growing crystals and so produce differences in polymorphism or crystal habit.

6.1.2 Synthesis

Three pharmaceutically relevant compounds were selected for investigation. Carbamazepine (CBZ) was selected owing to its use in previous studies. The recent discovery of form V carbamazepine growth on the crystal surface of a related compound,[243] and of form IV on polymer heteronucluei,[237] makes it a promising candidate for investigation. A study using polymer heteronuclei found the hydrophobicity of polymer side chains influences the polymorphism of acetaminophen (ACP) and it would be interesting to see if the same effect was observed in gels.[262] 5-Methyl-2-[(2-nitrophenyl)amino]-3-thiophenecarbonitrile, known as ROY for its red, orange and yellow crystals, has a large number of readily distinguishable polymorphs making it an interesting candidate for further study.[268]

Building on previous success with hexamethylene spaced bis-urea gelators (Chapters 2-4), compounds **39**, **21** and **42** were designed to incorporate functionalities mimicking carbamazepine (CBZ), acetaminophen (ACP) and ROY respectively (Scheme 3). Later studies identified a second core, 4,4'-methylenebis(2,6-diethyphenylurea) which is utilised in the same way for compounds **40**, **41**, **43**. Phenylalanine derived gelators **44**, initially synthesised as part of parallel studies into the crystallisation of amino acids from gels, provides a good reference compound with which to compare the effects of the other gelators.

Initial attempts to prepare **39** by direct reaction of carbamazepine with 1,6-diisocyanatohexane in chloroform showed no evidence of reaction, presumably due to the low nucleophilicity of the urea nitrogen lone pair in carbamazepine. Attempts were made to reduce the urea to a primary amine using lithium aluminium hydride, however this resulted in the formation of a bright orange compound. The product could not be identified but NMR

spectroscopy indicated a mixture of compounds and disruption of the aromatic rings. Carbamazepine was unaffected by reaction with less strongly reducing $NaBH_4$.

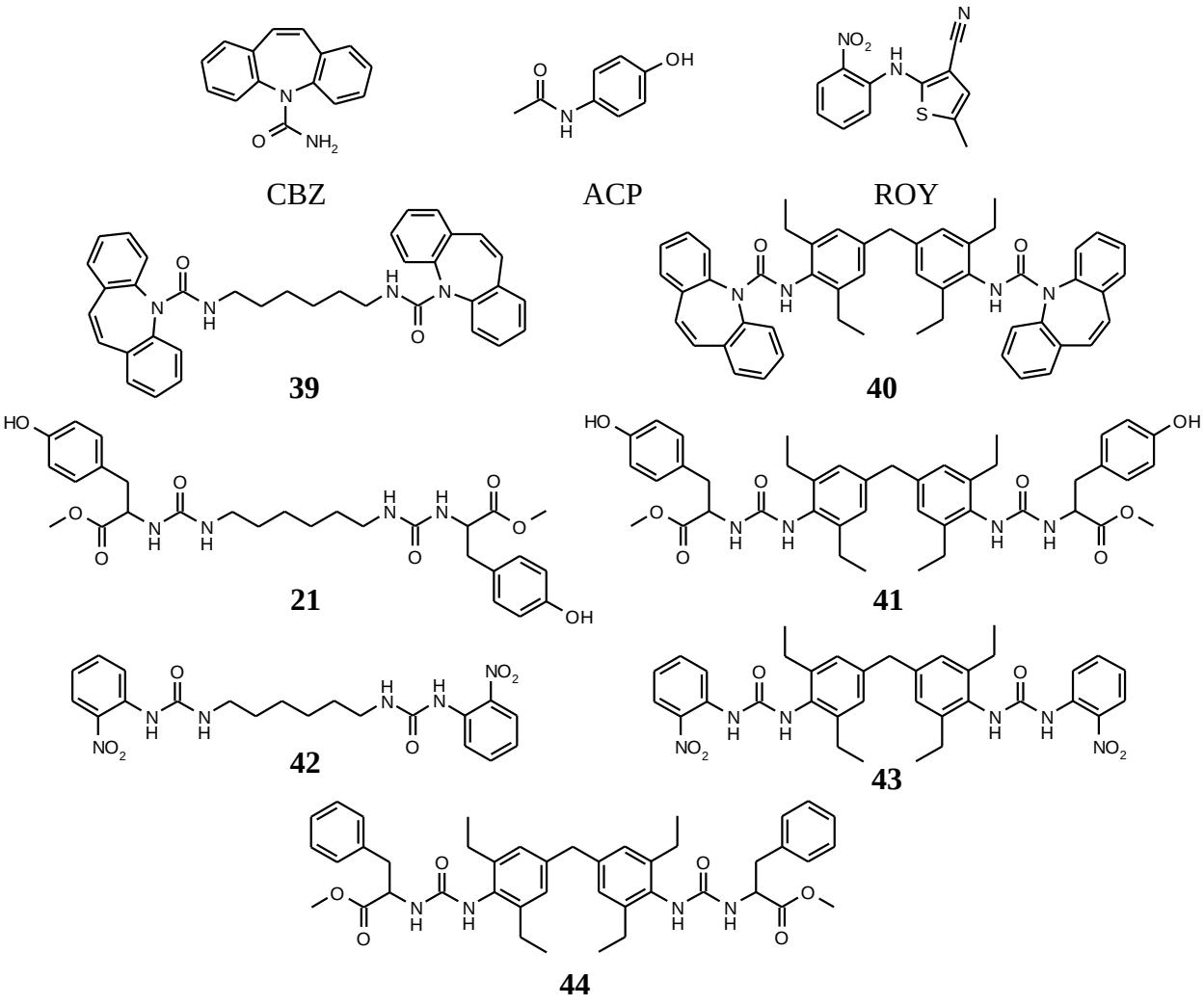

Scheme 3 Gelators mimicking functionality of: carbamazepine (**39** and **40**), acetaminophen (**21** and **41**), ROY (**42** and **43**), and phenylalanine derived gelator **44**.

Compound **39** was successfully synthesised by reacting the commercially available acyl-chloride derivative of carbamazepine, dibenz[b,f]azepine-5-carbonyl chloride, with diaminohexane. The initial procedure using only two equivalents of triethylamine led to the precipitation of significant quantities of 1,6-diamino hexane hydrochloride salt resulting in a low yield (22%) of **39**. Higher yields could be achieved using a higher concentration of triethylamine to sequester chloride ions as they are produced and prevent precipitation.

Attempts to synthesise **40** by heating under reflux dibenz[b,f]azepine-5-carbonyl chloride with 4,4'-methylenebis(2,6-diethylphenylamine) in chloroform with an excess of

triethylamine for 18 hours produced only starting material. The reaction was repeated using pyridine as a base but no reaction was observed after several days of heating under reflux.

Compound **21** was successfully synthesised, along with its butylene spacer analogue **27**. The experimental procedures are reported along with the other amino-acid derived gelators in Chapter 2. The product is obtained from the chloroform reaction mixture as an immiscible oil and a white solid can be obtained either by drying the oil in a drying pistol at 110°C or by recrystallisation from water.

Reaction of tyrosine methylester hydrochloride in chloroform and triethylamine with 4,4′-methylenebis(2,6-diethylphenylisocyanate) produced **41**. A number of other amino-acid derived gelators based on the 4,4′-methylenebis(2,6-diethylphenylurea) core were also synthesised using this same approach. Phenylalanine derived gelator **44**[269] was formed in good yield by the reaction of 4,4′-methylenebis(2,6-diethylphenylisocyanate with the phenylalanine methylester hydrochloride in the presence of triethylamine.

Attempts to react 2-nitroaniline with hexamethylene isocyanate were unsuccessful. This is likely to be due to the nitro-group on the aniline ring reducing the nucleophilicity of the amine. Addition of 1,6-diaminohexane to a solution in chloroform of 2-nitrophenylisocyanate resulted in the rapid precipitation of a yellow solid which was filtered, washed and identified as compound **42**. 2-Nitrophenylisocyanate also reacted readily with 4,4′-methylenebis(2,6-diethylphenylamine) producing a gelatinous precipitate from the chloroform reaction mixture.

6.1.3 Gelation studies

Compounds **21**, **39** and **41**-**44** were tested in a range of solvents for evidence of gel formation. The compound (0.01 g) was heated in 1ml of solvent (1 % w/v) in a sealed vial until fully dissolved. The samples were cooled rapidly by placing the vials in a water bath at room temperature. They were sonicated briefly at the first sign of precipitation to aid homogeneous gel formation. The results upon cooling to room temperature are recorded in Table 18. Gel formation was characterised by a simple vial inversion test; if the solvent was fully immobilised it was considered to have gelled. The term partial gel was ascribed to samples where only partial trapping of the solvent occurred.

Table 18: Screening of compounds **21**, **39** and **41**-**44** for gelation behaviour in a range of solvents

Solvent	Compound					
	21	**39**	**41**	**42**	**43**	**44**
Water	P	I	I	I	I	I
Acetonitrile	O	S	G	G	G	G
Methanol	O	S	PG	G[a]	G	G
Ethanol	S	S	G	G[a]	G	G
Acetone	O	S	G	G	G	G
THF	O	S	G	PG	PG	G
DCM	O	S	I	G	G	G
Ethylacetate	O	S	G	G[a]	G	G
Chloroform	O	S	I	G	G	G
Toluene	O	S	I	G	G	G

P = precipitate, S = solution, G = Gel, PG = partial gel, O = oil, I = insoluble with heating, unstable over time. [a] = gel unstable and breaks down over time.

Carbamazepine derivative **39** is highly soluble and forms clear solutions at room temperature in most solvents, even at higher concentrations (tested up to 10 % w/v), and no gels were observed. The compound is insoluble in water and addition of water to a concentrated methanol solution produces a fine white precipitate. Slow evaporation of a toluene solution gave crystals suitable for single crystal X-ray diffraction. This technique revealed the sample to be a toluene solvate of **39** by XRD.

In contrast to other hexamethylene spaced gelators discussed in Chapter 2, the hexylene chain has an anticlinal orientation with respect to the carbonyl group with a torsion angle of 118.62°. This lies between the cis conformation adopted by **23** form B and the all-*trans* conformation observed for the other gelators. The hexamethylene spacer gives the urea groups an antiparallel orientation. However, steric hindrance from the bulky aromatic rings of the carbamazepine groups prevents hydrogen bonding between the free NH and carbonyl of the urea moieties. Instead, the carbonyl groups interact with the aromatic hydrogen atoms on an adjacent carbamazepine moiety (O1-C3 3.31 Å) resulting in anti-parallel chains of hydrogen bonding interactions. Surprisingly, the hydrogen bonding potential of the NH (N1) remains unsatisfied. Disordered toluene is found in the large cavities between the chains of molecules. Slightly longer interactions (O1-C7 3.4 Å) between adjacent chains link stacks in π-stacking between pairs of carbamazepine groups to give packing in the other dimensions. The lack of strong hydrogen bonding interactions is possibly due to the presence of the bulky end group and explains the high solubility of **39** and the lack of gel formation observed.

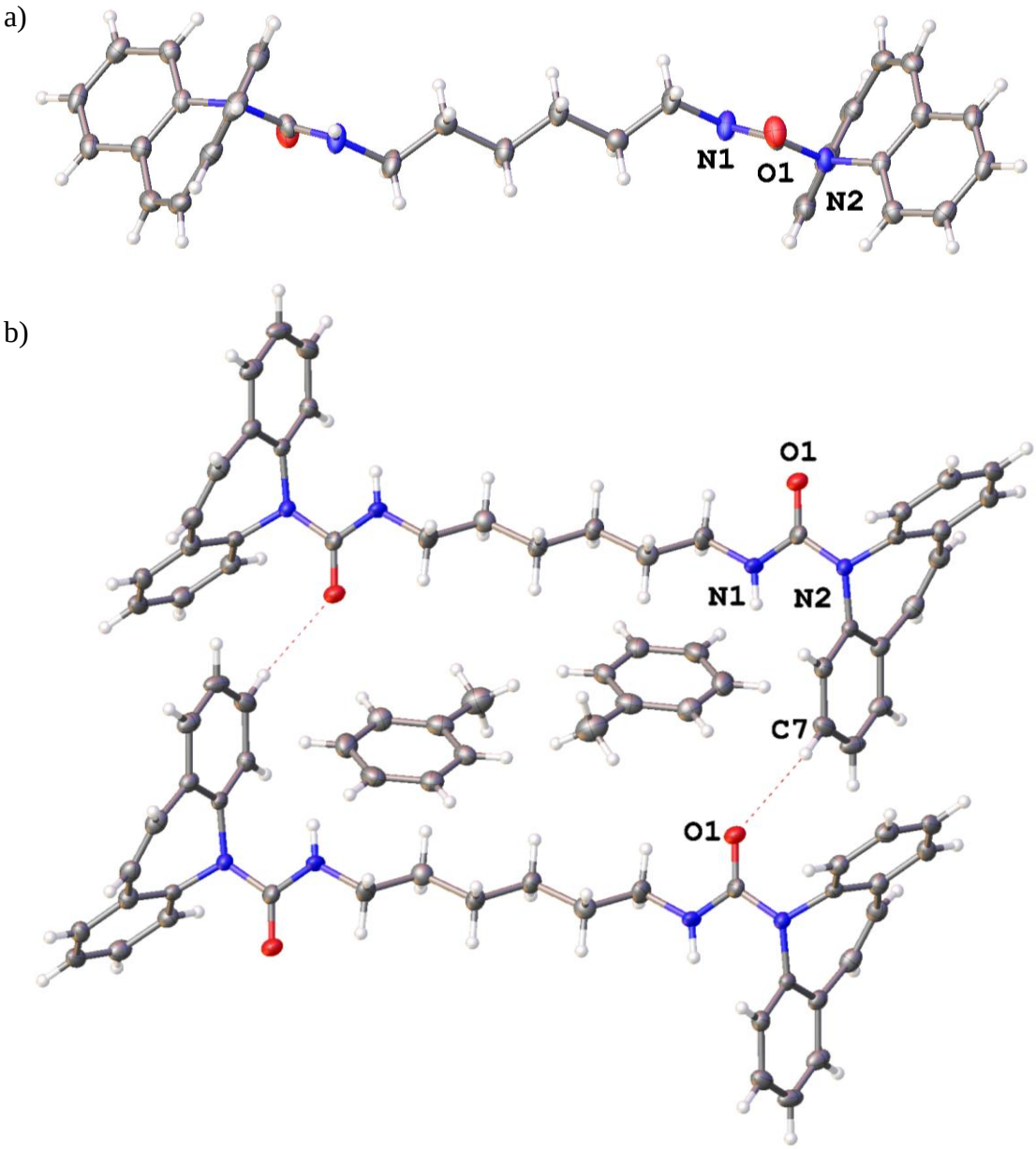

Figure 108: X-ray molecular and crystal structure and packing of a toluene solvate of **39**, O1-C7 = 3.31 Å.

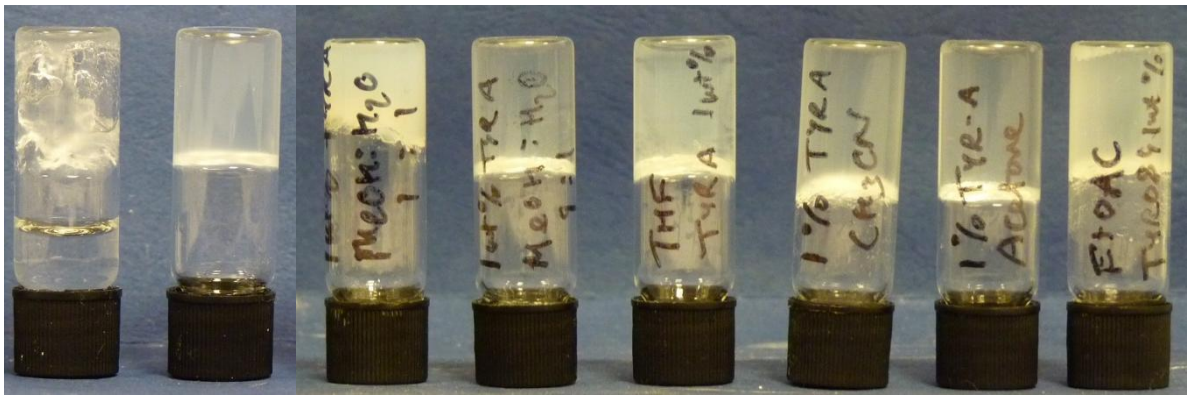

Figure 109 Gels comprising 1 % w/v **41** in (left to right) methanol, ethanol, 1:1 and 9:1 methanol:water, THF, acetonitrile, acetone and ethyl acetate.

As discussed in Chapter 2, no gelation was observed for hexamethylene spaced tyrosine derivative **21** which instead forms immiscible oils in a range of solvents. In contrast, diphenyl methyl **41** forms robust, translucent gels in a range of solvents such as ethanol, THF, acetonitrile, acetone and ethyl acetate (Figure 109). At 1 % w/v only partial gels were observed for **41** in methanol but higher concentrations of gelator or the addition of water resulted in complete gel formation. The compound is insoluble in less polar solvents such as toluene and chloroform as well as water.

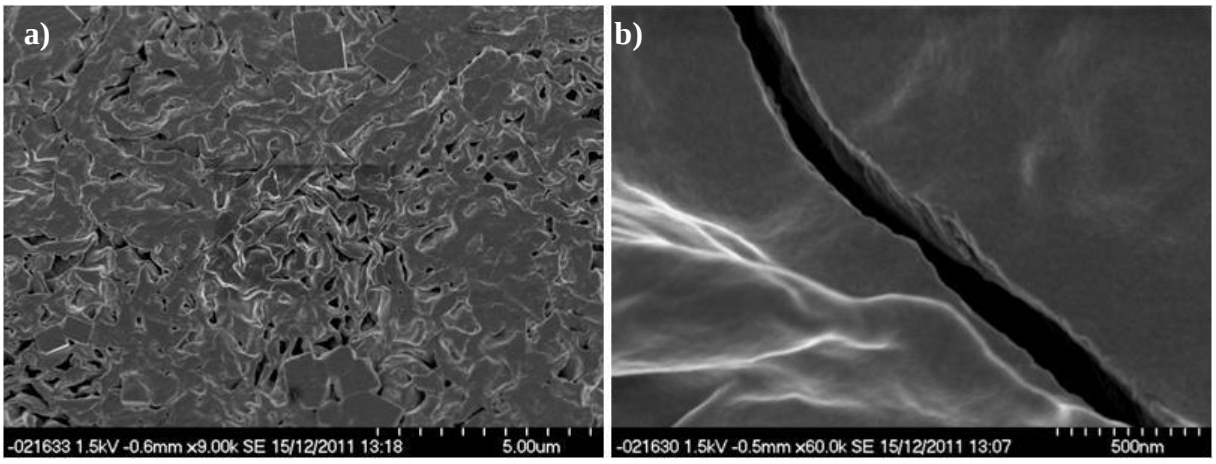

Figure 110 SEM images showing xerogels formed from 1 % w/v gels of **41** in a) acetone b) acetonitrile.

Small amounts of gel sample were applied to silicon chips using a cocktail stick and the solvent was allowed to evaporate under atmospheric pressure. Acetonitrile and acetone gels of **41** prepared in this way showed no evidence of fibre formation within the resolution of the instrument. Instead, a number of plate-like structures were observed against a textured but continuous background. The gel samples from which the xerogels were prepared were unchanged in appearance over the course of the experiment and remained stable over a number of weeks. The morphology observed may be due to conversion of the xerogel to a different crystal form or precipitation of dissolved material on top of the gel as the solvent is removed. Cryo-SEM could be used to ascertain the nanoscopic structure of the gel.

The formation of oils by **21** is thought to be due to competition between different potential hydrogen bonding motifs involving the urea and phenol groups. It may be that the less flexible aromatic spacer pre-organises the molecule allowing the formation of urea tapes and preventing competing interactions. Phenylalanine diphenylmethane spaced gelator **44** also showed a greater range of gelation behaviour than its alkylene spacer analogue **20**. The full range of gelation behaviour by **44** is discussed in Chapter 7.

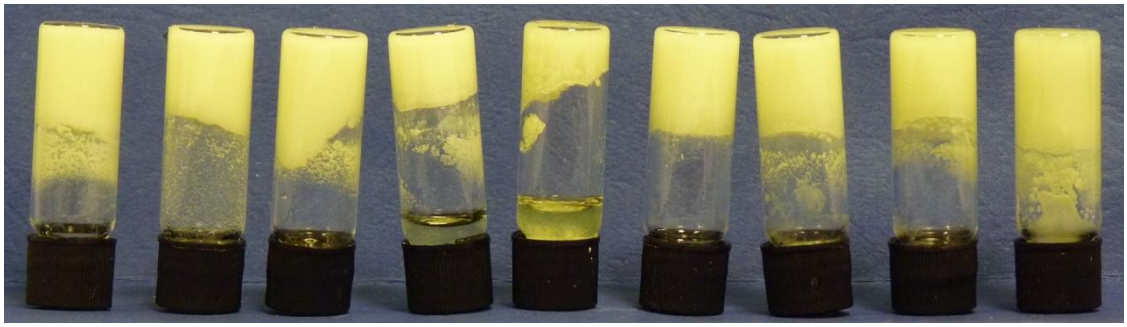

Figure 111: Gels of 1 % w/v **42** in (left to right) acetonitrile, methanol, ethanol, acetone, THF, DCM, ethylacetate, chloroform and toluene.

Unlike the other hexamethylene spaced analogues, ROY mimic **42** forms gels with rapid cooling and sonication in the full range of solvents with the exceptions of water and THF. However, the gels are opaque and fragile, breaking apart to form a precipitate if gently shaken. Gels form without sonication but tend to be less homogeneous with clumps of gel and free solvent. The chloroform, toluene, acetonitrile and acetone gels are unstable and form a precipitate after a number of days whilst gels from other solvents remain stable.

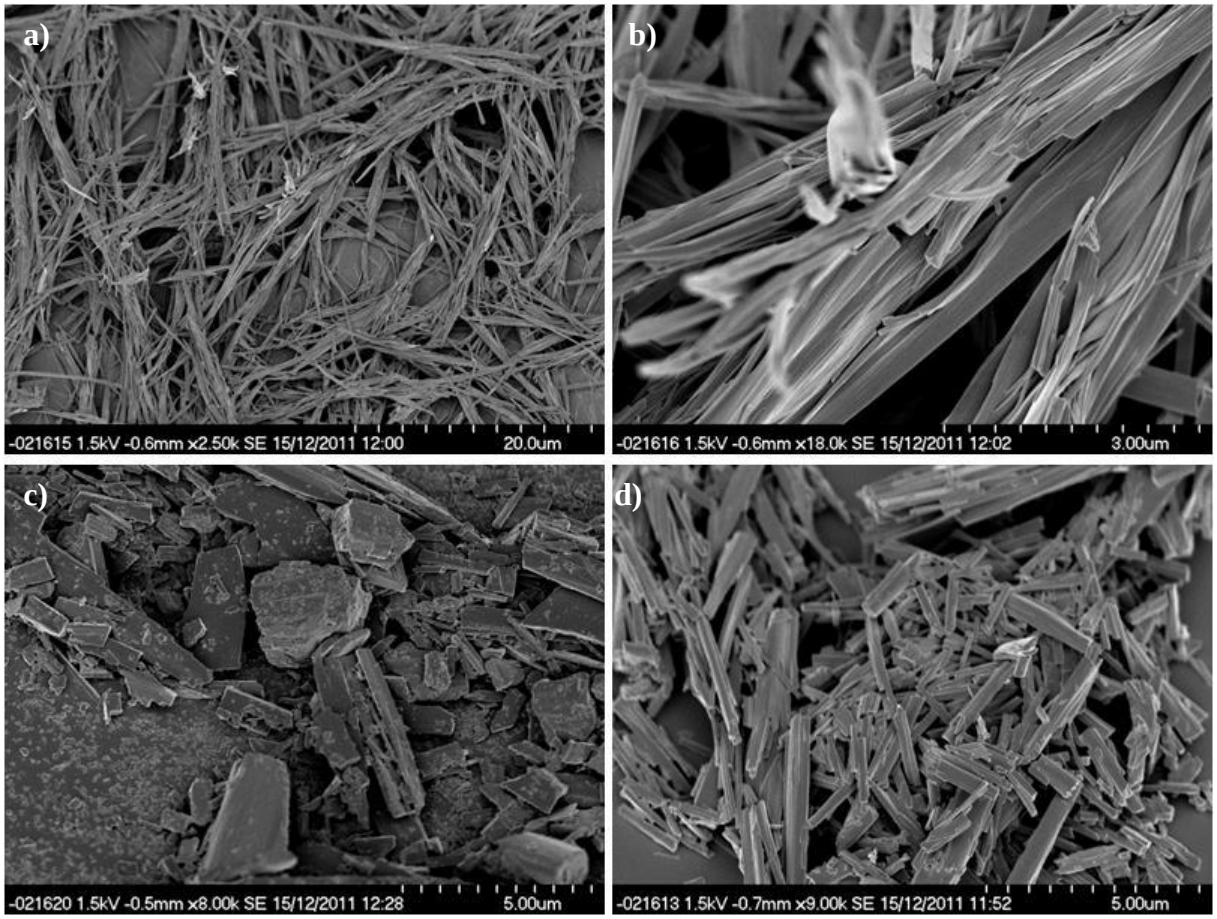

Figure 112 SEM images showing xerogels formed from 1 % w/v gels of **42** in acetonitrile (a and b), toluene (c) and acetone (d).

SEM images of xerogels formed from 1 % w/v gels of **42** in acetonitrile showed a mesh of poorly defined rectangular fibres with a rectangular cross section. The fibres are hundreds of nanometres thick, several microns long and bunch together with fibres merging into each other. A variety of larger plate and block shaped structures were obtained from toluene and acetone which may represent the precipitates observed when the gels break down. It would be interesting to understand whether a polymorphic transition is responsible for the break-down of the gels as observed for compounds **17**, **23** and **24** in Chapter 2.

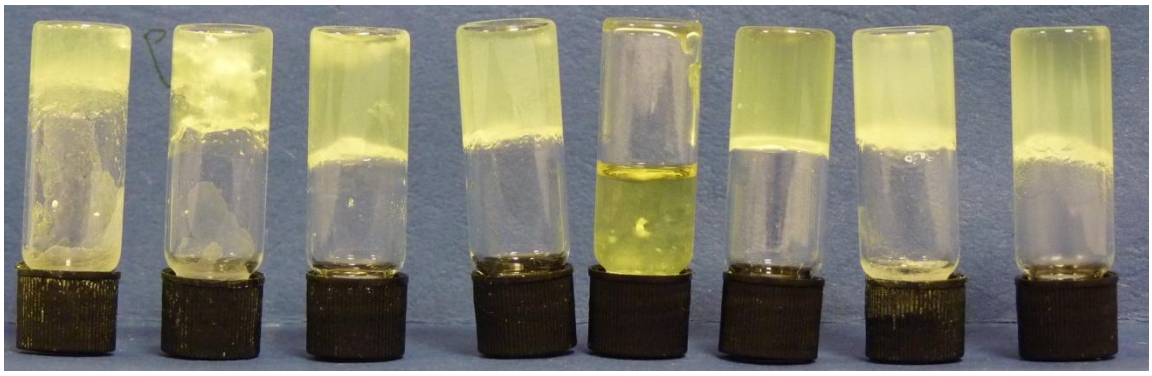

Figure 113: 1 % w/v **43** in (left to right) acetonitrile, methanol, ethanol, acetone, THF, DCM, ethylacetate and toluene.

ROY derived compound **43** forms robust, stable, translucent gels in a wide range of solvents including acetonitrile, methanol, acetone, THF, ethylactetate and toluene as shown in Figure 113. Compound **43** is much less soluble than **42** failing to dissolve fully in a number of the solvents at 1 % w/v. Undissolved material tends to inhibit gel formation and the use of lower concentrations of gelator results in more translucent and homogeneous gels. SEM indicates that the gels consist of entangled networks of fine fibres. The small diameter of the fibres observed (~20 nm) is consistent with the translucent appearance of the gels which are not opaque, unlike the gels of **42**.

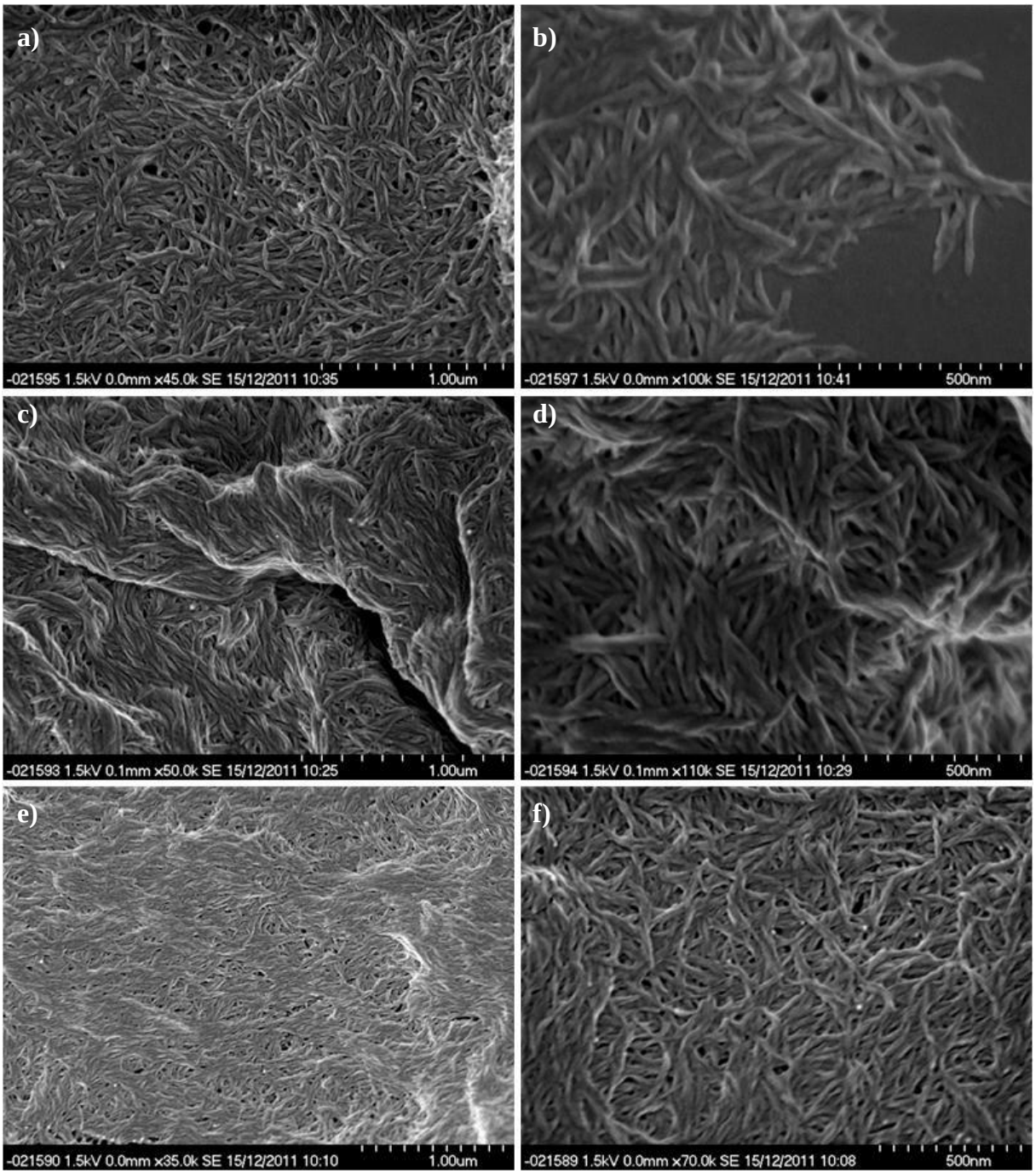

Figure 114 SEM images at two different magnifications showing xerogels formed from 1 % w/v gels of **43** in a-b) toluene, c-d) acetonitrile e-f) acetone.

6.2 Crystallisation from tailored gelators

6.2.1 The polymorphism of ROY

ROY was first synthesised by medicinal chemists at Eli Lilly as a reagent to prepare olanzapine, a schizophrenia drug. There are ten known crystal forms of ROY of which seven crystal structures have been obtained. Whilst this does not make ROY the most polymorphic compound on record (as water for example has ten known solid state forms) ROY is remarkable in that all seven forms can be crystallised and are kinetically stable enough to be studied under near-ambient conditions.[270] Different crystal forms are represented by initials reflecting the distinct colour and habits adopted by different polymorphs. The names and properties of various ROY polymorphs are given in Table 19. The different colours of ROY originate from conformational isomerism. The distinct differences in appearance allow for relatively facile *in-situ* monitoring of crystal growth and the different forms are unambiguously distinguishable by infrared spectroscopy.[268]

Table 19 Selected properties of ROY polymorphs[268]

Form	Y	YT04	R	OP	ON	YN	ORP
Description	Yellow prism	Yellow prism	Red Prism	Orange Plate	Orange needle	Yellow needle	Orange-red plate
θ(deg)	104.7	112.8	21.7	46.1	52.6	104.1	39.4
$\bar{\nu}_{CN}$	2231	2224	2212	2226	2224	2222	2217
H-H_Y, KJ/mol	0	0.9	1.4	1.9	2.6	3.0	4.1

The Y form is most stable under ambient conditions with enthalpies increasing in the order Y < YTO4 < R < OP < ON < YN < ORP. However, all of these forms are kinetically stable over months or years and often grow concomitantly from both solution and the melt.[268] Some of the polymorphs are known to nucleate on and outgrow those of other crystal forms.[271, 272] The polymorphism of ROY is altered by crystallisation from liquids in contact with polymer surfaces,[262] gold islands,[273] in capillary tubes,[274] porous solids[275] and from micro-emulsions[276] and micro-gels.[155]

Compounds **42** and **43** were designed to mimic the functionality of ROY by incorporating a nitrophenyl substituent as part of the chemical structure of a bis-urea derivative, a known gel forming motif.[51, 52, 170] The nitrophenyl groups are expected to comprise the exterior of the gel

fibres upon assembly of the gel by the classic urea α-tape motif, presenting ROY molecules with an ordered fibre surface on which to nucleate. This may favour the nucleation of different polymorphs to those found in solution or which homo-nucleate within a more conventional gel that does not interact with the substrate. In order to establish whether any differences observed are due to specific interactions with the gelator, rather than generic effects of a gel environment, crystallisations of ROY were undertaken from a range of different gels as well as solution.

6.2.2 Crystallisation of ROY from different gelators

A solution containing 100 mg/ml of ROY was allowed to crystallise from toluene gels of the designer gelator **43**, as well as four different generic gelators used in previous studies (compounds **17**, **20**, **32** and **38**). Toluene was selected as the solvent because a wide variety of the gelators reliably form gels in the solvent without sonication. The opacity and instability of hexamethylene spaced ROY mimic **42** in toluene made it unsuitable for use in this study.

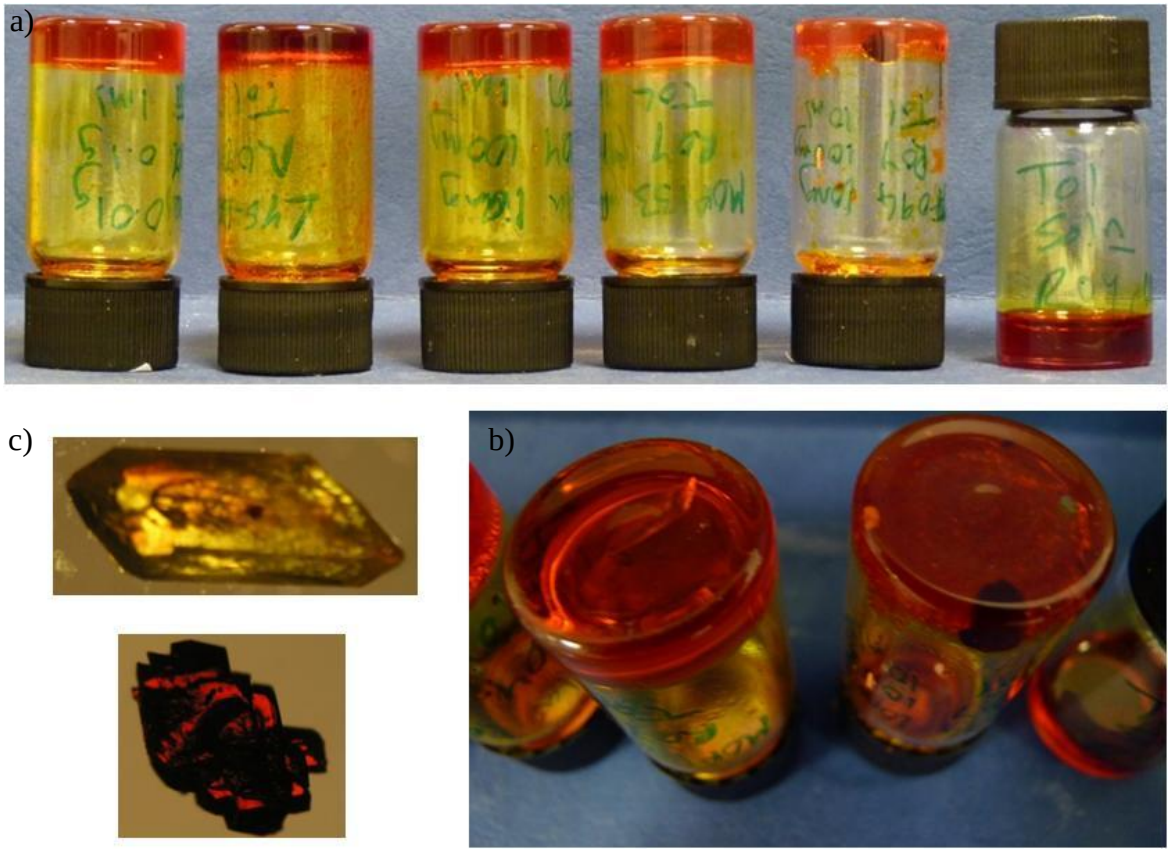

Figure 115 (a) Crystals of ROY grown from five different gels (left to right: **17**, **20**, **32**, **38**) and a solution phase control experiment (b) red crystals growing in a gel of **43** which is designed to mimic ROY, (right) and yellow crystals in a non-specific gel (**38**)(left), (c) isolated crystals of Y and R forms.

After one month the generic gelators and solution produced large yellow blocks identified by single crystal X-ray unit cell determination as the thermodynamically most stable Y form. Under the same conditions, 1 % w/v gels of **43** produced red crystals corresponding to the R form. Figure 115 shows images of the crystals obtained from different gels. These preliminary results appear to indicate that the designer gelator, **43**, induces the crystallisation of a different polymorph of ROY to that obtained from solution or a range of generic gels.

In order to test this observation, five repeats using the same concentration of ROY in toluene (100 and 200 mg/ml) were undertaken along with a samples at lower (50 mg/ml) and higher (150 mg/ml) concentrations. Crystallisations from gels of ROY mimic **43** were compared with solution samples and three different generic gelators: hexamethylene spaced **20** and **17** and diphenylmethane spaced gelator **44**. Gels were formed with 1 % w/v of gelator in each case except for compound **44** which, for solubility reasons, was used at 0.5 % w/v. An additional sample containing a non-gelling solution saturated with **43** at room temperature was also investigated. The purpose of this reference was to test whether any differences observed were due to the gel state or compound **43** acting as a solution-based additive.

Samples were prepared from stock solutions in crimp top vials, sealed, and heated until all solids had completely dissolved. Samples were allowed to cool on the bench to room temperature without sonication. Crystallisation generally took place over several hours to weeks and results are recorded at various time intervals in Table 20. Clear differences in crystal colour and shape allow the different polymorphs to be distinguished and intermediate assignment of crystal form is purely on the basis of visual observation. Assignments of the final crystal forms were confirmed by IR spectrometry. XRPD patterns for each of the different crystal forms were compared with generated patterns taken from the CSD to confirm the assignments.

Table 20 Crystallisation and polymorphism of ROY crystallised from different gelators and solution over time

Gelator	ROY mg/ml toluene	Crystal form observed at time interval 24 hours	72 hours	96 hours	2 weeks	>1 month
20	100	Y	Y	Y	Y	Y
	100	Y	Y	Y	Y	Y
	100	-	-	-	-	R
	100	-	Y	Y	Y	Y
	100	-	-	-	-	R
	50	-	-	-	-	-
	150	Y	Y	Y	Y	Y
	200	-	Y	Y	Y	Y
37	100	R+Y	Y	Y	Y	Y
	100	R	R	R	R	R
	100	R+Y	R+Y	R+Y	Y	Y
	100	-	-	R	R	R
	100	-	-	R	R+Y	Y
	50	-	-	-	-	Y
	150	-	Y	Y	Y	Y
	200	R	R	R	R	R
44	100	-	-	-	Y	Y
	100	-	-	Y	Y	Y
	100	-	R	R	R	R
	100	-	-	-	R	R
	100	-	R	R	R	Y
	50	-	-	-	-	Y
	150	-	-	-	Y	Y
	200	-	-	Y	Y	Y
43	100	R	R	R	R+Y	Y
	100	-	-	-	R	R
	100	-	-	-	R	R
	100	-	-	-	R	R
	100	-	ON	ON	ON	ON
	50	-	-	-	-	Y
	150	R	R	R	R	R
	200	-	R	R	R	R
Solution (no gelator)	100	Y	Y	Y	Y	Y
	100	-	R	R	R	R
	100	R	R	R	R	R
	100	-	Y	Y	Y	Y
	100	-	-	-	Y	Y
	50	-	-	-	Y	Y
	150	Y	Y	Y	Y	Y
	200	Y	Y	Y	Y	Y
Solution saturated with **43** at 20°C	100	Y	Y	Y	Y	Y
	100	-	-	-	Y	Y
	100	R	R	R	R	R
	100	-	Y	Y	Y	Y
	100	-	R	R	R	R
	50	-	-	-	-	Y
	150	Y	Y	Y	Y	Y
	200	-	Y	Y	Y	Y

Y, R, ON refer to the crystal form of ROY obtained. R+Y indicates concomitant polymorphism. All gelators used at 1% w/v in toluene except **38** which was used at 0.5 % w/v.

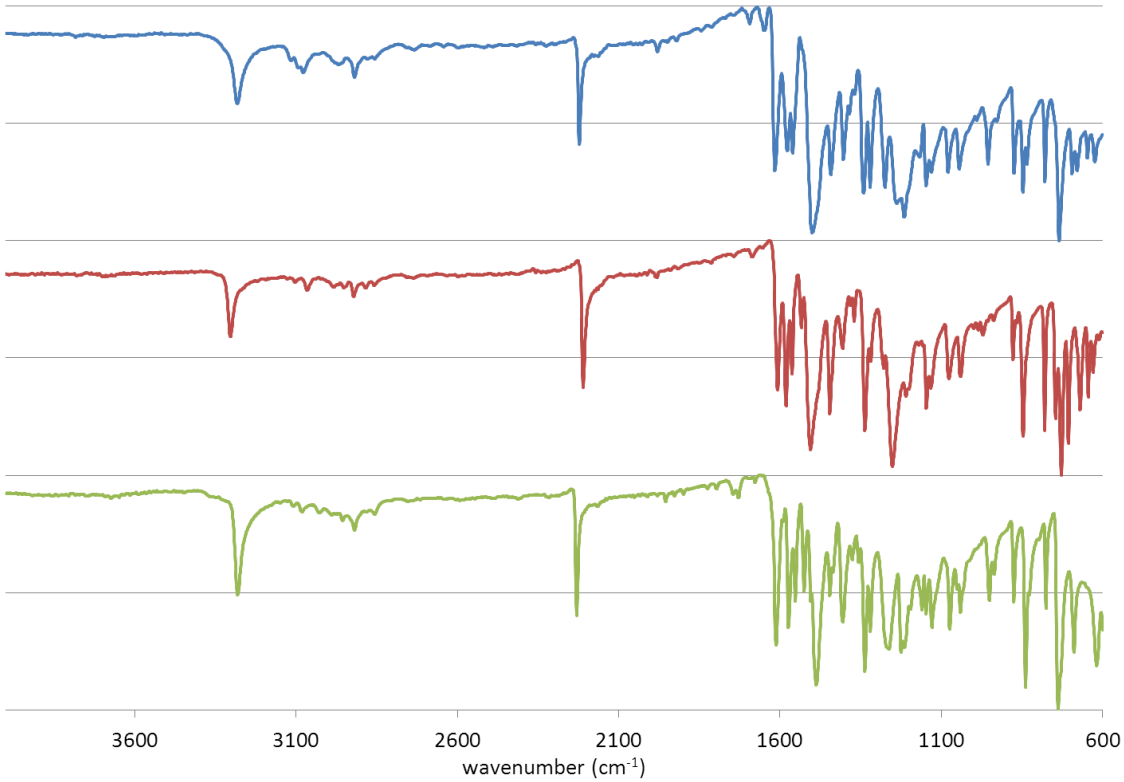

Figure 116 Typical IR spectra for ON (blue), R (red) and Y (green) polymorphs of ROY grown from gels**.**

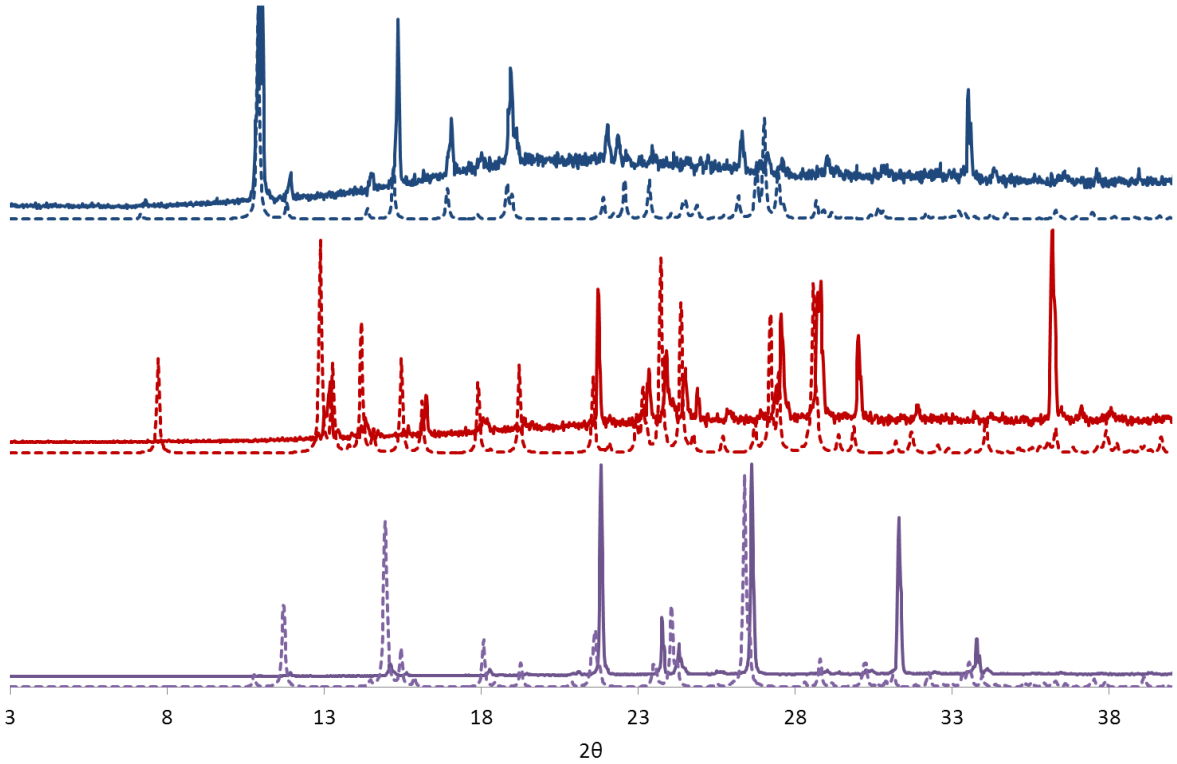

Figure 117 Assignment of crystal forms of ROY based on comparison of experimental (unbroken lines) and calculated (dotted lines) XRPD patterns: ON form, QAXMEH (blue),[268] R form, QAXMEH02 (red),[268] Y form, QAXMEH01 (purple).[268]

There is considerable variation in the time taken before crystals are first observed, ranging from hours to weeks for a single set of conditions. Three different polymorphs, the Y, R and ON crystal forms, were identified. No trend in the time at which particular polymorphs are observed could be deduced with both the R and Y forms first appearing in samples after less than 24 hours and more than one month. A number of cases of concomitant crystal growth between the R and Y forms were observed. Over time crystals of the Y form began to appear in a number of the samples where only crystals of the R form were observed previously. Where both the Y and R form are present, the R form gradually converts into the more stable Y form. However, in the absence of the Y form, crystals of R remain stable after several months in both the gel and solution phases.

In solution samples without any gelator at 100 mg/ml of ROY, the R form is observed in two cases whilst Y was observed in three. Higher concentrations of ROY gave the Y form which was also observed in the 50mg/ml sample after two weeks. The same pattern was observed for the non-gelling **43** solution reference indicating **43** has no significant effect on crystal growth as a solution based additive. In most cases, many more individual crystals formed from solution than in the gel phase samples, although there was considerable variation between repeats.

In the gels of **44** and **17** the R form was observed slightly more often than from solution. This is particularly true in the case of **17** where the R form was also observed at higher concentrations. In gels of **20** only the Y form was produced across all samples, although the R form was later observed after several months in two of the samples which had failed to crystallise. The Y form was observed for all samples in the 50 mg/ml samples.

In gels of the designer gelator **43**, large single blocks of R were seen in five of the eight samples. One of the 100 mg/ml repeats produced jagged yellow/orange needles growing from the surface which were identified as ON by IR spectrometry and XRPD. The 150 mg/ml sample produced many separate smaller crystals which were also identified as the R form by IR and XRPD. After >6 months the Y form was eventually observed in the 50mg/ml sample.

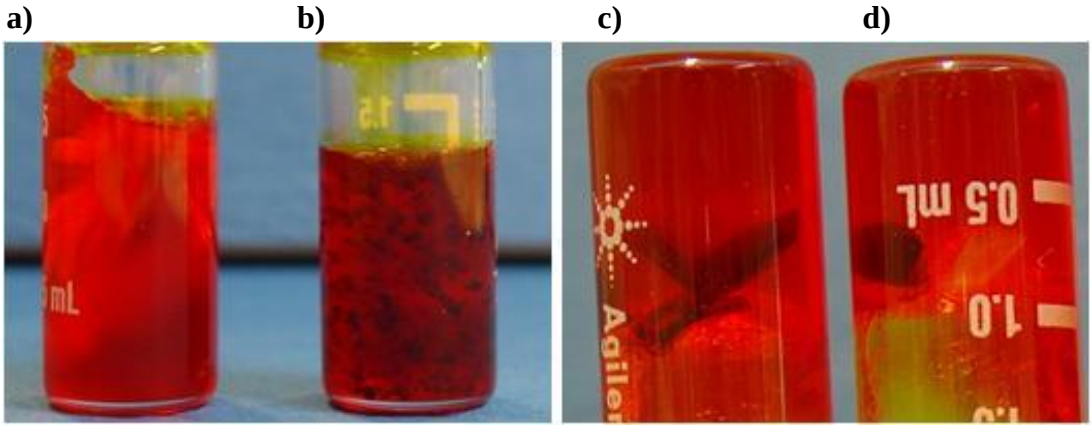

Figure 118 Photographs showing crystallisation of a) ON form, b) and c) different morphologies of the R form and d) concomitant crystal growth of the R and Y forms.

One possible explanation for the differences in polymorphic behaviour observed is that the gels were heated to different extents in order to dissolve the different gelators, resulting in slightly different cooling profiles. Thermostatically controlled conditions would remove this variable but were not possible due to the high temperatures required to dissolve the gels in some instances. However, the toluene solutions are saturated with ROY at 60°C which is well below the dissolution temperature of all of the gelators. Furthermore, crystal growth is typically observed after several days and no correlation between crystal form and the time at which the crystals are first observed could be determined. An additional factor to consider is that in some samples the crystals grow against the sides of the vials and on the surface of the gels. In these cases heteronucleation on the glass vial or from dust at the gel surface may determine the crystal form rather than the gel matrix. However, both the Y and R forms were observed growing against the glass vials and on the gel surface indicating that this is unlikely to account for the variation in polymorphism observed.

With more repeats, the effect of different gelators on the crystallisation of ROY is less clear cut than indicated by the preliminary experiments. In the absence of gelator both the R and Y forms are observed. A mixture of the R and Y forms is also observed in all of the gel samples. Gels of **20** show more instances of the Y form than observed from solution whilst gels of **17** and **44** showed slightly higher instances of the R form. The largest difference in polymorphic outcome compared with solution was observed in gels containing the ROY mimic **43**. The ON form is produced which is not observed in any of the other samples. Otherwise, the R form is almost exclusively observed with the Y form only produced in the 50 mg/ml ROY sample after several months. Evidence that these differences are due to **43** in

the gel state rather than solution come from the reference samples containing a non-gelling solution of **43** where no difference in polymorphism was observed compared to solution.

Because multiple forms of ROY crystallise under the same conditions, and even concomitantly from the same sample, many more repeats are required to establish whether the differences in polymorphism observed are statistically significant. The stochastic nature of the crystallisation of ROY from solution is well documented.[155, 268] In one study a solution of ROY evaporated from 10,000 500 μm gold islands on a single plate produced six out of the seven stable forms of ROY.[273]

6.3 Conclusion

Incorporating specific functionalities into low molecular weight gelators offers an interesting new approach to influencing crystallisation. A variety of functional groups, mimicking those of pharmaceutical compounds, were successfully incorporated into bis-urea molecules. The presence of sterically bulky groups or competing hydrogen bonding functionalities prevented gel formation in some cases. However, a number of the compounds were found to form gels in a variety of solvents showing that such groups can be incorporated in principle. The aromatic spaced gelators showed particularly strong gelation behaviour with a number of different end groups. Investigations were undertaken into the influence of different gelators on the polymorphism of ROY but proved inconclusive due to the large number of stable polymorphs at room temperature. More detailed studies into the effect of crystallising pharmaceutical compounds from different LMWGs and into interactions between crystals and gel fibres are required to establish the utility of this approach.

6.4 Experimental section

6.4.1 Source of compounds

Compound MOP 133 was synthesised by Dr Marc Piepenbrock. Compound **38** was synthesised by Masters student Gary Cameron under the supervision of Jonathan Foster.[269] Compound **5** was originally synthesised by Jonathan as part of work submitted for assessment as part of his Masters thesis.[179]

6.4.2 Synthesis

Instrumentation and general procedures for the analysis of compounds and gels are as described in the experimental section of Chapter 2. ROY was kindly provided by Dr Sharon Cooper. Other drug compounds and all solvents and reagents were obtained from standard commercial sources.

N-[6-(benzo[b][1]benzazepine-11-carbonylamino)hexyl]benzo[b][1]benzazepine-11-carboxamide (**39**)

Dibenz[b,f]azepine-5-carbonyl chloride (95%) (1.00 g, 3.9 mmol, fibrous green solid) was dissolved in chloroform (30 ml) in an ice bath to produce a light green solution. Addition of 1,6- diamino hexane (0.22 g, 1.9 mmol) and triethylamine (0.40 g, 3.9 mmol) dropwise over 30 mins produced an orange solution. The reaction was allowed to proceed at room temperature for two hours and a white crystalline precipitate formed. The solution was filtered and the precipitate identified as 1,6-diamino hexane hydrochloride salt by NMR spectroscopy. The organic layer was washed twice with water, dried with $MgSO_4$, filtered and reduced under vacuum to produce a pink gum. After 1 hour under vacuum in a drying pistol (110°C) a green solid was produced. The solid was washed then recrystallized from toluene to produce a white powder which was dried in a heating pistol for 30 minutes (0.233 g, 0.42 mmol, 22%). ^{1}H NMR (500MHz, DMSO-d_6, *J*/Hz): 7.45 – 7.40 (4 H, m, Ar-H), 7.39 – 7.36 (2 H, m, ArH), 7.35 – 7.30 (2 H, m, ArH), 6.96 (2 H, s, C<u>H</u>), 5.35 (1 H, t, *J* 5.8, N<u>H</u>CH_2), 2.86 (2 H, q, *J* 6.5, NHC<u>H</u>$_2$), 1.22 (2 H, t, *J* 7.1, $NHCH_2C$<u>H</u>$_2$), 1.10 – 0.97 (2 H, d, *J* 3.8, CH_2CH_2C<u>H</u>$_2$). ^{13}C{^{1}H} NMR (126MHz, DMSO-d_6),156.17 (s, <u>C</u>O), 141.06 (s, Ar<u>C</u>), 135.67 (s, ArC), 130.94 (s, <u>C</u>H), 129.97 (s, Ar<u>C</u>H), 129.96 (s, Ar<u>C</u>H) 129.86 (s, Ar<u>C</u>H), 40.87-39.60 (s, under DMSO multiplet, NH<u>C</u>H_2), 30.24 (s, $NHCH_2$<u>C</u>H_2), 26.54 (s, CH_2CH_2<u>C</u>H_2). m/z (ES^+-MS): 577.294 ([M+Na], 100%), 555.342 ([M+H], 51.69%) CHN expected $C_{36}H_{34}N_4O_2$: C, 77.95; H, 6.18; N, 10.10. Found: C, 77.26; H, 6.02; N, 9.70.

Crystal data for **39:** $C_{43}H_{42}N_4O_2$, M =646.81, clear colourless plate, 0.3 x 0.2 x 0.01 mm^3, triclinic space group $P\bar{1}$ (No. 2), V = 853.55(10) Å^3, Z = 1, D_c = 1.258 g/cm^3, F_{000} = 344, Bruker SMART CCD 6000 area detector, MoKα radiation, λ = 0.71073 Å, T = 120K, $2\theta_{max}$ = 55.0°, 10606 reflections collected, 3917 unique (R_{int} = 0.0727). Final *GooF* = 0.985, R_1 = 0.0539, wR_2 = 0.147, R indices based on 1928 reflections with $I > 2\sigma(I)$ (refinement on F^2), 255 parameters, 0 restraints. Lp and absorption corrections applied, μ = 0.078 mm^{-1}.

Methyl (2S)-2-[[4-[[3,5-diethyl-4-[[(1S)-1-[(4-hydroxyphenyl)methyl]-2-methoxy-2-oxo-ethyl]carbamoylamino]phenyl]methyl]-2,6-diethyl-phenyl]carbamoylamino]-3-(4-hydroxyphenyl)propanoate (**41**)

Tyrosine methylester hydrochloride (6.39 g, 27.5 mmol) and triethylamine (3 g) were dissolved by heating under reflux in chloroform (500 ml). 4,4′ methylenebis(2,6-diphenylisocyanate) (5g, 13.7 mmol), dissolved in chloroform (20 ml) was added and the mixture heated under reflux for 24 hours. Upon cooling the precipitate was filtered, washed with chloroform and dried. NMR indicated the product contained triethylamine so the solid was ground and washed with water (50 ml) by sonication for 1 hour at 60 °C. The product was filtered and dried in a heating pistol to give a white solid (8.7053 g, 11.56 mmol, 84%) ^{1}H NMR (600MHz, DMSO-d$_6$, *J*/Hz): 9.21 (1 H, s, ArOH), 7.5 (1 H, s, ArNH), 6.94 (2 H, s, Ar<u>H</u>), 6.88 (2 H, s, Ar<u>H</u>), 6.70 – 6.60 (1 H, m), 6.36 (1 H, s, ArN<u>H</u>), 4.37(2 H, d, *J* 6.4, C*<u>H</u>), 3.77 (1H, s, ArC<u>H</u>$_2$Ar), 3.58 (3 H, s, OC<u>H</u>$_3$), 2.85 (1 H, d, *J* 24.8, C*C<u>H</u>$_2$), 2.41 (4 H, d, *J* 6.5, C<u>H</u>$_2$CH$_3$), 1.02 (6 H, t, *J* 7.5, CH$_2$C<u>H</u>$_3$). ^{13}C{^{1}H} NMR (151 MHz, DMSO-d$_6$) 173.28 (s, <u>C</u>OOH), 156.47 (NH<u>C</u>O), 142.22 (s, Ar<u>C</u>), 139.63 (s, Ar<u>C</u>), 132.62 (s, Ar<u>C</u>), 130.52 (s, Ar<u>C</u>), 127.34 (s, Ar<u>C</u>), 126.59 (s, Ar<u>C</u>), 115.47 (s, Ar<u>C</u>),54.63 (s, <u>C</u>*), 52.09 (s, O<u>C</u>H3), 41.15 (Ar<u>C</u>H$_2$Ar), 37.25 (s, C*<u>C</u>H$_2$), 24.82 (s, <u>C</u>H$_2$CH$_3$), 15.10 (s, CH$_2$<u>C</u>H$_3$). m/z (ASAP$^+$-MS): 499.9 (100%) CHN expected $C_{43}H_{52}N_4O_8$: C, 68.60; H, 6.96; N, 7.44. Found: C, 65.61; H, 6.97, N; 7.04.

1-(2-nitrophenyl)-3-[6-[(2-nitrophenyl)carbamoylamino]hexyl]urea (**42**)

1,6 diamino hexane (0.35 , 3.046 mmol) dissolved in chloroform (20 ml) was added dropwise to a solution of 2-nitrophenyl isocyanate (1 g, 6.093 mmol) in chloroform (20 ml). A bright yellow precipitate rapidly formed from the solution which was stirred for a further hour at room temperature. The precipitate was filtered, washed with DCM and dried in a heating pistol for 10 minute to give the product as a bright yellow solid (1.3 g, 2.99 mmol, 84%). ^{1}H

NMR (600MHz, DMSO-d_6, *J*/Hz): 9.30 (1 H, s, ArN<u>H</u>), 8.30 (1 H, dd, *J* 8.6, 1.3, Ar<u>H</u>), 8.02 (1 H, dd, *J* 8.6, 1.3, Ar<u>H</u>), 7.60 (1 H, ddd, *J* 8.7, 7.2, 1.6, Ar<u>H</u>), 7.48 (1 H, t, *J* 5.0, N<u>H</u>), 7.08 (1 H, ddd, *J* 8.4, 7.2, 1.3, Ar<u>H</u>), 3.08 (2 H, td, *J* 6.9, 5.4, NHC<u>H</u>$_2$), 1.44 (2 H, p, *J* 6.7, NHCH$_2$C<u>H</u>$_2$), 1.36 – 1.27 (2 H, m, CH$_2$CH$_2$C<u>H</u>$_2$). ^{13}C{^{1}H} NMR (151 MHz, DMSO-d_6): 154.63 (s, CO), 137.09 (s, Ar<u>H</u>), 136.47 (s, Ar<u>H</u>), 135.39 (s, ArH), 125.72 (s, Ar<u>H</u>), 122.30 (s, Ar<u>H</u>), 121.64 (s, Ar<u>H</u>), 40.87-39.60 (s, under DMSO multiplet, NH<u>C</u>H$_2$), 29.79 (s, NHCH$_2$<u>C</u>H$_2$), 26.56 (s, CH$_2$CH$_2$<u>C</u>H$_2$). CHN expected $C_{20}H_{42}N_4O_6$: C, 54.05; H, 5.44; N, 18.9. Found: C, 52.59; H 5.24; N: 13.19.

1-[4-[[3,5-diethyl-4-[(2-nitrophenyl)carbamoylamino]phenyl]methyl]-2,6-diethyl-phenyl]-3-(2-nitrophenyl)urea (**43**)

2-Nitrophenylisocyanate (5g, 30.47 mmol) and 4,4 methylenebis(2,6 diethylanilene) (4.729 g, 15.23 mmol were dissolved in chloroform (100 ml) and stirred at room temperature. A gelatinous precipitate rapidly formed but the mixture was heated under reflux for 18 hours. The reaction mixture was cooled, filtered, washed with chloroform (2 x 25 ml) and diethylether then dried in a heating pistol for 10 minutes. The solid was ground to give **36** as a fine yellow powder (8.3 g, 12.99 mmol, 85.3 %). δ_H (600 MHz, $CDCl_3$) 9.56 (1 H, s, NO_2ArN<u>H</u>), 8.70 (1 H, d, *J* 8.2, Ar<u>H</u>), 8.02 (1 H, d, *J* 7.9, Ar<u>H</u>), 7.52 (2 H, t, *J* 7.8, Ar<u>H</u>), 7.03 (4 H, s, Ar<u>H</u>), 6.96 (2 H, t, *J* 7.8, Ar<u>H</u>), 5.99 (1 H, s, ArN<u>H</u>), 3.99 (2 H, s, ArC<u>H</u>$_2$Ar), 2.60 (8 H, dd, *J* 29.2, 6.5, C<u>H</u>$_2$CH$_3$), 1.10 (12 H, t, *J* 7.5, CH$_2$C<u>H</u>$_3$). δ_C (151 MHz, $CDCl_3$) 143.35(s, <u>C</u>OO), 135.76 (s, Ar<u>C</u>H), 135.55 (s, N<u>C</u>O), 128.3 (s, Ar<u>C</u>H), 121.62 (s, Ar<u>C</u>H), 121.12 (s, Ar<u>C</u>H), 41.64 (s, Ar<u>C</u>H$_2$Ar), 24.82 (s, C<u>H</u>$_2$CH$_3$), 14.80 (s, CH$_2$C<u>H</u>$_3$) m/z (ASAP$^+$-ms, 350°C): 474.2 (M-CONHPhNO_2, 100 %), 336.3 (75 %), 307.2 (50 %), 620.2 (15%) CHN expected $C_{35}H_{38}N_6O_6$: C, 65.82; H, 6.00; N, 13.16. Found: C, 65.47; H, 5.97; N,13.19,

Methyl (2S)-2-[[4-[[4-[[(1S)-1-benzyl-2-methoxy-2-oxo-ethyl]carbamoylamino]-3,5-diethyl-phenyl]methyl]-2,6-diethyl-phenyl]carbamoylamino]-3-phenyl-propanoate (**44)**

Phenylalanine methyl ester hydrochloride (0.50 g, 2.32 mmol) was dissolved in 20 ml of chloroform and an excess of triethylamine added. 4,4′-methylenebiz(2,6-diethylphenylisocyanate) (0.42 g, 1.16 mmol) in 20 ml chloroform solution was added dropwise and the reaction was then left stirring at 70°C for 18 hours. The solution was washed with water and the product isolated by removing the solvent on a rotary evaporator. **38** was isolated as a white powder (0.42 g, 0.58 mmol, 50 %): ^{1}H NMR (500 MHz, DMSO-

d_6, *J*/Hz): 7.54 (2H, s, ArN<u>H</u>), 7.33-7.24 (10 H, m, Ar<u>H</u>), 6.90 (4H, s, Ar<u>H</u>), 6.49 (2H, s, CHN<u>H</u>), 4.49-4.44 (2H, m C<u>H</u>), 3.79 (2H, s, ArC<u>H_2</u>Ar), 3.61 (6H, s, OC<u>H_3</u>), 2.99 (4H, d, *J* 9.8, CHC<u>H_2</u>Ar), 2.44-2.39 (8H, m, ArC<u>H_2</u>), 1.03 (12H, t, *J* 7.4, CH_2C<u>H_3</u>). ^{13}C NMR{^{1}H} (126 MHz, DMSO-d_6, *J*/Hz): 173.5 (s, <u>C</u>OO), 156.7 (s, NH<u>C</u>O), 142.5 (s, Ar<u>C</u>), 139.9 (s, Ar<u>C</u>), 145.0 (s, Ar<u>C</u>), 137.8 (s, Ar<u>C</u>), 128.9 (s, Ar<u>C</u>), 127.2 (s, Ar<u>C</u>), 126.9 (s, Ar<u>C</u>), 54.7 (s, <u>C</u>H), 52.4 (s, O<u>C</u>H3), 41.4 (s, Ar<u>C</u>H_2Ar), 25.1 (s, Ar<u>C</u>H_2CH_3), 15.4 (s, $ArCH_2$<u>C</u>H_3). m/z (ES^+-MS): 102.2 $(Et_3N+H]^+$, 100%, 822.6 $([M+Et_3N]^+$, 42 %), 823.6 $([M+Et_3N]^+$, 30%). Anal. calc'd for $C_{43}H_{52}N_4O_6$: C, 71.64; H, 7.27; N, 7.77 %. Found: C, 71.29; H, 7.30; N, 7.70 %.

Chapter 7: Can supramolecular gels be used as part of an industrial polymorph screening procedure?

7.1 The importance of crystal form in the pharmaceutical industry

Most pharmaceutical products are formulated as solids with the active pharmaceutical ingredient (API) in a crystalline state.[277] The success of a drug therefore depends not only on the structure of the drug molecule itself, but also how it packs together in the solid state. Polymorphism describes two or more crystalline phases with the same molecular composition but different crystal packing arrangements.[234] Different polymorphs can have very different physical properties such as habit, solubility, stability, colour and melting point. This dependence of properties on solid form is particularly important in the pharmaceutical industry where the solubility of different crystal forms impacts upon the bioavailability of a drug compound meaning conversion of one form to another can render a drug ineffective or dangerous.[278] Other properties such as crystal habit, density, hardness and compressibility can determine how easy to process and tablet a compound is and are important considerations in selecting a crystal form. Incorporation of solvent molecules into the crystal lattice gives rise to solvates (or hydrates in the case of water) and can also lead to differences in physical properties. Screening of drug compounds as salts[279] with different counter ions, or as co-crystals[280] by the incorporation of other neutral molecules has been used as an effective strategy for optimising the properties of API crystals. Amorphous solids, which lack long range order, are another possibility offering the advantage of high solubility, however there is a danger of physical instability and rearrangement to more stable crystalline forms.[281]

A classic case study into the costly effects of a previously unidentified polymorph emerging once a product has gone to market is that of the antiretroviral Ritonovir.[235] Originally marketed as gel-filled capsules containing a solution of Ritonovir, the emergence of a more stable, and less soluble, crystal form rendered the formulation unsafe and unmanufacturable.[282] As well as their physical implications, new crystal forms with ‘novel’ and ‘non-obvious’ properties can be patented.[283] This legal dimension means there are huge financial implications associated with the discovery, or failure to discover, new crystal forms. Different polymorphs or co-crystals can also provide patenting opportunities, and a possible means of designing around the existing rights of other companies.[278]

For these reasons, considerable investment has been made by pharmaceutical companies into ensuring that all crystal forms have been identified and that the solid state behaviour of an API is well understood. A collaboration with GlaxoSmithKline was developed which led to a month long industrial placement in their Particle Science group in Stevenage. The placement initially lasted three weeks and was followed a month later by a shorter stay of three days. The objective of the visit was to identify the feasibility and utility of incorporating crystallisation from LMWGs into the early polymorph screening procedures undertaken at GSK.

7.2 Methodological Development

A wide range of crystallisation procedures are undertaken at GSK Stevenage by the particle science group in order to characterise the polymorphic behaviour of candidate drug compounds. Pertinent to this investigation are cooling crystallisations undertaken as part of polymorph screens. Software is used to assist in the generation of 96 different combinations of solvents based on solubility data from a preliminary screen of the drug compound. The drug and solvent combinations are then automatically dispensed into ninety six well arrays and the compound slurried at a set temperature to create saturated solutions. After filtration to remove undissolved solid, the solutions cooled either to room temperature, or to 4^{o}C in a fridge. Once crystallisation has taken place, the crystals are filtered and characterised either by Raman spectrosocpy or XRPD in order to identify the crystal form. The whole process is highly optimised with automation used where possible and with each stage anticipating the requirements of the next. The approach is high-throughput and, combined with other routes, probes a wide range of crystallisation conditions in a systematic and reproducible way.

The aim of this project is to adapt the process in order to develop a screening procedure for crystallisation from supramolecular gels. The specialist equipment available also provides an excellent opportunity to test the influence of the gel phase on crystallisation from a wide range of conditions. Preliminary studies set out to establish what equipment, gelators and APIs would be best to use for further studies.

7.2.1 Compound selection

A number of candidate drug compounds were made available by GSK for use in the study. Due to commercial sensitivities these compounds will be refered to as **GSKA**-**E**. Preliminary

experiments involving **GSK-A** and **GSK-B** are described in section 5.5. **GSK-C** has been used by a number of other groups so the compound used in this study is designated **GSK-D** for consistency. **GSK-D** crystallises readily and has three non-solvated crystal forms and two solvates making it an interesting system for further investigation. **GSK-E** is formulated as a salt and the tosylate, mesylate, citrate and hydrochloride API salts were available for testing.

7.2.2 Gelator selection

The high throughput screening procedure outlined in Section 7.2 endeavours to create suitable and diverse crystallisation conditions for the candidate drug compound using mixtures of solvents. Ideally only one or a small number of gelators should be required to form gels in the full range of solvents. The amount of gelator required to gel a given solvent combination would also ideally be standardised to simplify screening procedures. The gels should also be able to form in the presence of all (or at least most) drug compounds which can vary enormously in their functionality and reactivity. However, most LMWGs require very specific conditions (solvent, gelator concentration, heating profile) and the gelator may be disrupted by the presence of some drug compounds.

Gel formation is usually achieved by heating the solid gelator in a solvent using a heat gun until it is fully dissolved with the gel forming upon cooling of the solution to room temperature. In order to scale up the crystallisation process, rather than heating each vial individually, blocks of vials are heated collectively. However, many of the gelators developed within the Steed group require high temperatures to fully dissolve, in some instances above that of the boiling point of the solvent. Great care is therefore required when collectively heating samples. Solvents with boiling points of less than 50°C were treated separately and only exposed to high temperatures for short periods of time. Samples were heated in HPLC vials sealed with silicone caps. It is important to ensure the caps form a good seal to the vials otherwise the solvent evaporates upon heating. It is not possible to insert needles into the vials as the build-up of pressure is necessary to prevent evaporation of the solvent at the high temperatures required to dissolve the gelator. Great care must therefore be taken whilst heating the samples.

The equipment used to heat the blocks of vials in the slurrying experiments has a maximum heating temperature of 60°C, well below that required to dissolve most of the gelators. Temperature controlled reactor blocks with 48 wells were available which could reach

temperatures of approximately 120°C or 150°C. This is well below the approximately 400°C heating range of a heat gun. The cooling rate of the equipment was also limited to 5°C/min which proved detrimental to gel formation in some instances.

Preliminary studies were undertaken into gel formation in eight different solvents by five different gelators. Initially a standard gelator concentration was used for all samples of 0.5 % w/v with 1 ml of solvent used. The samples were heated and the solubility at 5°C intervals was noted. Once the maximum temperature of 120°C had been reached, the samples were cooled in the block at ~5°C/min. The temperature at which the gelator dissolved and the phase of the mixtures upon cooling are recorded in Table 21.

Phenylalanine derived hexylene spaced gelator **20** proved the most soluble, but only forms gels in one of the solvents under the conditions tested. Alanine derived hexylene spaced gelator **17** is less soluble but forms partial gels in four of the solvents tested. Phenylalanine derived diphenylmethane spaced compound **44** is poorly soluble in most of the solvents but nevertheless forms strong clear gels in all solvents apart from toluene where a partial gel is formed. ROY mimic compound **43** forms strong gels in some mixtures but is poorly soluble in toluene and chlorobenzene and highly soluble in THF. Compound **41** is poorly soluble in most of solvents except THF with insoluble material forming a crust on the surface of the solvent.

The concentrations of the gelators in the different solvents were adjusted on the basis of this data and the experiment was rerun (Table 22). Whilst the higher concentrations of compound helped ensure gel formation in some cases, e.g. **20** in ethylacetate or **17** in acetonitrile, this was not always sufficient to ensure gel formation. In some cases homogeneous gels failed to form in compositions where they have previously been shown to form with the aid of fast cooling and sonication. Compound **41** produced gels in five of the solvents, but with undissolved material remaining at 120°C in three of them. Compound **44** was observed to consistently form strong clear gels at 0.2 % w/v across all of the solvents tested and was therefore selected for further studies.

Table 21 Temperature at which 0.5 wt% of gelator dissolved (T_s) in various solvents and phase upon cooling to 20°C.

Gelator / Solvent	20		17		44		41		43	
	T_s(°C)	Phase (20°C)	T_s(°C)	Phase (20°C)	T_s(°C)	Phase (20°C)	T_s(°C)	Phase (20°C)	T_s(°C)	Phase (20°C)
Acetone	70	S	90	PG	>120	G[c]	105	G	95	PG
Acetonitrile	90	S	90	PG	120[a]	G	105[a]	G	>120 [b]	G[b]
THF	80	S	90	PG	90	G	85	S	85	S
EtOAc	90	P	120[a]	P	>120	G[c]	>120	G[c]	>120 [b]	PG
Toluene	115	G	>120	PG	>120	PG[c]	>120	P	120[a]	PG
Ethanol	85	S	60	S	>120	G	95	PG	>120[b]	P
Propan-2-ol	85	S	85	S	>120	G	105	PG	>120 [b]	PG[b]
Chlorobenzene	105	P	120[a]	P	>120	G	>120	I	120	PG

S = solution, P= precipitate, G= Gel, PG= Partial gel, (a) all dissolved except small amounts of undissolved material remained, (b) Crust of undissolved material developed on surface of solvent (c) contains precipitate belonging to undissolved material.

Table 22 Phase of gelator at 120°C and at 20°C in various solvents at different concentrations of gelator

Gelator / Solvent	20			17			44			41			43		
	Gelator wt%	Phase at		Gelator . wt%	Phase at		Gelator . wt%	Phase at		Gelator . wt%	Phase at		Gelator . wt%	Phase at	
		120°C	20°C		120°C	20°C		120°C	20°C		120°C	20°C		120°C	20°C
Acetone	1	S	S	1	S	PG	0.2	S	G	0.5	S	G	-	-	-
Acetonitrile	1	S	P	1	S	G	0.2	S[a]	G	0.5	S	G	0.2	S	PG
THF	1	S	S	1	S	PG	0.2	S	PG	1	S[a]	S[a]	-	-	-
EtOAc	1	S	G	1	S[a]	PG	0.2	S[a]	G	1	I	G	1	I	G
Toluene	0.5	S	G	1	I	G	0.2	S	G	-	-	-	-	-	-
Ethanol	-	-	-	-	-	-	0.2	S	G	1	S[a]	G	-	-	-
Propan-2-ol	-	-	-	-	-	-	0.2	S	G	1	S[a]	G	-	-	-
Chlorobenzene	-	-	-	-	-	-	0.2	S	G	-	-	-	1	I	G[a]

G= Gel, PG= Partial gel, (a) small amounts of undissolved material remained

7.2.3 Gelation Screen of compound 44

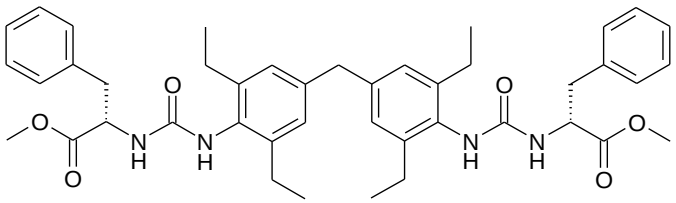

44

Compound **44** was originally synthesised by Masters student Gary Cameron as part of his Masters studies under the supervision of Jonathan Foster. The compound was identified as forming robust, clear gels in an unusually wide range of solvents. In order to establish just how versatile a gelator **44** is, it was screened for gelation behaviour in as wide a range of solvents as possible. Compound **44** (5 mg) was dispensed into crimp-top vials and 0.5 ml of solvent (1 % w/v gel) was dispensed by hand into the vials using a pipette. The samples were heated to an arbitrary temperature using a heat gun until all solids had dissolved where possible. In some instances sonication was used to aid dissolution. The samples were then cooled on the bench at room temperature. Table 23 records the results of these experiments.

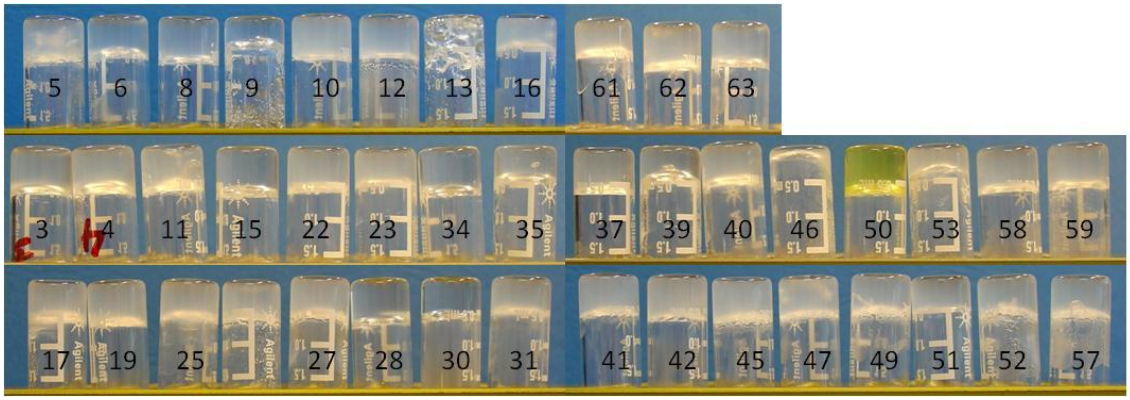

Figure 119 Photographs of gels of **44** in various solvents; numbers refer to solvents described in Table 23

Table 23 Test for solubility and gelation behaviour of **44** in different solvents

	Solvent	Type	% w/v	Hot	20°C
1	Water	Water	1	I	I
2	Methanol	Alcohol	1	S	G
3	2-Methoxyethanol	Alcohol	1	S	G
4	1-Propanol	Alcohol	1	S	G
5	Nitromethane	Nitro	1	S	G
6	Acetonitrile	Nitrile	1	S	G
7	Dimethyl sulfoxide	Sulfoxide	5	S	G
8	Acetone	Ketone	0.1	S	G
9	2-Butanone	Ketone	0.2	S	G
10	Dichloromethane	CHC	1	S	G
11	Methyl actetate	Ester	1	PS	G
12	Methylisobutyl ketone	Alcohol	1	S	G

	Solvent	Type	% w/v	Hot	20°C
13	Chloroform	CHC	1	S	G
14	Ethyl acetate	Ester	0.1	S	G
15	Chlorobenzene	Aryl Halide	1	S	G
16	Tetrahydrofuran	Ether	0.1	S	G
17	1,4-Dioxane	Ether	1	S	G
18	Diethyl ether	Ether	1	I	I
19	Toluene	Aromatic	0.1	S	G
20	Cyclohexane	HC	1	I	I
21	Heptane	HC	1	I	I
22	1-butanol	Alcohol	1	S	G
23	2-Propanol	Alcohol	0.2	S	G
24	Trifluoroethanol	Alcohol	1	S	S
25	Dimethyl carbonate	Carbonate ester	1	S	G
26	Formamide	Amide	1	S	P
27	Carbon disulphide	Sulfide	1	PS	G
28	Ethanol	Alcohol	0.1	S	G
29	Acetic acid	Acid	5	S	G
30	3-Methyl-1-butanol	Alcohol	1	S	G
31	N,N-dimethylacetamide	Alkyl amide	1	S(cold)	S
32	1-Methyl-2-pyrrolidininone	Lactam	10	S	G
33	Pyridine	Amine	1	S	S
34	Anisole	Amine	1	S	G
35	Tetrachloroethylene	PCC	1	S	G
36	Hexane	HC	1	I	I
37	1-Pentanol	Alcohol	1	S	G
38	Pentane	HC	1	I	I
39	p-Xylene	Aromatic	1	S	G
40	2-methyl-1-propanol	Alcohol	1	S	G
41	2-butanol	Alcohol	1	S	G
42	Isopropyl acetate	Ester	1	S	G
43	Isopropyl ether	Ether	1	I	I
44	N,N-dimethyl formamide	Amide	5	S	G
45	1,2-Dimethoxyethane	Ether	1	S	G
46	Ethylene glycol	Alcohol	1	S	G
47	Isobutyl acetate	Ester	1	S	G
48	Methylcyclohexane	HC	1	I	I
49	Benzonitrile	Nitrile	1	S	G
50	Nitrobenzene	Nitro	1	S	G
51	Benzyl-alcohol	Alcohol	1	S	G
52	2-Pentanol	Alcohol	1	S	G
53	Cyclopentyl methyl ether	Ether	1	PS	G
54	2-Methyl-2-butanol	Alcohol	1	S	G
55	2-Pentanone	Ketone	0.2	S	PG
56	Butyronitrile	Nitrile	0.2	S	G
57	diisobutyl ketone	Ketone	0.2	I	I
58	1-Hexanol	Alcohol	1	S	G
59	1-Heptanol	Alcohol	1	S	G
60	1-Octanol	Alcohol	1	S	PG
61	3-Methyl-2-butanol	Alcohol	1	S	G
62	2-Ethyl-1-hexanol	Alcohol	1	S	G
63	Diethylene glycol dimethyl ether	Ether	1	S	G
64	Cyclohexanone	Ketone	0.5	S	G
65	Cyclopentanone	Ketone	0.5	S	G
66	Benzene	Aromatic	0.2	S	G
67	Ethyl formate	Ester	0.2	S	G
68	Diisopropyl ether	Ether	1	I	I
69	Trifluoroacetic acid	Acid	1	S	S

HC = hydrocarbon, CHC = chlorohydrocarbon, S = soluble/solution, PS= partially soluble, I = Insoluble G= Gel, PG= Partial Gel, P = precipitate.

The gels formed were typically highly transparent and example images are shown in Figure 119. Of the sixty nine solvents investigated, strong gels form in fifty two of the systems with partial or weak gels forming in a further two. The compound remained as a solution upon cooling at the concentrations tested in seven cases and was insoluble in nine solvents. In one case (formamide) a non-gelling precipitate formed from solution. Formamide is known to decompose upon heating and it is not known if this was responsible for the precipitate.

In order to form a gel, the compound must dissolve in the solvent at high temperature, but come out of solution as a gel at low temperature. Compound **44** is poorly soluble in highly apolar solvents such as ethers and hydrocarbons. The low boiling point of these solvents further limits their potential to dissolve the gelator. Compound **44** is highly insoluble in water but tends to be highly soluble in polar aprotic solvents such as DMSO, DMF, NMP and DMAc with 1 % w/v of gelator dissolving at room temperature without heating. Gels were formed using higher concentrations of **44** in DMSO (5 % w/v), DMF (5 % w/v) and NMP (10 % w/v). The solvents are strong hydrogen bond acceptors so are likely to compete strongly with the carbonyl of the urea inhibiting urea tape formation.[38] Adding small amounts of anti-solvents such as water or alkanes reduces the solubility of the gelator and induces gel formation at lower concentrations. Acetic acid and pyridine were also found to fully dissolve **44** at room temperature, as was trifluoroethanol. This was found to be due to high solubility rather than pH with gels forming in acetic acid at 5 % w/v. Gels also form in acetone with trifluoroacetic acid or triethylamine added to give solutions ranging from pH 1-9 and weaker gels form between pH 9-11.

Compound **44** is able to reliably form gels in the presence of a diverse array of functionalities including: alcohols, esters, aromatics, chlorohydrocarbons, ketones, nitrile and nitro compounds. Gels may still be formed in the presence of non-gel forming solvents and solubility appears to be key the key factor in determining gel formation.

7.2.4 Binary Solvent Mixtures

At GSK, binary mixtures of solvents are used as part of solution based studies in order to create varied conditions which match the solubility of the API. Based on experimental solubility data of **GSK-D** in a number of solvents, solubility prediction software[284] was used to create ninety six binary mixtures of solvents in which a reasonable amount of **GSK-D** was

soluble at high temperature and insoluble at the lower temperature. The results of the crystallisation experiment are discussed in detail in sections 7.3 and 7.4.

Compound **44** was tested for gelation behaviour in the ninety six different solvent combinations used in the study in the absence of drug compound. A low concentration of gelator, 0.2 % w/v, was selected in order to ensure dissolution of the gelator below 120°C in as many solvents as possible. Compound **44** (2 mg) was automatically dispensed into ninety six vials and 1 ml of solvent mixture added. The vials were transferred to a thermostatically controlled heating block and heated to 120°C. In some cases sonication was used to help dissolve the gelator. Once the gelator was fully dissolved, the vials were cooled to room temperature then in a fridge to test for gelation behaviour. A summary of the results are provided in Table 23 and full details are given in Table 30 which can be found in the experimental section.

Of the ninety six solvent combinations studied during cooling from 120°C to room temperature, seventeen form gels at 0.2 % w/v from a clear solution, a further seventeen form partial gels, thirty seven remain as solutions and two form precipitates. In sixteen cases the compound did not fully dissolve at high temperatures but of these mixtures six still formed gels and ten more formed partial gels. In six solvent mixtures the sample was unchanged upon heating or after cooling with the gelator remaining insoluble throughout. Refrigerating the samples strengthened two of the weak gels so that they were fully self-supporting and induced gelation from solution in one case and partial gelation in five other samples.

The binary study again demonstrates the importance of solubility, rather than the presence of particular functional groups or solvent properties, in enabling gel formation. Gels formed in the presence of high concentrations of anti-solvents such as water, diethyl ether and cyclohexane. Indeed, the presence of anti-solvents enabled gel formation from solvents where the compound was highly soluble. Increasing the concentration of gelator to 0.5 or 1 % w/v may aid gel formation in cases where solutions or only partial gels formed. This has been seen experimentally for example in chloroform where **44** remains soluble at 0.2 % w/v but forms gels at 1 % w/v. Decreasing the concentration may help in cases where the compound didn’t dissolve at 120°C but formed gels or partial gels. Being able to heat to higher

temperatures would also increase the solubility of the gelator in all samples enabling gelation in a greater range of solvent mixtures at a higher standard concentration.

Figure 120 Photograph showing 0.2 % w/v **44** in different binary solvent mixtures.

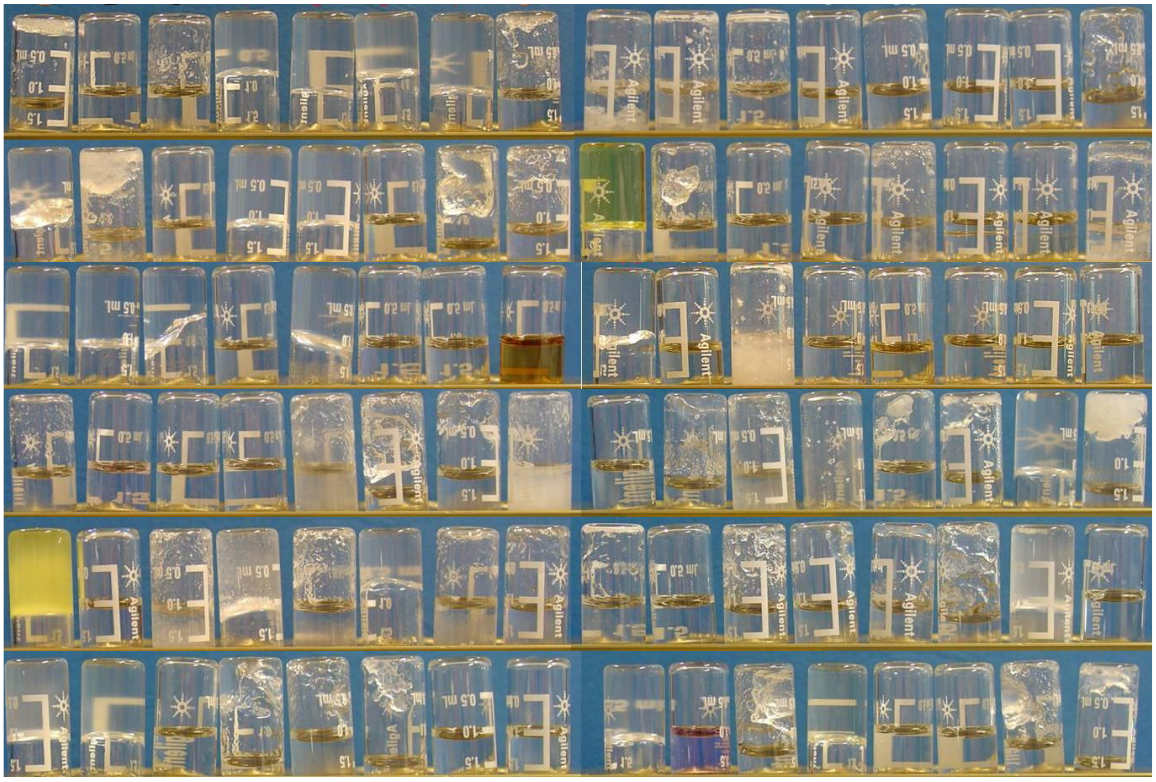

Table 24 Summary of phase transitions in the various solvent systems with 0.2 % w/v gelator **44** going from 120-5°C

Transition	S-G	S-PG	S-S	S-P	PS-G	PS-PG	I-I
120-20°C	17	17	37	2	6	10	6
120-5°C	19	21	31	2	6	10	6

S= clear solution, PS= Small amounts of insoluble material remained, I= larger amounts of insoluble material remained, S(cold)= soluble without heating at 20°C, P= precipitate, G=Gel, PG=Partial gel

7.2.5 Conclusion

The low solubility of **44** is essential to its success in forming gels in a wide range of solvents at a low concentration. However, the same low solubility also means it is difficult to ensure complete dissolution of even low concentrations of the gelator at 120°C. Being able to heat to higher temperatures and pressures would allow uniformly higher concentrations of gel to be used, but presents safety and equipment issues. Another issue is the thermal stability of the drug compounds being tested which are likely to react or degrade at high temperatures. One solution would be to modify the solubility prediction software to select only solvent/gel

combinations which were compatible with gel formation at moderate temperatures whilst still maintaining a diverse range of environments. Ultimately, issues with solubility are likely to be a limiting factor in the utility of using thermally formed LWMGs and a different approach may be required (see section 7.5).

7.3 GSK-D study low temperature (20°C-5°C)

Following preliminary investigations **GSK-D** was selected for use in crystallisation studies. Characterisation of this compound from the solution phase had already been undertaken by GSK and the aim of this investigation was to mimic that study and compare the results. In order to establish the influence of the gelator on crystallisation, it is desirable to follow the procedures used in the solution phase study as closely as possible. The procedure being replicated was the crystallisation of the API from saturated solutions of ninety six different solvent combinations at room temperature by cooling in a fridge. The experiment was scaled down and only forty eight of the solvent combinations were investigated. Thirty one solvent combinations were selected because crystallisation had been observed from these mixtures in the solution based screen in order to allow comparison of the resulting crystal forms. Solvents with boiling points of less than 50°C were excluded from the screen. The remaining binary-solvents were selected because it was thought they were likely to form gels and because they represented a diverse range of conditions.

Saturated solutions were prepared using the same procedures as the solution based screen. An excess of API was dispensed into vials and a total of 1 ml for each of the ninety six solvents was dispensed into the vials. The samples were sealed and slurried for 24 hours at room temperature. After 24 hours the slurries were filtered into glass tubes.

In the solution based screen, the glass tubes were then refrigerated inducing crystallisation over a period of days to weeks. In the gel phase study, an automated solvent dispenser was used to transfer the saturated solutions into new vials containing a weighed amount of gelator (2 mg). The new vials were sealed, heated to 120°C until the gelator was fully dissolved and cooled to room temperature allowing the gels to form. Technical problems meant that the transfer of solution was not 100% efficient with most samples receiving approximately 0.7 ml of solvent but some as low as 0.1 ml of solvent and in one case none at all. The volume of

solution for crystallisation varied considerably and the concentration of gelator deviated significantly from 0.2 % w/v.

Table 25 Comparison of phase transition undergone by **44** in the absence and presence of GSK-D

Phase transition upon cooling (120-5°C)	**S-G**	**S-PG**	**PS-G**	**PS-PG**	**S-S**	**I-I**	**X**
0.2 % w/v **44**	12	12	3	6	13	2	-
+ **GSK-D**	15	1	10	1	15	3	3

S= clear solution, PS= Small amounts of insoluble material remained, I= larger amounts of insoluble material remained, S(cold)= soluble without heating at 20°C, P= precipitate, G=Gel, PG=Partial gel, X= sample failed.

Table 25 summarises the phase transitions which took place in both this study and in the absence of gelator. Twelve samples were found to completely gel where only partial gels had been obtained in the absence of **GSK-D** with 0.2 % w/v of gelator. It is possible that this strengthening of the gel is due to some supramolecular interaction of **GSK-D** molecules with the gel fibres or mechanical strengthening of the gel by the crystals. However, a more likely explanation is that incomplete transfer of the solvent resulted in increased gelator concentrations and so stronger gelation. Low volumes of solvent are also the most likely explanation for the eight additional cases where the compound did not dissolve. In two cases solutions were observed where partial gels had formed in the absence of the API. This may indicate a weak disruptive effect of **GSK-D** on the gelator in some solvent mixtures.

Once gelled, the samples were refrigerated and left to crystallise. After 24 hours crystals were observed in seventeen samples and after ~1 month crystals were observed in a further sixteen. The total of thirty four crystals obtained from gels is comparable with thirty five crystals obtained from solution. In ten cases, crystals were observed in the gel sample but not from solution and in eight from solution but not the gel. Of the samples in which crystals were observed, eleven corresponded to cases where strong gels had formed from clear solutions. One crystal was formed from a partial gel and seven were formed from a strong gel but where the gelator had not completely dissolved at 120°C. In ten cases crystals had grown from solution in samples where the gelator had dissolved but had not formed a gel and in one case where the gelator was insoluble.

Samples obtained previously during the solution phase screen were characterised by Raman spectroscopy using an automated procedure to isolate, characterise and cluster the results. The same procedure was followed for the gel samples with gel samples transferred for

filtration by hand using a glass pipette or spatula. Given the diversity of solvent mixtures being used, dissolution using anions was not attempted. Small amounts of gelator were therefore present in the samples being analysed, however this did not appear to cause any problems. During the first visit, technical difficulties during filtration meant insufficient sample was available for characterisation in a number of cases.

A second approach developed was to analyse the crystals *in situ*, in the gel, without filtering. The vial was inserted into the spectrometer on a stage which could be adjusted so that the Raman laser was aligned with an individual crystal suspended in the gel sample. Where crystals grew in the centre or on the surface of the sample they had to be isolated using a spatula and analysed on a glass slide. This approach allowed much smaller crystals to be analysed and crystals with different habits or grown in different environments (e.g. surface, above the gel, in the gel) to be analysed separately. In-situ analysis potentially allows polymorphic transitions to be monitored over time. However, this approach was less effective where the crystals were dispersed throughout the sample and the process would be less easy to automate as software is likely to struggle to distinguish between crystal and gel.

GSK-D is known to form three different polymorphs as well as solvates with DMSO, NMP and benzonitrile. Form 2 is the most stable at room temperature and form 1 the least stable. Heating of form 2 or form 3 to higher temperatures produces form 1. Slurrying of form 1 at room temperature produces form 2 or form 3 which eventually converts to form 2. The DMSO, benzonitrile and NMP solvates can be formed by addition of solvent to form 1. The non-solvated forms 1-3 and solvates can be readily distinguished by Raman spectroscopy with key peaks in the 3000-3400 cm^{-1} region. There are no significant peaks in this region in the Raman spectra for compound **44**. Mixtures containing DMSO were further checked for solvate formation by comparing the fingerprint region of spectra. In most cases overlap from solvent peaks did not prove problematic in identifying spectra, however in a number of cases there was insufficient material for the spectra to be assigned.

Table 26 Summary of samples where crystallisation took place in the gel

No.	Solvent (3:7)	Phase		Description		Crystal Form	
		120°C	0°C	Colour	Crystal Habit	Gel	Sol.
8	acetone:acetone	S	G	O	Fine needles, Plates above	2 and 3	UA
10	2-butanone:2-butanone	S	G	Y	Plate above	3	2
15	methyl acetate:2-methoxyethanol	S	G	O	Small needles	X	2
16	methyl acetate:1,2-dimethoxyethane	S	G	Y	Plate above	3	2
22	ethyl acetate:acetonitrile	S	G	O	Yellow needles	2?	-
27	tetrahydrofuran:nitromethane	S	G	Y	Cylinders	1	-
28	tetrahydrofuran:acetone	S	G	YO	Needles on surface	2	2
51	tetrachloroethylene:ethanol	S	G	OY	Needles from surface	1	2
61	2-butanol:toluene	S	G	YO	Needles above and below	1	2
87	cyclohexanol:isopropyl acetate	S	G	Y	Fine needle above	1	2
88	t-butanol:butyronitrile	S	G	O	Fine needle above	1	2
9	acetone:tetrachloroethylene	PS	G	Y	Plate above	3	2
11	2-butanone:methyl acetate	PS	G	Y	Long needles/plates	1/3 and 3	-
23	ethyl acetate	PS	G	Y	Blocks above	3	-
30	toluene:ethyl acetate	PS	G	Y	Mesh of needles	1	-
62	isopropyl acetate:methylisobutyl ketone	PS	G	Y	Yellow needles	1	-
71	methylcyclohexane:nitrobenzene	PS	G	Y	Clump of plates/needles	1	3
79	2-pentanone	PS	G	Y	Needles above	1	-
91	3-methyl-2-butanol:cyclopentyl methyl ether	PS	G	OR	Needles above	UA	2
5	2-methoxyethanol	S	PG	O	Needles	X	2
7	acetonitrile:chloroform	S	S	Y	Needles and plates	2	3
21	chloroform:chloroform	S	S	Y	Block above	2	3
25	chlorobenzene:dimethyl sulfoxide	S	S	Y	Mesh of needles	UA	DMSO
37	2-propanol:chloroform	S	S	Y	Cylinders	2	3
40	N,N-dimethylacetamide:anisole	S	S	O	Cylinders	2	
45	1-methyl-2-pyrrolidinone:acetic acid	S	S	O	Clump of needles above	1	UA
52	tetrachloroethylene:acetic acid	S	S	R	Long fine needles	1	UA
56	p-xylene:methanol	S	S	O	Needles above	UA	2
57	p-xylene:dimethyl sulfoxide	S	S	OY	Needles	UA	DMSO
89	2-ethyl-1-hexanol:chloroform	S	S	Y	Needles/plates	2	2
95	methanol:THF	S	S	O	Thick needles above	1	-
96	methanol:1-methyl-2-pyrrolidine	S	S	O	Blocks	2	-
78	2-pentanone:p-xylene	I	I	Y	Yellow needles	1	2

S= Solution, PS=Partially solution, I= Insoluble, G=Gel, PG= Partial Gel, O=orange, Y=yellow, R= Red, YO/OY/OR- colours inbetween, UA = unassigned.

GSK-D produced solutions of a variety of colours ranging from yellow and orange to red. The colours of different solutions are noted in Table 26 and Table 30. No correlation between solution colour and crystal form could be identified with crystals of all polymorphs being yellow in colour. There was some variation in the habit of crystals between the different forms. Form 3 tended to be plate like, form 2 thicker needles or blocks and form 1 finer

needles. Representative images of crystal habits are shown in Figure 121 although considerable variation was observed.

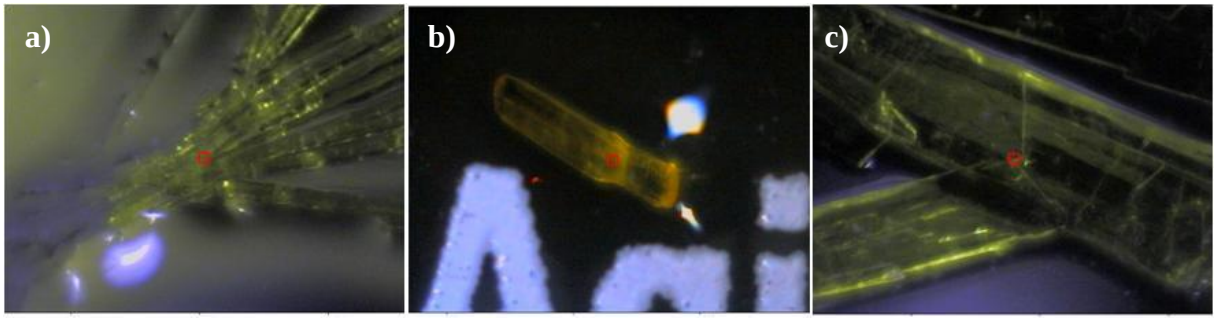

Figure 121 Images of **GSK-D** showing a) needles of form 1, b) blocks of form 2 c) plates of form 3.

Considerable differences in polymorphic behaviour of **GSK-D** were observed in the gel phase compared with solution. The correlation between crystal forms obtained from a particular solvent combination in the different screens is low with only one successfully assigned match. In the solution phase screen, form 2 was obtained from all systems apart from four cases where form 3 was obtained and two where the DMSO solvate was obtained. In the gel phase study by contrast, form 1 was obtained in fourteen cases with form 2 obtained nine times and form 3 six times.

The increase in the less thermodynamically stable form 1 in the gel screen could indicate some form of templation by the gel fibres or slowing of the rate of conversion to more stable forms. However, form 1 is also the most stable form at high temperatures and the gel phase samples had an additional step where they were heated to 120°C, possibly inducing nucleation of form 1. Within the gel phase study where all the samples were heated, form 2 was observed more often in samples that remained as solutions upon cooling than in those that formed gels. However, this could be due to differences in solvent mixtures and a repeat of the full solution phase study in which the samples are heated to 120°C would provide a fair test and allow direct comparison between samples.

A further complication in the analysis is that in some of the samples the crystals were observed growing either on the surface of the gel or on the glass of the vial above the gel. All of the reported plates of form 3 were found growing above the gel as were a number of crystals of form 1 and 2. This could be due to heteronucleation on impurities on the gel surface and walls occurring more readily than homonucleation in the gel phase. This would

indicate the gel is behaving as an inert environment. Because the crystals are not immersed in the solvent the rate of transformation to the more stable form 2 would be slowed compared with the solution phase study. This might further help explain the increased prevalence of the less stable forms.

7.4 GSK-D high temperature study (60°C- 20°C)

As part of routine polymorph screening procedures undertaken at GSK, a second solution based crystallisation study had been undertaken by cooling solutions saturated with **GSK-D** at 60°C to room temperature. The larger temperature gradient creates different growth conditions and can lead to different polymorphs. Unfortunately it was not possible to replicate this study using the procedure used for the lower temperature gel phase crystallisation study described in section 7.4. This is because the transfer and filtration of saturated solutions into vials containing pre-weighed gelator could only be undertaken at room temperature using the equipment available.

A second approach was therefore developed to allow a study using crystallisation from higher temperatures to room temperature. All 96 solvent combinations used in the low temperature solution based screen were used in this study. Both API and gelator were weighed directly into the same vial before solvent was added. The vial was then heated to 120°C until all material had been dissolved (where possible) then allowed to cool on the bench to room temperature.

The mass of API was selected to be either 10mg or 20mg depending on whether 40 or 60 milligrams respectively of compound had been used to create saturated solutions in the solution based screen. This approach had the advantage that it involved far fewer steps and so was much quicker than the previous method. It also enabled higher levels of supersaturation and faster rates of crystal growth to be achieved. Potential disadvantages of this approach are that the API may not fully dissolve at high temperatures or could crash out of solution upon cooling before the gel has fully formed. However, solvents are selected by solubility software[284] to ensure reasonable solubility of the API at room temperature and are then heated to 120°C meaning that low solubility is unlikely to be problematic. Preliminary studies showed that many of the gels form and are stable above 80°C, in some cases 120°C, and gels form very rapidly so premature crystallisation is also unlikely to be problematic.

The high temperature study of **GSK-D** was also designed with adjusted concentrations of gelator. For solvent combinations in which gels had formed successfully in the **44** gel screen, 0.2 % w/v of gelator was used again. Where the gelator was soluble at 120°C the amount of gelator was increased to 0.5 % w/v where partial gels formed upon cooling and to 1 % w/v where no gels formed. Where gels were formed but the compound did not fully dissolve a lower concentration of 0.1 % w/v was used. Other cases were judged individually.

These adjustments were found to have a positive impact upon the number of samples where the gelator fully dissolved at 120°C and in terms of gel formation. Of the ninety six gel solvent combinations, sixty formed gels with the adjusted concentrations compared to twenty five at 0.2 % w/v in the absence of drug compounds. No record was kept as to whether complete dissolution had taken place at 120°C for the first forty eight solvent combinations. Of the last forty eight samples where dissolution was recorded, only six failed to fully dissolve at 120°C compared to fifteen in the same solvents when a constant concentration of 0.2 % w/v was used. Adjustments to the concentration of gelator meant that gels formed in sixty of the ninety six samples with partial or weak gels in a further eight. Varying the concentration of gelator for different solvent mixtures achieves much better results for ensuring both the dissolution of the gelator at high temperatures and gel formation at low temperatures. However, in a small minority of solvent combinations gelator remained undissolved at high temperatures and no gelation was observed. In such cases simply adjusting the concentration of gelator would never achieve gel formation from a clear solution.

Crystallisation was observed in sixty nine out of the ninety six solvent combinations in this experiment. Comparing the forty eight crystallisations used in the low temperature study, crystals were only observed in twenty seven of the samples compared to thirty four in the low temperature studies. The choice of 10 or 20 mg of **GSK-D** in each vial was too low to induce crystallisation in many of the samples. This highlights a limitation of this approach as the solubility of compounds is difficult to predict. With hindsight, undissolved material was unlikely to have been a significant problem had higher concentrations of **GSK-D** been used as the samples were heated well above 60°C in order to dissolve the gelator.

Form 2 was the most prevalent crystal form and was identified in twenty seven of the samples. Form 1 was observed in sixteen cases and form 3 in just one. The prevalence of form 2 may reflect the lower levels of supersaturation resulting in formation of the thermodynamically more stable form. Needles and plates were observed growing on the wall of the vials above the gel and such samples are noted in Table 30 with an asterisk. Time pressure meant priority was given to assigning crystals observed growing in the gels so the form of these crystals was not identified. In the low temperature study, all of the crystals identified by Raman as form 3 grew above the surface of the gel. It is likely therefore that many of the crystals whose form was not identified are form 3, which may account for the low number of form 3 crystals observed in this study compared to the low temperature gel study.

Comparing crystal forms obtained in this study with those observed in the low temperature gel and solution phase studies is complicated by differences in temperature, method, concentration of **GSK-D**, gelator, whether crystallisation had taken place and if the crystal forms could be assigned. Comparison of the two gel phase studies showed poor correlation between the crystal forms observed (different in nine cases, the same in six). This lack of correlation indicates that there is not a strong templating effect by the gelator and that other effects such as concentration and temperature are more important in determining crystal form. However, the stochastic nature of crystallisation and complexity of comparing data means it is difficult to draw many conclusions from this study.

One interesting phenomenon demonstrated by the gel phase is shown in Figure 122. The image shows an orange block assigned by Raman spectroscopy as form 2 growing out of yellow needles assigned as form 1. Because material remains suspended in the gel phase, a depletion zone can be seen around the growing block of form 2 as it cannibalises the surrounding needles. This provides a good visual demonstration of the stability relationship observed between forms 1 and 2.

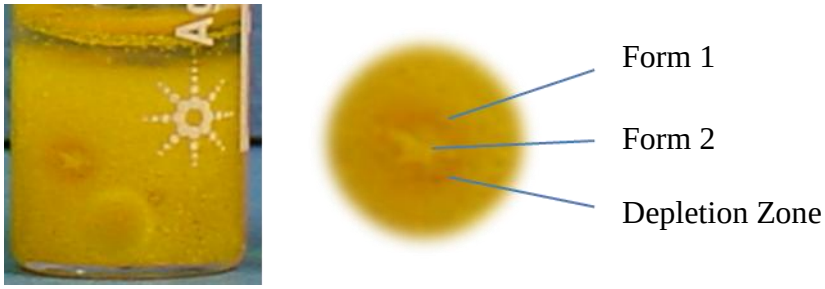

Figure 122 Photograph showing depletion of fine needles of **GSK-D** form 1 by a growing crystal of form 2 suspending in a 0.2 % w/v gel of **44**.

7.5 Compatibility of LMWGs with API salts

As well as forming gels in a wide variety of solvents, to be industrially relevant LMWGs must tolerate a variety of industrially relevant drug compounds. Proof of principle for the compatibility of drug compounds from supramolecular gels was established in Chapters 5 and 6. Compound **44** is able to form stable gels in the presence of a wide range of different neutral drug compounds as well as ibuprofen sodium salt.

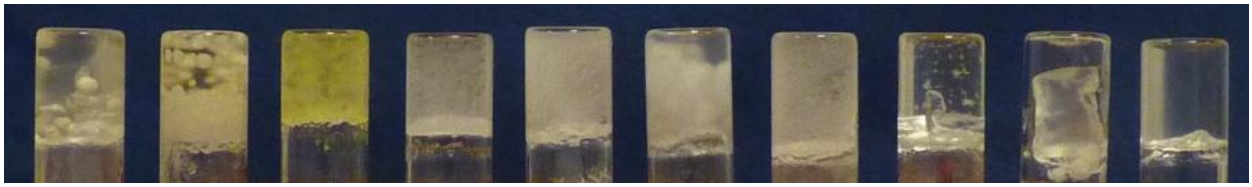

Figure 123 Left to right: Piroxicam, Indomethacin, Sparfloxacin, Theophyline, Caffeine, Ibuprofen sodium salt, Acetaminophen, Carbamazepine, **GSK-A**, and **GSK-B** crystallised from toluene gels of **44.**

The formulation of APIs as salts has proved a useful technique for increasing the solubility of compounds and adjusting other properties through the careful choice of counterion.[279] Given the tendency of supramolecular gels to dissolve in the presence of anions such as acetate it was interesting to understand whether API salts can be crystallised from supramolecular gels. **GSK-E** is one such API which is marketed as a salt and a variety of **GSK-E** salts were available for testing. Conditions were selected to match screens previously carried out on a variety of free base APIs (and Na-Ibuprofen) using 1 % w/v **44** in five different solvent systems. The same conditions were also replicated using **44** and solution phase crystallisations undertaken for comparison. Salts of **GSK-E** with four different anions: chloride, tosylate, mesylate and citrate were investigated.

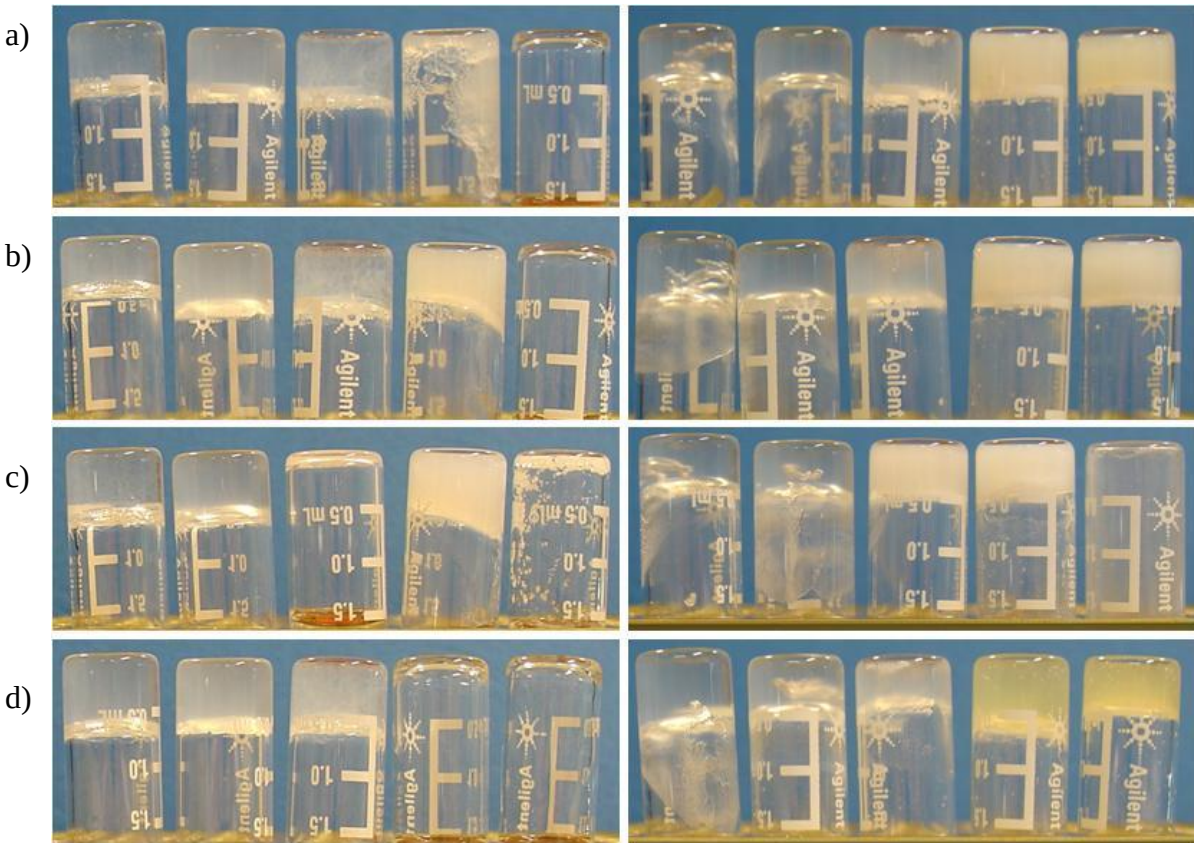

Figure 124 Gels of left hand side- 1 % w/v **20**, right hand side- 1 % w/v **44**, made with saturated solutions (at 60°C) of **GSK-E** a) hydrochloride, b) tosylate, c) mesylate, d) citrate salts in (left to right) 9:1 toluene:$CHCl_3$, 9:1 toluene:CH_3CN, Ethylacetate, 1:1 DMSO:H_2O, 3:2 Methanol:water.

Saturated solutions were formed by slurrying the **GSK-E** salts in selected solvents at 60°C overnight. The resulting solutions were hot filtered into vials containing 1 % w/v gelator using syringes capped with filtration devices. In three instances (noted by superscript 'a' in Table 27 and Table 28) fully saturated solutions were not formed at 60°C due to the very high solubility of the salt in the solvent mixture. The sample was heated using a heat gun until fully dissolved and then allowed to cool to room temperature.

Table 27 Gel formation by 1 % w/v **20** gelator from various solutions of **GSK-E** salts

Solvent / **GSK-E**	1:9 CH_3CN:Tol	1:9 $CHCl_3$:Tol	EtOAc	1:1 DMSO:H_2O	3:2 MeOH:H_2O
HCl	G	G	G	PG	S[a]
Tosylate	G	G	G	G	S
Mesylate	G	G	P	G	P
Citrate	G	G	G	S[a]	S[a]

G= Gel, PG= Partial Gel, P= precipitate, S= solution, * solution not fully saturated with API salt.

Compound **20** formed gels in all of the non-aqueous solvent systems in the presence of all four salts of **GSK-E**, except for the mesylate salt which disrupted gel formation in the ethylacetate sample. Gelation was generally weaker in the aqueous systems with some gels and partial gels forming in DMSO: H_2O mixtures but none forming in MeOH:H_2O mixtures. This is likely to be due in part to the greater solubility of the **GSK-E** salts in the aqueous solutions. Precipitates were observed for the mesylate salt in the methanol:water and ethylacetate solutions with gels forming in other cases.

Previous studies investigating the use of anions to break down gels have found them to be ineffective in aqueous systems, thought to be due to hydration of the anions. Urea hydrogen bonding is also thought to be more important to gel formation in less polar environments whilst hydrophobic effects are more important in aqueous systems. The ability of the gels to form in the presence of significant quantities of anions in non-aqueous systems, and to dissolve gels in aqueous systems is therefore an interesting observation which requires broader investigation.

Table 28 Gel formation by 1 % w/v **44** gelator from various solutions of **GSK-E** salts

Solvent / **GSK-E**	1:9 CH_3CN:Tol	1:9 $CHCl_3$:Tol	EtOAc	1:1 DMSO:H_2O	3:2 MeOH:H_2O
HCl	G	G	G	G	G
Tosylate	G	G	G	G	G
Mesylate	G	G	G	G	G
Citrate	G	G	G	G	G

Compound **44** formed gels with all four salts in all of the solvent systems investigated. This is remarkable given the high concentrations of anions used, particularly in the aqueous systems. It would be interesting to see if more variation is seen at lower concentrations of gelator as 1 % w/v is relatively concentrated for this system. The ability of **44** to reliably form gels in a wide range of solvent systems in the presence of high concentrations of anions provides proof of principle for the use of LMWGs as a medium for the crystallisation of API salts.

7.6 Freeze-drying study

Many of the problems encountered during this study have been due to the need for high temperatures to form the gels. One possible solution investigated is to pre-form a gel in a suitable solvent, freeze-dry it to remove the solvent, then resolvate the gel with a solution containing the drug molecule to be crystallised. This would overcome many of the

complications associated with forming the gels *in situ*, greatly simplify the crystallisation process and allowing the crystallisation of thermally sensitive drug molecules from the gels. It would also potentially allow crystallisation from solvent systems where gels do not normally form due to issues with solubility.

To test this, 1 % w/v gels of **44** were formed in a variety of suitable solvents (0.5ml) and freeze-dried. Of the eight gels attempted, four successfully formed stable aerogels and one an aerogel which collapsed slightly. The aerogels appeared as a homogeneous, opaque white solid which occupied approximately the same space as that of the gel. The collapsed aerogel contained a similar looking white solid but had not retained its shape and consisted of many fragments at the bottom of the vial. The other samples contained white solid coating the sides of the flask or free-flowing precipitates at the bottom of the flask.

Table 29 The effect of freeze-drying gels formed from various solvents and of the addition of a second solvent to the aerogels

No.	Starting Solvent	Phase	Effect of freeze-drying	Addition of solvent
17	1,4-dioxane	G	Aerogel	1,4-dioxane- Partial Gel
59	2-methyl-2-butanol	G	Aerogel	Water-imiscible layers
25	Dimethyl-carbonate	G	Aerogel	Hexane-fine precipitate
5	Nitromethane	G	Thick coating on vial walls	
6	Acetonitrile	G	Xerogel	
49	1,2-dimethoxyethane	G	Fine coating on vial walls	
43	2-butanol	G	Fine coating on walls + solid	
57	2-pentanol	G	Fine coating on walls + solid	

In order to test whether or not the aerogels could be resolvated, three scenarios were tested. Firstly, 1,4-dioxane was added to an aerogel formed from the same solvent. This resulted in the collapse of the aerogel to give a precipitate which trapped some of the solvent. Upon standing, a stable, translucent gel formed which retained approximately half of the solvent upon inversion. A much clearer and more complete gel was achieved by sonication of the sample in a water bath for approximately 30minutes during which time the water had heated to 40°C.

The xero-gel fibres appear capable of re-gelling the solvent, however destruction of the aero-gel upon addition of the solvent means that the macroscopic structure is broken preventing a sample-spanning gel reforming. Sonication appears to aid the formation of a sample-spanning structure. Further investigations have shown that gels can be formed by **44** in solvents such as

NMP, cyclohexanone, chlorobenzene and chloroform by sonicating a sample of the solid gelator in the solvent. After ten minutes of sonication a fine suspension is formed which gradually gels over a period of minutes to hours. This potentially provides an alternative route to gel formation which does not require heating.

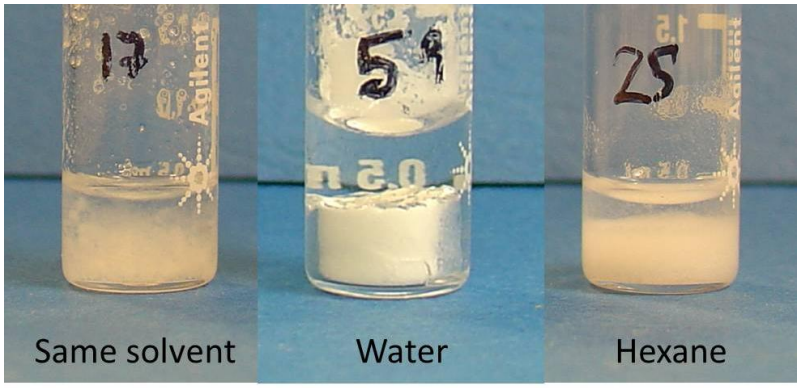

Figure 125 Effect of careful addition of (left to right) 1,4-dioxane, water and hexane to aerogels formed by 1wt% **44** from 1,4-dioxane, 2-methyl-2-butanol, dimethyl-carbonate

In a second experiment, water was added to an aerogel formed from 2-methyl-2-butanol. Compound **44** is insoluble in water so it is not possible to form a hydrogel. The water initially formed a layer resting on top of the aerogel which did not collapse. After several minutes the layers inverted with the denser water layer going to the bottom and the aerogel floating intact on top. After several months the aerogel remained floating on the water in three large blocks. The hydrophobic nature of the aerogel and high-surface tension and viscosity of water are likely to account for the lack of wetting of the aerogel.

In a third experiment, hexane was added to an aerogel formed from dimethylcarbonate. Compound **44** is insoluble in hexane and other apolar solvents and therefore does not form gels. Addition of the hexane resulted in the immediate collapse of the aerogel leaving a fine precipitate. No evidence of gelation behaviour was observed over several weeks.

7.7 Conclusions

Industrial polymorph screening procedures have been successfully adapted for crystallisation of an API that is currently being commercially developed. Most stages could make use of existing processes and equipment with only one additional heating step required. However, the high temperatures required to ensure dissolution of the gelator coupled with variations in the boiling points of different solvent combinations meant that this additional step was

problematic. Attempts to circumnavigate this problem using pre-formed aerogels provideed an attractive solution which requires further investigation.

The gelator, **44**, was remarkably robust at forming gels from a wide variety of solvent conditions, particularly when the concentration of the gelator was adjusted according to the solvent used. Gelation was unaffected by the presence of a wide range of different drug compounds including a number of API salts.

Raman spectroscopy was successfully used to identify crystal forms in the presence of gelator either by filtration or *in situ*. Large differences in the solid form and prevalence of each polymorph were observed between the solution and gel phase studies. However, the additional heating step used in the gel but not the solution study and the tendency for crystals to form outside of the gel complicates the analysis. No new crystal polymorphs or solvates of **GSK-D** were discovered.

Overall this high throughput study demonstrates that with some achievable modifications to procedure and gel structure, LMWGs could be adapted for use in industrial polymorph screening procedures. However, further work is required to demonstrate that the differences in polymorphism observed are due to the gel phase and that this route potentially provides access to polymorphs not identified by conventional techniques if it is to be adopted.

7.8 Experimental Section

Drug compounds **GSKA-E** were supplied by GSK and further details regarding compound structure and polymorphism can not be provided due to commercial sensitivity. Compound **44** was synthesised by Masters student Gary Cameron under the supervision of Jonathan Foster. Further details regarding the synthesis of compounds **17** and **20** are provided in Chapter 2 and **41**, **43** and **44** in Chapter 6. The low temperature solution phase study was undertaken by Reshma Chudasama. Raman spectroscopic measurements were preformed on a Thermo Scientific, Nicolet, NXR9650 Raman spectrometer.

Table 30 Summary of phases found at various temperature for 0.2wt% **44**, assignments of crystal forms from previously undertaken solution study, gelation and crystal data for 20-4°C gel phase study of **GSK-D** of studies in various binary solvent mixtures.

	Solvent System (3:7)	44 Gel study[a]			Sol.[b]	Low Temperature GSK-D study[c]					mg/ml		High temperature GSK-D study[d]				
		120°C	20°C	4°C	Form	120°C	4°C	Colour	Description	Form	44	GSK-D	120°C	20°C	Colour	Description	Form
1	water:formamide	I	I	I							1	20		S	Y	Precipitate	2
2	water:ethylene glycol	I	I	I							1	20		S	Y	Precipitate	2
3	methanol:water	I	I	I							1	20		S	Y	Precipitate	2
4	methanol:methanol	S	PG	PG	-	S	G	O	-	-	5	10		G	Y	Yellow Precipitate + Blocks	2+2
5	2-methoxyethanol:2-methoxyethanol	S	S	PG	2	S	PG	O	Needles	X	5	10		G	O	Red crystal + yellow needles above	2+1
6	2-methoxyethanol:dichloromethane	S	S	S							10	10		P		White fibres/yellow precip	1
7	acetonitrile:chloroform	S	S	PG	3	S	S	Y	Needles and plates	2	5	10		PG	Y	Long blocks	2
8	acetone:acetone	S	G	G	UA	S	G	O	Fine needles + Plates above	2 +3	2	20		G	Y	Block	2
9	acetone:tetrachloroethylene	S	G	G	2	PS	G	Y	Plate above	3	2	10		S	S	Block	2
10	2-butanone:2-butanone	S	G	G	2	S	G	Y	Plate above	3	2	20		S		O block on surface, Y block above	2+1
11	2-butanone:methyl acetate	S	G	G	-	PS	G	Y	Long needles/plates	1/3	2	20		G	Y	Block	2
12	2-butanone:ethylene glycol	S	S	S							10	20		G	O	Block	2
13	dichloromethane:methanol	S	S	S							10	20		G		Blocks	2
14	dichloromethane:ethylene glycol	S	P	P							10	10		Oil	O	Oil	-
15	methyl acetate:2-methoxyethanol	S	S	PG	2	S	G	O	Small needles	X	5	10		G	O	Plates above	-
16	methyl acetate:1,2-dimethoxyethane	S	G	G	2	S	G	Y	Plate above	3	2	10		G	Y	-	
17	methylisobutyl ketone:1-propanol	S	G	G							2	10		G	Y	-	
18	methylisobutyl ketone	PS	PG	PG	-	PS	PG	Y	-	-	1	20		G	Y	Long blocks	2
19	methylisobutyl ketone:nitrobenzene	S	G	G							2	20		G	Y	White precipitate	3
20	chloroform:nitromethane	S	PG	PG							5	20		G	Y	Fibres on bottom + blocks above	1+2
21	chloroform:chloroform	S	S	S	3	S	S	Y	Block above	2	10	10		G	Y	White fibrous material	
22	ethyl acetate:acetonitrile	S	G	G	-	S	G	O	Yellow needles	2?	2	20		G	Y	Block	2
23	ethyl acetate:ethyl acetate	PS	G	G	-	PS	G	Y	Blocks above	3	1	10		G	Y	Needles above	*

	Solvent System (3:7)	44 Gel study[a]			Sol.[b]	Low Temperature GSK-D study[c]					mg/ml		High temperature GSK-D study[d]				
		120°C	20°C	4°C	Form	120°C	4°C	Colour	Description	Form	44	GSK-D	120°C	20°C	Colour	Description	Form
24	ethyl acetate:1-methyl-2-pyrrolidinone	S	S	S	-						10	10		S	O	-	
25	chlorobenzene:dimethyl sulfoxide	S	S	S	DMSO	S	S	Y	Mesh of needles	UA	10	10		S	Y	-	
26	chlorobenzene:N,N-dimethylformamide	S	S	S	-						10	10		PG	R	-	
27	tetrahydrofuran:nitromethane	S	PG	PG	-	S	G	Y	Cylinders	1	5	10		G	Y	Blocks	2
28	tetrahydrofuran:acetone	S	PG	PG	2	S	G	YO	Needles on surface	2	5	20		G	Y	Blocks + needles above	*
29	diethyl ether:chloroform	S	P	P							5	10		G	Y	Blocks + needles above	*
30	toluene:ethyl acetate	PS	G	G	-	PS	G	Y	Mesh of needles	1	1	10		G	Y	Blocks + needles above	*
31	toluene:tetrahydrofuran	S	G	G	-	S	G	YO			2	10		GW	Y	-	
32	cyclohexane:1-methyl-2-pyrrolidinone	S	S	S	-						10	10		S	Y	-	
33	cyclohexane:N,N-dimethylformamide	S	S	S	-						10	10		S	O	-	
34	heptane:ethyl acetate	PS	WG	PG	-						1	10		PG	Y	-	
35	heptane:tetrahydrofuran	S	G	G	-						2	10		G	Y	Cloudy	
36	1-butanol:tetrachloroethylene	S	G	WG	2	S	G	YO	-		5	20		G	Y	Block needles	1
37	2-propanol:chloroform	S	S	S	3	S	S	Y	Cylinders	2	10	20		S	Y	P + fine needles above	*
38	3-methyl-1-butanol:3-methyl-1-butanol	S	WG	G	-	S	G	O	-		5	10		G	Y	Fine needles	1
39	DMAc:carbon disulfide	S	S	S	-						10	10		S	Y	-	
40	N,N-dimethylacetamide:anisole	S	S	S	-	S	S	O	Cylinders	2	10	20		G	Y	Precipitate	2
41	1-methyl-2-pyrrolidinone:water	I	I	I	-						1	10		S	Y	Precipitate	
42	1-methyl-2-pyrrolidinone:2-butanone	S	S	S	2	S	S	YO	-		10	10		PG	Y	-	
43	1-methyl-2-pyrrolidinone:toluene	S	S	S	-						10	20		G	Y	-	
44	1-methyl-2-pyrrolidinone:carbon disulfide	S	S	S	-						10	10		S	Y	-	
45	1-methyl-2-pyrrolidinone:acetic acid	S	S	S	UA	S	S	O	Clump of needles above	1	10	10		S	Y	Blocks	2
46	1-methyl-2-pyrrolidinone:DMAc	S	S	S	-						10	10		S	Y	-	
47	pyridine:2-methoxyethanol	S	S	S	-						10	20		G	R	Needles above	*
48	pyridine:1,4-dioxane	S	S	S	-						10	20		G	Y	Needles above	*

	Solvent System (3:7)	44 Gel study[a]			Sol.[b]	Low Temperature GSK-D study[c]					mg/ml		High temperature GSK-D study[d]				
		120°C	20°C	4°C	Form	120°C	4°C	Colour	Description	Form	44	GSK-D	120°C	20°C	Colour	Description	Form
49	anisole:N,N-dimethylformamide	S	S	S	-						10	20	S	G	O	-	
50	tetrachloroethylene:acetonitrile	S	PG	PG	-						5	20	S	G	Y	Needles above and in gel	1
51	tetrachloroethylene:ethanol	S	PG	PG	2	S	G	OY	Needles from surface	1	5	20	S	G	Y	Fine needles	1
52	tetrachloroethylene:acetic acid	S	S	S	UA	S	S	R	Long fine needles-solution	1	10	20	S	S	Y	Needles	1
53	hexane:carbon disulfide	S	PG	PG	-						5	20	I	I	Y	Blocks	2
54	1-pentanol:pentane	x	X	X	-						2	10	PS	G	Y	Blocks	2
55	pentane:methylisobutyl ketone	I	I	I	-						1	10	S	WG	Y	Needles	1
56	p-xylene:methanol	S	S	S	2	S	S	O	Needles above	UA	10	10	S	G	YO	Needles	2
57	p-xylene:dimethyl sulfoxide	S	S	S	DMSO	S	S	OY	Needles	UA	10	10	S	S	YO	-	
58	p-xylene:chlorobenzene	S	WG	WG	2	PS	G	Y	-		5	10	PS	G	Y	Gelator	
59	2-methyl-1-propanol:diethyl ether	PS	PG	PG	-						1	10	PS	G	Y	Blocks	2
60	2-methyl-1-propanol:diisobutyl ketone	PS	G	G	-						1	20	PS	G	Y	Long needles	1
61	2-butanol:toluene	S	PG	PG	2	S	G	YO	Needles above and below	1	5	10	S	G	Y	Needles above	*
62	isopropyl acetate:methylisobutyl ketone	PS	PG	PG	-	PS	G	Y	Yellow needles	1	1	20	S	G	Y	Blocks	2
63	isopropyl acetate:heptane	PS	PG	PG	-						1	20	I	I	Y	Blocks + gelator	2
64	isopropyl ether:isobutyl acetate	PS	G	G	-						1	20	PS	G	Y	Fine needles	1
65	DMF:tetrahydrofuran	S	S	S	-						10	20	S	G	Y	-	
66	N,N-dimethylformamide:2-propanol	S	S	PG	-						5	20	S	G	O	Needles	UA
67	1,2-dimethoxyethane:benzonitrile	S	WG	WG	-						5	20	S	G	Y	Needles	UA
68	ethylene glycol:acetonitrile	S	S	PG	-						5	20	S	S	O	Fibres + orange block	1
69	isobutyl acetate:1,2-dimethoxyethane	S	WG	WG	-						5	20	S	G	Y	-	
70	isobutyl acetate:isobutyl acetate	I	I	I	2	X	X	X	-		1	10	S	?			2
71	methylcyclohexane:nitrobenzene	S	G	G	3	PS	G	Y	Clump of plates/needles	1	2	10	S	G	Y	Cloudy	
72	benzonitrile:cyclohexane	PS	G	G	-						1	10	S	G	Y	Needles	1
73	benzonitrile:1-methyl-2-pyrrolidinone	S	S	S	-						10	10	S	S	Y	-	
74	benzyl alcohol:benzyl alcohol	S	S	S	2	S	S	O	-		10	10	S	G	Y	-	

	Solvent System (3:7)	44 Gel study[a]			Sol.[b]	Low Temperature GSK-D study[c]					mg/ml		High temperature GSK-D study[d]				
		120°C	20°C	4°C	Form	120°C	4°C	Colour	Description	Form	44	GSK-D	120°C	20°C	Colour	Description	Form
75	2-pentanol:2-pentanone	S	G	G	-						2	10	S	G	Y	Needles above	*
76	2-methyl-2-butanol:acetic acid	S	S	S	-						10	10	S	G	Y	Branched needles	1
77	2-pentanone:methyl-t-butyl ether	PS	PG	PG	2	I	I	Y	-		1	10	S	G	Y	Needles above	*
78	2-pentanone:p-xylene	PS	G	G	2	I	I	Y	Yellow needles	1	1	10	S	G	Y	-	
79	2-pentanone:2-pentanone	PS	PG	PG	-	PS	G	Y	Needles above	1	1	10	S	WG	Y	Orange block	2
80	butyronitrile:1-butanol	S	WG	G	-						5	10	S	G	Y	Orange blocks + fine needles	2+1
81	butyronitrile:butyronitrile	S	G	G	-	X	X	X	-		2	10	S	S	Y	Needles	1
82	diisobutyl ketone:1,4-dioxane	S	G	G	-						2	10	S	G	Y	-	
83	diisobutyl ketone:DMAc	S	S	G	-						5	10	S	S	Y	-	
84	diisobutyl ketone:diisobutyl ketone	I	I	I	-	I	I	Y	-		1	10	PS	S	Y	Needles	2
85	1-octanol:pyridine	S	S	S	-						10	10	S	G	O	Plates above	*
86	1-octanol:1-octanol	PS	WG	WG	-	I	X	X	-		1	20	S	G	Y	Fine needles	1
87	cyclohexanol:isopropyl acetate	S	G	G	2	S	G	Y	Fine needle above	1	2	20	S	G	Y	Branched needles	1
88	t-butanol:butyronitrile	S	G	G	2	S	G	O	Fine needle above	1	2	20	S	G	O	Orange blocks	2
89	2-ethyl-1-hexanol:chloroform	S	S	S	2	S	S	Y	Needles/plates	2	10	10	S	P		White precip	2
90	1-heptanol:cyclopentyl methyl ether	PS	PG	PG	2	PS	G	-	-		1	10	S	G	Y	-	
91	3-methyl-2-butanol:cyclopentyl methyl ether	S	WG	PG	2	PS	G	OR	Needles above	UA	5	10	S	G	R	Needle blocks above	*
92	1-hexanol:dimethyl carbonate	S	WG	WG	-						5	10	S	G	Y	-	
93	Methanol:acetic acid (80%)	S	PG	PG	-						5	10	S	G	Y	Fine precip	2
94	1-methyl-2-pyrrolidinone	S	PG	PG	2	S	S	O	-		5	10	S	G	Y	Needles	1
95	methanol:THF	S	S	S	-	S	S	O	Thick needles above	1	10	10	S	PG	Y	-	
96	Methanol:1-methyl-2-pyrrolidine	S	S	S	-	S	S	O	Blocks	2	10	10	S	G	RO	-	

S = Solution/soluble, PS = partially soluble, I = Insoluble, G= Gel, PG= Partial Gel, WG = Weak gel, A,B,C refer to non-solvated forms A-C, DMSO refes to DMSO solvate, colour refers to solution with Y = yellow, O=orange, R=Red, YO, OY, OR colours in between Blank space= experiment not undertaken, - no result reported, * insufficient time to complete experiment. [a] Mixed solvents were dispensed into vials containing 0.2 % w/v **44** and heated to 120°C then cooled to 20°C and 4°C. [b] Results of solution phase experiment previously undertaken [c] Filtered solutions saturated at room temperature with **GSK-D** were added to vials containing 0.2 % w/v **44** and heated to 120°C then cooled to 4°C. [d] Given masses of **44** and **GSK-D** were dispensed into vials along with 1 ml of mixed solvent. The vial was sealed and heated until all solid was dissolved and allowed to cool to room temperature.

Chapter 8: Conclusion

This thesis has contributed a number of new urea based gelators to the growing body of LMWGs in the literature. The bis-urea motif employed proved highly successful at bringing about gelation in molecules functionalised with a range of different spacer and peripheral groups. The series based on oligomethylene spacers functionalised with different amino acids identified a number of 'optimal' compounds (notably **17** and **20**) which produced robust gels in a variety of solvents. Small differences in spacer length and R-group were found to have a dramatic impact upon gelation behaviour and conformational flexibility resulted in extensive polymorphism. The series was successfully extended to include 1- and 2- pyrenylalanine gelators (**35** and **36**) which proved effective gelators as well as ROY and CBZ mimics (**39** and **42**). In general the more rigid diphenyl methyl spacer proved more tolerant of competing hydrogen bonding functionalities and in reliably forming gels in a wider range of solvents. Compound **44** was particularly remarkable in reliably forming gels in over 52 different solvents at very low gelator concentrations (typically 0.2 % w/v).

The complex, hierarchical nature of gels with their solid-like structure but predominantly liquid-like composition presents a number of challenges to their study. Solid state analytical techniques such as crystallography, XRPD and IR revealed the importance but inadequacy of molecular packing in explaining gelation behaviour. SEM provided valuable insight into the higher order structure of the gels revealing a number of distinct fibre morphologies associated with different gelators, polymorphs and mixed gel systems. Analysis of polymers templated by gelators **17** and **20** corroborated the differences in fibre shape and size distribution observed in the xerogels. Rheometry allowed characterisation of the gels in their native state and confirmed gelation in the systems tested. The use of fluorescent gelators provided another handle with which to investigate gelator behaviour both in solution and in the gel state. However, as with a number of the other mixed gel systems, the pyrenylalanine gelators were found to induce changes in gel fibre morphology and molecular packing.

As observed in related urea systems, anions were found to disrupt urea hydrogen bonding interactions leading to dissolution of the gels. Disruption of the macroscopic structure of the gels as measured by rheology was found to occur at considerably lower concentrations of anions than required to prevent aggregation of the gelator molecules as measured by fluorescence. This mechanism was effectively utilised to aid recovery of crystals grown in

LMWGs. However, limitations due to the solubility and effectiveness of anions in different solvents, and their tendency to dissolve crystals, mean gels which respond to alternative stimuli (e.g. electrochemical, light etc.) may be more suitable for this application.

The gels were developed towards a number of applications. The different architectures of gelators **17** and **20** enabled the templation of porous polymers with different pore shapes which may find applications in filtration. The fluorescent response exhibited by gelators **35** and **36** upon binding to acteate, but not tetrafluoroborate, makes them suitable for use as an anion sensor. The ability to turn gelation on and off or tune the rheology of the gel system using anions allows the gels to be used as 'smart' materials for applications such as drug delivery and crystal recovery.

Proof of principle was demonstrated for the crystallisation of a wide range of pharmaceutically relevant compounds from LMWGs. A number of differences were observed in crystal habit and polymorphism in crystals grown from gels compared with those grown from solution. It proved possible to design LMWGs which incorporate specific functionalities into their structure which mimic those of the drug compound being crystallised. Gelator **43,** which incorporated a nitroaniline group to mimic that of ROY, showed some promise in bringing about a higher proportion of the R-form than observed from solution or generic gels and should be investigated further. The potential of supramoelcular gels for use in early stage screening of pharmaceutical compounds in an industrial setting was shown to be feasible during a placement with the particle science group at GSK in Stevenage. The high temperatures required to form the gels and need to control sample cooling are two factors which require further development. The inherent reversibility of the gels, their ability to gel a wide range of solvents and opportunity to design gelators incorporating specific functionalities mean LMWGs hold great promise as a medium for crystal growth.

9 References

1. Flory, P.J., *Faraday Discuss.*, 1974, **57**, 7.
2. Wang, R., Liu, X.-Y., Xiong, J. & Li, J., *J. Phys. Chem. B*, 2006, **110**, 7275.
3. Dolle, C., Magrone, P., Riva, S., Ambrosi, M., Fratini, E., Peruzzi, N. & Lo Nostro, P., *J. Phys. Chem. B*, 2011, **115**, 11638.
4. Mieden-Gundert, G., Klein, L., Fischer, M., Vogtle, F., Heuze, K., Pozzo, J.L., Vallier, M. & Fages, F., *Angew. Chem. Int. Ed.*, 2001, **40**, 3164.
5. Araki, K. & Yoshikawa, I. Low Molecular Mass Gelators: Design, Self-Assembly, Function (ed. Fages, F.) 133 (Springer-Verlag Berlin, Berlin, 2005).
6. Ajayaghosh, A., Praveen, V.K., Vijayakumar, C. & George, S.J., *Angew. Chem. Int. Ed.*, 2007, **46**, 6260.
7. Brouwer, Arwin J., Mulders, Suzanne J.E. & Liskamp, Rob M.J., *Eur. J. Org. Chem.*, 2001, **2001**, 1903.
8. Suzuki, M. & Hanabusa, K., *Chem. Soc. Rev.*, 2009, **38**, 967.
9. Adhikari, B., Palui, G. & Banerjee, A., *Soft Matter*, 2009, **5**, 3452.
10. Bhuniya, S. & Kim, B.H., *Chem. Commun.*, 2006, 1842.
11. Frkanec, L. & Zinic, M., *Chem. Commun.*, 2010, **46**, 522.
12. Piepenbrock, M.-O.M., Lloyd, G.O., Clarke, N. & Steed, J.W., *Chem. Rev.*, 2009, **110**, 1960.
13. Foster, J.A. & Steed, J.W., *Angew. Chem. Int. Ed.*, 2010, **49**, 6718.
14. Hirst, A.R. & Smith, D.K., *Chem. Eur. J.*, 2005, **11**, 5496.
15. Babu, P., Sangeetha, N.M., Vijaykumar, P., Maitra, U., Rissanen, K. & Raju, A.R., *Chem. Eur. J.*, 2003, **9**, 1922.
16. Basit, H., Pal, A., Sen, S. & Bhattacharya, S., *Chem. Eur. J.*, 2008, **14**, 6534.
17. Moffat, J.R. & Smith, D.K., *Chem. Commun.*, 2008, 2248.
18. Byrne, P., Lloyd, G.O., Applegarth, L., Anderson, K.M., Clarke, N. & Steed, J.W., *New J. Chem.*, 2010, **34**, 2261.
19. Piepenbrock, M.M., Clarke, N. & Steed, J.W., *Langmuir*, 2009, **25**, 8451.
20. Adhikari, B. & Banerjee, A., *Soft Matter*, 2011, **7**, 9259.
21. Samanta, S.K., Pal, A., Bhattacharya, S. & Rao, C.N.R., *J. Mater. Chem.*, 2010, **20**, 6881.
22. Yang, X.Y., Zhang, G.X., Zhang, D.Q., Xiang, J.F., Yang, G. & Zhu, D.B., *Soft Matter*, 2011, **7**, 3592.
23. Wang, Q., Mynar, J.L., Yoshida, M., Lee, E., Lee, M., Okuro, K., Kinbara, K. & Aida, T., *Nature*, 2010, **463**, 339.
24. Terech, P. & Weiss, R.G., *Chem. Rev.*, 1997, **97**, 3133.
25. Estroff, L.A. & Hamilton, A.D., *Chem. Rev.*, 2004, **104**, 1201.
26. van Bommel, K.J.C., van der Pol, C., Muizebelt, I., Friggeri, A., Heeres, A., Meetsma, A., Feringa, B.L. & van Esch, J., *Angew. Chem. Int. Ed.*, 2004, **43**, 1663.
27. Mohmeyer, N. & Schmidt, H.-W., *Chem. Eur. J.*, 2007, **13**, 4499.
28. Dastidar, P., *Chem. Soc. Rev.*, 2008, **37**.
29. Anderson, K.M., Day, G.M., Paterson, M.J., Byrne, P., Clarke, N. & Steed, J.W., *Angew. Chem. Int. Ed.*, 2008, **47**, 1058.
30. Braga, D., d'Agostino, S., D'Amen, E. & Grepioni, F., *Chem. Commun.*, 2011, **47**, 5154.
31. Roubeau, O., Colin, A., Schmitt, W. & Clerac, R., *Angew. Chem. Int. Ed.*, 2004, **43**, 3283.
32. Wang, Y., Tang, L. & Yu, J., *Cryst. Growth Des.*, 2008, **8**, 884.
33. Cui, J., Shen, Z. & Wan, X., *Langmuir*, 2010, **26**, 97.
34. Edwards, W., Lagadec, C.A. & Smith, D.K., *Soft Matter*, 2011, **7**, 110.
35. Chen, J., Kampf, J.W. & McNeil, A.J., *Langmuir*, 2010, **26**, 13076.
36. Muro-Small, M.L., Chen, J. & McNeil, A.J., *Langmuir*, 2011, **27**, 13248.

37. Terech, P., Pasquier, D., Bordas, V. & Rossat, C., *Langmuir*, 2000, **16**, 4485.
38. Steed, J.W., *Chem. Soc. Rev.*, 2010, **39**, 3686.
39. Smith, M.M. & Smith, D.K., *Soft Matter*, 2011, **7**, 4856.
40. Terech, P., Rossat, C. & Volino, F., *J. Colloid Interface Sci.*, 2000, **227**, 363.
41. Hirst, A.R., Coates, I.A., Boucheteau, T.R., Miravet, J.F., Escuder, B., Castelletto, V., Hamley, I.W. & Smith, D.K., *J. Am. Chem. Soc.*, 2008, **130**, 9113.
42. Saha, A., Manna, S. & Nandi, A.K., *Langmuir*, 2007, **23**, 13126.
43. Abdallah, D.J., Sirchio, S.A. & Weiss, R.G., *Langmuir*, 2000, **16**, 7558.
44. Escuder, B., Llusar, M. & Miravet, J.F., *J. Org. Chem.*, 2006, **71**, 7747.
45. Bernstein, J., Davis, R.E., Shimoni, L. & Chang, N.-L., *Angew. Chem. Int. Ed.*, 1995, **34**, 1555.
46. George, M., Tan, G., John, V.T. & Weiss, R.G., *Chem. Eur. J.*, 2005, **11**, 3243.
47. Kim, J.-U., Schollmeyer, D., Brehmer, M. & Zentel, R., *J. Colloid Interface Sci.*, 2011, **357**, 428.
48. van Esch, J.H., Schoonbeek, F., de Loos, M., Kooijman, H., Spek, A.L., Kellogg, R.M. & Feringa, B.L., *Chem. Eur. J.*, 1999, **5**, 937.
49. Brinksma, J., Feringa, B.L., Kellogg, R.M., Vreeker, R. & van Esch, J., *Langmuir*, 2000, **16**, 9249.
50. de Loos, M., van Esch, J., Kellogg, R.M. & Feringa, B.L., *Angew. Chem. Int. Ed.*, 2001, **40**, 613.
51. Lloyd, G.O., Piepenbrock, M.O.M., Foster, J.A., Clarke, N. & Steed, J.W., *Soft Matter*, 2012, **8**, 204.
52. Piepenbrock, M.O.M., Lloyd, G.O., Clarke, N. & Steed, J.W., *Chem. Commun.*, 2008, 2644.
53. Bond, A.D., *CrystEngComm*, 2006, **8**, 333.
54. de Loos, M., Ligtenbarg, Alette G.J., van Esch, J., Kooijman, H., Spek, Anthony L., Hage, R., Kellogg, Richard M. & Feringa, Ben L., *Eur. J. Org. Chem.*, 2000, **2000**, 3675.
55. Stanley, C.E., Clarke, N., Anderson, K.M., Elder, J.A., Lenthall, J.T. & Steed, J.W., *Chem. Commun.*, 2006, 3199.
56. Zhou, Y., Yi, T., Li, T., Zhou, Z., Li, F., Huang, W. & Huang, C., *Chem. Mater.*, 2006, **18**, 2974.
57. Takizawa, M., Kimoto, A. & Abe, J., *Dyes Pigments*, 2011, **89**, 254.
58. Reddy, L.S., Basavoju, S., Vangala, V.R. & Nangia, A., *Cryst. Growth Des.*, 2005, **6**, 161.
59. Wood, D.M., Greenland, B.W., Acton, A.L., Rodriguez-Llansola, F., Murray, C.A., Cardin, C.J., Miravet, J.F., Escuder, B., Hamley, I.W. & Hayes, W., *Chemistry (Weinheim an der Bergstrasse, Germany)*, 2012, **18**, 2692.
60. Lloyd, G.O. & Steed, J.W., *Nat. Chem.*, 2009, **1**, 437.
61. Piepenbrock, M.-O.M., Clarke, N., Foster, J.A. & Steed, J.W., *Chem. Commun.*, 2011, **47**, 2095.
62. Piepenbrock, M.-O.M., Lloyd, G.O., Clarke, N. & Steed, J.W., *Chem. Rev.*, 2010, asap article.
63. Piepenbrock, M.O.M., Clarke, N., Foster, J.A. & Steed, J.W., *Chem. Commun.*, 2011, **47**, 2095.
64. Yang, H., Yi, T., Zhou, Z., Zhou, Y., Wu, J., Xu, M., Li, F. & Huang, C., *Langmuir*, 2007, **23**, 8224.
65. Esteban-Gomez, D., Fabbrizzi, L. & Licchelli, M., *J. Org. Chem.*, 2005, **70**, 5717.
66. Swinburne, A.N., Paterson, M.J., Beeby, A. & Steed, J.W., *Org. Biomol. Chem.*, 2010, **8**, 1010.

67. Becker, T., Goh, C.Y., Jones, F., McIldowie, M.J., Mocerino, M. & Ogden, M.I., *Chem. Commun.*, 2008, 3900.
68. Lloyd, G.O. & Steed, J.W., *Soft Matter*, 2011, **7**, 75.
69. Byrne, P., Turner, D.R., Lloyd, G.O., Clarke, N. & Steed, J.W., *Cryst. Growth Des.*, 2008, **8**, 3335.
70. Applegarth, L., Clark, N., Richardson, A.C., Parker, A.D.M., Radosavljevic-Evans, I., Goeta, A.E., Howard, J.A.K. & Steed, J.W., *Chem. Commun.*, 2005, 5423.
71. Piepenbrock, M.O.M., Clarke, N. & Steed, J.W., *Soft Matter*, 2010, **6**, 3541.
72. Hirst, A.R., Escuder, B., Miravet, J.F. & Smith, D.K., *Angew. Chem., Int. Ed.*, 2008, **47**, 8002.
73. Banerjee, S., Das, R.K. & Maitra, U., *J. Mater. Chem.*, 2009, **19**, 6649.
74. Yang, X., Zhang, G. & Zhang, D., *J. Mater. Chem.*, 2012, **22**, 38.
75. Zhou, J.L., Chen, X.J. & Zheng, Y.S., *Chem. Commun.*, 2007, 5200.
76. Collier, J.H., Hu, B.H., Ruberti, J.W., Zhang, J., Shum, P., Thompson, D.H. & Messersmith, P.B., *J. Am. Chem. Soc.*, 2001, **123**, 9463.
77. Chu, Z. & Feng, Y., *Chem. Commun.*, 2011, **47**, 7191.
78. Hsueh, S.-Y., Kuo, C.-T., Lu, T.-W., Lai, C.-C., Liu, Y.-H., Hsu, H.-F., Peng, S.-M., Chen, C.-h. & Chiu, S.-H., *Angew. Chem. Int. Ed.*, **49**, 9170.
79. Shome, A., Debnath, S. & Das, P.K., *Langmuir*, 2008, **24**, 4280.
80. Chung, J.W., An, B.-K. & Park, S.Y., *Chem. Mater.*, 2008, **20**, 6750.
81. Gasnier, A.l., Royal, G. & Terech, P., *Langmuir*, 2009, **25**, 8751.
82. Chen, J. & McNeil, A.J., *J. Am. Chem. Soc.*, 2008, **130**, 16496.
83. Muraoka, T., Koh, C.-Y., Cui, H. & Stupp, S.I., *Angew. Chem. Int. Ed.*, 2009, **48**, 5946.
84. Qiu, Z., Yu, H., Li, J., Wang, Y. & Zhang, Y., *Chem. Commun.*, 2009, 3342.
85. Wang, S., Shen, W., Feng, Y. & Tian, H., *Chem. Commun.*, 2006, 1497.
86. Naota, T. & Koori, H., *J. Am. Chem. Soc.*, 2005, **127**, 9324.
87. Li, Y., Wang, T. & Liu, M., *Tetrahedron*, 2007, **63**, 7468.
88. Bardelang, D., Zaman, M.B., Moudrakovski, I.L., Pawsey, S., Margeson, J.C., Wang, D.S., Wu, X.H., Ripmeester, J.A., Ratcliffe, C.I. & Yu, K., *Adv. Mater.*, 2008, **20**, 4517.
89. Panda, J.J., Mishra, A., Basu, A. & Chauhan, V.S., *Biomacromolecules*, 2008, **9**, 2244.
90. van Bommel, K.J.C., Stuart, M.C.A., Feringa, B.L. & van Esch, J., *Org. Biomol. Chem.*, 2005, **3**, 2917.
91. Vemula, P.K., Li, J. & John, G., *J. Am. Chem. Soc.*, 2006, **128**, 8932.
92. Bhuniya, S., Seo, Y.J. & Kim, B.H., *Tetrahedron Lett.*, 2006, **47**, 7153.
93. Gao, Y., Kuang, Y., Guo, Z.-F., Guo, Z., Krauss, I.J. & Xu, B., *J. Am. Chem. Soc.*, 2009, **131**, 13576.
94. Yang, Z., Gu, H., Zhang, Y., Wang, L. & Xu, B., *Chem. Commun.*, 2004, 208.
95. Yang, Z., Liang, G., Guo, Z., Guo, Z. & Xu, B., *Angew. Chem. Int. Ed.*, 2007, **46**, 8216.
96. Yang, Z.M., Xu, K.M., Guo, Z.F., Guo, Z.H. & Xu, B., *Adv. Mater.*, 2007, **19**, 3152.
97. Yang, Z., Liang, G. & Xu, B., *Acc. Chem. Res.*, 2008, **41**, 315.
98. Komatsu, H., Matsumoto, S., Tamaru, S.-i., Kaneko, K., Ikeda, M. & Hamachi, I., *J. Am. Chem. Soc.*, 2009, **131**, 5580.
99. Chung, J.W., Yoon, S.-J., Lim, S.-J., An, B.-K. & Park, S.Y., *Angew. Chem. Int. Ed.*, 2009, **48**, 7030.
100. Matsumoto, S., Yamaguchi, S., Wada, A., Matsui, T., Ikeda, M. & Hamachi, I., *Chem. Commun.*, 2008, 1545.
101. Zhou, S.L., Matsumoto, S., Tian, H.D., Yamane, H., Ojida, A., Kiyonaka, S. & Hamachi, I., *Chem. Eur. J.*, 2005, **11**, 1130.
102. Yang, Z.M., Gu, H.W., Zhang, Y., Wang, L. & Xu, B., *Chem. Commun.*, 2004, 208.

103. Semino, C.E., Merok, J.R., Crane, G.G., Panagiotakos, G. & Zhang, S., *Differentiation*, 2003, **71**, 262.
104. Kisiday, J., Jin, M., Kurz, B., Hung, H., Semino, C., Zhang, S. & Grodzinsky, A.J., *P. Natl. Acad. Sci. USA*, 2002, **99**, 9996.
105. Silva, G.A., Czeisler, C., Niece, K.L., Beniash, E., Harrington, D.A., Kessler, J.A. & Stupp, S.I., *Science*, 2004, **303**, 1352.
106. Ellis-Behnke, R.G., Liang, Y.X., You, S.W., Tay, D.K.C., Zhang, S.G., So, K.F. & Schneider, G.E., *P. Natl. Acad. Sci. USA*, 2006, **103**, 5054.
107. Ellis-Behnke, R.G., Liang, Y.-X., David, K.C., Kau, P.W.F., Schneider, G.E., Zhang, S., Wu, W. & So, K.-F., *Nanomed-Nanotechnol*, 2006, **2**, 207.
108. Li, Y. & Liu, M., *Chem. Commun.*, 2008, 5571.
109. Adhikari, B., Nanda, J. & Banerjee, A., *Chem. Eur. J.*, 2011, **17**, 11488.
110. Ikeda, M., Ueno, S., Matsumoto, S., Shimizu, Y., Komatsu, H., Kusumoto, K.-i. & Hamachi, I., *Chem. Eur. J.*, 2008, **14**, 10808.
111. Wu, J., Tian, Q., Hu, H., Xia, Q., Zou, Y., Li, F., Yi, T. & Huang, C., *Chem. Commun.*, 2009, 4100.
112. Smith, D.K., *Nat. Chem.*, 2010, **2**, 162.
113. Mizrahi, S., Gun, J., Kipervaser, Z.G. & Lev, O., *Anal. Chem.*, 2004, **76**, 5399.
114. Yamamichi, S., Jinno, Y., Haraya, N., Oyoshi, T., Tomitori, H., Kashiwagi, K. & Yamanaka, M., *Chem. Commun.*, 2011, **47**, 10344.
115. Mizrahi, S., Rizkov, D., Hayat, N. & Lev, O., *Chem. Commun.*, 2008, 2914.
116. Yoshio, M., Shoji, Y., Tochigi, Y., Nishikawa, Y. & Kato, T., *J. Am. Chem. Soc.*, 2009, **131**, 6763.
117. Desvergne, J.-P., Olive, A.G.L., Sangeetha, N.M., Reichwagen, J., Hopf, H. & Del Guerzo, A., *Pure Appl. Chem.*, 2006, **78**, 2333.
118. Ajayaghosh, A., Praveen, V.K., Vijayakumar, C. & George, S.J., *Angew. Chem. Int. Ed.*, 2007, **46**, 6260.
119. Puigmarti-Luis, J., Laukhin, V., del Pino, A.P., Vidal-Gancedo, J., Rovira, C., Laukhina, E. & Amabilino, D.B., *Angew. Chem. Int. Ed.*, 2007, **46**, 238.
120. Wang, G. & Hamilton, A.D., *Chem. Eur. J.*, 2002, **8**, 1954.
121. Llusar, M. & Sanchez, C.m., *Chem. Mater.*, 2008, **20**, 782.
122. van Bommel, K.J.C., Friggeri, A. & Shinkai, S., *Angew. Chem. Int. Ed.*, 2003, **42**, 980.
123. Nagasawa, J.i., Kudo, M., Hayashi, S. & Tamaoki, N., *Langmuir*, 2004, **20**, 7907.
124. van Bommel, K.J.C., Friggeri, A. & Shinkai, S., *Angew. Chem. Int. Ed.*, 2003, **42**, 980.
125. Ouhib, F., Bugnet, E., Nossov, A., Bonardet, J.-L. & Bouteiller, L., *Polymer*, 2010, **51**, 3360.
126. Srinivasan, S., Babu, P.A., Mahesh, S. & Ajayaghosh, A., *J. Am. Chem. Soc.*, 2009, **131**, 15122.
127. Mann, S., *Nature*, 1988, **332**, 119.
128. Burguete, M.I., Galindo, F., Gavara, R., Izquierdo, M.A., Lima, J.C., Luis, S.V., Parola, A.J. & Pina, F., *Langmuir*, 2008, **24**, 9795.
129. Beginn, U., Sheiko, S. & Möller, M., *Macromol. Chem. Phys.*, 2000, **201**, 1008.
130. Gu, W.Q., Lu, L.D., Chapman, G.B. & Weiss, R.G., *Chem. Commun.*, 1997, 543.
131. Simon, F.-X., Khelfallah, N.S., Schmutz, M., Díaz, N. & Mésini, P.J., *J. Am. Chem. Soc.*, 2007, **129**, 3788.
132. J. H. Hafkamp, R., P. A. Kokke, B., M. Danke, I., P. M. Geurts, H., E. Rowan, A., C. Feiters, M. & J. M. Nolte, R., *Chem. Commun.*, 1997, 545.
133. Wei, Q. & James, S.L., *Chem. Commun.*, 2005, 1555.
134. Mitra, R.N. & Das, P.K., *J. Phys. Chem. C.*, 2008, **112**, 8159.
135. Dutta, S., Shome, A., Debnath, S. & Das, P.K., *Soft Matter*, 2009, **5**, 1607.

136. Piepenbrock, M.O.M., Clarke, N. & Steed, J.W., *Soft Matter*, 2011, **7**, 2412.
137. Escuder, B., Rodriguez-Llansola, F. & Miravet, J.F., *New J. Chem.*, 2010, **34**, 1044.
138. Pal, A., Srivastava, A. & Bhattacharya, S., *Chem. Eur. J.*, 2009, **15**, 9169.
139. Miljanic, S., Frkanec, L., Biljan, T., Meic, Z. & Zinic, M., *Langmuir*, 2006, **22**, 9079.
140. Piepenbrock, M.-O.M., Clarke, N. & Steed, J.W., *Soft Matter*, 2011, **7**, 2412.
141. Mullin, J.W. Crystallization (Reed Educational and Professional Publishing Ltd, Oxford, 2001).
142. Kashchiev, D. & van Rosmalen, G.M., *Cryst. Res. Technol.*, 2003, **38**, 555.
143. Achlioptas, D., D'Souza, R.M. & Spencer, J., *Science*, 2009, **323**, 1453.
144. Chen, C., Cook, O., Nicholson, C.E. & Cooper, S.J., *Cryst. Growth Des.*, **11**, 2228.
145. Ostwald, W.Z., *Phys. Chem.* , 1897, **22**, 289.
146. Holmes, H.N., *J. Phys. Chem.*, 1917, **21**, 709.
147. Henisch, H.K. & Garciaruiz, J.M., *J. Cryst. Growth*, 1986, **75**, 203.
148. Desiraju, G.R., Curtin, D.Y. & Paul, I.C., *J. Am. Chem. Soc.*, 1977, **99**, 6148.
149. Yaghi, O.M., Li, G.M. & Li, H.L., *Chem. Mater.*, 1997, **9**, 1074.
150. Henisch, H.K. Crystal Growth in Gels (The Pennsylvania State University Press, University Park, PA, 1976).
151. Duffus, C., Camp, P.J. & Alexander, A.J., *J. Am. Chem. Soc.*, 2009, **131**, 11676.
152. Cudney, R., Patel, S. & McPherson, A., *Acta crystallographica. Section D, Biological crystallography*, 1994, **50**, 479.
153. Pauchet, M., Morelli, T., Coste, S., Malandain, J.-J. & Coquerel, G., *Cryst. Growth Des.*, 2006, **6**, 1881.
154. Xiao, J., Zhu, Y., Liu, Y., Liu, H., Zeng, Y., Xu, F. & Wang, L., *Cryst. Growth Des.*, 2008, **8**, 2887.
155. Diao, Y., Whaley, K.E., Helgeson, M.E., Woldeyes, M.A., Doyle, P.S., Myerson, A.S., Hatton, T.A. & Trout, B.L., *J. Am. Chem. Soc.*, 2012, **134**, 673.
156. Leng, B., Jiang, F., Lu, K., Ming, W. & Shao, Z., *CrystEngComm*, 2010, **12**, 730.
157. Petrova, R.I., Patel, R. & Swift, J.A., *Cryst. Growth Des.*, 2006, **6**, 2709.
158. Oaki, Y. & Imai, H., *Cryst. Growth Des.*, 2003, **3**, 711.
159. Imai, H. & Oaki, Y., *Angew. Chem. Int. Ed.*, 2004, **43**, 1363.
160. Oaki, Y. & Imai, H., *J. Am. Chem. Soc.*, 2004, **126**, 9271.
161. Li, H. & Estroff, L.A., *J. Am. Chem. Soc.*, 2007, **129**, 5480.
162. Li, H.Y. & Estroff, L.A., *CrystEngComm*, 2007, **9**, 1153.
163. Iafisco, M., Marchetti, M., Morales, J.G., Hernandez-Hernandez, M.A., Ruiz, J.M.G. & Roveri, N., *Cryst. Growth Des.*, 2009, **9**, 4912.
164. Petrova, R.I. & Swift, J.A., *J. Am. Chem. Soc.*, 2004, **126**, 1168.
165. Sangeetha, N.M. & Maitra, U., *Chem. Soc. Rev.*, 2005, **34**, 821.
166. Abdallah, D.J. & Weiss, R.G., *Adv. Mater.*, 2000, **12**, 1237.
167. Estroff, L.A. & Hamilton, A.D., *Angew. Chem. Int. Ed.*, 2000, **39**, 3447.
168. Estroff, L.A., Addadi, L., Weiner, S. & Hamilton, A.D., *Org. Biomol. Chem.*, 2004, **2**, 137.
169. Hartgerink, J.D., Beniash, E. & Stupp, S.I., *Science*, 2001, **294**, 1684.
170. Foster, J.A., PiepenbrockMarc-Oliver, M., Lloyd, G.O., Clarke, N., HowardJudith, A.K. & Steed, J.W., *Nat. Chem.*, 2010, **2**, 1037.
171. Steed, J.W., *Chem. Commun.*, 2011, **47**, 1379.
172. van Esch, J., Schoonbeek, F., de Loos, M., Kooijman, H., Spek, A.L., Kellogg, R.M. & Feringa, B.L., *Chem. Eur. J.*, 1999, **5**, 937.
173. Menger, F.M. & Caran, K.L., *J. Am. Chem. Soc.*, 2000, **122**, 11679.
174. Smith, D.K., *Chem. Soc. Rev.*, 2009, **38**, 684.

175. Friggeri, A., van der Pol, C., van Bommel, K.J.C., Heeres, A., Stuart, M.C.A., Feringa, B.L. & van Esch, J., *Chem. Eur. J.*, 2005, **11**, 5353.
176. Cravotto, G. & Cintas, P., *Chem. Soc. Rev.*, 2009, **38**, 2684.
177. Fujita, N., Sakamoto, Y., Shirakawa, M., Ojima, M., Fujii, A., Ozaki, M. & Shinkai, S., *J. Am. Chem. Soc.*, 2007, **129**, 4134.
178. Lloyd, G.O. in Chemistry (Durham University, Durham, 2010).
179. Foster, J.A. in Chemistry (Durham University, Durham, 2008).
180. Wu, X., Ji, S., Li, Y., Li, B., Zhu, X., Hanabusa, K. & Yang, Y., *J. Am. Chem. Soc.*, 2009, **131**, 5986.
181. Brizard, A., Oda, R. & Huc, I., *Top. Curr. Chem.*, 2005, **256**, 167.
182. Sheldrick, G.M. in SHELXS-97 (University of Göttingen, 1997).
183. Dolomanov, O.V., Bourhis, L.J., Gildea, R.J., Howard, J.A.K. & Puschmann, H., *Journal of Applied Crystallography*, 2009, **42**, 339.
184. Adhikari, B., Nanda, J. & Banerjee, A., *Soft Matter*, 2011, **7**, 8913.
185. Rajamalli, P. & Prasad, E., *Org. Lett.*, 2011, **13**, 3714.
186. Kim, T.H., Choi, M.S., Sohn, B.H., Park, S.Y., Lyoo, W.S. & Lee, T.S., *Chem. Commun.*, 2008, 2364.
187. Montalti, M., Dolci, L.S., Prodi, L., Zaccheroni, N., Stuart, M.C.A., van Bommel, K.J.C. & Friggeri, A., *Langmuir*, 2006, **22**, 2299.
188. Hahma, A., Bhat, S., Leivo, K., Linnanto, J., Lahtinen, M. & Rissanen, K., *New J. Chem.*, 2008, **32**, 1438.
189. Das, R.K., Kandanelli, R., Linnanto, J., Bose, K. & Maitra, U., *Langmuir*, 2010, **26**, 16141.
190. Kamikawa, Y. & Kato, T., *Langmuir*, 2006, **23**, 274.
191. Kim, T.H., Choi, M.S., Sohn, B.-H., Park, S.-Y., Lyoo, W.S. & Lee, T.S., *Chem. Commun.*, 2008, 2364.
192. Sagawa, T., Fukugawa, S., Yamada, T. & Ihara, H., *Langmuir*, 2002, **18**, 7223.
193. Ikeda, M., Ochi, R., Wada, A. & Hamachi, I., *Chemical Science*, 2010, **1**, 491.
194. Ribou, A.-C., Vigo, J. & Salmon, J.-M., *Photochem. Photobiol.*, 2004, **80**, 274.
195. Kaden, P., Mayer-Enthart, E., Trifonov, A., Fiebig, T. & Wagenknecht, H.-A., *Angew. Chem. Int. Ed.*, 2005, **44**, 1636.
196. Berezin, M.Y. & Achilefu, S., *Chem. Rev.*, 2010, **110**, 2641.
197. Figueira-Duarte, T.M. & Muellen, K., *Chem. Rev.*, 2011, **111**, 7260.
198. Ham, J.S., *J. Chem. Phys.*, 1953, **21**, 756.
199. Crawford, A.G., Dwyer, A.D., Liu, Z., Steffen, A., Beeby, A., PaÌŠlsson, L.-O., Tozer, D.J. & Marder, T.B., *J. Am. Chem. Soc.*, **133**, 13349.
200. Li, W.-S., Teng, M.-J., Jia, X.-R. & Wei, Y., *Tetrahedron Lett.*, **51**, 5336.
201. Li, Y., Wang, T. & Liu, M., *Soft Matter*, 2007, **3**, 1312.
202. Coventry, D.N., Batsanov, A.S., Goeta, A.E., Howard, J.A.K., Marder, T.B. & Perutz, R.N., *Chem. Commun.*, 2005, 2172.
203. Crawford, A.G., Liu, Z., Mkhalid, I.A.I., Thibault, M.-H., Schwarz, N., Alcaraz, G., Steffen, A., Collings, J.C., Batsanov, A.S., Howard, J.A.K. & Marder, T.B., *Chemistry – A European Journal*, **18**, 5022.
204. Vyas, P.V., Bhatt, A.K., Ramachandraiah, G. & Bedekar, A.V., *Tetrahedron Lett.*, 2003, **44**, 4085.
205. Rodriguez, A., Miller, D.D. & Jackson, R.F.W., *Org. Biomol. Chem.*, 2003, **1**, 973.
206. Oswald, C.L., Carrillo-Marquez, T., Caggiano, L. & Jackson, R.F.W., *Tetrahedron*, 2008, **64**, 681.
207. Jackson, R.F.W., Wishart, N., Wood, A., James, K. & Wythes, M.J., *J. Org. Chem.*, 1992, **57**, 3397.

208. Kalyanasundaram, K. & Thomas, J.K., *J. Am. Chem. Soc.*, 1977, **99**, 2039.
209. Winnik, F.M., *Chem. Rev.*, 1993, **93**, 587.
210. Bains, G., Patel, A.B. & Narayanaswami, V., *Molecules*, 2011, **16**, 7909.
211. Kollar, J., Hrdlovic • , P. & Chmela, S., *J. Photoch. Photobio. A.*, **214**, 33.
212. Swinburne, A.N., Paterson, M.J., Beeby, A. & Steed, J.W., *Chem. Eur. J.*, 2010, **16**, 2714.
213. Wenzel, M., Hiscock, J.R. & Gale, P.A., *Chem. Soc. Rev.*, 2012, **41**, 480.
214. Maeda, H., *Chem. Eur. J.*, 2008, **36**, 11274.
215. Yamanaka, M., Nakamura, T., Nakagawa, T. & Itagaki, H., *Tetrahedron Lett.*, 2007, **48**, 8990.
216. Sahai, R., Loper, G.L., Lin, S.H. & Eyring, H., *P. Natl. Acad. Sci. USA*, 1974, **71**, 1499.
217. Swinburne, A.N., Paterson, M.J., Beeby, A. & Steed, J.W., *Chemistry-a European Journal*, **16**, 2714.
218. Gans, P. (University of Leeds, Leeds, 2006).
219. Yun, H.-S., Park, J.-W., Kim, S.-H., Kim, Y.-J. & Jang, J.-H., *Acta Biomaterialia*, **7**, 2651.
220. Yoshizawa, S., Utsugi, T., Shibano, K., Goto, S. & Yajima, H., *T. Mrs. Jap.*, 2005, **30**, 1155.
221. Shan, Z., Maschmeyer, T. & Jansen, J.C. (ABB Lummus Global Inc, USA Technische Universiteit Delft, Neth., US, 2004).
222. Audouin, F., Birot, M., Pasquinet, E., Besnard, O., Palmas, P., Poullain, D. & Deleuze, H., *Macromolecules*, 2011, **44**, 4879.
223. Sing, K.S.W., Everett, D.H., Haul, R.A.W., Moscou, L., Pierotti, R.A., Rouquerol, J. & Siemieniewska, T., *Pure Appl. Chem.*, 1985, **57**, 603.
224. Lowell, S., Shields, J.E., Thomas, M.A. & Thommes, M. Characterization of porous solids and powders: surface area, pore size and density (Springer, The Netherlands, 2006).
225. Daiguebonne, C., Deluzet, A., Camara, M., Boubekeur, K., Audebrand, N., Gerault, Y., Baux, C. & Guillou, O., *Cryst. Growth Des.*, 2003, **3**, 1015.
226. Pauchet, M., Morelli, T., Coste, S., Malandain, J.J. & Coquerel, G., *Cryst. Growth Des.*, 2006, **6**, 1881.
227. Li, H., Fujiki, Y., Sada, K. & Estroff, L.A., *CrystEngComm*, 2011, **13**, 1060.
228. McCauley, J.W. & Roy, R., *Am. Mineral.*, 1974, **59**, 947.
229. Dastidar, P., *Chem. Soc. Rev.*, 2008, **37**, 2699.
230. George, M. & Weiss, R.G., *Acc. Chem. Res.*, 2006, **39**, 489.
231. Smith, D.K. Organic Nanostructures (eds. Atwood, J.L. & Steed, J.W.) 111 (Wiley-VCH, Weinheim, 2008).
232. Rodríguez-Llansola, F., Escuder, B. & Miravet, J.F., *J. Am. Chem. Soc.*, 2009, **131**, 11478.
233. Kuroiwa, K., Shibata, T., Takada, A., Nemoto, N. & Kimizuka, N., *J. Am. Chem. Soc.*, 2004, **126**, 2016.
234. Bernstein, J. Polymorphism in Molecular Crystals (Clarendon Press, Oxford, 2002).
235. Stahly, G.P., *Cryst. Growth Des.*, 2007, **7**, 1007.
236. Grzesiak, A.L., Lang, M.D., Kim, K. & Matzger, A.J., *J. Pharm. Sci.*, 2003, **92**, 2260.
237. Lang, M.D., Kampf, J.W. & Matzger, A.J., *J. Pharm. Sci.*, 2002, **91**, 1186.
238. Dabros, M. & Thalladi, V.R., *Chem. Commun.*, 2007, 2476.
239. Florence, A.J., Bedford, C.T., Fabbiani, F.P.A., Shankland, K., Gelbrich, T., Hursthouse, M.B., Shankland, N., Johnston, A. & Fernandes, P., *CrystEngComm*, 2008, **10**, 811.
240. Gelbrich, T. & Hursthouse, M.B., *CrystEngComm*, 2006, **8**, 448.

241. Harris, R.K., Ghi, P.Y., Puschmann, H., Apperley, D.C., Griesser, U.J., Hammond, R.B., Ma, C.Y., Roberts, K.J., Pearce, G.J., Yates, J.R. & Pickard, C.J., *Org. Process Res. Dev.*, 2005, **9**, 902.
242. Lang, M.D., Grzesiak, A.L. & Matzger, A.J., *J. Am. Chem. Soc.*, 2002, **124**, 14834.
243. Arlin, J.-B., Price, L.S., Price, S.L. & Florence, A.J., *Chem. Commun.*, 2011, **47**, 7074.
244. Fernandes, P., Shankland, K., Florence, A.J., Shankland, N. & Johnston, A., *J. Pharm. Sci.*, 2007, **96**, 1192.
245. McMahon, L.E., Timmins, P., Williams, A.C. & York, P., *J. Pharm. Sci.*, 1996, **85**, 1064.
246. Burnett, D.J., Thielmann, F. & Sokoloski, T.D., *J. Therm. Anal. Calorim.*, 2007, **89**, 693.
247. Fleischman, S.G., Kuduva, S.S., McMahon, J.A., Moulton, B., Walsh, R.D.B., Rodriguez-Hornedo, N. & Zaworotko, M.J., *Cryst.Growth Des.*, 2003, **3**, 909.
248. Vrečer, F., Vrbinc, M. & Meden, A., *Int. J. Pharm.*, 2003, **256**, 3.
249. deIlarduya, M.C.T., Martin, C., Goni, M.M. & MartinezOharriz, M.C., *J. Pharm. Sci.*, 1997, **86**, 248.
250. Llinas, A., Box, K.J., Burley, J.C., Glen, R.C. & Goodman, J.M., *J. Appl. Crystallogr.*, 2007, **40**, 379.
251. Otsuka, M., Kato, F. & Matsuda, Y., *Analyst*, 2001, **126**, 1578.
252. Llinas, A., Burley, J.C., Prior, T.J., Glen, R.C. & Goodman, J.M., *Cryst. Growth Des.*, 2008, **8**, 114.
253. Ebisuzaki, Y., Boyle, P.D. & Smith, J.A., *Acta Crystallogr. C.*, 1997, **53**, 777.
254. Sun, C.Q., Zhou, D.L., Grant, D.J.W. & Young, V.G., *Acta Crystallogr. E*, 2002, **58**, 368.
255. Phadnis, N.V. & Suryanarayanan, R., *J. Pharm. Sci.*, 1997, **86**, 1256.
256. Airaksinen, S., Karjalainen, M., Rasanen, E., Rantanen, J. & Yliruusi, J., *Int. J. Pharm.*, 2004, **276**, 129.
257. Krzyzaniak, J.F., Williams, G.R. & Ni, N.N., *J. Pharm. Sci.*, 2007, **96**, 1270.
258. Griesser, U.J. & Burger, A., *Int. J. Pharm.*, 1995, **120**, 83.
259. Derollez, P., Dudognon, E., Affouard, F., Danede, F., Correia, N.T. & Descamps, M., *Acta Crystallogr. B*, 2010, **66**, 76.
260. Zhang, Y.G. & Grant, D.J.W., *Acta Crystallogr. C.*, 2005, **61**, 435.
261. Moynihan, H.A. & O'Hare, I.P., *Int. J. Pharm.*, 2002, **247**, 179.
262. Price, C.P., Grzesiak, A.L. & Matzger, A.J., *J. Am. Chem. Soc.*, 2005, **127**, 5512.
263. McGregor, P.A., Allan, D.R., Parsons, S. & Pulham, C.R., *J. Pharm. Sci.*, 2002, **91**, 1308.
264. Parkin, A., Parsons, S. & Pulham, C.R., *Acta Crystallogr. E*, 2002, **58**, 1345.
265. Fabbiani, F.P.A., Allan, D.R., David, W.I.F., Moggach, S.A., Parsons, S. & Pulham, C.R., *CrystEngComm*, 2004, **6**, 504.
266. Fabbiani, F.P.A., Allan, D.R., Dawson, A., David, W.I.F., McGregor, P.A., Oswald, I.D.H., Parsons, S. & Pulham, C.R., *Chem. Commun.*, 2003, 3004.
267. Cudney, R., Patel, S. & McPherson, A., *Acta Crystallogr. D.*, 1994, **50**, 479.
268. Yu, L., Stephenson, G.A., Mitchell, C.A., Bunnell, C.A., Snorek, S.V., Bowyer, J.J., Borchardt, T.B., Stowell, J.G. & Byrn, S.R., *J. Am. Chem. Soc.*, 2000, **122**, 585.
269. Cameron, G.J. in Chemistry (University of Durham, Durham, 2011).
270. Yu, L., *Acc. Chem. Res.*, 2010, **43**, 1257.
271. Chen, S., Xi, H. & Yu, L., *J. Am. Chem. Soc.*, 2005, **127**, 17439.
272. Chen, S., Guzei, I.A. & Yu, L., *J. Am. Chem. Soc.*, 2005, **127**, 9881.
273. Singh, A., Lee, I.S. & Myerson, A.S., *Cryst. Growth Des.*, 2008, **9**, 1182.

274. Hilden, J.L., Reyes, C.E., Kelm, M.J., Tan, J.S., Stowell, J.G. & Morris, K.R., *Cryst. Growth Des.*, 2003, **3**, 921.
275. Ha, J.-M., Wolf, J.H., Hillmyer, M.A. & Ward, M.D., *J. Am. Chem. Soc.*, 2004, **126**, 3382.
276. Nicholson, C.E., Chen, C., Mendis, B. & Cooper, S.J., *Cryst. Growth Des.*, 2011, **11**, 363.
277. Lee, A.Y., Erdemir, D. & Myerson, A.S., *Annu. Rev. Chem. Biomol. Eng.*, 2011, **2**, 259.
278. Mangin, D., Puel, F. & Veesler, S., *Org. Process Res. Dev.*, 2009, **13**, 1241.
279. Bastin, R.J., Bowker, M.J. & Slater, B.J., *Org. Process Res. Dev.*, 2000, **4**, 427.
280. Qiao, N., Li, M., Schlindwein, W., Malek, N., Davies, A. & Trappitt, G., *Int. J. Pharm.*, 2011, **419**, 1.
281. Chieng, N., Rades, T. & Aaltonen, J., *J. Pharm. Biomed. Anal.*, 2011, **55**, 618.
282. Bauer, J., Spanton, S., Henry, R., Quick, J., Dziki, W., Porter, W. & Morris, J., *Pharm. Res.*, 2001, **18**, 859.
283. Bernstein, J., *Cryst. Growth Des.*, 2011, **11**, 632.
284. Song, Y. & Chen, C.-C., *Ind. Eng. Chem. Res.*, 2009, **48**, 5522.